Universidade do Minho
Escola de Engenharia

Rui Miguel Correia da Silva

Designing synthetic *Ashbya* cell factories

março de 2019

FCT
Fundação para a Ciência e a Tecnologia
MINISTÉRIO DA CIÊNCIA, TECNOLOGIA E ENSINO SUPERIOR

PD-F

[DP_AEM]
DOCTORAL PROGRAM IN APPLIED AND ENVIRONMENTAL MICROBIOLOGY

COMPETE 2020
PROGRAMA OPERACIONAL COMPETITIVIDADE E INTERNACIONALIZAÇÃO

UNIÃO EUROPEIA
Fundo Europeu de Desenvolvimento Regional

PORTUGAL 2020

NORTE 2020
PROGRAMA OPERACIONAL REGIONAL DO NORTE

Rui Miguel Correia da Silva **Designing synthetic *Ashbya* cell factories**

UMinho | 2019

Universidade do Minho
Escola de Engenharia

Rui Miguel Correia da Silva

Designing synthetic *Ashbya* cell factories

Tese de Doutoramento em Engenharia Química e Biológica

Trabalho efetuado sob a orientação da
Doutora Lucília Maria Alves Ribeiro Domingues
e da
Doutora Tatiana Sofia da Quinta Vidal Aguiar

março de 2019

STATEMENT OF INTEGRITY

I hereby declare having conducted my thesis with integrity. I confirm that I have not used plagiarism or any form of falsification of results in the process of the thesis elaboration. I further declare that I have fully acknowledged the Code of Ethical Conduct of the University of Minho.

University of Minho, 28/03/2019

Full Name: Rui Miguel Correia da Silva

Signature:

Rui Miguel Correia da Silva

Ignoramus

Yuval N. Harari

ACKNOWLEDGEMENTS

Esta tese de doutoramento representa o maior desafio intelectual que abracei até ao momento. Como é regra em desafios desta dimensão, a sua concretização só é possível devido à contribuição de muitos, a quem dirijo o meu sincero agradecimento.

Em primeiro lugar às minhas orientadoras. À Professora Lucília Domingues, obrigado pelas oportunidades que me concedeu e pela confiança depositada em mim. Agradeço-lhe a disponibilidade para sempre me ouvir, me guiar e ajudar a desenvolver o meu pensamento critico, autonomia e rigor. À Doutora Tatiana Aguiar, fonte infindável de ideias, agradeço o acompanhamento incansável ao longo destes anos, todos os conselhos, e a constante preocupação com o meu bem-estar profissional e pessoal.

Ao Centro de Engenharia Biológica (CEB) da Universidade do Minho, pelas condições de trabalho fornecidas.

To all my co-authors, for the readiness to collaborate in the studies described in this thesis and for the way they have enriched the work presented with their different visions. A special thank is due to Professor Rui Oliveira and Professor José Luis Revuelta for having received me in their labs.

A todos os meus colegas de laboratório e de grupo (LBM e LF), pela boa disposição e alegria que sempre pude encontrar no trabalho.

A todas as pessoas envolvidas no DP_AEM, em especial aos meus companheiros e companheiras que iniciaram comigo este trajeto.

À Joana Cunha e à Sara Baptista, por sempre contribuírem e torcerem pelo meu sucesso, e pela partilha de experiências, preocupações, visões e ambições. Podia descrever as inúmeras situações pelas quais vos agradeço, mas tudo se resume ao enorme sentimento de amizade que nutro por cada uma de vós.

Aos meus amigos de sempre, tenho a felicidade de os ter por perto constantemente. Cada um à sua maneira, obrigado por estarem sempre lá para me apoiar e inspirar.

Ao Diogo e à Cristiana, por me incentivarem a dar o exemplo.

À Vera. Sempre à Vera. Obrigado por te tornares nessa mulher extraordinária com quem tenho o privilégio de partilhar a minha vida. Tanto que já construímos, tanto ainda por construir. Obrigado pelo amor, pela partilha, pelo passado, pelo presente e pelo futuro (tão próximo).

Aos três pilares da minha vida, a quem dedico esta tese. À minha madrinha Fernanda, por depositar todo o seu cuidado e carinho em mim. À minha mãe Matilde, por me mostrar todos os dias o que é o amor incondicional. Ao meu pai César, pelos valores que me transmitiu e que definem em grande parte o homem que sou hoje. O vosso bem-estar e harmonia é essencial para mim. Obrigado por todos os dias mostrarem o orgulho e o amor que têm por mim. Obrigado pela vida que me proporcionaram.

Lastly, the author would like to acknowledge the Fundação para a Ciência e Tecnologia (FCT) for having financially supported the work presented in this thesis through the FCT Doctoral Program in Applied and Environmental Microbiology (DP_AEM) - PhD grant PD/BD/113812/2015. The author would also like to thank for: the strategic funding of UID/BIO/04469/2013 and UID/BIO/04469/2019 unit; COMPETE 2020 (POCI-01-0145-FEDER-006684); and BioTecNorte operation (NORTE-01-0145-FEDER-000004) funded by the European Regional Development Fund under the scope of Norte2020 - Programa Operacional Regional do Norte.

ABSTRACT

Designing synthetic *Ashbya* cell factories

Industrial biotechnology is a segment of the bioeconomy in which microorganisms are considered core assets, playing a central role as cell factories in fermentation processes. Despite numerous proof-of-concept studies performed in industrial models, many commercial bioprocesses are based on non-conventional microorganisms with optimized innate metabolic potential. In fact, the choice between engineering microbial models or improving the innate metabolism of non-conventional microorganisms has been a major question in the field.

Ashbya gossypii is a filamentous fungus that stands in the intersection between industrial models and non-conventional microorganisms. It is considered a paradigm of the industrial biotechnology owing to the success of the bioprocess implemented almost 30 years ago that makes use of its overwhelming capacity to overproduce riboflavin (vitamin B_2). Until the beginning of this decade, its biotechnological relevance remained restricted to this application. Since then, interesting potentialities of its natural metabolism have been unravelled. Therefore, with the objective of developing *A. gossypii* as an alternative cell factory and of identifying novel biotechnological products, this thesis focused on the systematic exploration of this fungus natural metabolism through its physiological and molecular characterization.

The overproduction of riboflavin is the most distinctive trait of this hemiascomycete. It has been proposed to act as an ecological defence, as it is triggered by environmental stress. Envisioning a better understanding of this trait, a presumed genotoxic effect associated with the overproduction of riboflavin was investigated. For assessing that, the *Ashbya* Comet Assay was developed, which was able to reproducibly measure DNA damage. Using this protocol, exposure to sun-mimicking light during growth was found to significantly increase DNA damage in riboflavin-overproducing cells, but not in non-overproducing ones. In overproducing cells, light induced the intracellular accumulation of reactive oxygen species and increased the production of riboflavin 1.5-fold. These results draw attention for the importance of controlling the exposure to light of riboflavin biotechnological processes.

Proceeding with the influence of riboflavin overproduction on the global metabolism of *A. gossypii*, the molecular basis for the unusual sensitivity to uracil displayed by the *A. gossypii Agura3* pyrimidine auxotroph was identified. Uracil phosphoribosyltransferase (UPRTp) is the pyrimidine salvage pathway enzyme responsible for converting uracil to uridine monophosphate in the presence of phosphoribosyl pyrophosphate (PRPP). Characterization of the *A. gossypii* UPRTp,

produced and purified from *Escherichia coli*, revealed that uracil concentrations above 1 mM negatively affected its activity, thus explaining the hypersensitivity of the *Agura3* mutant to uracil. Decreased UPRT activity ultimately favours the preservation of PRPP, which may be directed to promote riboflavin production. Thus, this UPRTp modulation reveals a putative means of saving precursors essential for riboflavin overproduction.

The *A. gossypii Agura3* mutant, which displays a riboflavin-overproducing phenotype, was further identified as a suitable host for the production of a novel high-value compound, orotic acid. This strain was found to accumulate and excrete orotic acid to culture supernatants. Evidences are discussed indicating that the metabolic feature crucial for this phenotype is a putative mitochondrial dihydroorotate dehydrogenase encoded by *AgURA9*. Further engineering of this strain with the overexpression of a gene involved in glycerol metabolism (*AgGUP1*) improved its glycerol consumption profile, as well as its glycerol-dependent hyperosmotic tolerance. Thus, a flexible and robust strain for the production of high-value chemicals was constructed, which is able to sustain their production from a medium completely based on industrial by-products.

Finally, an alternative production process for γ-lactones is presented. The biotechnological exploration of these valuable fragrances relied solely in biotransformation processes, which limited their production from more sustainable substrates. Here, the innate ability of *A. gossypii* for *de novo* biosynthesis of γ-lactones from glucose was uncovered and improved. Characterization of nine strains of this fungus revealed the presence of seven chemically different γ-lactones. To understand this biosynthetic process, metabolic engineering strategies were applied to the fatty acid biosynthesis and the β-oxidation pathways. Overexpression of *AgDES589*, encoding a desaturase for the conversion of oleic acid into linoleic acid, and deletion of *AgELO624,* which encodes an elongase that catalyzes the formation of longer fatty acids increased the production of γ-lactones up to 6.4-fold. Further substitution of *AgPOX1* by a codon-optimized *POX2* gene from *Yarrowia lipolytica* fine-tuned the biosynthesis of γ-decalactone. By means of metabolic engineering, this study elucidated key steps in the biosynthesis of these compounds, and demonstrated the potential of *A. gossypii* as a model and future platform for the *de novo* biosynthesis of γ-lactones.

In sum, this thesis contributed to the goal of establishing *A. gossypii* as an alternative cell factory by disclosing two novel biotechnological applications that emerged from the exploration and understanding of this fungus natural metabolism.

RESUMO

Desenho de fábricas sintéticas de *Ashbya*

A biotecnologia industrial é um segmento da bioeconomia no qual os microrganismos são considerados ativos nucleares, desempenhando um papel central como fábricas celulares em processos de fermentação. Apesar de numerosos estudos de prova de conceito realizados em modelos industriais, muitos bioprocessos comerciais são baseados em microrganismos não-convencionais com potencial metabólico inato otimizado. De facto, a escolha entre modificar geneticamente modelos industriais ou melhorar o metabolismo inato de microrganismos não-convencionais tem sido uma das principais questões da área.

O *Ashbya gossypii* é um fungo filamentoso que se posiciona na interseção entre os modelos industriais e os microrganismos não-convencionais. Este é considerado um paradigma da biotecnologia industrial devido ao sucesso do bioprocesso implementado há quase 30 anos que faz uso da sua tremenda capacidade de superproduzir riboflavina (vitamina B_2). No entanto, até ao início desta década a sua relevância biotecnológica manteve-se restrita a esta aplicação. Desde então, potencialidades interessantes do seu metabolismo natural começaram a ser desvendadas. Assim, com o objetivo de desenvolver o *A. gossypii* como uma fábrica celular alternativa e de identificar novos produtos biotecnológicos, esta tese focou-se na exploração sistemática do seu metabolismo natural através da sua caracterização fisiológica e molecular.

A superprodução de riboflavina é a característica mais marcante deste hemiascomiceto. Esta tem vindo a ser proposta como uma defesa ecológica, já que é desencadeada por stress ambiental. Na busca de uma melhor compreensão desta característica, um possível efeito genotóxico associado à superprodução de riboflavina foi investigado. Para avaliar isso, o *Ashbya* Comet Assay foi desenvolvido, o qual permitiu medir danos no DNA de forma reprodutível. A partir deste protocolo, descobriu-se que a exposição durante o crescimento a uma fonte de luz com espetro similar ao da luz solar aumenta significativamente os danos no DNA em células com fenótipo de superprodução de riboflavina, mas não em células sem este fenótipo. A exposição destas células (superprodução de riboflavina) à luz induziu ainda a acumulação intracelular de espécies reativas de oxigénio e aumentou a produção de riboflavina 1,5 vezes. Estes resultados chamam a atenção para a importância de controlar a exposição à luz de processos biotecnológicos de produção de riboflavina.

Na continuação da influência da superprodução de riboflavina sobre o metabolismo global de *A. gossypii*, foi identificada a base molecular para a sensibilidade incomum ao uracilo apresentada pela estirpe auxotrófica de pirimidinas *A. gossypii Agura3*. A uracilo fosforibosiltransferase (UPRTp) é a enzima da via *salvage* das pirimidinas que converte uracilo em uridina monofosfato na

presença de fosforibosil pirofosfato (PRPP). A caracterização da UPRTp de *A. gossypii*, produzida e purificada a partir de *Escherichia coli*, revelou que concentrações de uracilo acima de 1 mM afetaram negativamente a sua atividade, explicando assim a hipersensibilidade do mutante *Agura3* ao uracilo. Em última instância, a atividade reduzida da UPRT favorece a preservação de PRPP, que pode ser direcionado para promover a produção de riboflavina. Assim, esta modulação revela uma forma putativa de poupar precursores essenciais para a superprodução de riboflavina.

O mutante *A. gossypii Agura3*, que exibe um fenótipo de superprodução de riboflavina, foi ainda identificado como um hospedeiro adequado para a produção de um novo composto de valor acrescentado, o ácido orótico. Evidências são discutidas que indicam que a característica metabólica crucial para este fenótipo é uma putativa dihidroorotato desidrogenase mitocondrial codificada pelo gene *AgURA9*. Engenharia adicional desta estirpe com a sobre-expressão de um gene envolvido no metabolismo do glicerol (*AgGUP1*) melhorou o perfil de consumo de glicerol bem como a sua resistência ao stress híper-osmótico de forma dependente do glicerol. Assim, uma estirpe flexível e robusta para a produção de químicos de valor acrescentado foi construída, que é capaz de sustentar a sua produção a partir de um meio completamente baseado em subprodutos industriais.

Finalmente, é apresentado um processo de produção de γ-lactonas alternativo. A exploração biotecnológica destas valiosas fragrâncias baseava-se em processos de bio-transformação, o que limitava a sua produção a partir de substratos mais sustentáveis. Aqui, a habilidade inata do *A. gossypii* para a biossíntese *de novo* de γ-lactonas a partir de glucose foi descoberta e melhorada. A caracterização de nove estirpes deste fungo revelou a presença de sete γ-lactonas quimicamente diferentes. A sobre-expressão do gene *AgDES589*, que codifica uma desaturase para a conversão de ácido oleico em linoleico, e a eliminação do gene *AgELO624*, que codifica para uma elongase que catalisa a formação de ácidos gordos de cadeia mais longa, aumentaram a produção de γ-lactonas até 6,4 vezes. A substituição adicional do gene *AgPOX1* pelo gene *POX2* de *Yarrowia lipolytica* com codão otimizado, afinou a biossíntese de γ-decalactona. Por meio de engenharia metabólica, este estudo elucidou passos chave na biossíntese destes compostos, e mostrou o potencial de *A. gossypii* como um modelo e futura plataforma para a biossíntese *de novo* de γ-lactonas.

Em suma, esta tese contribuiu para o objetivo de estabelecer o *A. gossypii* como uma fábrica celular alternativa ao revelar duas novas aplicações biotecnológicas que emergiram da exploração e compreensão do metabolismo natural deste fungo.

LIST OF PUBLICATIONS

Articles in peer reviewed journals

Silva R, Aguiar TQ, Coelho E, Jiménez A, Revuelta JL, Domingues L. Metabolic engineering of *Ashbya gossypii* for deciphering the *de novo* biosynthesis of γ-lactones. Microbial Cell Factories 2019; DOI:10.1186/s12934-019-1113-1.

Silva R*, Aguiar TQ*, Oliveira C, Domingues L. Physiological characterization of a pyrimidine auxotroph exposes link between uracil phosphoribosyltransferase regulation and riboflavin production in *Ashbya gossypii*. New Biotechnology 2019; 50:1–8. DOI: 10.1016/j.nbt.2018.12.004. *Equal contributions.

Silva R, Aguiar TQ, Oliveira R, Domingues L. Light exposure during growth increases riboflavin production, ROS accumulation and DNA damage in *Ashbya gossypii* riboflavin-overproducing strains. FEMS Yeast Research 2019; 19: DOI: 10.1093/femsyr/foy114.

Aguiar TQ, **Silva R**, Domingues L. New biotechnological applications for *Ashbya gossypii*: challenges and perspectives. Bioengineered 2017; 8:309–315. DOI: 0.1080/21655979.2016.1234543.

Aguiar TQ*, **Silva R***, Domingues L. *Ashbya gossypii* beyond industrial riboflavin production: A historical perspective and emerging biotechnological applications. Biotechnology Advances 2015; 33:1774–1786. DOI: 10.1016/j.biotechadv.2015.10.001. *Equal contributions.

Oral communications

Silva R, Aguiar TQ, Oliveira R, Domingues L. *Ashbya gossypii* riboflavin overproducing strains are highly susceptible to light-induced oxidative DNA damage. Book of Abstracts of MicroBiotec'17 - Congress of Microbiology and Biotechnology, Porto, Portugal, 7–9 December, 2017.

Silva R, Aguiar TQ, Domingues L. Engineering osmotic stress tolerance in the riboflavin producer *Ashbya gossypii*. Book of Abstracts of the 1st Iberoamerican Congress on Biotechnology (Bio.Iberoamérica 2016), Salamanca, Spain, 5–8 June, 2016.

Oral communications by invitation

Silva R, Coelho E, Aguiar TQ, Jiménez A, Revuelta JL, Domingues L. Improved *de novo* biosynthesis of lactones by engineered *Ashbya gossypii*. 3rd Joint BIOTECnico and AEM PhD Programs Workshop, Lisbon, Portugal, 11–12 June, 2018.

Silva R, Aguiar TQ, Domingues L. Designing synthetic *Ashbya* cell factories. 2nd Joint Workshop of the PhD Programs in Applied and Environmental Microbiology (DP_AEM) and Molecular and Environmental Biology (PDBMA), Braga Portugal, 25–29 September, 2017.

Silva R, Aguiar TQ, Domingues L. Designing synthetic terpenoid-producing fungal cell factories: Metabolic profiling of aroma volatile compounds produced by *Ashbya gossypii* wild strains. 2nd Joint BIOTECnico and AEM PhD Programs Workshop, Lisbon, Portugal, 15–16 February, 2017.

Silva R, Aguiar TQ, Domingues L. *Ashbya gossypii* beyond industrial riboflavin production: A historical perspective and emerging biotechnological applications. 1st Joint BIOTECnico and AEM PhD Programs Workshop, Lisbon, Portugal, 21–22 January, 2016.

Poster communications

Silva R, Coelho E, Aguiar TQ, Jiménez A, Revuelta JL, Domingues L. Volatile compounds' profiling and engineering of *Ashbya gossypii* strains for de novo biosynthesis of lactones. ME12 - Metabolic Engineering 12, Munich, Germany, 24–28 June, 2018.

Aguiar TQ, **Silva R**, Oliveira C, Domingues L. Substrate inhibition of Uracil Phosphoribosyltransferase (UPRT) in distinct microbial species and its implications in the phenotype of uracil auxotrophs. Book of Abstracts of MicroBiotec'17 - Congress of Microbiology and Biotechnology, Porto, Portugal, 7–9 December, 2017.

Silva R, Aguiar TQ, Domingues L. Why does uridine supplementation properly rescue the growth of *Ashbya gossypii* uracil auxotrophs, but not uracil? XIX National Congress of Biochemistry (SPB2016), Guimarães, Portugal, 8–10 December, 2016.

Silva R, Aguiar TQ, Domingues L. Analysis of the sensitivity of different fungal species to uracil. Book of Abstracts of the 6th Conference on Physiology of Yeast and Filamentous Fungi (PYFF6), Lisbon, Portugal, 11–14 July, 2016.

Poster communications by invitation

Silva R, Aguiar TQ, Domingues L. Deciphering the uracil growth sensitivity of *Ashbya gossypii* pyrimidine auxotrophs. Symposium 30 Years Molecular Biology of *Ashbya gossypii*, Basel, Switzerland, 28 April, 2017.

Silva R, Oliveira R, Aguiar TQ, Domingues L. The *Ashbya gossypii* Comet Assay: Measuring oxidative and non-oxidative damage in the DNA. Symposium 30 Years Molecular Biology of *Ashbya gossypii*, Basel, Switzerland, 28 April, 2017.

Silva R, Coelho E, Aguiar TQ, Domingues L. Metabolic profiling of aroma volatile compounds produced by *Ashbya gossypii* wild strains. 2nd Joint BIOTECnico and AEM PhD Programs Workshop, Lisbon, Portugal, 15–16 February, 2017.

CONTENTS

ACKNOWLEDGEMENTS VII

ABSTRACT IX

RESUMO XI

LIST OF PUBLICATIONS XIII

CONTENTS XVII

LIST OF FIGURES XXI

LIST OF TABLES XXXI

LIST OF ABBREVIATIONS AND ACRONYMS XXXIII

MOTIVATION AND OUTLINE OF THE THESIS 1

Motivation 2

Outline of the thesis 3

CHAPTER I

GENERAL INTRODUCTION 5

1.1 Industrial Biotechnology: a global overview 7

1.1.1 Microbial cell factories: a core element within the sector 8

1.1.2 Industrial models vs non-conventional microbial hosts 9

1.2 *Ashbya gossypii* 12

1.2.1 Niche, taxonomy and morphology 13

1.2.2 Biochemistry and physiology 16

1.2.3 Genetics and molecular tools 24

1.3 Commercial and emerging biotechnology of *A. gossypii* 28

1.3.1 Vitamins 28

1.3.2 Recombinant proteins 34

1.3.3 Single cell oil and *de novo* biosynthesis of lipids 37

1.3.4 Flavours 39

1.4 Standpoint of *A. gossypii* as a cell factory 42

1.5 References 45

CHAPTER II

LIGHT EXPOSURE DURING GROWTH INCREASES RIBOFLAVIN PRODUCTION, ROS ACCUMULATION AND DNA DAMAGE IN *ASHBYA GOSSYPII* RIBOFLAVIN-OVERPRODUCING STRAINS 57

Abstract 59

2.1 Introduction 60

2.2 Material and methods 62

2.2.1 Strains and media 62

2.2.2 Radial growth conditions and cell treatments 62

2.2.3 The *Ashbya gossypii* comet assay 62

2.2.4 Analysis of intracellular ROS accumulation 64

2.2.5 Statistical analyses 64

2.3 Results and discussion 65

2.3.1 The *Ashbya* Comet Assay is able to measure oxidative and non-oxidative DNA damage 65

2.3.2 Light exposure during growth affects riboflavin production and increases DNA damage and intracellular oxidation in *A. gossypii* 69

2.4 References 74

CHAPTER III

PHYSIOLOGICAL CHARACTERIZATION OF A PYRIMIDINE AUXOTROPH EXPOSES LINK BETWEEN URACIL PHOSPHORIBOSYLTRANSFERASE REGULATION AND RIBOFLAVIN PRODUCTION IN *ASHBYA GOSSYPII* 77

Abstract 79

3.1 Introduction 80

3.2 Materials and methods 82

3.2.1 Strains and media 82

3.2.2 Radial growth conditions for *A. gossypii* strains 82

3.2.3 AgUPRTp sequence analysis, recombinant production and purification 83

3.2.4 Enzyme activity assays 84

3.2.5 Statistical analyses 84

3.3 Results and discussion 85

3.3.1 Growth-rescuing effect of various pyrimidine supplements on *A. gossypii Agura3* 85
3.3.2 AgUPRTp sequence analysis, recombinant production and purification 89
3.3.3 AgUPRTp activity is negatively affected by high uracil concentrations 92
3.4 Conclusions 96
3.5 References 97

CHAPTER IV

EXPLORATION OF THE *ASHBYA GOSSYPII* PYRIMIDINE AUXOTROPH *AGURA3* FOR OROTIC ACID PRODUCTION 101
Abstract 103
4.1 Introduction 104
4.2 Material and methods 107
4.2.1 Strains 107
4.2.2 Media and fermentations 108
4.2.3 Construction of the integration cassette and transformation of *A. gossypii* strains 109
4.2.4 Radial growth of *A. gossypii* strains in hyperosmotic stress conditions 110
4.2.5 Analytical methods 110
4.3 Results and discussion 112
4.3.1 *A. gossypii Agura3* produces and excretes orotic acid to the medium 112
4.3.2 Effects of *AgGUP1* overexpression on the glycerol consumption profile and hyperosmotic stress tolerance of *A. gossypii Agura3* 113
4.3.3 Exploring culture conditions for orotic acid production by *A. gossypii* 117
4.4 Conclusions 121
4.5 References 122

CHAPTER V

METABOLIC ENGINEERING OF *ASHBYA GOSSYPII* FOR DECIPHERING THE *DE NOVO* BIOSYNTHESIS OF γ-LACTONES 125
Abstract 127
5.1 Introduction 128
5.2 Materials and methods 132
5.2.1 Chemicals 132
5.2.2 Strains and media 132

5.2.3 Culture conditions for the analysis of the VOCs produced by *A. gossypii* non-engineered strains 133
5.2.4 Construction of integration cassettes and transformation of *A. gossypii* 134
5.2.5 Culture conditions for the analysis of the *de novo* biosynthesis of γ-lactones by *A. gossypii* engineered strains 135
5.2.6 Volatiles extraction and analysis by GC–MS 135
5.2.7 Statistical analyses 136
5.3 Results and discussion 137
5.3.1 *A. gossypii* predominantly produced γ-lactones and higher alcohols as VOCs 137
5.3.2 The major lactone produced by *A. gossypii* was γ-decalactone 138
5.3.3 Redirection of the metabolic fluxes of the fatty acid biosynthesis modulated the *de novo* biosynthesis of γ-lactones in *A. gossypii* 141
5.3.4 Combinatorial engineering fine-tuned the biosynthesis of γ-decalactone in *A. gossypii* 145
5.4 Conclusions 147
5.5 References 148
CHAPTER VI
GENERAL CONCLUSIONS AND FUTURE PERSPECTIVES 151
APPENDIX 157

LIST OF FIGURES

CHAPTER I

Figure 1.1. *A. gossypii* biotechnological applications. Following its established industrial use in riboflavin production, emerging biotechnological applications for this fungus are: other vitamins, recombinant proteins, single-cell oil (SCO) and flavours production. The technological approaches used for the development of these biotechnological applications are presented in the closing circle.

Figure 1.2. Schematic representation of the *A. gossypii* life cycle. The colony photo represents growth for eight days on agar-solidified complex medium.

Figure 1.3. Pathways and genes involved in the *A. gossypii* metabolism that have been targeted for biotechnological purposes. The pathways are identified according to the following colour scheme: glycolysis and gluconeogenesis (light blue), β-oxidation and fatty acid biosynthesis (red), TCA cycle and glyoxylate cycle (purple), pentose phosphate pathway (brown), *de novo purine* biosynthetic pathway (dark blue), glycine pathways (grey), *de novo* pyrimidine biosynthetic pathway (yellow), riboflavin biosynthetic pathway (orange), leucine and phenylalanine degradation (Ehrlich pathway; green) and folates biosynthesis (light green). Dashed arrows indicate a multi-step pathway, dotted arrows indicate regulatory roles and filled arrow indicates a transport reaction. (E)-2-(MCM)B, (E)-2-8(methoxycarbonylmethyl)butenedioate; DHAP, dihydroxy-acetone-phosphate; GAR, 5'-phosphoribosylglycinamide; GMP, guanosine-5'-phosphate; M-CoA, malonyl-CoA; PRA, 5-P-β-D-ribosyl-amine; Trans-2,3-DA-CoA, Trans-2,3-dehydroacyl-CoA; XMP, xanthosine-5-phosphate. *An*, *Aspergillus niger*; *Bs*, *Bacillus subtilis*; *Mm*, *Mus musculus*.

CHAPTER II

Figure 2.1. Measurement of H_2O_2-mediated oxidative DNA damage in *A. gossypii* ATCC 10895 with the *Ashbya* Comet Assay. **(A)** Data are presented as mean ± standard error of the mean of the tail length of at least forty comets obtained from two independent experiments for each concentration (as described in Materials and methods). Before harvesting, cells were grown for three days at 30 °C on agar-solidified AFM containing different concentrations of H_2O_2 (5, 10 or 25 mM). Asterisks represent significant differences compared to the control (0 mM H_2O_2). * ($p < 0.05$), ** ($p < 0.01$) and *** ($p < 0.001$). **(B)** Representative images of the comets obtained with

the Comet Assay protocol adapted in this work for control cells (0 mm H_2O_2) and cells exposed to 10 mM H_2O_2. DNA was stained with GelRed™. White bar = 50 μm.

Figure 2.2. Exposure to **(A)** menadione (oxidative agent) or **(B)** camptothecin (CPT; non-oxidative agent) induces DNA damage in *A. gossypii* ATCC 10895. Data are presented as mean ± standard error of the mean of the tail length of at least forty comets obtained from two independent experiments for each concentration (as described in Materials and methods). Before harvesting, cells were grown for three days at 30 °C on agar-solidified AFM containing different concentrations of menadione (1, 5 or 10 μM) and CPT (10, 20 or 40 μM). Asterisks represent significant differences compared to the control (0 μM menadione/CPT). * ($p < 0.05$), ** ($p < 0.01$) and **** ($p < 0.0001$).

Figure 2.3. Exposure to light during growth induces DNA damage in the *A. gossypii* riboflavin-overproducing strain A8, but not in strain ATCC 10895. **(A)** Data are presented as mean ± standard error of the mean of the tail length of at least forty comets obtained from two independent experiments for each condition (as described in "Materials and methods"). Before harvesting, cells were grown for three days on agar-solidified AFM at 30 °C, in the dark or exposed to light. Asterisks represent significant differences between strains and conditions. **** ($p < 0.0001$). **(B)** Representative images of the colonies from where cells were harvested for DNA damage measurement with the *Ashbya* Comet Assay.

Figure 2.4. Exposure to light during growth induces intracellular ROS accumulation in the *A. gossypii* riboflavin-overproducing strain A8, but not in strain ATCC 10895. **(A)** Fluorescence intensity of cell suspensions loaded with H_2DCFDA determined by fluorimetry (as described in Material and methods) presented as mean ± standard deviation of two biological replicates. Asterisks represent significant differences between strains and conditions. * ($p < 0.05$) and ** ($p < 0.01$). **(B)** Representative overlaid images (obtained from bright-field and fluorescence microscopy) of *A. gossypii* cell suspensions loaded with H_2DCFDA. White bar = 25 μm. Before harvesting, cells were grown for three days on agar-solidified AFM at 30 °C, in the dark or exposed to light.

CHAPTER III

Figure 3.1. Schematic representation indicating the *de novo* and salvage pathways of pyrimidine ribonucleotides. Red × marks where the *de novo* pyrimidine biosynthetic pathway is blocked in the *A. gossypii Agura3* uracil auxotroph. Dashed arrows indicate a multi-step pathway. UMP: uridine monophosphate; PRPP: phosphoribosyl pyrophosphate. Numbers indicate the enzymes involved in each step of the pyrimidine pathways. 1: nucleosidase/uridine nucleosidase; 2: cytidine deaminase; 3: cytosine deaminase; 4: uridine kinase; 5: uracil phosphoribosyltransferase; 6: orotate phosphoribosyltransferase; 7: orotidine-5'-phospate decarboxylase.

Figure 3.2. Maximum relative growth of *A. gossypii Agura3* on agar-solidified MM supplemented with different concentrations of intermediates from the pyrimidine salvage pathway. The percentage of maximum relative growth was normalized to the radial growth of the best condition tested (5 mM uridine). Data are representative of three biological replicates after 8 days of growth. Letters represent significant differences ($p < 0.05$) between bars with the same supplement concentration.

Figure 3.3. Radial growth curves and colony morphologies of *A. gossypii Agura3* on agar-solidified **(A)** SC or **(B)** AFM supplemented with 5 mM uridine, uracil or cytosine. **(C)** Maximum relative growth and colony morphology of *A. gossypii Agura3* overexpressing the gene Ag*FUR1* on agar-solidified AFM supplemented with 5 mM uridine or uracil. Letters represent significant differences ($p < 0.05$) between bars (supplementation). The control conditions represent media without added supplement. The growth observed in AFM without any added supplement is due to the presence of small quantities of various pyrimidines in the complex constituents of this rich medium. Data represent the average ± standard deviation from three (A and B) or two (C) biological replicates. Where not seen, error bars were smaller than the symbols. Images were recorded after 8 days of growth.

Figure 3.4. Alignment of AgUPRTp with other UPRTs and corresponding phylogenetic tree. **(A)** UPRTp amino acid sequences from *A. gossypii* (Agos, NP_985599), *K. marxianus* (Kmar, XP_022674246), *S. cerevisiae* (Scer, NP_011996), *Y. lipolytica* (Ylip, XP_506088), *D. hansenii* (Dhan, XP_002770455), *P. guilliermondii* (Pgui, XP_001482408), *L. donovani* (Ldon, XP_003864273) and *T. gondii* (Tgon, XP_002364470). Four conserved regions from human to prokaryotes are shaded in grey (Li et al., 2007). The residues that constitute a β-arm, a flex-loop

and the PRPP and uracil binding sites identified previously (Schumacher et al., 1998) are marked with black lines. Boxed residues represent positions where mutations were reported to increase resistance to 5-Flucytosine or 5-Fluorouracil. Asterisks (*) represent fully conserved residues, colons (:) represent residues with strongly similar properties and periods (.) represent residues with weakly similar properties. **(B)** Phylogenetic tree resultant from the alignment performed by ClustalO, which was drawn with FigTree v1.4.3. Indicated values represent the percentage of sequence identity to AgUPRTp.

Figure 3.5. SDS-PAGE analyses of the **(A)** production and **(B)** purification of AgUPRTp from *E. coli*. Lane 1, crude extract of cells producing AgUPRTp fusion with TrxA (TrxA-AgUPRTp); Lanes 2, molecular weight marker; Lane 3, supernatant containing the soluble protein fraction after lysis of the TrxA-AgUPRTp producing cells; Lane 4, AgUPRTp cleaved and purified from TrxA-AgUPRTp.

Figure 3.6. AgUPRTp activity at varying concentrations of uracil and PRPP. Specific AgUPRTp activity was determined spectrophotometrically as a function of uracil concentration in the presence of **(A)** 1 mM PRPP, and as a function of PRPP concentration in the presence of **(B)** 0.5 mM uracil concentration. Data represent average ± standard deviation from three experimental replicates.

Figure 3.7. Effect of increasing uracil concentrations on AgUPRTp activity. AgUPRTp activity was determined spectrophotometrically at a set-saturating PRPP concentration (1 mM) and represented as percentage of the maximum activity. Data represent average ± standard deviation from three experimental replicates. Asterisks represent significant differences (* $p < 0.05$; ** $p < 0.01$) compared to the maximum activity.

CHAPTER IV

Figure 4.1. Schematic representation of the *de novo* biosynthetic pathway of pyrimidines in *A. gossypii*. Red × marks where the *de novo* pyrimidine biosynthetic pathway is blocked in the *A. gossypii Agura3* auxotroph. Dashed arrows indicate a multi-step pathway. Relevant gene names are represented in italic and bold. Acronyms near the gene names represent the corresponding enzyme: DHOD, dihydroorotate dehydrogenase; O-5'PD, orotidine-5'-phosphate decarboxylase. UMP: uridine monophosphate.

Figure 4.2. Engineering strategy and integration cassette used for the overexpression of *AgGUP1*.

Figure 4.3. Time-course quantification of the orotic acid produced and excreted by *A. gossypii Agura3* during growth at 28 °C and 200 rpm in AFM (20 g/L glucose) or AFM-glycerol (20 g/L glycerol). Cultivations were stopped when the concentration of orotic acid stabilized. Data represent average values and standard deviations of biological duplicates. Where not seen, error bars were smaller than the symbols.

Figure 4.4. Orotic acid production and glycerol consumption by *A. gossypii Agura3* and *A. gossypii Agura3*_GUP1 in AFM-glycerol **(A)** without $CaCO_3$ and **(B)** with $CaCO_3$ (2 g/L). *A. gossypii Agura3* is represented by circles (●) and *A. gossypii Agura3*_GUP1 by squares (■). Filled symbols represent orotic acid and empty symbols glycerol. Strains were grown for 8 days at 28 °C and 200 rpm. Data represent average values and standard deviations of biological duplicates. Where not seen, error bars were smaller than the symbols.

Figure 4.5. **(A)** Radial growth of *A. gossypii* strains on agar-solidified AFM with 1 M KCl. Strains were grown for 7 days at 30 °C. The small graphic represents the same data but with smaller scale of the vertical axis to allow a better comparison. **(B)** Relative radial growth (%) of strains overexpressing *AgGUP1* (ATCC_GUP1 and *Agura3*_GUP1). Relative growth was obtained by calculating the ratio between the final radial growth of each strain in 1 M KCl and in the AFM without KCl. Data represent average values and standard deviations. Where not seen, error bars were smaller than the symbols.

Figure 4.6. Performance of *A. gossypii Agura3*_GUP1 during a controlled bioreactor fermentation using AFM (20 g/L glucose). **(A)** Orotic acid and biomass production (CDW) and **(B)** pH and dissolved oxygen concentration (pO2) profiles during 3 days (72 h) of culture at 30 °C using 300 rpm of agitation and 2 vvm of aeration.

Figure 4.7. Effect of aeration on orotic acid production by *A. gossypii Agura3*_GUP1 during shake-flask fermentation in AFM-glycerol (40 g/L glycerol). Superior levels of aeration were achieved by increasing the headspace in shake-flasks (to a ratio of 1:10) through reduction of the working volume of the medium (25 mL in shake-flasks of 250 mL) or by using a shake-flask with higher capacity (50 mL in shake-flasks of 500 mL). The control condition consisted in 50 mL of working volume in shake-flaks of 250 mL (ratio of 1:5). Strains were grown at 28 °C and 200 rpm. Data represent average values and standard deviations of biological duplicates. Where not seen, error bars were smaller than the symbols.

Figure 4.8. **(A)** Orotic acid production and **(B)** carbon source consumption by *Agura3*_GUP1 in shake-flask fermentations using crude glycerol (GLY_{CR}; ~2.5 % v/v) or sugarcane molasses (SM; ~2.5 % w/v) as main carbon source. Fermentations were carried out at 28 °C and 200 rpm in 250 mL shake-flasks containing 25 mL medium. The percentages (%) indicated for RYE, CSL are expressed in w/v. All medium formulations were buffered with 2 g/L $CaCO_3$. Data represent average values and standard deviations of biological duplicates. Where not seen, error bars were smaller than the symbols.

CHAPTER V

Figure 5.1. Metabolic engineering of the *de novo* biosynthesis of lactones in *A. gossypii*. **(A)** Schematic diagram of the interconnection between the metabolic pathways involved in the *de novo* biosynthesis of lactones. An $acyl_{n-2}$-CoA represents a fatty acid from which two carbons of the initial chain length were removed after 1 cycle of β-oxidation. **(B)** Heterologous overexpression cassette constructed using the Golden-Gate rapid assembly. Grey-circled names represent the genes targeted for engineering. Dashed lines represent multi-reactions. Abbreviations used: M-CoA, malonyl-CoA; trans-2,3-DA-Coa, trans-2,3-dehydroacyl-CoA.

Figure 5.2. Quantitative and qualitative VOCs profiling by GC-MS of *A. gossypii* strains. **(A)** Total VOCs production. **(B)** Distribution of the VOCs produced by families of aromas according to their chemical structure and their relative presence in each strain. The *S. cerevisiae* CEN.PK113-7D (CEN.PK) and *Y. lipolytica* W29 were used as controls to help evaluate which VOCs were distinctively produced by *A. gossypii*. Cultures were carried out in MA2 medium for 48 h. Data are presented as mean ± standard deviation of at least two biological replicates.

Figure 5.3. Specific productions (μg/g_{CDW}) of the seven chemically different γ-lactones identified in cultures of *A. gossypii*. **(A)** Production levels of the minor γ-lactones identified. **(B)** Production levels of the major γ-lactone identified, γ-decalactone. Data are presented as mean ± standard deviation of at least two biological replicates.

Figure 5.4. Improved biosynthesis of γ-lactones by engineered *A. gossypii* strains. **(A)** Volumetric (μg/L) and **(B)** specific (μg/g_{CDW}) production of total γ-lactones. Data are presented as mean ± standard deviation of three biological replicates. Cultures were carried out in AFM for 72 h. Asterisks represent significant differences to the control (ATCC). **($p < 0.01$), ***($p < 0.001$) and ****($p < 0.0001$).

CHAPTER VI

Figure 6.1. Graphical schematic representation of the contributions of this thesis for the development of *A. gossypii* as a cell factory. The biotechnological applications identified and explored here are shown in white. The scientific and technical approaches most applied during this thesis are written in bold in the closing circle.

APPENDIX

Figure A2.1 Representative image of the microscopic field obstructed with *A. gossypii* spores, which if not removed by using paraffin, impeded the visualization of the comets and consequently the comet assay protocol adapted in this work.

Figure A2.2. Measurement of H_2O_2-induced DNA damage in *A. gossypii* ATCC10895. Data are presented as mean ± standard error of the mean of the % DNA tail of at least forty comets obtained from two independent experiments for each concentration of H_2O_2 (5, 10 or 25 mM). Experimental procedure is described in the Materials and methods section of Chapter II. Statistical differences were tested by one-way ANOVA followed by post-hoc Dunnett's multiple comparison tests. Asterisks represent significant differences compared to the control (0 mM H_2O_2). ** ($p < 0.01$), *** ($p < 0.001$) and **** ($p < 0.0001$).

Figure A2.3. Exposure to **(A)** menadione or **(B)** camptothecin (CPT; non-oxidative agent) induces DNA damage in *A. gossypii* ATCC10895. Data are presented as mean ± standard error of the mean of the % DNA tail of at least forty comets obtained from two independent experiments for each concentration of menadione (1, 5 or 10 μM) and CPT (10, 20 or 40 μM). Experimental procedure is described in the Materials and methods section of Chapter II. Statistical differences were tested by one-way ANOVA followed by post-hoc Dunnett's multiple comparison tests. Asterisks represent significant differences compared to the control (0 μM menadione/CPT).* ($p < 0.05$), ** ($p < 0.01$) and **** ($p < 0.0001$).

Figure A3.1. Radial growth curve and colony morphology of *A. gossypii* ATCC10895 at 30 °C on agar-solidified SC supplemented with 5 mM of uracil. The control condition represents medium without any added supplement. Data represent the average ± standard deviation from three biological replicates. Where not seen, error bars were smaller than the symbol. Images were recorded after 4 days of growth. Previously, we observed that the addition of uracil to SC medium negatively affected the growth of *A. gossypii* ATCC 10895, the parental strain of the *Agura3* mutant (Silva et al., 2015; see section "3.5 References"). However, during this study we realized that happened due to inadequate buffering of the medium pH, which after addition of a basic uracil stock solution increased to values that impair the growth of *A. gossypii* ATCC 10895. With this medium pH issue overcome, here we show that the growth and morphology of *A. gossypii* ATCC 10895 on SC medium is not affected by the presence of 5 mM uracil or cytosine. In fact, concentrations of uracil up to 10 mM did not affect the phenotype of this strain (data not shown). Therefore, the phenotypic traits displayed by the *A. gossypii Agura3* on uracil-supplemented media are exclusive of this mutant.

Figure A3.2. DNA damage was assessed by the *Ashbya* Comet Assay (single cell gel electrophoresis) in cells exposed to 5 mM uracil during 7 days of growth on solid SC medium. Control condition represents medium without uracil. Data are presented as mean ± standard error of the mean of the tail length of 50 comets analysed by condition. Experimental procedure applied for the Comet Assay is described in the "2.2 Materials and methods" section of Chapter II.

Figure A3.3. Growth curve (OD_{600nm}) of pyrimidine auxotrophic **(A)** *S. cerevisiae* CEN.PK113-5D, **(B)** *K. marxianus* KMS2 and **(C)** *Y. lipolytica* Po1f in liquid SC medium supplemented with

different concentrations of uracil or uridine. Control condition represents medium without any added supplement. Data represent average ± standard deviation from three biological replicates. Where not seen, error bars were smaller than the symbol. Growths were performed in 24-well microplates containing 1 mL of medium at 30 °C and 200 rpm. The inoculum was defined to an initial OD_{600nm} of 0.1 from an overnight pre-inoculum in YPD (10 g/L yeast extract, 20 g/L peptone, 20 g/L glucose). The optical density at 600 nm was measured using a Synergy Mx / Cytation 3 microplate reader (Biotek) at the indicate time points.

Figure A3.4. SDS-PAGE analyses of the production AgUPRTp from *E. coli* without any fusion partner. Lane 1, insoluble fraction; Lane 2, soluble fraction; Lane 3, molecular weight marker; Lane 4, whole protein content of non-induced cells. Both insoluble and soluble fractions were obtained after lysis of cells producing AgUPRTp.

Figure A4.1. Confirmation of correct genomic integration of *AgGUP1* overexpression cassette upstream the initiator codon of *AgGUP1*. Expected size of amplification using primers annealing outside the overexpression cassette integration (AgGUP1p-fw) and within the *KanMX4* selection marker (kanB-rv) of the cassette: 378 bp. Lane M, molecular weight marker; Lane 1, ATCC 10895 (WT); Lane 2, ATCC_GUP1; Lane 3, *Agura3*_GUP1.

Figure A5.1. Confirmation of genotypes by analytical PCR. **(A)** Confirmation of correct genomic integration of *YlPOX2* overexpression cassette in the *AgPOX1* locus of 4 independent clones (strain DES589/elo624Δ/YlPOX2). Expected size of amplification using primers annealing outside the overexpression cassette (Pox1a3-fw) and within the *KanMX4* selection marker (kanB-rv) of the cassette: 908 bp. Lane M, molecular weight marker. The correct integration of deletion cassette of *AgELO624* gene cannot be shown since no digital image was possible to get from the equipment used. **(B)** Confirmation of homokaryotic genotype of each strain. Lane M, molecular weight marker; Lane 1, ATCC 10895 (WT); Lane 2, YlPOX2; Lane 3, DES589/elo624Δ/YlPOX2; Lane 4, DES589/ Lane elo624Δ. Expected size (Pox1a3-fw & -rv) for ATCC 10895 genotype: 894 bp. Expected size (elo624-fw & -rv) for ATCC 10895 genotype: 601 pb. Absence of WT genotypes confirms homokaryotic genotype of engineered strains.

Figure A5.2. Specific productions (μg/gCDW) of the two major higher alcohols identified in cultures of non-engineered *A. gossypii* strains. Production levels of **(A)** 2-phenylethanol and **(B)** isoamyl alcohol. Data are presented as mean ± standard deviation of at least two biological replicates.

Figure A5.3. Comparison of the amino acid sequence of *A. gossypii* AgDes589p with other fatty acid desaturases, hydroxylases and bifunctional desaturase/hydroxylases. Asterisks (*) represent conserved residues, colons (:) represent residues with strong similar properties and periods (.) represent residues with weak similar properties. The amino acid residues that differ between oleate desaturases and hydroxylases are indicated in boxes. Red boxes represent the two important amino acids residues for the catalytic activity that are conserved between AgDes589p and hydroxylases or bifunctional enzymes. Accession numbers for the sequences are: *F.* x *ananassa* desaturase FaFAD1p (KF887973), *Y. lipolytica* YlYALI0B10153p (XP_500707.1), *A. thaliana* AtFAD2p (AAA32782), *R. comunis* hydroxlase RcFAH12 (AAC49010), (MDP0000288297) and *L. fendleri* bifunctional desaturase/hydroxylase LfAH12 (AAC32755).

LIST OF TABLES

CHAPTER I

Table 1.1. Random engineering approaches applied in *A. gossypii* for biotechnological purposes.

Table 1.2. Target genes of rational genetic engineering strategies in *A. gossypii* for different biotechnological applications.

Table 1.3. Production levels and approaches taken for emerging biotechnological applications in *A. gossypii*. Comparisons with other microorganisms are also presented. The term "engineered" refers to strains target of a rational approach, while "mutants" were obtained randomly.

CHAPTER II

Table 2.1. Colony radial growth of *A. gossypii* ATCC 10895 after three days of growth at 30 °C on agar-solidified AFM containing different concentrations of H_2O_2. Data are presented as mean ± standard deviation of three biological replicates. Superscript letters represent significant differences compared to the control (0 mM H_2O_2).

Table 2.2. Colony radial growth and specific riboflavin production for the *A. gossypii* strains ATCC 10895 and A8, measured after three days of growth on agar-solidified AFM at 30 °C, in the dark or exposed to light. Data are presented as mean ± standard deviation of at least five biological replicates. Superscript letters represent significant differences between specific riboflavin productions by the same strain under different conditions.

CHAPTER III

Table 3.1. Maximum radial growth rates and lag phases of *A. gossypii Agura3* on agar-solidified MM supplemented with different concentrations of intermediates from the pyrimidine salvage pathway. Data are representative of three biological replicates. Radial growth rates are expressed as mean ± standard deviation. Superscripts represent significant differences ($p < 0.05$) between values of the same column (supplement concentration).

CHAPTER IV

Table 4.1. *A. gossypii* strains and primers used in this work. Lower case sequences correspond to homologous recombination sites.

CHAPTER V

Table 5.1. *A. gossypii* strains used and generated in this work.

Table 5.2. MS fragmentation pattern for each γ-lactone. Numbers between brackets represent percentages of m/z ions.

Table 5.3. Specific production (μg/g_{CDW}) of different γ-lactones by engineered *A. gossypii* strains. Underlined values represent the percentage (%) of γ-decalactone regarding the total γ-lactones produced by different high-producing engineered strains. Data are presented as mean ± standard deviation of three biological replicates. Superscript letters represent significant differences to the control (ATCC) between values of the same column. Superscript letters of underlined values represent significant differences between relative productions. a,b ($p < 0.05$), a,c ($p < 0.01$), a,d ($p < 0.001$) and a,e ($p < 0.0001$).

APPENDIX

Table A2.1. Colony radial growth of *A. gossypii* ATCC10895 after three days of growth at 30 °C on agar-solidified AFM containing different concentrations of menadione or CPT. Data are presented as mean ± standard deviation of three biological replicates.

Table A5.1. Primers used in this work. Lower case sequences correspond to homologous recombination sites. Recognition sequences for restriction enzymes are underlined.

Table A5.2. Lactones produced by *A. gossypii* non-enginereed strains above their odour perception threshold. Values of the thresholds either in complex (*e.g.*, wine) or simple (*e.g.*, aqueous solutions) samples were retrieved from the literature (Coelho et al., 2015; Jackson et al., 2009). Data are presented as mean of at least two biological replicates. (–), not detected or detected at concentrations below the odour perception threshold of the compound.

LIST OF ABBREVIATIONS AND ACRONYMS

(E)-2-(MCM)B	(E)-2-8(methoxycarbonylmethyl)butenedioate
5-FC	5-flucytosine
5-FU	5-fluorouracil
AFM	*Ashbya* Full Medium
AMP	Adenosine monophosphate
ARS	Autonomous replicating sequences
bp	Base pairs
CPT	Camptothecin
CSL	Corn steep liquor
CDW	Cell dry weight
DBTL	Design, Build, Test and Learn
DHAP	Dihydroxy-acetone-phosphate
DHOD	Dihydroorotate dehydrogenase
EMS	Methane sulfonate
EU	European Union
EUR	Euro
FA	Fatty acids
FAD	Flavin adenine dinucleotide
FMN	Flavin mononucleotide and
G418	Geneticin
GAR	5'-phosphoribosylglycinamide
GC–MS	Gas chromatography–mass spectrometry
GLYcr	Crude glycerol
GMP	Guanosine-5'-phosphate
GTP	Guanosine-5-triphosphate
H_2DCFDA	2',7'-dichlorofluorescein diacetate
HPLC	High-Performance Liquid Chromatography
LVLV	Large-volume, low-value chemicals
LVHV	Low-volume, high-value chemicals
MAP	Mitogen-activated protein
M-CoA	Malonyl-CoA
MM	Minimal medium
MNNG	N-methyl-N'-nitro-N-nitrosoguanidine ethyl

NOHBY	No homolog in Baker's yeast
O-5'PD	Orotidine-5'-phosphate
ORF	Open reading frame
PCR	Polymerase Chain Reaction
PKA	Protein kinase A
PRA	5-P-β-D-ribosyl-amine
PRPP	Phosphoribosyl pyrophosphate
PUFAs	Polyunsaturated fatty acids
Ribulose 5-P	Ribulose 5-phosphate
ROS	Reactive oxygen species
RYE	Raw yeast extract
SC	Synthetic complete
SCO	Single cell oil
SM	Sugarcane molasses
Trans-2,3-DA-Coa	Trans-2,3-dehydroacyl-CoA
TCA	Tricarboxylic acid
TrxA	Thioredoxin A
TYR	Titers, yields and rates
UHPLC	Ultra high-performance liquid chromatography
UMP	Uridine monophosphate
UPRT	Uracil phosphoribosyltransferase
US	United States of America
UV	Ultraviolet
VOCs	Volatile organic compounds
VVM	Volumes of air per volume of liquid per minute
WGD	Whole genome duplication
XMP	Xanthosine-5-phosphate
YPD	Yeast extract-peptone-glucose

MOTIVATION AND OUTLINE OF THE THESIS

Motivation

Ashbya gossypii is an industrial filamentous fungus used for riboflavin production for almost 30 years. Despite this process was considered a paradigm of the industrial biotechnology, until the beginning of the present decade, the relevance of this fungus within the sector was confined to this application. However, since then, its metabolism (*e.g.*, biosynthesis of lipids, nucleosides and flavours) has attracted some attention, resulting in some well-designed proof of concept studies of yet unexplored biotechnological potential. The expansion of the catalogue of chemicals produced by *A. gossypii*, as well as the generation of platform/chassis strains are essential to fulfil the requisites of a cell factory envisaged for industrial biotechnology. However, much remains to be addressed in order to achieve these goals, namely the systematic exploration of this fungus natural metabolism through well defined principles.

The recent advancements in the biotechnology of *A. gossypii* were possible due to the accumulated physiological and molecular data gathered throughout years of fundamental and applied research, which intriguingly were rarely crossed with each other. This positioned *A. gossypii* in the intersection between those considered to be industrial microbial models (*e.g.*, *Saccharomyces cerevisiae*) and non-conventional microorganisms. Thus, making the most out of the *A. gossypii*'s natural metabolism deserves to be the effective future path for cell design. Identification of novel target compounds should not be solely based on their commercial value, but rather focused on the exploration of final/precursor compounds for which the chassis strain already demonstrates innate biosynthetic potential. In addition, the optimization of the biosynthesis of selected high-value chemicals should be combined with the exploration of more sustainable feedstocks for their production. In doing so, one must keep in mind that the use of metabolic engineering approaches to improve the production of these compounds will be dependent on the fungus metabolic and physiologic regulation, which needs to be continuously characterized throughout the repertoire of strains available, either non-engineered or engineered.

Therefore, the purpose of this thesis is to contribute for the development of *A. gossypii* as an alternative cell factory, helping to close the gap between this fungus and industrial models by identifying novel biotechnological applications that fit within the potentialities of its metabolism. To achieve this goal this thesis focused on the physiological and molecular characterization of different *A. gossypii* strains.

Outline of the thesis

The thesis presented herein reports the main outcomes obtained from research undertaken at CEB – Centre of Biological Engineering, University of Minho (Braga, Portugal) under the supervision of Professor Lucília Domingues and Doctor Tatiana Q. Aguiar.

This thesis is organized into the following chapters:

Chapter I starts by defining the importance of microbial cell factories within the industrial biotechnology and, after presenting a global and comprehensive perspective of *A. gossypii* briefly establishes the standpoint of this fungus as a cell factory.

Chapter II discloses the effects to which *A. gossypii* riboflavin-overproducing cells are exposed to during growth under sun-mimicking light conditions. The adaptation of a Comet Assay protocol for measuring DNA damage under these conditions is also presented. Professor Rui Oliveira (CEB/CITAB — Centre for the Research and Technology of Agro-Environmental and Biological Sciences, University of Minho) participated in the adaptation of the Comet Assay protocol.

Chapter III addresses the physiological characterization of an *A. gossypii* pyrimidine auxotroph, which presents hypersensitivity to uracil, and the identification of the molecular cause for this unusual phenotype. Doctor Carla Oliveira (CEB, University of Minho) performed the production and purification of the recombinant AgUPRTp.

In **Chapter IV**, the same *A. gossypii* pyrimidine auxotroph studied in the previous chapter is identified as a suitable chassis strain for the production of orotic acid, a high-value chemical produced from the *de novo* pyrimidine biosynthetic pathway. Furthermore, an engineering strategy designed to improve the capacity of this strain to utilize a biodiesel industrial by-product (glycerol) is presented.

Chapter V describes the deciphering of the *de novo* biosynthesis of γ-lactones in *A. gossypii* by means of metabolic engineering and presents this fungus as a promising microbial host for the production of these fragrances. Part of the engineered strains presented in this study were constructed by the author during a period abroad at the Department of Microbiology and Genetics, University of Salamanca (Salamanca, Spain). Professor Alberto Jiménez and Professor

José Luis Revuelta (University of Salamanca) participated in the construction of strains. Eduardo Coelho (CEB, University of Minho) performed the volatiles extraction and GC-MS analyses.

Finally, **Chapter VI** presents the main conclusions, specifying the contributions of this thesis for the development of *A. gossypii* as a cell factory and some future perspectives.

CHAPTER I

General introduction

This chapter is partially based on the following publications:

Aguiar TQ*, Silva R*, Domingues L. *Ashbya gossypii* beyond industrial riboflavin production: a historical perspective and emerging biotechnological applications. Biotechnol Adv 2015;33:1774–86. *Equal contributions.

Aguiar TQ, Silva R, Domingues L. New biotechnological applications for *Ashbya gossypii*: Challenges and perspectives. Bioengineered 2017;8:309–15.

1.1 Industrial Biotechnology: a global overview

In 2012, the National Bioeconomy Blueprint developed by the United States (US) administration stated that the bioeconomy was all around us, redefining the sector as the "one based on the use of research and innovation in the biological sciences to create economic activity and public benefit" (Connelly et al., 2015). In the same year, the European Union (EU) in its Strategy and Action Plan stated a similar, but more specific, definition: "production of biological resources and the conversion of these resources and waste streams into value added products such as food, feed, bio-based products and bio-energy" (Nattrass et al., 2016). Although some economic data is still difficult to obtain, since established companies have their headquarters and manufacturing facilities geographically spanned, it is clear that we are talking about a relevant, continuously growing sector that, in 2017, accounted for EUR 122.4 thousand million in revenues worldwide (Ernst & Young, 2017). Moreover, the Biotech market witnessed the greatest five-year bull run between 2011–2015 (Booth, 2016), finally revealing signs of maturation after 40 years as a sector and outperforming leading indexes such as the S&P 500 (which represents the 500 major US publicly traded companies). In general, estimations set that bio-based products already represent more than 5–10 % of the whole chemical market. The US are the leading player of the sector, representing EUR 98.4 thousand million in revenues (4 % annual growth rate; data from 2017), obtained by 449 companies traded in public market exchanges. In turn, the EU biotech industry accounts for 259 public companies, which presented an overall revenue of EUR 23.7 thousand million in 2017 (19 % annual growth rate) (Ernst & Young, 2017). To support the thriving of the bioeconomy, government strategic funding has been significant, ascending to EUR 505 million in the US (without period description) and to EUR 3.6 billion in the EU (2014–2024) (Nattrass et al., 2016). Besides the UE and the US, which have dedicated bioeconomy strategies, other relevant players of the sector include China, Canada, Brazil, Malaysia and more recently Japan (Ernst & Young, 2017; Nattrass et al., 2016). Despite all the geopolitical complexities (*e.g.*, Brexit) and controversies around the sector (*e.g.*, CRISPR twins; Cyranoski and Ledford, 2018) faced at the moment, biotechnology companies continue to strongly invest in the sector, even when it is forecasted the next global economic and financial contraction.

Footnote to the reader: All the values presented were converted from USD to EUR on 27th February 2019 using the Converter from Banco de Portugal (https://www.bportugal.pt/en/conversor-moeda). The conversion rate at the time was 1 EUR = 1.13860 USD.

1.1.1 Microbial cell factories: a core element within the sector

Within the bioeconomy, industrial biotechnology (*syn.* white biotechnology) regards the use of biology (*e.g.*, cells and enzymes) for the production of chemicals for industrial and consumer use, which excludes health (*e.g.*, gene therapies) and agricultural (*e.g*, genetically modified crops) applications (Connelly et al., 2015). The type of products obtained can be categorized in two different ways: large-volume, low-value chemicals (LVLV, bulk or commodity chemicals) or low-volume, high-value chemicals (LVHV, specialty chemicals). For instance, the first category includes biofuels and polymer intermediates, while the second comprises pharmaceuticals and fragrances. The manufacturing of chemicals was the foundation of the industrial development and the main driving force for economic growth, which since the beginning of the 20th century has been leveraged on the understanding of crude oil and its chemistry (Connelly et al., 2015). However, the world needs to reduce its dependency on crude oil, not only because it is a non-renewable resource connected to severe environmental problems, such as climate change, as its global reserves are forecasted to be insufficient to fulfil the future needs of a continuously growing world population.

Industrial biotechnology offers the possibility to produce chemicals through the establishment of biorefineries in a more sustainable way than petrochemical refineries. Taking advantage of the high specificity and selectivity of biological systems, it enables the production of new molecules that were unfeasible to obtain using traditional chemical synthesis. Moreover, it also allows the production of complex chemicals that are normally found in nature only in small quantities and mainly in plants. The extraction and isolation of such molecules from the source are connected to environmental problems, mostly related to severe harvesting, and to economic concerns derived from the fact that cultivation yields are climate-dependent, which leads to price fluctuations of the final product. On the other hand, chemical synthesis does not present itself as a viable alternative, as the high complexity of these molecules requires an operational process with numerous steps (Tippmann et al., 2013).

Currently, industrial biotechnology represents an estimated production of about 50 million tons of bio-based chemicals each year (Connelly et al., 2015). It was forecasted that until 2025 at least 20 % of the petrochemical products can be replaced by biotechnological products (Connelly et al., 2015). This switch holds the advantages of reducing the greenhouse gas emission, increasing the production speed and boosting the innovation potential. Indeed, more optimistic predictions exist, since in Denmark about 40 % of the bio-based chemical manufacturing is already

obtained with a cell factory (Connelly et al., 2015). However, it is accepted that biotechnological processes should be placed as a complement to chemical synthesis, and not as a vehicle to abolish it. Thus, it is essential to direct concerted efforts between scientific disciplines like synthetic chemistry, metabolic engineering, synthetic biology and process engineering so that in the future the combination of biology and traditional chemistry gives rise to more successful cases, such as the semi-synthetic drug artemisinin (Paddon and Keasling, 2014).

The current relentless pace of scientific and technological revolution, which for instance consent DNA reading and synthesis to be faster and cheaper, feeds the expectation of having an increasingly higher number of biotechnological processes reaching the market, and thus fulfilling the purposes of the white biotechnology. To achieve that, the committee on Industrialization of Biology, created by request of the US Department of Energy and the National Science Foundation, identified six core categories in which fundamental and applied research should invest in order to boost the establishment of industrial biotechnology over petrochemical manufacturing (Connelly et al., 2015). These areas are: i) feedstocks and pre-processing; ii) fermentation and processing; iii) organism: chassis; iv) organism: pathway; v) design toolchain; and vi) test and measurement. Among them, feedstocks and fermentation assets are the categories that have the highest impact on the overall cost of the bioprocess. Therefore, it is crucial to identify new feedstocks (*e.g.*, C1 carbon sources) and to fully use those already explored, such as industrial wastes (*e.g.*, crude glycerol) and lignocellulosic biomass. In turn, fermentation technologies should guarantee ideal conditions for high titers, yields and rates (TYR) through new modes of operation (continuous fermentation vs batch fermentation). However, regarding the TYR, it is consensual that the microbial chassis is the key determinant for the economic competitiveness of white biotechnology processes, either for commodity or specialty chemicals production (Connelly et al., 2015; Nielsen and Keasling, 2016). Although it is possible to implement cell-free systems, to date, the advancements in this area are still very short. Moreover, synthesis of complex chemical structures as well as operations for their production at large-scale were not yet demonstrated. Therefore, microbial fermentation is the main alternative bioprocess chosen to complement the dominant petrochemical industry, and consequently, microorganisms are the core assets of industrial biotechnology.

1.1.2 Industrial models vs non-conventional microbial hosts

Finding and developing the best microbial hosts for the production of a myriad of

compounds, from fuels to pharmaceuticals, is of critical importance. Unlike recombinant proteins, commodity and specialty chemicals require several genes and, in most cases, even different metabolic pathways for their biosynthesis. Since microorganisms have evolved to grow and survive using efficiently the specific resources of their niches (Goddard and Greig, 2015), which are not comparable to those found in industrial processes, industrial microbes for biotechnological applications have certainly to be engineered (Alper and Stephanopoulos, 2009; Connelly et al., 2015; Czajka et al., 2017). For every metabolic engineering approach, the iterative DBTL (Design, Build, Test and Learn) cycle is applied, where after the tailoring of the metabolism is planed and executed, the phenotypes of the engineered strain are tested and evaluated. However, there have been two distinct philosophies for choosing and developing industrial microbial hosts: engineering microbial models (such as *Escherichia coli* and *Saccharomyces cerevisiae*) or improving the innate metabolic potential of non-conventional microorganisms (Alper and Stephanopoulos, 2009; Czajka et al., 2017).

Microbial models are easily controlled in laboratorial conditions and are characterized in detail at the physiological and molecular level. Moreover, significant molecular and *in silico* toolboxes are available for their engineering and it is straightforward to obtain approval for a bioproduct using a host that was already approved for other industrial use. Thus, it is easy to construct platform strains with enriched cellular pools of precursor metabolites (*e.g.*, acetyl-CoA), which can be used as a starting point for the production of several commercial chemicals. On the other hand, non-conventional microorganisms present natural metabolic and physiological abilities to produce several chemicals and are able to use unusual substrates. Therefore, they naturally present a chassis more prone to a specific application. Thus, despite the numerous proof of concept studies performed with microbial models, only few commercial cases can be reported (Nielsen and Keasling, 2016). On the other hand, many commercial production bioprocesses of chemicals are based on non-conventional microorganisms with optimized innate metabolic potential (Czajka et al., 2017). As practice, these non-conventional microorganisms have also been used as bioprospecting archetypes, where the factors conferring the favourable phenotype are evaluated and identified before their genetic determinants are transferred to a microbial model chassis (Adrio and Demain, 2010).

As mentioned above, the reasons why the microbial models are so extensively used are the broad list of genetic tools available for their engineering, together with all the fundamental knowledge gathered about them. However, these microbial chassis will not be the most appropriate

for all compounds, since the metabolic and physiological requirements for their production are very divergent. In addition, while native pathways and subsequent phenotypes are generally the result of adaptive evolutions faced by the microbial host in its niche (Goddard and Greig, 2015), introduction of complete heterologous pathways may lead to severe bottlenecks due to the hosts' metabolic regulations and underground metabolism, especially under suboptimal conditions (Czajka et al., 2017; Rosenberg and Commichau, 2019). Therefore, the committee on Industrialization of Biology (Connelly et al., 2015) highlighted the importance of "expanding the palette of domesticated microbial [...] platforms", by strongly investing in fundamental science and in the development of technologies for microorganisms other than the established models. Furthermore, they set as a goal that until 2022 the field should have the ability to domesticate any microbial type.

In the intersection of these two philosophies (microbial models vs non-conventional microorganisms) there are microorganisms that, due to the interest that their natural abilities arouse several years ago, have been doing an approximation towards the genetic toolbox and the fundamental knowledge presented by industrial models. *Ashbya gossypii* (*syn. Eremothecium gossypii*) is a filamentous fungus in which the scientific community has put its interest on due to two main traits: (i) its tremendous natural ability to overproduce riboflavin (vitamin B_2) and (ii) the incredible high degree of homology and synteny that its genome shares with that of the baker's yeast *S. cerevisiae* (Dietrich et al., 2004). Indeed, *A. gossipii* has been industrially exploited for riboflavin production by the chemical company BASF (Germany) since 1990. Nonetheless, much still need to be done regarding the exploration of its natural potential in order to bring *A. gossypii* closer to industrial models.

1.2 *Ashbya gossypii*

The filamentous hemiascomycete *A. gossypii* has recently emerged as a microorganism with attractive potential to be an alternative cell factory for the production of yet unexplored high-value products. Industrially exploited almost for 30 years due to its natural ability to overproduce riboflavin, *A. gossypii* is considered a remarkable example of the sustainable white biotechnology business model (Kato and Park, 2012; Lim et al., 2001; Stahmann et al., 2000; zu Berstenhorst et al., 2009). Nevertheless, the scientific prominence of *A. gossypii* is not limited to its biotechnological potential, since it is also extensively used as a model organism in fungal developmental and evolutionary biology studies (Perez-Nadales et al., 2014; Schmitz and Philippsen, 2011; Wendland and Walther, 2005). Its industrial relevance and the basic knowledge accumulated along the years promoted the development of molecular and *in silico* tools that, in turn, have allowed the continuous engineering of *A. gossypii* strains with improved riboflavin production traits, either through random or rational approaches.

The overwhelming capacity of *A. gossypii* to produce riboflavin will and should continue to be targeted for optimization, even more with the advent of systems biology and synthetic biology. However, since the beginning of this decade, we have witnessed the increasingly stronger shift of the *A. gossypii* biotechnological paradigm from riboflavin to other commercially interesting high-value compounds, such as recombinant proteins (Ribeiro et al., 2010), single cell oil (SCO; Ledesma-Amaro et al., 2014a) and fatty-acids (Lozano-Martínez et al., 2016), flavour compounds (Ravasio et al., 2014; Ledesma-Amaro et al., 2015a) and folates (Serrano-Amatriain et al., 2016). In this section, the emerging biotechnological potential of this promising cell factory that nowadays goes far beyond riboflavin production (Figure 1.1) will be comprehensively described. However, first, a global perspective over this fungus will be presented, highlighting its relevant genetic, metabolic and physiological traits, together with the molecular toolbox established and available for *A. gossypii* engineering. To conclude, future challenges and directions that should be taken in order to guide these and other emerging biotechnological applications through the successful track of riboflavin production are identified.

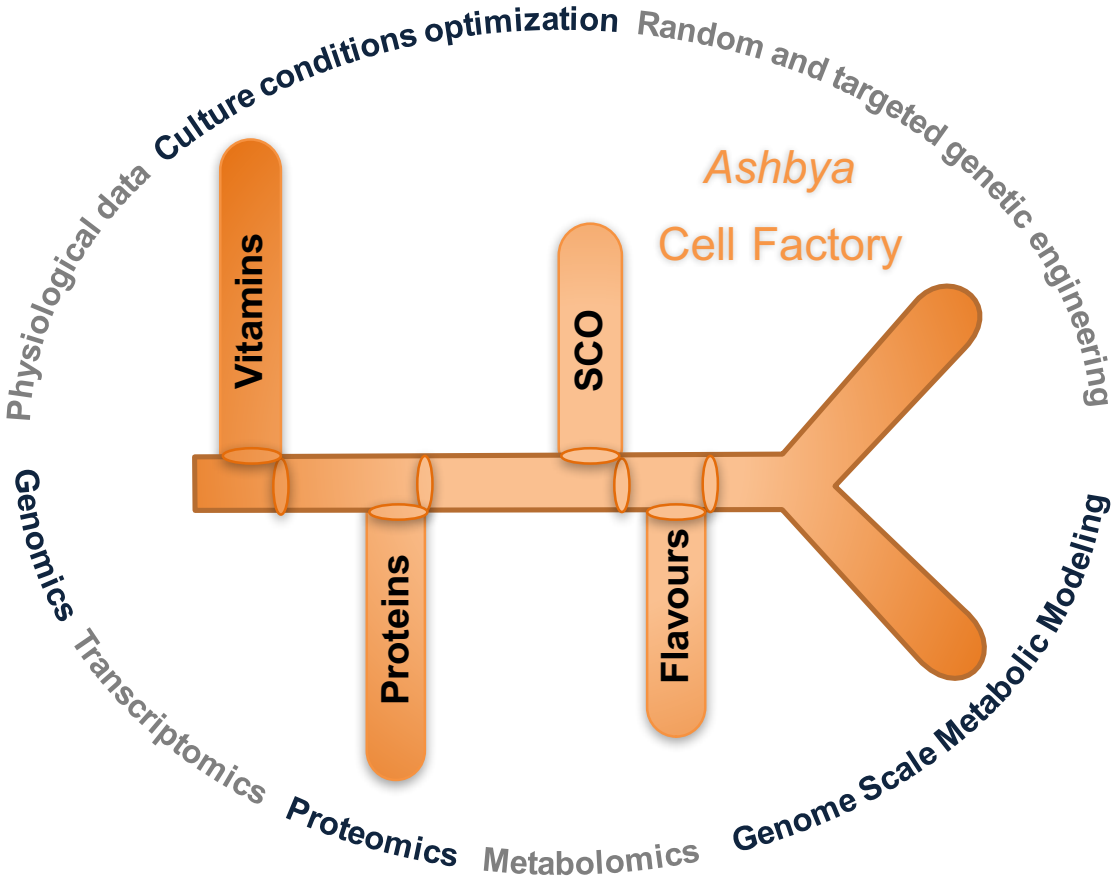


Figure 1.1. *A. gossypii* biotechnological applications. Following its established industrial use in riboflavin production, emerging biotechnological applications for this fungus are: other vitamins, recombinant proteins, single-cell oil (SCO) and flavours production. The technological approaches used for the development of these biotechnological applications are presented in the closing circle.

1.2.1 Niche, taxonomy and morphology

A. gossypii was one of the causative agents of the stigmatomycosis disease that mainly infected cotton plants in the Caribbean region (Ashby and Nowell, 1926). Other crops in the tropics and sub-tropics regions of America and Africa such as coffee, citrus fruits and tomatoes were also infected (Batra, 1973; Pridham and Raper, 1950). More recently, nearly 50 years after the isolation and identification of the first available *A. gossypii* strains, this fungus was again isolated in nature from large milkweed bugs found feeding on oleander in Florida, US (Dietrich et al., 2013). Since this fungus is incapable of penetrating healthy tissues, it requires an insect vector (generally of the Heteroptera suborder) to transfer its spores or mycelia into the plant (Batra, 1973; Pridham and Raper, 1950). Thus, application of insecticides to crops revealed an effective way of controlling the widespread of *A. gossypii* (Dammer and Ravelo, 1990).

The classification of *A. gossypii* has differed along the years. Initially named *Nematospora gossypii* (Ashby and Nowell, 1926), due to its similarity with some *Nematospora* species, this fungus was a couple of years later included in the class Hemiascomycetes and given a new genus name, *Ashbya*. This separation was based in morphological differences, as it grew exclusively as mycelia and had polynucleated cells as source of sporangia (Fragoso and Ciferri, 1928; Guilliermond, 1928). Later, with the first pieces of genomic and ribosomal DNA of *A. gossypii* being analysed (Altmann-Jöhl and Philippsen, 1996; Kurtzman, 1995; Steiner and Philippsen, 1994) its close relationship with *S. cerevisiae* and its placement in the Saccharomycetaceae family became obvious. Since the advent of the genome sequencing of several fungi, phylogenomic studies have consistently classified *A. gossypii* as a member of the order Saccharomycetales, close to other pre-whole-genome duplication (pre-WGD) species (Fitzpatrick et al., 2006; Wang et al., 2009).

A. gossypii is as an attractive model to study fungal developmental biology (reviewed in Perez-Nadales et al., 2014; Schmitz and Philippsen, 2011; Wendland and Walther, 2005), not only due to its close relationship to yeast, small genome size and easy genetic manipulation, but also because it has one of the simplest life cycles studied (Figure 1.2). *A. gossypii* starts the germination of its uninucleate haploid spores with the formation of a spherical germ bubble at the centre of the spores (Alberti-Segui et al., 2001; Wendland and Philippsen, 2000). Then, it switches permanently to polarized growth, emerging the first germ tube, followed by the formation of the first septum (Knechtle et al., 2003). On the opposite side, another germ appears, giving rise to a bipolar germling (Wendland and Philippsen, 2000). Subsequently, new hyphae start forming by lateral branching, generating a young mycelium. As the mycelium becomes mature, the growth speed increases at hyphal tips, which starts to undergo dichotomous branching, leading to the formation of Y-shaped hyphal filaments (Ayad-Durieux et al., 2000). Septation and nuclear division are uncoupled events in *A. gossypii*, and thus each hyphal compartment encloses multiple nuclei (Kaufmann and Philippsen, 2009; Wendland and Philippsen, 2000). These exhibit asynchronous division cycles and variable ploidy, despite sharing a common cytoplasm (Anderson et al., 2015; Gladfelter et al., 2006). To deal with the high demand for novel cell surface at the growing tip, secretory vesicles containing new membrane and cell wall components are transported along the actin cytoskeleton to the tip of fast-growing hyphae, where they accumulate in Spitzenkörper-like spherical structures and fuse with the plasma membrane, releasing their content to the extracellular space (Köhli et al., 2008). The secretion of proteins required for cell wall synthesis

and lysis of substrates is thus thought to occur preferentially (although not exclusively) at the hyphal tip (Read, 2011).

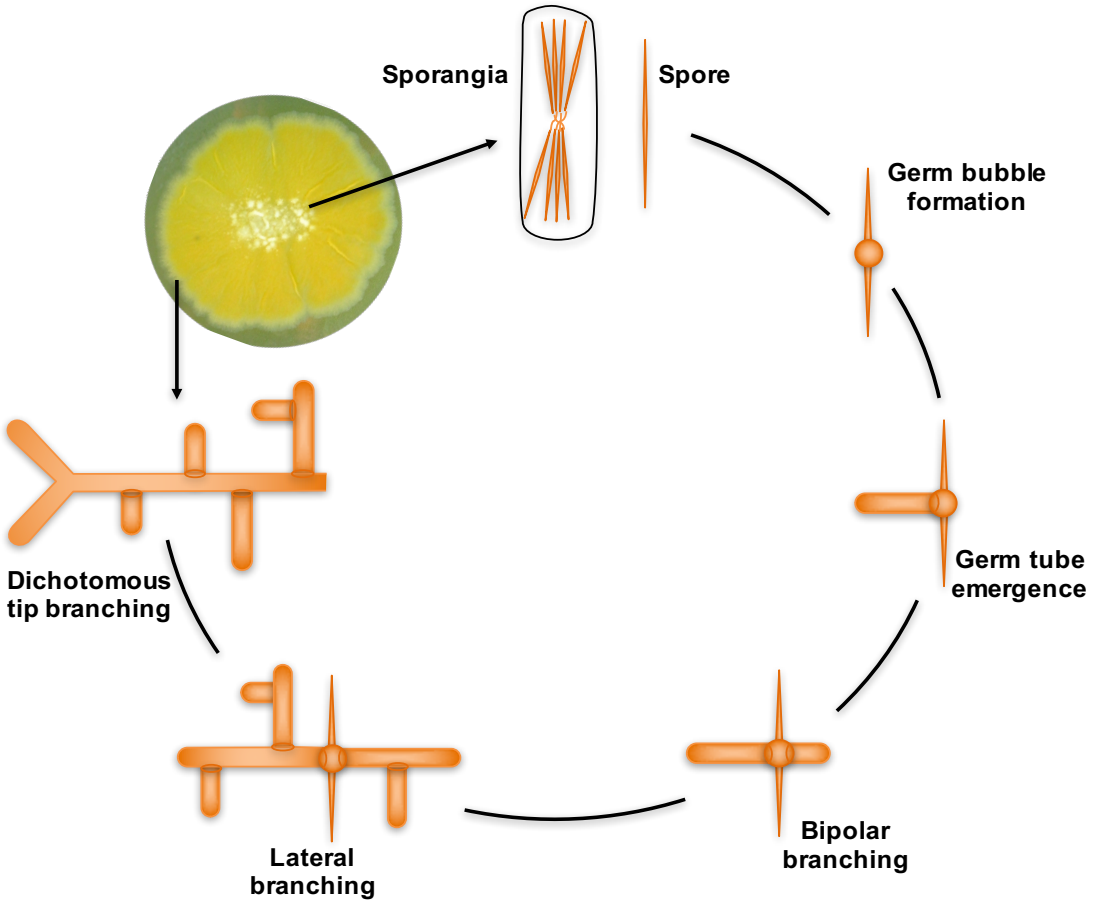


Figure 1.2. Schematic representation of the *A. gossypii* life cycle. The colony photo represents growth for eight days on agar-solidified complex medium.

The vegetative growth of *A. gossypii* ceases upon nutrient limitation and old mycelia eventually undergo sporulation, event that is linked with the overproduction of riboflavin (Stahmann et al., 2001). However, riboflavin production is not exclusively connected to sporulation, as non-sporulating mycelia also accumulate riboflavin (Walther and Wendland, 2012). Generally, eight spores bound by filaments are released from *A. gossypii* sporangia, which are formed in old hyphae that fragments at septal sites (Wendland and Walther, 2005). On solid media, the sporulation zone is rich in strongly aggregated hyphae that rise above the agar and form synnemata-like structures (Grünler et al., 2010). In liquid media, old mycelia undergo autolysis during the latest phase of its life cycle (Pridham and Raper, 1950). Sporulation in *A. gossypii* is affected by the mitogen-activated protein (MAP)-kinase pathway that governs the mating pheromone response and the

starvation/filamentous growth response, and by the cyclic adenosine monophosphate/protein kinase A (cAMP/PKA) pathway that governs all aspects of cell physiology, particularly morphogenesis, growth and sporulation (Wasserstrom et al., 2013, 2015; Wendland et al., 2011). However, the specific mechanisms of spore formation in *A. gossypii* are still poorly understood, not being clear whether there is a meiotic component to sporulation (Wasserstrom et al., 2013, 2015). Moreover, the last sequenced strain, *FDAG1* isolated from large milkweed bugs, encodes not only *MAT**a*** genes, but also *MAT*α sequences, which are not found in the reference strain ATCC 10895. Therefore, and contributing to the complexity of this discussion, these data suggest that at least some *A. gossypii* strains likely have a sexual cycle (Dietrich et al., 2013).

1.2.2 Biochemistry and physiology

The main metabolic and physiological trait of *A. gossypii* is, undoubtedly, the overproduction of riboflavin, the yellowish vitamin B_2 (Wickerham et al., 1946). In liquid cultures, the production of this vitamin is accentuated at the stationary phase, when the growth rate declines and the nutrients become limited, in simultaneous with sporulation (Karos et al., 2004; Stahmann et al., 2001). Since the production kinetics of this metabolite is similar to other secondary metabolites, riboflavin was classified as a pseudo-secondary metabolite of *A. gossypii* (Schlösser et al., 2001). The two main precursors for *de novo* riboflavin biosynthesis in *A. gossypii* are guanosine-5-triphosphate (GTP) and ribulose 5-phosphate (ribulose 5-P), which are converted through a pathway controlled by six genes (*AgRIB1*, *AgRIB2, AgRIB3, AgRIB4*, *AgRIB5* and *AgRIB7*) (Karos et al., 2004). These genes are regulated at the transcription level, in particular *AgRIB3*, *AgRIB4* and *AgRIB5*, which suffer a strong increase in expression during the production of riboflavin (Schlösser et al., 2001, 2007; Walther and Wendland, 2012).

Environmental stimuli, such as nutritional and oxidative stress, were shown to trigger riboflavin overproduction (Kavitha and Chandra, 2009, 2014; Silva et al., 2015; Schlösser et al., 2007; Walther and Wendland, 2012). Alongside with the induction of riboflavin overproduction and secretion, oxidative stress has been shown to also induce the activity of enzymes that are involved in the detoxification of reactive oxygen species (ROS), *e.g.* catalase and superoxide dismutase (Kavitha and Chandra, 2009, 2014). Therefore, riboflavin production in *A. gossypii* and, consequently, its secretion was hypothesized as a defence mechanism against the stress imposed by the ROS produced by plant defences (Walther and Wendland, 2012). Recently, another link was made between oxidative stress and riboflavin production, connecting the highly active tricarboxylic

acid (TCA) cycle displayed by *A. gossypii* during the growth phase and the riboflavin production phase with ROS production due to inefficient mitochondrial respiration (Schwechheimer et al., 2018b). In this regard, the transcription factor AgYap1p, which is known to play a major role in guiding the cellular responses to various stresses in *S. cerevisiae*, was demonstrated to direct an increase in the production of riboflavin during an event of oxidative stress, likely through the regulation of the *AgRIB4* expression (Walther and Wendland, 2012). AgYap1p also seems to regulate the expression of *AgRIB3* and *AgGSH1* (gene encoding γ-glutamyl cysteinyl synthase, a rate-limiting enzyme in the biosynthesis of glutathione, which is a molecule involved in the *A. gossypii* antioxidant defence), both of which have been shown to be up-regulated in response to oxidative stress (Kavitha and Chandra, 2014). These evidences show that riboflavin overproduction by *A. gossypii* is related with regulatory mechanisms rather than with metabolic capabilities. Indeed, comparatively with its close relatives *S. cerevisiae* and *Kluyveromyces lactis* that do not overproduce riboflavin, *A. gossypii* does not possess exclusive enzymes directly involved in the riboflavin biosynthetic pathway that could explain its overproducing trait (Gomes et al., 2014). On the other hand, significant differences exist at the intergenic level between *A. gossypii* and its non-flavinogenic relatives (Brachat et al., 2003; Wendland et al., 2011), which hints at the existence of regulatory differences between them.

Despite all the advances made to understand it and all the strain improvements achieved along the years, riboflavin production by *A. gossyppi* is an extremely complex process. This is a dual-stage (growth and riboflavin production phases), multi-pathway and multi-compartment (*e.g.*, peroxisome and cytosol) metabolic process performed in complex culture conditions (*e.g.*, yeast extract and vegetable oils) (Schwechheimer et al., 2018b). Therefore, to continue meeting industrial requirements, a continuous effort is still being made to comprehensively deconstruct its underlying mechanisms. In this regard, through ^{13}C tracer isotopic labelling analysis, Schwechheimer et al. (2018b) recently deciphered the core metabolism under industrial production conditions of an overproducing *A. gossypii* strain during the growth and riboflavin production phases. This study focused on three building blocks: glycine, serine and formate. Interestingly, glycine, which contributes to the formation of the pyrimidine ring of riboflavin as a two-carbon donor, was almost exclusively acquired from the medium. In turn, serine and formate contributed as one-carbon donors for riboflavin biosynthesis. Both micronutrients were mainly uptake from the medium or synthesized from the glycine pools. Since the one-carbon metabolism was identified as a bottleneck in the earlier production phases of riboflavin, increasing the supply

of formate at specific time points allowed to increase the production of riboflavin by 45 % (Schwechheimer et al., 2018b). This study is a clear example of the positive impact that isotopic labelling analyses can have in providing insights that could be translated in culture condition optimizations (in this case of minor elements or micronutrients) of biotechnological processes. A similar approach was followed to determine the importance of macronutrients for growth and riboflavin production, which demonstrated that vegetable oils contributed 81 % to the formation of riboflavin, definitely establishing this as the best-suited substrate for this purpose (Schwechheimer et al., 2018a).

Driven by industrial interest, the physiology of this fungus started to be disclosed early in the last century, when the first studies reported the production of a yellow pigment by *A. gossypii* during investigation of its nitrogen requirements (Farries and Bell, 1930). In this regard, *A. gossypii* was not able to use potassium nitrate and ammonium salts (Farries and Bell, 1930; Buston et al, 1938). However, in the beginning of this decade, Ribeiro et al. (2012) showed that this fungus is able to grow in defined media containing ammonium at pH 6.5, but scarcely at pH 4.5, and therefore the lack of growth previously observed was likely due to low pH of the medium. In accordance, *A. gossypii* owns the genetic elements for ammonium metabolism.

A. gossypii does not tolerate well low pH (pH 4), which is deleterious for growth and riboflavin production (Tanner et al., 1949). While the interval between pH 4.5 – 5.5 revealed to be acceptable for growth (but not for riboflavin), pH above 5.5 (ideally between pH 6.0 – 7.0) gave the highest riboflavin yields (Tanner et al., 1949). Regarding temperature, there is also a disparity between growth and riboflavin production. Growth has been observed between 20 – 40 °C, while the optimum range lies between 30 – 35 °C. In turn, riboflavin accumulation is higher at temperatures between 26 – 28 °C (Özbas and Kutsal, 1986; Pfeifer et al., 1950; Tanner et al., 1949). The presence of low concentrations of NaCl and Na_3PO_4, or slightly higher concentrations of mannitol, sorbitol and KCl, highly inhibit the growth of *A. gossypii*, which displays acute sensitivity to hyperosmotic stress (Förster et al., 1998; Nikolaou et al., 2009).

The main micronutrients needed for *A. gossypii* growth are myo-inositol and biotin (Buston and Pramanik, 1931; Farries and Bell, 1930; Kögl and Fries, 1937), since this fungus is unable to biosynthesize them (Gomes et al., 2014). In fact, the requirement of *A. gossypii* for biotin played an important role in the discovery of this vitamin (Kögl and Fries, 1937). Thiamine is also necessary for adequate growth, as *A. gossypii* synthesises it in sub-optimal amounts (Pridham and Raper, 1950). These “accessory factors” are supporting elements that when added to the medium allow

A. gossypii to use amino acid mixtures, ammonium aspartate and asparagine (Buston and Kasinathan, 1933; Demain, 1972). However, concerning nitrogen sources, peptone and casein are the most suitable for this fungus (Farries and Bell, 1930).

Yeast extract is recognized for a long time as a good source of several nutrients necessary for *A. gossypii*'s growth (Wickerhan et al., 1946). However, its crucial role for growth and, at a lower but significant extent, for riboflavin production by *A. gossypii* was only recently disclosed (Schwechheimer et al., 2018b). In this study, yeast extract was shown to be the major source of carbon used by *A. gossypii* for growth, contributing also with 9 % of carbon for riboflavin biosynthesis. Besides yeast extract, other complex substrates, such as crude nitrogen and micronutrient sources (*e.g.*, corn steep liquor) have been also employed in large-scale riboflavin production (Pfeifer et al., 1950; Schwechheimer et al., 2018a; Smiley et al., 1951; Tanner et al., 1949).

This fungus can utilize a wide range of carbon sources, such as glucose, fructose, sucrose, starch, maltose, glycerol and plant oils (Kutsal and Özbas, 1989; Ledesma-Amaro et al. 2014a; Pridham and Raper, 1950; Ribeiro et al., 2012; Tanner et al., 1949). At a lower extent, ethanol can also support growth (Pridham and Raper, 1950). However, plant oils, namely corn oil and soybean oil, are the preferred substrate for riboflavin production and obviously for lipid accumulation. Cellulose, pentoses (arabinose, xylose), galactose and lactose are not utilized as carbon sources (Pridham and Raper, 1950; Ribeiro et al., 2012), which for some cases may be explained by the absence of enzymes and/or pathways necessary for the metabolism of these substrates in *A. gossypii* (Gomes et al., 2014; Ribeiro et al., 2012). Correlated with this, the variety and amount of hydrolytic enzymes secreted by *A. gossypii* to the extracellular medium is rather low (Aguiar et al., 2014a; Ribeiro et al., 2010, 2013). Of these, only a lipase and an invertase have been experimentally characterized thus far (Aguiar et al. 2014b; Stahmann et al. 1997).

In aerobioisis, *A. gossypii* converts glucose mainly to carbon dioxide and water, also producing traceable amounts of ethanol, pyruvic, acetic and citric acid (Mickelson, 1950; Mickelson and Schuler, 1953). Volatile fusel alcohols and esters derived from the catabolism of amino acids are also formed via the Ehrlich pathway (Figure 1.3), with particularly high level production of isoamyl alcohol and 2-phenylethanol, which confer to *A. gossypii*'s cultures a characteristic fruity/floral aroma (Ravasio et al., 2014). In addition, *A. gossypii* is capable of fermenting glucose anaerobically, approaching the theoretical yield of a yeast alcoholic fermentation (Mickelson,

1950). Nonetheless, the *A. gossyppi* metabolism is clearly marked to aerobic conditions bias, as it is the case for riboflavin overproduction (Demain, 1972; Pfeifer et al., 1950; Tanner et al., 1949).

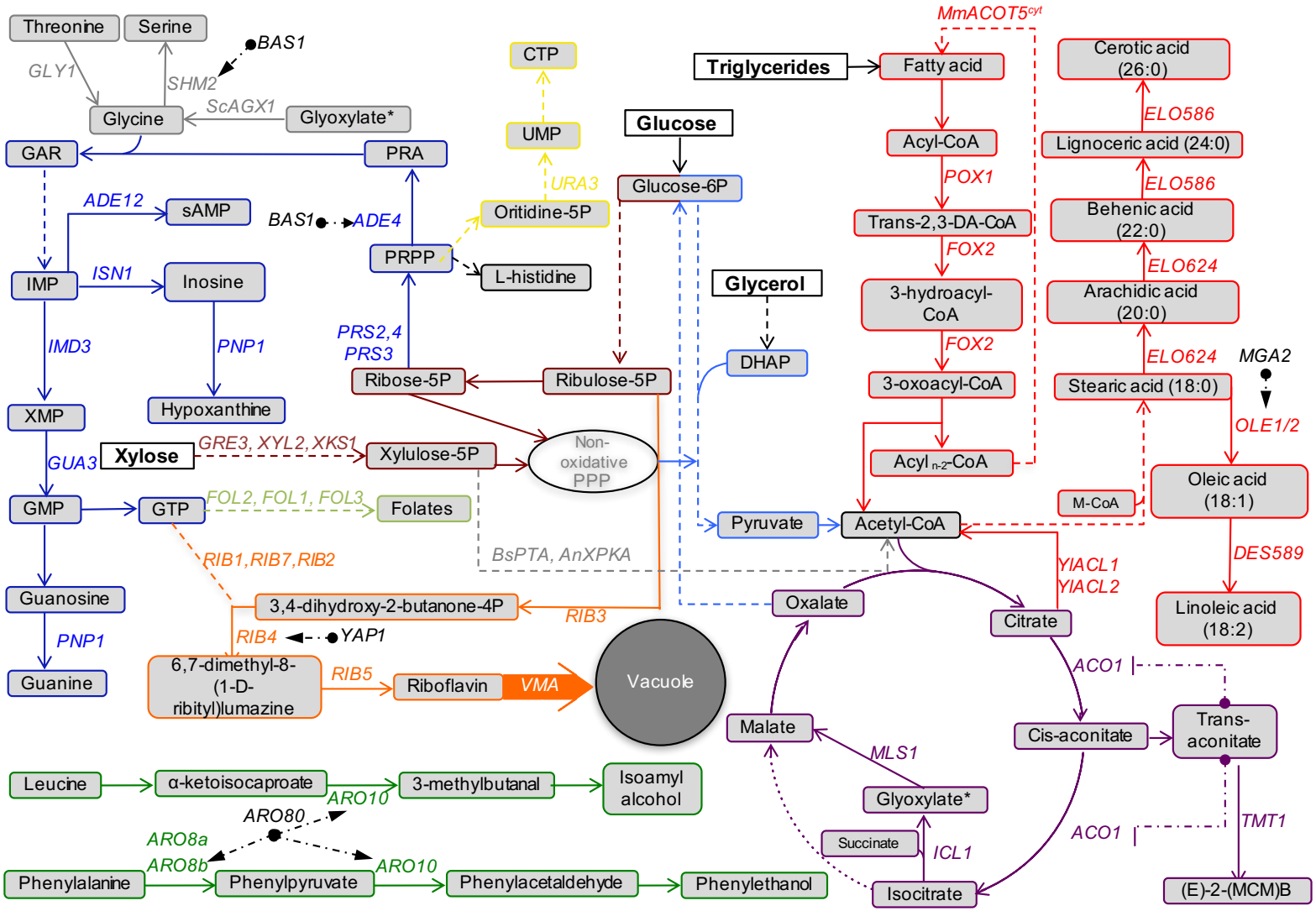

Threonine
Serine
BAS1
GLY1
SHM2
Glycine
ScAGX1
Glyoxylate*
GAR
PRA
ADE12
sAMP
BAS1
ADE4
IMP
ISN1
Inosine
IMD3
PNP1
XMP
Hypoxanthine
GUA3
Xylose
GRE3, XYL2, XKS1
Xylulose-5P
GMP
GTP
FOL2, FOL1, FOL3
Folates
RIB1,RIB7,RIB2
Guanosine
PNP1
Guanine
3,4-dihydroxy-2-butanone-4P
RIB3
RIB4
YAP1
6,7-dimethyl-8-(1-D-ribityl)lumazine
RIB5
Riboflavin
VMA
Vacuole
PRPP
PRS2,4
PRS3
Ribose-5P
Ribulose-5P
CTP
UMP
URA3
Oritidine-5P
L-histidine
Glucose
Glucose-6P
Glycerol
DHAP
Non-oxidative PPP
BsPTA, AnXPKA
Pyruvate
Acetyl-CoA
Oxalate
Citrate
Malate
MLS1
Glyoxylate*
Succinate
ICL1
Isocitrate
ACO1
Cis-aconitate
Trans-aconitate
TMT1
ACO1
(E)-2-(MCM)B
YIACL1
YIACL2
Leucine
α-ketoisocaproate
ARO10
3-methylbutanal
Isoamyl alcohol
ARO80
ARO8a
ARO8b
ARO10
Phenylalanine
Phenylpyruvate
Phenylacetaldehyde
Phenylethanol
Triglycerides
MmACOT5cyt
Fatty acid
Acyl-CoA
POX1
Trans-2,3-DA-CoA
FOX2
3-hydroacyl-CoA
FOX2
3-oxoacyl-CoA
Acyl n-2-CoA
M-CoA
Cerotic acid (26:0)
ELO586
Lignoceric acid (24:0)
ELO586
Behenic acid (22:0)
ELO624
Arachidic acid (20:0)
ELO624
Stearic acid (18:0)
MGA2
OLE1/2
Oleic acid (18:1)
DES589
Linoleic acid (18:2)

Figure 1.3.

Figure 1.3. *Continued.* Pathways and genes involved in the *A. gossypii* metabolism that have been targeted for biotechnological purposes. The pathways are identified according to the following colour scheme: glycolysis and gluconeogenesis (light blue), β-oxidation and fatty acid biosynthesis (red), TCA cycle and glyoxylate cycle (purple), pentose phosphate pathway (PPP) (brown), *de novo purine* biosynthetic pathway (dark blue), glycine pathways (grey), *de novo* pyrimidine biosynthetic pathway (yellow), riboflavin biosynthetic pathway (orange), leucine and phenylalanine degradation (Ehrlich pathway; green) and folates biosynthesis (light green). Dashed arrows indicate a multi-step pathway, dotted arrows indicate regulatory roles and filled arrow indicates a transport reaction. (E)-2-(MCM)B, (E)-2-8(methoxycarbonylmethyl)butenedioate; DHAP, dihydroxy-acetone-phosphate; GAR, 5'-phosphoribosylglycinamide; GMP, guanosine-5'-phosphate; M-CoA, malonyl-CoA; PRA, 5-P-β-D-ribosyl-amine; Trans-2,3-DA-CoA, Trans-2,3-dehydroacyl-CoA; XMP, xanthosine-5-phosphate. *An*, *Aspergillus niger*; *Bs*, *Bacillus subtilis*; *Mm*, *Mus musculus*.

A. gossypii has been shown to accumulate high amounts of lipid bodies as carbon and energy storage pools (Stahmann et al., 1994; Ledesma-Amaro et al., 2014a). Although the carbon sources utilized play a determinant role in its lipidogenic profile, *A. gossypii* predominantly accumulates unsaturated fatty acids (FA) (Stahmann et al., 1994; Ledesma-Amaro et al., 2014a). Using plant oils as substrate, their breakdown into fatty acids and glycerol is made by a lipase, one of the few extracellular proteins identified and characterized in *A. gossypii* (Maeting et al., 2000; Stahmann et al., 1997). Non-ionic agents added to the medium are able to stabilize it, consequently improving riboflavin production (Demain et al., 1972; Goodman and Ferrera, 1954; Stahmann et al., 1997). Inside the cell, the glyoxylate cycle plays the role of a connective shunt with the central carbon metabolism, since the main precursors of riboflavin are GTP and ribulose 5-P (Figure 1.3) (Schmidt et al., 1996a, 1996b). The main result of this anaplerotic pathway is a final conversion of fatty acids to carbohydrates through gluconeogenesis. This starts with the cleavage of isocitrate to succinate and glyoxylate by isoccitrate lyase (Aglclp), shifting the carbon flux from the TCA cycle towards a carbon-conserving pathway (Maeting et al., 1999; Schmidt et al., 1996a, 1996b). Despite the significant yield difference when plant oils are used as substrate, *A. gossypii* is also able to naturally biosynthesize *de novo* lipids from sugars like glucose. This turned out to be an improbable and tunable trait of the fungus (Ledesma-Amaro et al., 2014c; Lozano-Martínez et al., 2016).

Riboflavin biosynthesis is closely related to other biosynthetic pathways, such as the purine synthesis pathway and the pentose phosphate pathway, all of which compete for common precursors at specific pathway nodes (Figure 1.3). For instance, GTP is synthesized through the

purine pathway, which in turn starts from phosphoribosyl pyrophosphate (PRPP). On the other hand, GTP is also a committed intermediate for the biosynthesis of other high-value chemical naturally produced by this fungus, namely folic acid (Serrano-Amatriain et al., 2016). From a process point of view, intermediates of these pathways that feed the formation of these precursors are usually beneficial for riboflavin overproduction. For instance, addition of glycine to the medium enhances riboflavin production (Demain, 1972; Monschau et al., 1998). This amino acid is a precursor during the *de novo* purine biosynthetic pathway, which is formed from threonine by the action of AgGly1p (Monschau et al., 1998). Interestingly, *A. gossypii* was recently shown to secrete high amounts of inosine and guanosine, which are purine nucleosides produced via this same pathway (Ledesma-Amaro et al., 2015a). In turn, PRPP, a central intermediate of the primary metabolism, is required for the *de novo* and salvage pathways of purine, pyrimidine and pyridine (NAD^+, $NADP^+$) nucleotides, histidine biosynthesis (Figure 1.3) and tryptophan biosynthesis (Jiménez et al., 2008).

Regarding the physiology of *A. gossypii,* an aspect that needs to be stressed out, and whose importance has been overlooked, is the strain heterogeneity noted for several morphological and physiological parameters. For instance, Ribeiro et al. (2012) reported distinct sporulation efficiencies and colony radial growth for similar strains deposited in different culture collections. This inherent plasticity of *A. gossypii* also affects riboflavin production/accumulation, as Nieland and Stahmann (2013) showed that *A. gossypii* hyphal cells growing in the same culture exhibit phenotypic differences in what concerns overproduction and accumulation of riboflavin. Therefore, the analysis of data on the metabolism and physiology of *A. gossypii* should always be made under the scope of the strain(s) studied. Recent findings reporting the existence of differences between the mating type of different *A. gossypii* strains (Dietrich et al., 2013) and of variable degrees of ploidy within the same cell at different cell cycle stages (Anderson et al., 2015) may help explain why physiological and metabolic differences are observed between and within strains, and thus warrant further investigation. On the other hand, as the production of industrially interesting metabolites varies significantly among wild strains (Ledesma-Amaro et al., 2015a), the systematic exploration of this fungus natural biodiversity may unravel new biotechnological potential for *A. gossypii,* and should therefore be considered as a standard procedure in the development of novel applications.

1.2.3 Genetics and molecular tools

The sequencing and annotation of the *A. gossypii* genome elucidated the close relation between *A. gossypii* and *S. cerevisiae*, revealing homologs in *S. cerevisiae* for 94 % of the 4776 annotated protein-coding genes of *A. gossypii*, 90 % of which at syntenic positions (Brachat et al., 2003; Dietrich et al., 2004, 2013). Only 6 % of the *A. gossypii*'s protein-coding genes have no homolog in *S. cerevisiae*, the so-called NOHBY (no homolog in Baker's yeast) genes, but most of these have a syntenic homolog in other closely related species (Dietrich et al., 2004, 2013; Wendland et al., 2011; Wendland and Walther, 2014). The small size (9.12 Mb) and organization of the *A. gossypii*'s genome into only seven chromosomes also provided compelling evidence for an ancient whole-genome duplication (WGD) of the *Saccharomyces* lineage after its split from the *Ashbya* lineage (Dietrich et al., 2004).

Various genetic tools and molecular methods have been developed for use in *A. gossypii*, among which random mutagenesis with physical (ultraviolet (UV) radiation) or chemical (nitrogen mustard, N-methyl-N'-nitro-N-nitrosoguanidine (MNNG) and ethyl methane sulfonate (EMS)) mutagens followed by screening of colonies with the desired phenotype has been the methodology used for the longest time to generate and isolate *A. gossypii* mutants with improved traits (Park et. al, 2007; Pridham and Raper, 1952; Perlman, 1979; Ribeiro et al. 2013; Schmidt et al. 1996a; Tagima et al., 2009). In fact, random mutagenesis has been the main classical genetic approach used to manipulate *A. gossypii* strains, although adaptive evolution strategies under selective conditions also allowed isolating spontaneous mutants with improved phenotypes (Pfeifer et al., 1950; Sugimoto et al., 2010). Other random mutagenesis techniques that do not involve the use of chemical or physical mutagens have also been used to generate genetic diversity in *A. gossypii*, such as insertional mutagenesis by *in vitro* transposition (Santos et al., 2005) and disparity mutagenesis using an error-prone DNA polymerase (Park et. al, 2011). The absence of a known sexual cycle in this fungus has impeded the use of other classical genetic approaches (Dietrich et al., 2013; Wendland et al., 2011). A significant technical difficulty associated with the *A. gossypii* mutagenic screens that needs to be highlighted is the inability to easily isolate single spores, as they clump together via terminal filaments (Wendland et al., 2011).

With the introduction of recombinant DNA technology in *A. gossypii*, reverse genetic approaches have been added to mutational techniques as a means to further improve strains in a rational way. The methodology to introduce recombinant DNA using episomal vectors in *A. gossypii* was first developed by Wright and Philippsen (1991). Interestingly, *A. gossypii* has the ability to

replicate plasmids based on *S. cerevisiae* autonomously replicating sequences (ARS; *ARS1* and 2-micron). However, ARS elements of *A. gossypii* are not functional in *S. cerevisiae* (Schade et al., 2003), despite working well in the closely related dimorphic fungus *Holleya sinecauda* (Kurtzman, 1995). These *S. cerevisiae* genetic elements have been extensively used to drive the expression of homologous and heterologous genes in *A. gossypii* (Aguiar et al., 2014b; Altmann-Jöhl and Philippsen, 1996; Ayad-Durieux et al., 2000; Kato and Park, 2006; Magalhães et al., 2014; Monschau et al., 1998; Ribeiro et al., 2010). Following the mechanistic genetic similarities with yeasts, *A. gossypii* presents a very effective homologous recombination system, which is an exception among filamentous fungus (Steiner et al., 1995). Thus, it is possible to implement stable genetic integrations using PCR-based gene targeting (Wendland et al., 2000). Genome engineering in *A. gossypii* leads first to heterokaryotic transformants, containing wild and engineered nuclei. Subsequently, sporulation of these mycelia produce uninucleate spores, which can be isolated as homokaryotic clones under selective conditions (e.g., germinating in the presence of an antibiotic). In sum, genetic engineering of *A. gossypii* resembles in easiness to that of yeasts.

To feed continuous engineering of this fungus, several promoters needed to be used. Regarding strong and constitutive promoters, the natives *AgTEF* and *AgGPD* (Revuelta et al., 1999; Steiner and Philippsen, 1994) and the heterologous from *S. cerevisiae*'s *TEF2*, *PDC1*, *PGK1*, *LEU2* and *ADH1* were used (Kaufmann, 2009; Magalhães et al., 2014; Ribeiro et al., 2010; Wendland et al., 2000). More recently, the promoter *AgRIB7* appeared as a solution to drive low gene expression in *A. gossypii* (Ledesma-Amaro et al., 2015b). Regarding transient and tunable promoters, the native Ag*MET3* and *AgSUC2* promoters together with the heterologous from *S. cerevisiae THI13 and MET3* have been used (Aguiar et al., 2014b; Dünkler and Wendland, 2007; Kaufmann, 2009).

As tools for molecular studies, some auxotrophic strains were generated such as the threonine auxotroph *Agthr4*Δ (Altmann-Jöhl and Philippsen, 1996) and the leucine auxotroph *Agleu2*Δ (Ayad-Durieux et al., 2000), which are complemented by the *S. cerevisiae* homolog genes (Altmann-Jöhl and Philippsen, 1996; Ayad-Durieux et al., 2000). In addition, the green fluorescent protein (GFP) and prokaryotic and eukaryotic β-galactosidases have been used as reporter proteins (Ayad-Durieux et al., 2000; Dünkler and Wendland, 2007; Gladfelter et al., 2006; Magalhães et al., 2014; Monschau et al., 1998; Walther and Wendland, 2012). Furthermore, staining of subcellular compartments was addressed with various fluorescent dyes (Gladfelter et al., 2006; Walther and Wendland, 2004; Wendland and Philippsen, 2001). Several dominant selection markers for

resistance to antibiotics are also available for selection of *A. gossypii* engineered strains, such as the *GEN3*/geneticin (G418; Wendland et al., 2000), the *Hyg*/hygromycin (Jiménez et al. 2008; Mateos et al., 2006), the *NATPS*/nourseothricin (clonNAT; Hoepfner *in* Kaufmann, 2009) and the *BLE3*/phleomycin (Ribeiro et al., 2013) marker cassette/antibiotic combinations. Moreover, a whole set of modules combining different fluorescent protein tags and heterologous selection markers is also available for use in *A. gossypii* (Kaufmann, 2009).

Concerning biotechnological applications, strain engineering for stable industrial use should allow the removal and recycling of marker genes and leave only residual (or ideally be absent of) genetic scars. With this in mind, the Cre-*lox*P recombination system of the bacteriophage P1 was adapted for generating *A. gossypii* strains free of exogenous marker genes, opening new perspectives for the deletion and/or integration of multiple genes (Aguiar et al., 2014c). In the scope of that work, three heterologous recyclable drug marker cassettes and two Cre recombinase expression vectors were created, being suitable for use in both laboratorial and industrial *A. gossypii* strains, as they do not require any predetermined genetic background. These tools also allowed the generation of stable auxotrophic strains for uridine/uracil (*Agura3*Δ), adenine (*Agade1*Δ) and both (*Agura3*Δ, *Agade1*Δ) (Aguiar et al., 2014c). Unlike the others auxotrophies already mentioned (*A. gossypii Agleu2*Δ and *Agthr4*Δ strains), the corresponding *S. cerevisiae*'s homolog could not complement the deletion of *AgURA3* (Pompejus et al., 1999). Therefore, these auxotrophic strains will be important for future engineering projects as soon as a selection system based on the complementation of these auxotrophies becomes available.

All these molecular tools have been important for the development of stable *A. gossypii* strains for biotechnological purposes (as it will be discussed in the following section), but the improvement of existing tools and development of new ones will be crucial to meet the demands of the biotechnology industry and to further develop *A. gossypii* as cell factory. In this regard, the establishment of flexible genome editing methods (e.g., CRISPR-Cas9 system; DiCarlo et al., 2013) for engineering this fungus is of great interest. Moreover, as the number of characterized promoters currently available for use in *A. gopssypii* is limited, screening and identification of other promoters with desired characteristics will settle the basis for the development of new and more flexible gene expression tools. Similar screening strategies should be followed for designing new reporter proteins and secretion signal sequences for use in the scope of recombinant protein production. Beyond these pressing needs, a major outcome of the upcoming years may be related with the arising of forward genetic tools for *A. gossypii*, fading away the dependency on reverse genetics.

However, significant work is still needed in order to elucidate the conditions needed for sexual reproduction. The first step has already been taken with the isolation of wild *A. gossypii* strains possessing mating type regions distinct from those presented by the first sequenced strain, ATCC 10895 (Dietrich et al., 2013).

1.3 Commercial and emerging biotechnology of *A. gossypii*

There are some innate capacities of *A. gossypii* that have allowed this fungus to remain in a relevant role in industry for almost 30 years. From these, it can be highlighted its performance in large-scale fermentation processes using low-cost and waste-derived substrates (Park et al., 2007; Tajima et al., 2009; Wei et al., 2013). In addition, its ability to secrete metabolites/proteins to the culture medium and to undergo autolysis during the late stationary phase of growth or at low temperature is also industrially appealing, as they facilitate downstream product recovery (Aguiar et al., 2014a; zu Berstenhorst et al., 2009; Schwechheimer et al., 2016). The successful industrial process of riboflavin production by *A. gossypii*, together with the extensive molecular investigation to which it was subjected, led to a sharp increase in the molecular tools available for its engineering, as it was mentioned above. Therefore, the interest now has shifted for its maximum exploitation as a cell factory able to accomplish other biotechnological challenges. In addition, as any other microbial model, *A. gossypii* relies on well curated genome sequencing and annotation (Dietrich et al., 2013; Gomes et al., 2014). Therefore, two genome scale metabolic models (GSMM) were already developed in order to provide systems biology predictive power to optimize existing and develop new biotechnological applications (Gomes et al., unpublished results; Ledesma-Amaro et al., 2014b). With its stoichiometric reaction set compiled and successfully validated for experimental parameters such as biomass growth, riboflavin production and substrate utilization, it is possible to reliably simulate metabolic cell behaviour of this fungus. Together, the molecular and *in silico* toolbox of *A. gossypii* are leveraging its potential as a cell factory organism.

1.3.1 Vitamins

Riboflavin (vitamin B_2) is an essential vitamin for humans and animals, since these organisms do not have the ability to synthesize it. On the other hand, microorganisms and plants can efficient produce it to fulfil their needs. This vitamin is a precursor of flavins like flavin mononucleotide (FMN) and flavin adenine dinucleotide (FAD), present as co-factors in several enzymatic reactions (*e.g.*, dehydrogenases, oxidases, oxidoreductases). In humans, deficiency of this vitamin can led to skin and eye lesions as well as impairment of the fetus development during pregnancy (Schwechheimer et al., 2018a). This vitamin is supplied as formulation, yellow colorant and animal food additive. Until 1990, it was obtained by chemical synthesis, but since then *A. gossypii* has played a major role in the industrial production of riboflavin, producing it by fermentation and thus constituting a paradigm of the concept of the white biotechnology

(Schwechheimer et al., 2016; Stahmann et al., 2000). The industrial riboflavin production process employing *A. gossypii* completely replaced the chemical synthesis and remains an economically competitive process, contributing to an estimated annual market of 9000 tonnes (Schwechheimer et al., 2016). The continuous improvement of strains by random mutagenesis or rational engineering approaches that has been performed along the years greatly contributed for the success of this process (Kato and Park, 2012; Lim et al., 2001; Revuelta et al. 2016; Stahmann et al., 2000).

Wild *A. gossypii* strains have been reported to produce up to 5 g/L of riboflavin in optimized culture media, but randomly improved strains can produce from 14 to 20 g/L of riboflavin (Demain, 1972; Lim et al., 2001; Park et al., 2011; Schwechheimer et al., 2016). Many randomly improved *A. gossypii* strains for riboflavin production were obtained by several rounds of mutagenesis followed by screening of colonies with increased yellow pigmentation (Perlman, 1979). Since the industrial establishment of this process, different mutagenic agents and screening procedures were adopted and combined in different manners (Table 1.1). UV radiation (Park et al. 2007; Schmidt et al., 1996b; Wei et al., 2012), chemical mutagens (Lizama et al., 2007; Tajima et al., 2009) and disparity mutagenesis (Park et al., 2011) have been applied to create mutations. For the screening procedures, antimetabolites (mainly itaconate and oxalate) have been the most common way to isolate overproducing strains, essentially due to the correlation between the *A. gossypii* isocitrate lyase (Icl1p; glyoxylate cycle) activity and riboflavin production (Schmidt et al., 1996a, 1996b). In fact, Sugimoto et al. (2010) were able to isolate a riboflavin overproducing strain only by growing *A. gossypii* spores in a medium containing oxalate, without the application of any mutagenic agent. More recently, through the analysis of the itaconate metabolism and genetics, its related compounds *cis*-aconitate and *trans*-aconitate were detected in the riboflavin production phase and, as the latter has an inhibitory effect on aconitase in the TCA, the authors proposed *trans*-aconitate as a novel and more available antimetabolite for screening of riboflavin overproduction (Sugimoto et al., 2014).

Table 1.1. Random engineering approaches applied in *A. gossypii* for biotechnological purposes.

Mutagen	Screening	Application	Reference(s)
UV light	Antimetabolite (itaconate)	Riboflavin	Park et al. (2007); Schmidt et al. (1996b)
UV light	Yellow colour of the colonies	Riboflavin	Wei et al. (2012)
MNNG	Antimetabolite (itaconate)	Riboflavin	Lizama et al. (2007); Tajima et al. (2009)
–	Antimetabolite (oxalate)	Riboflavin	Sugimoto et al. (2010)
Mutated DNA polymerase δ	Antimetabolite (oxalate and hydrogen peroxide) Regeneration of the colonies by serial transfers in selective medium Stabilization of the colonies in non-selective medium and quantification of riboflavin production	Riboflavin	Park et al. (2011)
EMS	Selective medium containing CMC[a] (for EGI), starch (for α-amylase) or tributyrin (for lipase) Determination of specific enzymatic activities	Recombinant protein production	Ribeiro et al. (2013)

[a]carboxymethylcellulose

Since the 1990s, when BASF (Germany) launched a riboflavin production plant with *A. gossypii* (in South Korea), the performance of *A. gossypii* strains could be much improved by rational design as well. The constantly increasing molecular toolbox for this fungus and the deep understanding acquired along the last three decades about the *A. gossypii* riboflavin biosynthetic pathway (reviewed in Kato and Park, 2012; Revuelta et al., 2016) supported this. The rationale for improve riboflavin production has mainly followed two principles: increase the flux towards the riboflavin biosynthetic pathway and increase the flux of the *de novo* purine biosynthetic pathway (Table 1.2). For this, the engineering approaches made so far were: i) overexpression of the *AgRIBs* genes (Althöefer et al., 1999; Althöefer and Revuelta, 2003); ii) overexpression of *AgGLY1*, responsible for the conversion of threonine to glycine (Monschau et al., 1998); iii) deletion of *AgSHM2*, encoding a cytosolic serine hydroxymethyltransferase that converts glycine in serine (Schlüpen et al., 2003); iv) overexpression of the heterologous *AGX1* gene from *S. cerevisiae*, which

encodes an alanine:glyoxylate aminotransferase that converts glyoxylate in glycine (Kato and Park, 2006); v) overexpression of some key genes of the purine biosynthetic pathway such as *AgADE4* (Jiménez et al., 2005), *AgPRS2,4* and *AgPRS3* (Jiménez et al., 2008); vi) deregulation of the transcription factor AgBas1p that constitutively activates the purine and glycine biosynthetic pathways (Mateos et al., 2006); and vii) blockage of the *A. gossypii de novo* pyrimidine biosynthetic pathway by deletion of the *AgURA3* gene (Aguiar et al., 2014c) to increase the availability/accumulation of PRPP for the formation and/or accumulation of riboflavin precursors (GTP and ribulose-5P; Silva et al., 2015). Other strategies focused on improving riboflavin production from plant oils by overexpressing genes involved in the glyoxylate cycle, such as the *AgICL1* (Käsler et al., 1997) and the *AgMLS1* (encoding the malate synthase; Sugimoto et al., 2009), and on increasing the excretion of riboflavin into the medium by disrupting the gene encoding the vacuolar ATPase subunit A, *AgVMA1* (Förster et al., 1999). Recently, the rationally engineered strain producing the highest titter of riboflavin was reported (Ledesma-Amaro et al., 2015b). In this strain, five of the six *RIB* genes (*RIB1,2,3,5,7*) were overexpressed and the *ADE12* gene from the *de novo* purine biosynthesis, which deviates the metabolic flux for GTP formation towards adenosine monophosphate (AMP) formation, was subjected to low expression.

Table 1.2. Target genes of rational genetic engineering strategies in *A. gossypii* for different biotechnological applications.

Gene	Strategy and outcome	Reference(s)
	Riboflavin production	
AgRIB3-5	Overexpression increased the flux of the riboflavin biosynthetic pathway, which resulted in a 2.5-fold increase in riboflavin production	Althöefer et al. (1999)
AgRIB1,2,4, 7	Overexpression increased the flux of the riboflavin biosynthetic pathway, which resulted in an 1.4-fold increase in riboflavin production	Althöefer and Revuelta (2003)
AgRIB1-3,5,7 and *AgADE12*	Overexpression of the Ag*RIB* genes, which increased the flux of the riboflavin biosynthetic pathway and low expression of *AgADE12*, which fed more GTP for riboflavin, resulted in a 5.4-fold increase in riboflavin production	Ledesma-Amaro et al. (2015b)
AgGLY1	Overexpression increased glycine formation from threonine, which allowed a 9-fold increase in specific riboflavin production	Monschau et al. (1998)
AgSHM2	Disruption abolished the conversion of glycine into serine, which led to a 10.6-fold increase in specific riboflavin production	Schlüpen et al. (2003)

Table 1.2. *Continued.*

ScAGX1	Heterologous expression allowed glycine biosynthesis from glyoxylate, which resulted in an 1.3-fold increase in specific riboflavin production	Kato and Park (2006)
AgADE4	Overexpression and elimination of feedback inhibition by site directed mutagenesis increased the flux of the purine biosynthetic pathway, which resulted in a 10-fold increase in riboflavin production	Jiménez et al. (2005)
AgPRS2,4 and *AgPRS3*	Overexpression and elimination of feedback inhibition by site directed mutagenesis increased PRPP availability, which resulted in an 1.7- to 1.8-fold increase in riboflavin production	Jiménez et al. (2008)
AgBAS1	Deletion of the C-terminal interaction and regulatory domain constitutively activated the purine and glycine pathways, which resulted in a 9.4-fold increase in specific riboflavin production	Mateos et al. (2006)
AgURA3	Disruption blocked the pyrimidine biosynthetic pathway, thus increasing the availability of riboflavin precursors, which led to a 7.5-fold increase in specific riboflavin production	Aguiar et al. (2014c); Silva et al. (2015)
AgICL1	Overexpression increased riboflavin production from oils (by 2.2-fold)	Käsler et al. (1997)
AgMLS1	Overexpression increased riboflavin production from oils (by 1.7-fold)	Sugimoto et al. (2009)
AgVMA1	Disruption reduced the accumulation of riboflavin in the vacuole and increased its excretion to the culture medium (by 2-fold)	Förster et al. (1999)
	Recombinant protein production	
ShceIA1	Heterologous expression allowed the recombinant production of *S. halstedii* endo-β-1,4-glucanase	Althöefer et al. (2001)
TreglI and *TrcbhI*	Heterologous expression allowed the extracellular production of *T. reesei* EGI and CBHI	Ribeiro et al. (2010)
AnlacA	Heterologous expression allowed the extracellular production of *A. niger* β-galactosidase	Magalhães et al. (2014)
ScSUC2	Heterologous expression allowed the extracellular production of *S. cerevisiae* invertase	Aguiar et al. (2014b)
	Single cell oil production	
YlACL1/ YlACL2	Heterologous expression enabled the production of acetyl-CoA from citrate, which increased lipid accumulation during the trophic phase (by 1.3-fold)	Ledesma-Amaro et al. (2014a)
AgPOX1 and *AgFOX2*	Disruption blocked the beta-oxidation pathway, which triggered a 2- to 3.5-fold increase in lipid accumulation	Ledesma-Amaro et al. (2014a)

Table 1.2. *Continued.*

AgELO586	Overexpression increased cerotic acid (26:0) accumulation and disruption resulted in SCO with properties that meet some biodiesel quality standards	Ledesma-Amaro et al. (2014c)
AgELO624	Overexpression led to nervonic acid (24:1) production and disruption resulted in SCO with properties that meet some biodiesel quality standards	Ledesma-Amaro et al. (2014c)
AgDES589	Overexpression increased linoleic acid (18:2) accumulation	Ledesma-Amaro et al. (2014c)
	Flavours	
AgARO80	Overexpression increased isoamyl alcohol and isobutanol production (by 2.5-fold)	Ravasio et al. (2014)
AgADE12	Disruption increased the excretion of inosine (by 11.5-fold) and guanosine (by 1.2-fold)	Ledesma-Amaro et al. (2015)
AgIMD3	Disruption increased inosine excretion (by 1.6-fold) and overexpression increased guanosine excretion (by 1.5-fold)	Ledesma-Amaro et al. (2015)
AgPNP1	Disruption increased the excretion of inosine (by 1.9-fold) and guanosine (by 1.5-fold)	Ledesma-Amaro et al. (2015)
AgISN1	Disruption did not increase inosine excretion	Ledesma-Amaro et al. (2015)
AgGUA1	Overexpression increased riboflavin production but did not increase guanosine excretion	Ledesma-Amaro et al. (2015)
AgRIB1	Down regulation reduced riboflavin production but did not increase guanosine excretion	Ledesma-Amaro et al. (2015)

Ag, *A. gossypii*; *An*, *A. niger*; *Sc*, *S. cerevisiae*; *Sh*, *S. halstedii*; *Tr*, *T. reesei*; *Yl*, *Y. lipolytica*

An increasing number of evidences have shown that the triggering of riboflavin overproduction in *A. gossypii* is associated with the activation of intracellular stress signalling cascades in response to environmental changes (Kavitha and Chandra, 2009, 2014; Walther and Wendland, 2012; Nieland and Stahmann, 2013). Therefore, future attempts to further improve riboflavin production will rely on the better understanding of the overall stress responses of *A. gossypii*. Meanwhile, the knowledge already gained with *A. gossypii* will serve as a basis to guide the improvement of riboflavin production by other cell factories.

The other vitamin whose production was recently explored is vitamin B_9 (folates or as commonly named, folic acid). Physiologically, folates are co-factors in one-carbon transfer reactions that support the nucleic acid and amino acid anabolic metabolism. In humans, deficiency of this vitamin can lead to severe illness conditions, such as cancer and anemia, being a common

supplementation during pregnancy. Currently, it is industrially manufactured by chemical synthesis. Recently, *A. gossypii* was shown to be the first microbial system improved by metabolic engineering for the biosynthesis of folates (Serrano-Amatriain et al., 2016). For this, the authors overexpressed genes of the folate biosynthetic pathway (*AgFOL2* and *AgFOL3*) and redirected the metabolic flux from competing pathways like the riboflavin biosynthetic pathway (underexpression of Ag*RIB1*), as riboflavin and folic acid share the same precursor, GTP (Figure 1.3). In addition, deletion of *AgMET7* prevented the cellular accumulation of folate polyanions, which inhibit the folic acid biosynthetic pathway. Overall, the combination of these genetic modifications allowed the construction of a strain able to produce about 7000 μg/L of folates (146-fold more than the parental strain).

1.3.2 Recombinant proteins

Beyond riboflavin production, the exploration of *A. gossypii* as a host for the production of heterologous proteins has received much attention in the last years. An endo-β-1,4-glucanase (celA1) from *Streptomyces halstedii* (Althöefer et al., 2001), two cellulases from *Trichoderma reesei*, endoglucanase I (EGI) and cellobiohydrolase I (CBHI) (Ribeiro et al., 2010), a β–galactosidase from *A. niger* (Magalhães et al., 2014) and a *S. cerevisiae*'s invertase (Aguiar et al., 2014b) are among the repertoire of heterologous enzymes already produced in this host system (Table 1.2).

The ability to secrete native and heterologous enzymes to the extracellular medium and to recognize heterologous signal peptides is a valuable starting point for any potential host for recombinant protein production (Aguiar et al., 2014b; Althöefer et al., 2001; Magalhães et al., 2014; Ribeiro et al., 2010; Stahmann et al., 1997). The amount and variety of native proteins secreted by this fungus is low, being its secretory potential more similar to that of yeast than to that of other filamentous fungi (Aguiar et al., 2014a). In line with this observation, the protease activity in *A. gossypii* culture supernatants is negligible (Ribeiro et al., 2010). Together, these features represent important advantages for heterologous protein production in this host, as secreted products are less likely to be contaminated or degraded by native proteins, thus allowing cost-efficient downstream processing of low- and medium-value enzymes.

Another important trait of the host lies on its capacity to perform protein post-translation modifications. *A. gossypii* performs glycosylation and other modifications required for the biological activity and stability of proteins (Aguiar et al., 2013; Magalhães et al., 2014; Ribeiro et al., 2010),

with a tendency to hyperglycosylate secreted proteins less extensively than *S. cerevisiae* (Demain and Vaishnav, 2009). Examples can be found in the glycosylation pattern of the heterologous EGI, CBHI (Ribeiro et al., 2010) and β–galactosidase (Magalhães et al., 2014). This is advantageous for the production of proteins whose properties may be adversely affected by extensive glycosylation. A recent characterization of its secreted *N*-glycome corroborates these data, as *A. gossypii* revealed a processing system substantially distinct from that of *S. cerevisiae*, which allows the production of much shorter *N*-glycans (Aguiar et al., 2013). In fact, this study showed that *A. gossypii* predominantly produces *N*-glycans that are more similar in extent to those produced by non-conventional yeast hosts such as *Pichia pastoris*, *Hansenula polymorpha* and *Yarrowia lipolytica* (Aguiar et al., 2013). Nevertheless, the extent of *N*-glycosylation and *N*-glycan phosphorylation in *A. gossypii* is highly influenced by the culture medium used (Aguiar et al., 2013).

Despite these advantages, the production levels reported for the first heterologous proteins secreted by *A. gossypii* (EGI and CBHI) were low, although comparable to those obtained with *S. cerevisiae* (Ribeiro et al., 2010). In fact, the obtainment of reasonable amounts of these cellulases by recombinant microbial hosts in a biologically active form has been a challenging task (Ribeiro et al., 2010). Therefore, further investigation of *A. gossypii* as a recombinant protein production host went through the implementation of random engineering techniques to improve its general secretory capacity. In this context, the recombinant *A. gossypii* strain expressing EGI was exposed to the chemical mutagen EMS (Ribeiro et al., 2013). The following screening strategy was initially based on the diameter of the haloes formed around the mutant colonies on screening media for different enzymatic activities (Table 1.1). Among the activities tested, only cellulolytic activity gave a good correlation and allowed the selection of the most promising mutants (Ribeiro et al., 2013). Subsequently, these mutants were grown in submerged cultures and extracellular activities were determined for heterologous cellulase (*T. reesei* EGI), native α-amylase and native β-glucosidase. One mutant exhibiting a superior performance (of 1.4- to 2-fold) in all extracellular enzymatic activities was identified, suggesting a global improvement in its secretory capacity (Ribeiro et al., 2013). Other mutants also presented partial improvements (of 2- to 3-fold): two in EGI or β-glucosidase activity, and one in EGI and α-amylase activities (Ribeiro et al., 2013). Another attempt to increase the general secretory potential of this fungus involved the deletion of *AgGAS1* homologs (encoding a β-1,3-glucanosyltransglycosylase involved in cell wall assembly) to enhance the permeability of the cell wall, but the resulting mutants presented serious growth defects (Ribeiro et al., 2013).

Transcriptomic analysis performed in *A. gossypii* cells under recombinant protein secretion conditions and dithiothreitol-induced secretion stress subsequently provided useful information about possible strategies that could be used to further improve its productivity (Aguiar et al., 2014a). Among these, the use of strong promoters was found to be of upmost importance, as the heterologous *S. cerevisiae PGK1* constitutive promoter was proved to be inefficient in driving the overexpression of the EGI-encoding gene (Aguiar et al., 2014a). This study also revealed the existence in *A. gossypii* of alternative regulatory mechanisms to cope with protein secretion stress, other than the conventional unfolded protein response (UPR), which may offer novel ways of improving protein secretion in this fungus (Aguiar et al., 2014a).

The strength of several native (*A. gossypii TEF* and *GPD*) and heterologous (*S. cerevisiae PGK1* and *ADH1*) constitutive promoters was compared when producing a heterologous protein of other origin, the β-galactosidase from *A. niger* (Magalhães et al., 2014). Given the ease of detection of this secreted enzyme, the screening of transformants was facilitated. Moreover, as this protein had already been efficiently secreted by recombinant *S. cerevisiae* strains (Domingues et al., 2002, 2005; Oliveira et al., 2007; Ramakrishnan and Hartley, 1993), it provided a good model protein to further explore the potential of *A. gossypii* as a heterologous protein producer. The strong *A. gossypii*'s *TEF* promoter drove the highest production levels of this enzyme in *A. gossypii* and *S. cerevisiae* laboratorial strains, followed by the other native promoter tested, *GPD* (Magalhães et al., 2014). Using the *TEF* promoter, *A. gossypii* secreted up to 37-fold more active β-galactosidase than two different *S. cerevisiae* strains transformed with the same plasmids (Magalhães et al., 2014). In similar culture conditions, *A. gossypii* also produced 2.5-fold more extracellular β-galactosidase than that previously reported for a β-galactosidase high-producing *S. cerevisiae* strain transformed with a different plasmid under the control of the *S. cerevisiae*'s *ADH1* promoter (Domingues et al., 2002; Magalhães et al., 2014). However, much can still be improved just by manipulating the production conditions, as demonstrated by the 1.5-fold increase in β-galactosidase secretion when glucose was replaced by glycerol in the culture medium, which allowed reaching extracellular activity levels (1,127 U/mL) within the range of those reported for non-modified *A. niger* strains (152 to 3,000 U/mL) (Magalhães et al., 2014).

In summary, the potential of *A. gossypii* as a host for heterologous protein production is still underexplored and much could be learned about possible strategies to improve its productivity, among which: (i) culture medium optimization; (ii) screening for better promoters and secretion signal sequences; (iii) development of better expression strategies, preferably through the

integration of stable expression cassettes.

1.3.3 Single cell oil and *de novo* biosynthesis of lipids

The adaptation of *A. gossypii* for SCO production is a perfect example of how the molecular and *in silico* toolbox made available for this fungus allowed to rationally capitalize its natural abilities. Also known as microbial lipids, SCOs constitute a promising renewable source for the sustainable production of biodiesel and other value-added oleochemicals, as they do not affect food costs and security, and can be obtained in large amounts by fermentation of waste-derived substrates under controlled conditions that are not dependent on climate or soil conditions. (Beopoulos et al., 2011). SCOs may also be interesting as food supplements, as some microorganisms are able to produce high-value polyunsaturated fatty acids (PUFAs), such as those belonging to the omega-3 and omega-6 families. In spite of being considered a non-oleaginous microorganism (Vorapreeda et al., 2012), *A. gossypii* was metabolically engineered to fit the requisites of a candidate for SCO production (minimum of 20 % lipid content in relation to its cell dry weight (CDW)) (Ledesma-Amaro et al., 2014a; Lozano-Martínez et al., 2016).

Ledesma-Amaro et al., (2014a) tested different strategies to accomplish that: first, the genes *AgPOX1* and *AgFOX2*, which are involved in the β-oxidation pathway, were disrupted to avoid FA degradation; second, a heteromeric ATP-citrate lyase (Aclp) from *Y. lipolytica* was overexpressed in *A. gossypii* to enable the conversion of citrate into acetyl-CoA and thus increase the pool of this crucial building block of FAs. Single mutants (*pox1Δ* or *fox2Δ*) with the β-oxidation pathway blocked were able to improve the accumulation of FAs in media containing only glucose or glucose and plant oils (Ledesma-Amaro et al., 2014a). In turn, the double mutant strain (*pox1Δfox2Δ*) did not present any advantage in relation to the single mutants. When oils were supplied as the sole carbon source, all of these strains presented growth limitation (Ledesma-Amaro et al., 2014a). The *pox1Δ* mutant revealed to be the most efficient strain, reaching a lipid content of approximately 40 % (after 3 days of growth) and 70 % (after 7 days of growth) of its CDW, when grown in medium containing glucose and plant oils (Ledesma-Amaro et al., 2014a). The heterologous overexpression of *YlACL1/YlACL2* (encoding both subunits of Aclp from *Y. lipolytica*) also fulfilled the goal for which it was originally proposed, *i.e.*, increase the cellular pool of acetyl-CoA (Ledesma-Amaro et al., 2014a). Thus, the *A. gossypii YlACL1/YlACL2* strain presented superior lipid accumulation, achieving the requirements of oleaginous microorganisms in terms of lipid accumulation (but only when grown in medium containing glucose and plant oils). However, the *A. gossypii*

pox1Δ,YlACL1/YlACL2 strain did not translate the higher levels of acetyl-CoA available into more lipid accumulation in comparison with the *A. gossypii pox1Δ* (Ledesma-Amaro et al., 2014a). The *pox1Δ* strain revealed a metabolic unbalance that increased the acetyl-CoA pool independently of the Aclp presence and some other cellular mechanisms benefited from these higher levels of acetyl-CoA (Ledesma-Amaro et al., 2014a). Hence, as suggested by the authors, this increase in acetyl-CoA pools can be valuable in the future to explore the production of other relevant products beyond SCO, such as biobutanol.

The potential applications of SCO are strictly connected with the FA profile of the strain, which should be manipulated according to the requisites of a particular industry. This FA profile is largely defined by the action of enzymes such as elongases and desaturases, which are responsible for the length and unsaturations of FAs, respectively (Hashimoto et al., 2008). In this regard, Ledesma-Amaro et al. (2014c) performed a functional characterization of selected genes of the elongation (*AgELO586* and *AgELO624*) and desaturation (*AgDES589* and *AgDES079*) system of *A. gossypii*, which had been previously identified (Hashimoto et al., 2008). After testing the functionality of the respective proteins in *S. cerevisiae*, only *AgDES079* did not match its predicted function, not showing any notable role in FA desaturation (Ledesma-Amaro et al., 2014c). The regulation of these genes by the carbon source used (glucose or soybean oil) was also checked by analysis of their transcription levels. Once again, *AgDES079* was the only gene that did not present any changes (Ledesma-Amaro et al., 2014c). Finally, all genes were independently overexpressed or deleted in *A. gossypii*. Excluding *AgDES079*, the manipulation of the other three genes generated interesting strains with potential application in different industries according to their FA profile (Table 1.2). For instance, the engineered strains *A. gossypii elo586Δ* and *A. gossypii elo624Δ* fulfil the restrictive requirements established by the European biodiesel quality standard EN 14214, and are therefore very promising for application in this industry (Ledesma-Amaro et al., 2014c). The adaptation of *A. gossypii* for SCO presented very consistent and promising results. According to Ledesma-Amaro et al (2014a), the 70 % of lipid accumulation achieved in the engineered *A. gossypii* strains is among the highest accumulation levels reported so far in both oleaginous and non-oleaginous microorganisms. Moreover, the strains created by metabolic engineering of the elongation and desaturation systems have a wide application spectrum in other industrial sectors, such as cosmetics, food, paper and pharmaceutical industry (Ledesma-Amaro et al., 2014c).

Despite the substantial improvements mentioned above, both in terms of yield as in enrichment in desired fatty acids, given the importance of the cost/benefit ratios in microbial

biotechnology processes, production costs must be minimized as much as possible. A way to accomplish that passes by reducing the cost of raw materials. Thus, it is important to obtain good product yields and productivities from low-cost substrates, such as renewable raw materials and industrial wastes rich in carbohydrates (e.g., hexose and pentose sugars). To accomplish that, different strategies have been recently used to harness *A. gossypii* with improved *de novo* biosynthesis of lipids from these substrates. Given that in sugar-based media *A. gossypii* strains were only able to produce up to 5 % of their CDW as lipids, this fungus was further engineered to: i) increase the activity of its main native *Δ9* desaturase, by overexpressing a truncated version of its main regulator (*AgMGA2*), and ii) alleviate the feedback inhibition exerted by fatty acyl-CoA on the enzymes of the fatty acid biosynthetic pathway, by decreasing its celular pool through the expression of an heterologous thioesterase (*Mus musculus ACOT5*) (Lozano-Martínez et al., 2016). This approach led to an increase of about 4-fold in the lipid content *per* CDW and allowed *A. gossypii* to reach 20 % of lipid accumulation when grown in medium containing only glucose. In addition, *A. gossypii* was recently engineered to consume xylose (Díaz-Fernández et al., 2017). This fungus owns the genetic machinery (*AgGRE3*, *AgXYL2* and *AgXKS1*) for its metabolism, but naturally it can not grow using this carbon source. However, the overexpression of these genes resulted in a strain able to consume up to 80 g/L of xylose. Further redirection of the metabolic flux of xylose towards acetyl-CoA through overexpression of a heterologous phosphoketolase pathway led to improved lipid biosynthesis from this pentose sugar (Díaz-Fernández et al., 2017).

1.3.4 Flavours

The fermented beverages sector invests strongly in new products that can offer a new variety of flavour/aroma perceptions, which are determinant features for product quality. Traditionally, complex mixtures of aromatic alcohols (known as fusel alcohols) and esters have been obtained as part of food or beverage fermentation processes (e.g. cheese, beer, wine) at low concentrations, where they contribute to the overall flavour of the fermented products (Akacha and Gargouri, 2015). The strong interest of the fermented food and beverages sector in new products with interesting flavour/aroma perceptions has supported the continuous search for novel producing organisms. Therefore, there is a continuous effort for screening the biodiversity in order to find new natural producers. In this regard, there is a growing interest on non-*Saccharomyces* species as natural flavour producers, which many believe to remain largely underexplored (Domizio et al., 2010).

The Ehrlich pathway plays an important role in the metabolism of flavour/aromatic compounds and Wendland and Walther (2011) noticed significant genetic differences between *A. gossypii* and its closely related *Eremothecium cymbalariae* regarding this pathway. *E. cymbalariae* harbours only one gene related with this pathway (*ARO8a*), whereas *A. gossypii* encodes four genes (*AgARO8a*, *AgARO8b*, *AgARO10* and *AgARO80*). In comparison with *S. cerevisiae*, *A. gossypii* lacks *ARO9* (Ravasio et al., 2014). Therefore, these authors decided to characterize and explore the importance of this pathway in flavour production by *A. gossypii*. The profile of volatile compounds produced by *A. gossypii* is characterized by high levels of 2-phenylethanol (rose/flower aroma), which are residual in *E. cymbalariae*, and of isoamyl alcohol (banana/fruity aroma), also elevated in *E. cymbalariae*. Indeed, the production of 2-phenylethanol by *A. gossypii* was determined to be higher than that in *S. cerevisiae* strains, namely *Weihenstephan* lager yeast and laboratorial CEN.PK2 (Ravasio et al., 2014). *A. gossypii* single mutants for the *ARO* genes revealed a strong impairment in the production of 2-phenylethanol and also isoamyl alcohol (with exception for the *AgARO8a*) (Ravasio et al., 2014). As *AgARO80* encodes a transcriptional regulator of some of these genes, these authors overexpressed this gene. Although it was not possible to note significant differences in the production of 2-phenylethanol (possibly due to phenylalanine limitation in the culture medium), the engineered strain was able to produce about 2.5-fold more isoamyl alcohol and isobutanol than the parent strain (Ravasio et al., 2014). This work reinforced the idea that the exploration of non-*Saccharomyces* strains for flavour enhancement of fermented beverages may result in a new wide line of products.

Very recently, *A. gossypii* became the first eukaryotic microorganism presenting good potential for industrial nucleoside production, particularly inosine and guanosine (Ledesma-Amaro et al., 2015a). These flavour active compounds (umami flavour) are used by the food industry with various beneficial effects associated to them, such as antioxidant and immunomodulatory properties. Some wild strains have the ability to naturally secrete high levels of inosine and guanosine (Ledesma-Amaro et al., 2015a). Furthermore, as a natural riboflavin overproducer, *A. gossypii* has a strong metabolic flow through the purine biosynthetic pathway, the central biosynthetic pathway of these two compounds. Based on this, a series of *in silico* simulations by the GSMM iRL766 (Ledesma-Amaro et al., 2014b) allowed defining a set of target genes (Table 1.2) for disruption or overexpression in order to redirect the flux through inosine and/or guanosine biosynthesis. An engineered strain (overexpressing a deregulated *AgADE4*; Jimenez et al, 2005) with increased flux through the purine biosynthetic pathway, which served before to enhance

riboflavin production, was used as background strain to introduce more specific metabolic shifts (Ledesma-Amaro et al., 2015a). From a total of eight new engineered strains, the strain deleted for *AgADE12*, encoding the enzyme responsible for the conversion of inosine-5'-phosphate (IMP) into adenylo-succinate (sAMP), and for *AgPNP1,* encoding the enzyme responsible for the conversion of the nucleosides (inosine and guanosine) into nucleobases (hypoxanthine and guanine), was able to produce and excrete 24-fold more inosine (0.27 g/L) and 2-fold more guanosine (0.14 g/L) than the wild type strain (Ledesma-Amaro et al., 2015a).

The filamentous fungus *A. gossypii* demonstrated once again to possess a very interesting natural potential and the machinery needed to create improved engineered strains for different biotechnological applications, in this particular case as a natural flavour producer for the fermented beverages and food industries. The advent of systems biology has allowed leveraging this natural biotechnological potential of *A. gossypii* (Ledesma-Amaro et al., 2015a) and will continue playing a major role in the development of this fungus as a cell factory.

1.4 Standpoint of *A. gossypii* as a cell factory

Being in a core position in what concerns industrial riboflavin production, *A. gossypii* has beneficiated from constant and sustainable improvement of its natural abilities, thus keeping the commercial competitiveness of that process. Production of riboflavin by *A. gossypii* will always be a landmark for white biotechnology and further improvements will continue to be pursued. However, there is no doubt that the trend in the last years show that *A. gossypii* holds the potential to expand its biotechnological significance way beyond riboflavin production. While important advances have been accomplished in what concerns these new *A. gossypii* applications, even when compared with industrial microbial models (Table 1.3), several challenges still need to be overcome until these emerging applications can follow the successful commercial track of riboflavin production. Following this rationale, exploration of new biotechnological applications should take into account the following: strain engineering should focus on the exploitation of valuable metabolites belonging to pathways with naturally strong metabolic fluxes; on the other hand, studies should assess if the optimization, scale-up and intensification of these bioprocesses can support the obtainment of economically sustainable titers, yields and rates.

Table 1.3. Production levels and approaches taken for emerging biotechnological applications in *A. gossypii*. Comparisons with other microorganisms are also presented. The term "engineered" refers to strains that were target of a rational approach, while "mutants" were obtained randomly.

Species	Product	Genetic Background	Culture Conditions Optimization	Production Levels	Reference(s)
Recombinant proteins					
A. gossypii	Endoglucanase I	Engineered	No	Up to 400 μmol/min.L	Ribeiro et al. (2010, 2013)
S. cerevisiae		Engineered	No	Up to 1000 μmol/min.L	
A. gossypii	β-galactosidase	Engineered	No	Up to 1127 U/mL	Magalhães et al. (2014)
A. niger		Wild	No	Up to 3000 U/mL	

Table 1.3. *Continued.*

Microbial lipids					
A. gossypii	SCO	Engineered	No	Up to 70 % of CDW	Ledesma-Amaro et al. (2014a)
Y. lipolytica		Engineered	Yes	Up to 88 % of CDW	
A. gossypii	Linoleic acid	Engineered	No	16 % of total fatty acids	Ledesma-Amaro et al. (2014c)
Y. lipolytica		Wild type	Yes	31 % of total fatty acids	Fontanille et al. (2012)
Flavours					
A. gossypii	2-phenylethanol	Wild	No	Up to 0.2 g/L	Ravasio et al. (2014)
S. cerevisiae and *Kluyveromyces marxianus*		Wild	Yes	0.25 - 20 g/L	Morrissey et al. (2015)
A. gossypii	Isoamyl alcohol	Engineered	No	0.5 - 0.6 g/L	Ravasio et al. (2014)
S. cerevisiae		Mutants	Yes	0.4 - 0.5 g/L	Abe and Horikoshi (2005)
A. gossypii	Inosine	Engineered	No	Up to 2.2 g/L	Ledesma-Amaro et al. (2015a, 2016)
B. subtilis		Engineered	No	6 - 7 g/L	
A. gossypii	Guanosine	Engineered	No	Up to 0.14 g/L	Ledesma-Amaro et al. (2015a)
Bacillus amyloliquefaciens		Engineered mutant	No	Up to 13.5 g/L	Wang et al. (2014)

In the last years, the most promising biotechnological applications emerged from a deeper understanding of the natural metabolism of this fungus, particularly of the metabolic and regulatory biological processes governing riboflavin biosynthesis. As mentioned before, *A. gossypii* displays enhanced metabolic flux through the pathways of the riboflavin precursors ribulose-5P and GTP. This last is formed in the *de novo* purine biosynthetic pathway, which is also the central pathway for the formation of the nucleosides guanosine and inosine, both explored as target products (Ledesma-Amaro et al., 2015a). Moreover, riboflavin biosynthesis in *A. gosypii* is a multi-pathway

metabolic process based on lipids that the fungus accumulates or synthesizes during its growth (Schwechheimer et al., 2018b). That is why it is valuable to engineer it for SCO accumulation and/or for biosynthesis of high-value fatty acids (Ledesma-Amaro et al., 2014c; Lozano-Martínez et al., 2016). In addition, folates and riboflavin biosynthesis are also strongly connected: i) by their competition for GTP (Serrano-Amatriain et al., 2016) and ii) because folates serve as one-carbon donors for riboflavin biosynthesis (Schwechheimer et al., 2018b). Therefore, to make the most out of the *A. gosssypii* metabolism one should keep in mind that this fungus is as riboflavin overproducer and that this trait significantly defines its metabolic idiosyncrasies.

1.5 References

Abe F, Horikoshi K. Enhanced production of isoamyl alcohol and isoamyl acetate by ubiquitination-deficient *Saccharomyces cerevisiae* mutants. Cell Mol Biol Lett 2005;10:383–8;

Adrio JL, Demain AL. Recombinant organisms for production of industrial products. Bioeng Bugs 2010;1:116–31.

Aguiar TQ, Maaheimo H, Heiskanen A, Wiebe MG, Penttilä M, Domingues L. Characterization of the *Ashbya gossypii* secreted N-glycome and genomic insights into its N-glycosylation pathway. Carbohydr Res 2013;381:19–27.

Aguiar TQ, Ribeiro O, Arvas M, Wiebe MG, Penttilä M, Domingues L. Investigation of protein secretion and secretion stress in *Ashbya gossypii*. BMC Genomics 2014a;15:1137.

Aguiar TQ, Dinis C, Magalhães F, Oliveira C, Wiebe MG, Penttilä M, et al. Molecular and functional characterization of an invertase secreted by *Ashbya gossypii*. Mol Biotechnol 2014b;56:524–34.

Aguiar TQ, Dinis C, Domingues L. Cre-*lox*P-based system for removal and reuse of selection markers in *Ashbya gossypii* targeted engineering. Fungal Genet Biol 2014c;68:1–8.

Akacha NB, Gargouri M. Microbial and enzymatic technologies used for the production of natural aroma compounds: Synthesis, recovery modeling, and bioprocesses. Food Bioprod Process 2015;94:675-706.

Alberti-Segui C, Dietrich F, Altmann-Jöhl R, Hoepfner D, Phillipsen P. Cytoplasmic dynein is required to oppose the force that moves nuclei towards the hyphal tip in the filamentous ascomycete *Ashbya gossypii*. J Cell Sci 2001;114:975–86.

Alper H, Stephanopoulos G. Engineering for biofuels: exploiting innate microbial capacity or importing biosynthetic potential? Nat Rev Microbiol 2009;7:715–23.

Altmann-Jöhl R, Philippsen P. *AgTHR4*, a new selection marker for transformation of the filamentous fungus *Ashbya gossypii*, maps in a four-gene cluster that is conserved between *A. gossypii* and *Saccharomyces cerevisiae*. Mol Gen Genet 1996;250:69–80.

Althöefer H, Revuelta JL, Seulberg H, Zelder O. Genetic method for producing riboflavin. WO Patent No. 1999/061623 A2.

Althöefer H, Pompeus M, Revuelta JL, Santos M, Jiminez A, Benito R, et al. Protein production using *Ashbya gossypii*. WO Patent No. 2001/023576

Althöefer H, Revuelta JL. Genetic strain optimization for improving the production of riboflavin. WO Patent No. 2003/048367 A1.

Anderson CA, Roberts S, Zhang H, Kelly CM, Kendall A, Lee CH, et al. Ploidy variation in multinucleate cells changes under stress. Mol Biol Cell 2015;26: 1129–40

Ashby SF, Nowell W. The Fungi of Stigmatomycosis. Ann Bot 1926;40:69–84.

Ayad-Durieux Y, Knechtle P, Goff S, Dietrich F, Philippsen P. A PAK-like kinase is required for maturation of young hyphae and septation in the filamentous ascomycete *Ashbya gossypii*. J Cell Sci 2000;113:4563–75.

Batra LR. Nematosporaceae (Hemiascomycetidae): taxonomy, pathogenicity, distribution, and vector relations. US Dept Agr Tech Bull 1973;1469:1–71.

Beopoulos A, Nicaud J, Gaillardin C. An overview of lipid metabolism in yeasts and its impact on biotechnological processes. Appl Microbiol Biotechnol 2011;90:1193–206

Booth LB. This time may be different. Nat Biotechnol 2016;34:25–30.

Brachat S, Dietrich FS, Voegeli S, Zhang Z, Stuart L, Lerch A, et al. Reinvestigation of the *Saccharomyces cerevisiae* genome annotation by comparison to the genome of a related fungus: *Ashbya gossypii*. Genome Biol 2003;4:R45.

Buston HW, Pramanik NB. The accessory factor necessary for the growth of *Nematospora gossypii*. The chemical nature of the accessory factor. Biochem J 1931;25:1656–70.

Buston HW, Kasinathan S. The accessory factor necessary for the growth of *Nematospora gossypii*. III. The preparation of concentrates of the second accessory factor. Biochem J 1933;27:1859–68.

Buston HW, Kasinathan S, Wylie SM. The nitrogen requirements of *Nematospora gossypii* in synthetic media. Ann Bot 1938;2:373–9.

Connelly TM, Michelle CG, Clarke L, Ellington AD, Hillson NJ, Johnson RA, et al. Industrialization of biology: A roadmap to accelerate the advanced manufacturing of chemicals. National Academy of Sciences. Washington DC: National Academies Press; 2015.

Cyranoski D, Ledford H. International outcry over genome-edited baby claim. Nature 2018;563:607–8.

Czajka J, Wang Q, Wang Y, Tang Y. Synthetic biology for manufacturing chemicals: constraints drive the use of non-conventional microbial platforms. Appl Microbiol Biotechnol 2017;101:7427–34.

Dammer KH, Ravelo HG. Verseuchung von Leptoglossus gonagra (Fabr.) mit *Nematospora coryli* Peglion und *Ashbya gossypii* (Ashby et Nowell) Guilliermond in einer zitrusanlage der Republik Kuba. Arch Phytopathol Pflanzenschutz Berlin 1990;26:71–8.

Demain AL. Riboflavin oversynthesis. Annu Rev Microbiol 1972;26:369–88.

Demain AL, Vaishnav P. Production of recombinant proteins by microbes and higher organisms. Biotechnol Adv 2009;27:297–306.

Díaz-Fernández D, Lozano-Martínez P, Buey RM, Revuelta JL, Jiménez A. Utilization of xylose by engineered strains of Ashbya gossypii for the production of microbial oils. Biotechnol Biofuels 2017;10:3.

DiCarlo JE, Norville JE, Mali P, Rios X, Aach J, Church GM. Genome engineering in *Saccharomyces cerevisiae* using CRISPR–Cas systems. Nucleic Acids Res 2013;41:4336–43.

Dietrich FS, Voegeli S, Brachat S, Lerch A, Gates K, Steiner S, et al. The *Ashbya gossypii* genome as a tool for mapping the ancient *Saccharomyces cerevisiae* genome. Science 2004;304:304–7.

Dietrich FS, Voegelli S, Kuo S, Philippsen P. Genomes of *Ashbya* fungi isolated from insects reveal four mating-type loci, numerous translocations, lack of transposons, and distinct gene duplications. G3 (Bethesda) 2013;3:1225–39.

Domingues L, Teixeira JA, Penttilä M, Lima N. Construction of a flocculent *Saccharomyces cerevisiae* strain secreting high levels of *Aspergillus niger* β-galactosidase. Appl Microbiol Biotechnol 2002;58:645–50.

Domingues L, Lima N, Teixeira JA. *Aspergillus niger* β-galactosidase production by yeast in a continuous high cell density reactor. Process Biochem 2005;40:1151-4.

Domizio P, Romani C, Lencioni L, Comitini F, Gobbi M, Mannazu I, et al. Outlining a future for non-*Saccharomyces* yeasts: Selection of putative spoilage wine strains to be used in association with *Saccharomyces cerevisiae* for grape juice fermentation. Int J Food Microbiol 2010;147:170–80.

Dünkler A, Wendland J. Use of *MET3* promoters for regulated gene expression in *Ashbya gossypii*. Curr Genet 2007;52:1–10.

Ernst & Young. Beyond Borders: Staying in Course. Ernst & Young Annual Biotech Report 2017 (Ernst & Young, New York, 2017). https://www.ey.com/Publication/vwLUAssets/ey-biotechnology-report-2017-beyond-borders-staying-the-course/$FILE/ey-biotechnology-report-2017-beyond-borders-staying-the-course.pdf.

Farries EHM, Bell AF. On the metabolism of *Nematospora gossypii* and related fungi, with special reference to the source of nitrogen. Ann Bot 1930;44:423–55.

Fitzpatrick DA, Logue ME, Stajich JE, Butler G. A fungal phylogeny based on 42 complete genomes derived from supertree and combined gene analysis. BMC Evol Biol 2006;6:99.

Fontanille P, Kumar V, Christophe G, Nouaille R, Larroche C. Bioconversion of volatile fatty acids into lipids by the oleaginous yeast *Yarrowia lipolytica*. Bioresour Technol 2012;114:443–9.

Förster C, Marienfeld S, Wendisch VF, Krämer R. Adaptation of the filamentous fungus *Ashbya gossypii* to hyperosmotic stress: different osmoresponse to NaCl and mannitol stress. Appl Microbiol Biotechnol 1998;50:219–26.

Föster C, Santos M, Ruffert S, Krämer R, Revuelta JL. Physiological consequence of disruption of the *VMA1* gene in the riboflavin overproducer *Ashbya gossypii*. J Biol Chem 1999;274:9442–48.

Fragoso RG, Ciferri R. Hongos parasitos y saprifitos de la Republica Dominicana. Boll R Soc Espan Hist Nat 1928;28:377–88.

Gladfelter AS, Hungerbuehler AK, Philippsen P. Asynchronous nuclear division cycles in multinucleated cells. J Cell Biol 2006;3:347–62

Goddard MR, Greig D. *Saccharomyces cerevisiae*: a nomadic yeast with no niche? FEMS Yeast Res 2015;15:3.

Gomes D, Aguiar TQ, Dias O, Ferreira EC, Domingues L, Rocha I. Genome wide metabolic re-annotation of *Ashbya gossypii*: new insights into its metabolism through a comparative analysis with *Saccharomyces cerevisiae* and *Kluyveromyces lactis*. BMC Genomics 2014;15:810.

Goodman JJ, Ferrera RR. Synthesis of riboflavin by *Ashbya gossypii* grown in a synthetic medium. Mycologia 1954;46:556.

Grünler A, Walther A, Lämmel J, Wendland J. Analysis of flocculins in *Ashbya gossypii* reveals *FIG2* regulation by *TEC1*. Fungal Genet Biol 2010;47:619–628.

Guilliermond A. Recherches sur quelques Ascomycetes inferieurs isoles de la Stigmatomycose des graines de Cotonnier. Essai sur la phylogenie des Ascomycetes. Rev Gen Bot 1928;40:328–42; 397–414; 474–85; 555–74; 606–24; 690–704.

Hashimoto K, Yoshizawa AC, Okuda S, Kuma K, Goto S, Kanehisa M. The repertoire of desaturases and elongases reveals fatty acid variations in 56 eukaryotic genomes. J Lipid Res 2008;49:183–191

Jiménez A, Santos MA, Pompejus M, Revuelta JL. Metabolic engineering of the purine pathway for riboflavin production in *Ashbya gossypii*. Appl Environ Microbiol 2005;71:5743–51.

Jiménez A, Santos MA, Revuelta JL. Phosphoribosyl pyrophosphate synthetase activity affects growth and riboflavin production in *Ashbya gossypii*. BMC Biotechnol 2008;8:67–78.

Karos M, Vilariño C, Bollschweiler C, Revuelta JL. A genome-wide transcription analysis of a fungal riboflavin overproducer. J Biotechnol 2004;113:69–76.

Käsler B, Sahm H, Stahmann KP, Schmidt G, Boeddecker B, Seulberger H. Riboflavin-production process by means of microorganisms with modified isocitrate lyase activity. WO Patent No. 1997/03208 A

Kato T, Park EY. Expression of alanine:glyoxylate aminotransferase gene from *Saccharomyces cerevisiae* in *Ashbya gossypii*. Appl Microbiol Biotechnol 2006;71:46–52.

Kato T, Park EY. Riboflavin production by *Ashbya gossypii*. Biotechnol Lett 2012;34:611–18.

Kaufmann A. A plasmid collection for PCR-based gene targeting in the filamentous ascomycete *Ashbya gossypii*. Fungal Genet Biol 2009;46:595–603.

Kaufmann A, Philippsen P. Of Bars and Rings: Hof1-Dependent Cytokinesis in Multiseptated Hyphae of *Ashbya gossypii*. Mol Cell Biol 2009;29:771–83.

Kavitha S, Chandra TS. Effect of vitamin E and menadione supplementation on riboflavin production and stress parameters in *Ashbya gossypii*. Proc Bio 2009;44:934–8.

Kavitha S, Chandra TS. Oxidative Stress Protection and Glutathione Metabolism in Response to Hydrogen Peroxide and Menadione in Riboflavinogenic Fungus *Ashbya gossypii*. Appl Biochem Biotechnol 2014;174:2307–25

Knechtle P, Dietrich F, Philippsen P. Maximal polar growth potential depends on the polarisome component AgSpa2 in the filamentous fungus *Ashbya gossypii*. Mol Biol Cell 2003;14:4140–54.

Köhli M, Galati V, Boudier K, Roberson RW, Philippsen P. Growth-speed-correlated localization of exocyst and polarisome components in growth zones of *Ashbya gossypii* hyphal tips. J Cell Sci 2008;121:3878–89.

Kögl F, Fries N. Uber den einfluss von biotin, aneurin, und meso-inosit auf das Wachstum verschiedenen Pilzarten. 26. Mitteil-ung iiber pflanzliche wachstumstoffe. Ztschr Physiol Chem 1937;249:93–110.

Kurtzman CP. Relationships among the genera *Ashbya*, *Eremothecium*, *Holleya*, and *Nematospora* determined from rDNA sequence divergence. J Industr Microbiol 1995;14:523–30.

Kutsal T, Özbas MT. Microbial production of vitamin B2 (riboflavin). In: Vandamme EJ, editor. Biotechnology of Vitamins, Pigments and Growth Factors. London: Elsevier; 1989. p. 149–66.

Ledesma-Amaro R, Santos MA, Jiménez A, Revuelta JL. Strain design of *Ashbya gossypii* for single-cell oil production. Appl Environ Microbiol 2014a;80:1237–44.

Ledesma-Amaro R, Kerkhoven EJ, Revuelta JL, Nielsen J. Genome scale metabolic modeling of the riboflavin overproducer *Ashbya gossypii*. Biotechnol Bioeng 2014b;111:1191–9.

Ledesma-Amaro R, Santos MA, Jiménez A, Revuelta JL, Tuning single-cell oil production in *Ashbya gossypii* by engineering the elongation and desaturation systems. Biotechnol Bioeng 2014c;111:1782–91.

Ledesma-Amaro R, Buey RM, Revuelta JL. Increased production of inosine and guanosine by means of metabolic engineering of the purine pathway in *Ashbya gossypii*. Microb Cell Fact 2015a;14:58.

Ledesma-Amaro R, Serrano-Amatriain C, Jiménez A, Revuelta JL. Metabolic engineering of riboflavin production in *Ashbya gossypii* through pathway optimization. Microb Cell Fact 2015b;14:163.

Ledesma-Amaro R, Buey RM, Revuelta JL. The filamentous fungus *Ashbya gossypii* as a competitive industrial inosine producer. Biotechnol Bioeng 2016;113:2060–3.

Lim SH, Choi JS, Park EY. Microbial production of riboflavin using riboflavin overproducers, *Ashbya gossypii*, *Bacillus subtilis*, and *Candida famate*: An Overview. Biotechnol Bioprocess Eng 2001;6:75–88.

Lizama G, Moguel-Salazar F, Peraza-Luna F, Ortiz-Vázquez E. Riboflavin production from mutants of *Ashbya gossypii* utilising orange rind as a substrate. Ann Microbiol 2007;57:157–161.

Lozano-Martínez P, Buey RM, Ledesma-Amaro R, Jiménez A, Revuelta JL. Engineering Ashbya gossypii strains for de novo lipid production using industrial by-products. Microb Biotechnol 2017;10:425–33.

Maeting I, Schmidt G, Sahm H, Revuelta JL, Stierhofd YD, Stahmanna KP. Isocitrate lyase of *Ashbya gossypii* – transcriptional regulation and peroxisomal localization. FEBS Lett 1999;444:15–21.

Maeting I, Schmidt G, Sahm H, Stahmanna KP. Role of a peroxisomal NADP-specific isocitrate dehydrogenase in the metabolism of the riboflavin overproducer *Ashbya gossypii*. J Mol Catal B: Enzym 2000;10:335–43.

Magalhães F, Aguiar TQ, Oliveira C, Domingues L. High-level expression of *Aspergillus niger* β-

galactosidase in *Ashbya gossypii*. Biotechnol Prog 2014;30:261–8.

Mateos L, Jiménez A, Revuelta J, Santos M. Purine biosynthesis, riboflavin production, and trophic phase span are controlled by a Myb-related transcription factor in the fungus *Ashbya gossypii*. Appl Environ Microbiol 2006;72:5052–60.

Mickelson MN. The metabolism of glucose by *Ashbya gossypii*. J Bacteriol 1950;59:559–566.

Mickelson MN, Schuler MN. Oxidation of acetate by *Ashbya gossypii*. J Bacteriol 1953;65:297–304.

Monschau N, Sahm H, Stahmann KP. Threonine aldolase overexpression plus threonine supplementation enhanced riboflavin production in *Ashbya gossypii*. Appl Environ Microbiol 1998;64:4283–90.

Morrissey JP, Etschmann MMW, Schrader J, de Billerbeck GM. Cell factory applications of the yeast *Kluyveromyces marxianus* for the biotechnological production of natural flavour and fragrance molecules. Yeast 2015;32:3–16.

Nattrass L, Biggs C, Bauen A, Parisi C, Rodríguez-Cerezo E, Gómez-Barbero M. The EU bio-based industry: Results from a survey. EUR 27736 EN; doi:10.2791/806858.

Nieland S, Stahmann KP. A developmental stage of hyphal cells shows riboflavin overproduction instead of sporulation in *Ashbya gossypii*. Appl Microbiol Biotechnol 2013;97:10143–53.

Nielsen J, Keasling JD. Engineering Cellular Metabolism. Cell 2016;164:1185–97.

Nikolaou E, Agrafioti I, Stumpf M, Quinn J, Stansfield I, Brown AJP. Phylogenetic diversity of stress signalling pathways in fungi. Bmc Evol Biol 2009;9:44.

Oliveira C, Teixeira JA, Lima N, Da Silva N, Domingues L. Development of a stable flocculent *Saccharomyces cerevisiae* strain for continuous *Aspergillus niger* β-galactosidase production. J Biosci Bioeng 2007;103:318-24.

Özbas MT, Kutsal T. Comparative study of riboflavin production from two microorganisms: *Eremothecium ashbyi* and *Ashbya gossypii*. Enzyme Microb Technol 1986;8:593–6.

Paddon CJ, Keasling JD. Semi-synthetic artemisinin: a model for the use of synthetic biology in pharmaceutical development. Nat Rev Microbiol 2014;12:355–67.

Park EY, Zhang JH, Tajima S, Dwiarti L. Isolation of *Ashbya gossypii* mutant for an improved riboflavin production targeting for biorefinery technology. J Appl Microbiol 2007;103:468–76.

Park EY, Ito Y, Nariyama M, Sugimoto T, Lies D, Kato T. The improvement of riboflavin production in *Ashbya gossypii* via disparity mutagenesis and DNA microarray analysis. Appl Microbiol Biotechnol 2011;91:1315–26.

Perez-Nadales E, Nogueira MFA, Baldin C, Castanheira S, El Ghalid M, Grund E. Fungal model systems and the elucidation of pathogenicity determinants. Fungal Genet Biol 2014;70:42–67.

Perlman D. Microbial Process for riboflavin production. In: Pepplev HJ, Pevlman, D, editors. Microbial technology. New York: Academic Press; 1979. p. 521–7.

Pfeifer VF, Tanner FW, Vojnovich C, Traufler DH. Riboflavin by fermentation with *Ashbya gossypii*. Ind Eng Chem 1950;42:1776–81.

Pompejus M, Revuelta JL, Santos MA. Orotidine-5'-phosphate decarboxylase-gene, gene construct containing said gene and the utilization thereof. WO Patent No. 1999/036432.

Pridham TG, Raper KB. *Ashbya gossypii* – Its significance in nature and in the laboratory. Mycologia 1950;42:603–23.

Pridham TG, Raper KB. Studies on variation and mutation in *Ashbya gossypii*. Mycologia 1952;44:452–69.

Ramakrishnan S, Hartley BS. Fermentation of lactose by yeast cells secreting recombinant fungal lactase. Appl Environ Microbiol 1993;59:4230–5.

Ravasio D, Wendland J, Walther A. Major contribution of the Ehrlich pathway for 2-phenylethanol/rose flavor production in *Ashbya gossypii*. FEMS Yeast Res 2014;14:833-44

Read ND. Exocytosis and growth do not occur only at hyphal tips. Mol Microbiol 2011;81:4–7.

Revuelta JL, Santos MA, Pompejus M, Seulberger, H. Promoter from *Ashbya gossypii*. WO Patent No. 1999/033993.

Revuelta JL, Ledesma-Amaro R, Lozano-Martinez P, Díaz-Fernández D, Buey RM, Jiménez A. Bioproduction of riboflavin: a bright yellow history. J Ind Microbiol Biotechnol 2017;44:659–65.

Ribeiro O, Wiebe M, Ilmén M, Domingues L, Penttilä M. Expression of *Trichoderma reesei* cellulases CBHI and EGI in *Ashbya gossypii*. Appl Microbiol Biotechnol 2010;87:1437–46.

Ribeiro O, Domingues L, Penttilä M, Wiebe MG. Nutritional requirements and strain heterogeneity in *Ashbya gossypii*. J Basic Microbiol 2012;52:582–9.

Ribeiro O, Magalhães F, Aguiar TQ, Wiebe MG, Penttilä M, Domingues L. Random and direct mutagenesis to enhance protein secretion in *Ashbya gossypii*. Bioengineered 2013;4:1-10.

Rosenberg J, Commichau FM. Harnessing Underground Metabolism for Pathway Development. Trends Biotechnol 2019;37:29–37.

Santos MA, Mateos L, Stahmann KP, Revuelta JL. Insertional Mutagenesis in the Vitamin B_2 Producer Fungus *Ashbya gossypii*. Methods Biotechnol 2005;18:283–300.

Schade D, Walther A, Wendland J. The development of a transformation system for the dimorphic plant pathogen *Holleya sinecauda* based on *Ashbya gossypii* DNA elements. Fungal Genet Biol 2003;40:65–71.

Schlösser T, Schmidt G, Stahmann KP. Transcriptional regulation of 3,4-dihydroxy-2-butanone 4-phosphate synthase. Microbiology 2001;147:3377–86.

Schlösser T, Wiesenburg A, Gätgens C, Funke A, Viets U, Vijayalakshmi S, et al. Growth stress triggers riboflavin overproduction in *Ashbya gossypii*. Appl Microbiol Biotechnol 2007;76:569–78.

Schlüpen C, Santos MA, Weber U, De Graaf A, Revuelta JL, Stahmann KP. Disruption of the *SHM2* gene, encoding one of two serine hydroxymethyltransferase isozymes, reduces the flux from glycine to serine in *Ashbya gossypii*. Biochem J 2003;369:263–73.

Schmidt G, Stahmann KP, Kaesler B, Sahm H. Correlation of isocitrate lyase activity and riboflavin formation in the riboflavin overproducer *Ashbya gossypii*. Microbiology 1996a;142:419–26.

Schmidt G, Stahmann KP, Sahm H. Inhibition of purified isocitrate lyase identified itaconate and oxalate as potential antimetabolites for the riboflavin overproducer *Ashbya gossypii*. Microbiology 1996b;142:411–7.

Schmitz HP, Philippsen P. Evolution of multinucleated *Ashbya gossypii* hyphae from a budding yeast-like ancestor. Fungal Biol 2011;115:557–68.

Schwechheimer SK, Becker J, Peyriga L, Portais JC, Sauer D, Müller R, et al. Improved riboflavin production with *Ashbya gossypii* from vegetable oil based on 13C metabolic network analysis with combined labeling analysis by GC/MS, LC/MS, 1D, and 2D NMR. Metab Eng 2018a;47:357–73.

Schwechheimer SK, Becker J, Peyriga L,, Portais JC, Wittmann C. Metabolic flux analysis in *Ashbya gossypii* using 13C-labeled yeast extract: industrial riboflavin production under complex nutrient conditions. Microb Cell Fact 2018b;17:162.

Schwechheimer SK, Park EY, Revuelta JL, Becker J, Wittmann C. Biotechnology of riboflavin. Appl Microbiol Biotechnol. 2016;100:2107–19.

Serrano-Amatriain C, Ledesma-Amaro R, López-Nicolás R, Ros G, Jiménez A, Revuelta JL. Folic Acid Production by Engineered Ashbya gossypii. Metab Eng 2016;38:473–82.

Smiley KL, Sobolov M, Austin FL, Rasmussen RA, Smith MB, van Lanen JM, et al. Biosynthesis of riboflavin, *L. bulgaricus* factor, and other growth factors. Laboratory and pilot plant studies of biosynthesis by *A. gossypii* cultivated on grain stillage media. Ind Eng Chem 1951;43:1380–4.

Silva R, Aguiar TQ, Domingues L. Blockage of the pyrimidine biosynthetic pathway affects riboflavin production in *Ashbya gossypii*. J Biotechnol 2015;193:37–40.

Stahmann KP, Kupp C, Feldmann SD, Sahm H. Formation and degradation of lipid bodies found in the riboflavin-producing fungus *Ashbya gossypii*. Appl Microbiol Biotechnol 1994;42:121–7.

Stahmann KP, Böddecker T, Sahm H. Regulation and properties of a fungal lipase showing interfacial inactivation by gas bubbles, or droplets of lipid or fatty acid. Eur J Biochem 1997;244:220–5.

Stahmann KP, Revuelta JL, Suelberger H. Three biotechnical process using *Ashbya gossypii*, *Candida famata*, or *Bacillus subtilis* compete with chemical riboflavin production. Appl Microbiol Biotechnol 2000;53:509–16.

Stahmann KP, Arst Jr HN, Althöfer H, Revuelta JL, Monschau N, Schlüpen C, et al. Riboflavin, overproduced during sporulation of *Ashbya gossypii*, protects its hyaline spores against ultraviolet light. Environ Microbiol 2001;3:545–50

Steiner S, Philippsen P. Sequence and promoter analysis of the highly expressed *TEF* gene of the filamentous fungus *Ashbya gossypii*. Mol Gen Genet 1994;242:263–71.

Steiner S, Wendland J, Wright MC, Philippsen P. Homologous recombination as the main mechanism for DNA integration and cause of rearrangements in the filamentous ascomycete *Ashbya gossypii*. Genetics 1995;140:973–87.

Sugimoto T, Kanamasa S, Kato T, Park EY. Importance of malate synthase in the glyoxylate cycle of *Ashbya gossypii* for the efficient production of riboflavin. Appl Microbiol Biotechnol 2009;83:529–39.

Sugimoto T, Morimoto A, Nariyama M, Kato T, Park EY. Isolation of an oxalate-resistant *Ashbya gossypii* strain and its improved riboflavin production. J Ind Microbiol Biotechnol 2010;37:57–64.

Sugimoto T, Kato T, Park EY. Functional analysis of cis-aconitate decarboxylase and trans-aconitate metabolism in riboflavin-producing filamentous *Ashbya gossypii*. J Biosci Bioeng 2014;117:563–8.

Tajima S, Itoh Y, Sugimoto T, Kato T, Park EY. Increased riboflavin production from activated bleaching earth by a mutant strain of *Ashbya gossypii*. J Biosci Bioeng 2009;108:325–9.

Tanner FW Jr, Vojnovich C, Van Lanen JM. Factors affecting riboflavin production by *Ashbya gossypii*. J Bacteriol 1949;58:737–45.

Tippmann S, Chen Y, Siewers V, Nielsen J. From flavors and pharmaceuticals to advanced biofuels: production of isoprenoids in *Saccharomyces cerevisiae*. Biotechnol J 2013;8:1435–44.

Vorapreeda T, Chinae Thammarongtham C, Cheevadhanarak S, Laoteng K. Alternative routes of acetyl-CoA synthesis identified by comparative genomic analysis: involvement in the lipid production of oleaginous yeast and fungi. Microbiology 2012;158:217–28.

Walther A, Wendland J. Apical localization of actin patches and vacuolar dynamics in *Ashbya gossypii* depend on the *WASP* homolog Wal1p. J Cell Sci 2004;117:4947-58.

Walther A, Wendland J. Yap1-dependent oxidative stress response provides a link to riboflavin production in *Ashbya gossypii*. Fungal Genet Biol 2012;49:697–707.

Wang J, He K, Xu Q, Chen N. Mutagenetic study of a novel inosine monophosphate dehydrogenase from *Bacillus amyloliquefaciens* and its possible application in guanosine production. Biotechnol Biotechnol Equip 2014;28:102–6.

Wang H, Xu Z, Gao L, Hao B. A fungal phylogeny based on 82 complete genomes using the composition vector method. BMC Evol Biol 2009;9:195.

Wasserstrom L, Lengeler KB, Walther A, Wendland J. Molecular Determinants of Sporulation in *Ashbya gossypii*. Genetics 2013;195:87-99.

Wasserstrom L, Lengeler K, Walther A, Wendland J. Developmental growth control exerted via the A kinase *Tpk2* in *Ashbya gossypii*. Eukaryot Cell 2015;doi:10.1128/EC.00045-15.

Wei S, Hurley J, Jiang Z, Wang S, Wang Y. Isolation and characterization of an *Ashbya gossypii* mutant for improved riboflavin production. Braz J Microbiol 2012;441-8

Wei S, Zheng W, Zhao F, Jiang Z, Zhou D. Microbial conversion of waste cooking oil into riboflavin by *Ashbya gossypii*. Biosci J 2013;29:1000-6.

Wendland J, Ayad-Durieux Y, Knechtle P, Rebischung C, Philippsen P. PCR-based gene targeting in the filamentous fungus *Ashbya gossypii*. Gene 2000;242:381–91.

Wendland J, Philippsen P. Determination of cell polarity in germinated spores and hyphal tips of the filamentous ascomycete *Ashbya gossypii* requires a rhoGAP homolog. J Cell Sci 2000;113:1611–21.

Wendland J, Philippsen P. Cell polarity and hyphal morphogenesis are controlled by multiple Rho-protein modules in the filamentous ascomycete *Ashbya gossypii*. Genetics 2001;157:601–10.

Wendland J, Walther A. *Ashbya gossypii*: a model for fungal developmental biology. Nat Rev Microbiol 2005;3:421–9.

Wendland J, Walther A. Genome evolution in the *Eremothecium* clade of the *Saccharomyces* complex revealed by comparative genomics. G3 (Bethesda) 2011;1:539–48.

Wendland J, Dünkler A, Walther A. Characterization of α-factor pheromone and pheromonereceptor genes of *Ashbya gossypii*. FEMS Yeast Res 2011;11:418–29.

Wendland J, Walther A. Chromosome number reduction in *Eremothecium coryli* by two telomere-to-telomere fusions. Genome Biol Evol 2014;6:1186–98.

Wickerham LS, Flickinger MH, Johnson RM. Production of riboflavin by *Ashbya gossypii*. Arch Biochem 1946;9:95–8.

Wright MC, Philippsen P. Replicative transformation of the filamentous fungus *Ashbya gossypii* with plasmids containing *Saccharomyces cerevisiae* ARS elements. Gene 1991;109:99–105.

zu Berstenhorst SM, Hohmann HP, Stahmann KP. Vitamins and vitamin-like compounds: microbial production. In: Schaechter M, editor. Encyclopedia of Microbiology. Oxford: Academic Press; 2009. p. 549–61.

CHAPTER II

Light exposure during growth increases riboflavin production, ROS accumulation and DNA damage in *Ashbya gossypii* riboflavin-overproducing strains

The work reported on this chapter was published in:

Silva R, Aguiar TQ, Oliveira R, Domingues L. Light exposure during growth increases riboflavin production, ROS accumulation and DNA damage in *Ashbya gossypii* riboflavin-overproducing strains. FEMS Yeast Res 2019;19:foy114.

Abstract

The overproduction of riboflavin (vitamin B_2) by *Ashbya gossypii*, one of the most distinctive traits of this filamentous hemiascomycete, has been proposed to act as an ecological defence mechanism, since it is triggered by environmental stress. The interaction of endogenous riboflavin with light generates reactive oxygen species (ROS) and induces oxidative DNA damage in mammalian cells, but exogenous riboflavin was shown to protect *A. gossypii* spores against UV light. Envisioning a better understanding of this biotechnologically relevant trait, here we investigated the putative genotoxic effects associated with the overproduction of riboflavin by *A. gossypii*. For assessing that we developed the *Ashbya* Comet Assay, which was able to reproducibly measure oxidative (H_2O_2/menadione-mediated) and non-oxidative (camptothecin-mediated) DNA damage in *A. gossypii*. Using this protocol, we determined that exposure to sunlight-mimicking light during growth significantly increased the DNA damage accumulation in riboflavin-overproducing cells, but not in non-overproducing ones. The exposure of overproducing cells to light induced the intracellular accumulation of ROS and increased the production of riboflavin 1.5-fold. These results show that riboflavin-overproducing strains are highly susceptible to photo-induced oxidative DNA damage and draw attention for the importance of controlling the exposure to light of biotechnological riboflavin production processes with *A. gossypii*.

2.1 Introduction

A. gossypii occurrence in nature is as a plant wound pathogen in the warmer parts of the planet (*e.g.*, cotton plants in the tropics), usually in close relationship with certain plant-feeding insects (Aguiar et al., 2015). The overproduction of riboflavin (vitamin B_2) by *A. gossypii*, which is one of the most distinctive traits of this filamentous hemiascomycete, has been connected with sporulation and stress, and is thought to represent an ecological advantage for both the fungus and its insect vectors, by conferring them protection against plant defences. Both nutritional (Schlösser et al., 2007) and oxidative stress (Kavitha and Chandra, 2014; Walther and Wendland, 2012) can trigger riboflavin production in *A. gossypii*. Oxidative stress-inducing agents, such as H_2O_2 and menadione, have been shown to concomitantly increase riboflavin production and standard antioxidant defence mechanisms (Kavitha and Chandra, 2014), which are driven by an *Yap1*-dependent response (Walther and Wendland, 2012). Moreover, riboflavin was reported to have a protective effect for the spores of *A. gossypii* against ultraviolet (UV) light (Stahmann et al., 2001), as its addition to spore suspensions was shown to improve their UV resistance. However, riboflavin is a strong photosensitizer that upon interaction with UV light generates reactive oxygen species (ROS), which can cause oxidative damage to both DNA and proteins (Alam et al., 2015). Therefore, endogenous riboflavin in excess can become harmful to the cells, an effect that was already reported in several organisms, such as bacteria and mammalians (Alam et al., 2015; Besaratinia et al., 2007; Lloyd et al., 1990). Nevertheless, despite this well-recognized photo-induced cytotoxicity of riboflavin, until the date there are no studies investigating the potential genotoxic effects of riboflavin in *A. gossypii* overproducing strains.

The Comet Assay (Single Cell Gel Electrophoresis) is a simple, sensitive and versatile technique for measuring DNA damage (Collins, 2004). It has been applied to a wide variety of organisms (such as human cells, insects, plants and fungi) as a standard procedure for a wide range of applications, such as compounds' genotoxicity testing, ecological monitoring (environmental risk assessment), human studies (biomonitoring and nutritional studies), DNA repair studies, among others (Azevedo et al., 2011; Collins, 2004; Langie et al., 2015). The first report of this methodology is dated of 1984, when Ostling and Johanson used the Comet Assay to investigate the effect of radiation on the DNA damage of individual mammalian cells (Ostling and Johanson, 1984). The theoretical scientific basis of this technique consists on the relaxation of the negative supercoiling of genomic DNA when lesions (such as single strand breaks) are present, which increases its mobility when an electric field is applied. Thus, it is possible to establish a

direct correlation between the electrophoretic mobility of the DNA and the level of damage present (Collins, 2004; Oliveira and Johansson, 2012).

Given the photosensitizer role of riboflavin and the connection of its overproduction by *A. gossypii* with environmental stress, it was our objective to understand whether riboflavin itself may act as a stressor for this filamentous fungus and under what conditions. Therefore, envisioning a better understanding of this relevant trait, here we investigated the putative genotoxic effects associated with the interaction between riboflavin and light in overproducing and non-overproducing *A. gossypii* strains. In this context, a Comet Assay protocol was developed for assessing DNA damage in *A. gossypii*.

2.2 Material and methods

2.2.1 Strains and media

The *A. gossypii* strains ATCC 10895, kindly provided by Prof. Peter Philippsen (University of Basel), and A8 (Ledesma-Amaro et al., 2015), kindly provided by Prof. Jose Luis Revuelta (University of Salamanca), were used throughout this study. Stock cultures of these strains were kept as spores suspended in spore buffer containing 200 g/L glycerol, 8 g/L NaCl and 0.25 % (v/v) Tween 20 and stored at −80 °C. Spores were prepared as previously described (Magalhães et al., 2014) with slight modifications. The mycelium was digested with 4 mg/mL of lysing enzymes from *Trichoderma harzanium* (Sigma-Aldrich) for 2-3 h at 37 °C. Agar-solidified Ashbya Full Medium (AFM; 10 g/L tryptone, 10 g/L yeast extract, 20 g/L glucose, 1 g/L myo-inositol) was used for the cultivation of *A. gossypii* strains.

2.2.2 Radial growth conditions and cell treatments

Agar-solidified AFM plates (90 mm diameter) with or without supplementation of stress agents were inoculated with 10 µL of a spore suspension of *A. gossypii* (10^7 spores/mL) and incubated at 30 °C for three days. When indicated, the following stress agents were added to AFM: hydrogen peroxide (H_2O_2; 5, 10 or 25 mM), menadione (1, 5 or 10 µM) or camptothecin (CPT; Abcam; 10, 20 or 40 µM). All agents were of analytical grade and diluted or dissolved in ultra-pure water for use at specified concentrations. When indicated, growth under light exposure was done using a fluorescent lamp (LUMILUX T5 HE, OSRAM) with an irradiance level of 16 µmol/(m^2.s), measured by a LI-250 Light Meter with a LI-190 quantum sensor (LI-COR, US). Final colony radial growth (Brancato and Golding, 1953) was determined by measuring the diameter of colonies in two perpendicular directions, through two guide lines previously drawn on the lower outer face of the plates. Images of the colony morphology were recorded at the end of the growth. Total riboflavin quantification was done as previously described (Silva et al., 2015).

2.2.3 The *Ashbya gossypii* comet assay

The *Ashbya* Comet Assay was developed using as basis the protocol of the Yeast Comet Assay (Azevedo et al., 2011; Oliveira and Johansson, 2012), which was adapted and optimized for the filamentous fungus *A. gossypii*. The resulting protocol comprised the three following steps: (1) protoplast generation, (2) buffer incubations and electrophoresis, and (3) comets' analysis.

For protoplast generation, the protocol described by Nieland and Stahmann (2013) was used with slight modifications. Mycelium from *A. gossypii* strains was harvested with a sterile loop from the areas near the edges of the colonies growing on agar-solidified AFM under different conditions and suspended in solution A (1.2 M $MgSO_4$, 10 mM Na-phosphate buffer, pH 5.8) with lysing enzymes (5 mg/mL). This mixture was incubated at 30 °C for 1 h in order to release the protoplasts. Total liberation of protoplasts was verified by microscopic analysis. Afterwards, the mixture was centrifuged at 3000 rpm for 10 min (4 °C), washed with solution B (1 M sorbitol, 10 mM Tris–HCl, pH 7.5) and the protoplasts resuspended in the same solution. To avoid the contamination of the protoplast suspension with high amounts of spores, 1 mL of paraffin oil light (AppliChem) was added, mixed by vortexing and left resting until two phases were formed. Finally, the lower phase, containing the protoplasts, was collected and diluted (1:4) in solution B.

For the buffer incubations and electrophoresis, the protoplast suspension was harvested by centrifugation at maximum speed for 5 min at 4 °C and resuspended in 1.5 % (w/v) low melting agarose (LMA; GRS Agarose LMT, grisp) at 35 °C. Immediately after, the suspensions were spread onto microscopic glass slides pre-coated with 0.5 % (w/v) melted multipurpose agarose. Next, the suspensions were covered with coverslips and the microscopic slides were kept on ice for 5 min in order to solidify the LMA, thus creating a microgel. The coverslips were removed and the slides were then submerged in lysing buffer (30 mM NaOH, 1 M NaCl, 50 mM EDTA, 10 mM Tris–HCl, 0.05 % w/v lauroylsarcosine, pH 10) for 2 h at 4 °C. Then, the slides were transferred into pre-chilled electrophoresis buffer (30 mM NaOH, 10 mM EDTA, 10 mM Tris–HCl, pH 10) and incubated for 20 min. Subsequently, in the same buffer, an electric field of 0.7 V/cm was applied for 10 min to the slides. Finally, the samples were neutralized (10 mM Tris–HCl, pH 7.4) for 10 min, fixated in ethanol 96 % (v/v) for another 10 min and left to air-dry overnight at room temperature. All the buffers were prepared just before use.

For the analysis of the comets, the microgels were stained with 10 µL of 3300-fold diluted GelRed™ (Biotium) and several representative images from the total area of the microgel were acquired by fluorescence microscopy (Leica Microsystems DM fluorescence microscope), using a magnification of 200x or 400x. The images were analysed with the CometScore software and the tail length of the comets (µm) was chosen as the parameter to measure DNA damage. Alternatively, the same software was used to determine the percentage of DNA in the comet tail, another parameter used to determine DNA damage.

2.2.4 Analysis of intracellular ROS accumulation

Cells from the areas near the edges of *A. gossypii* ATCC 10895 and A8 colonies grown in the dark or exposed to light for three days on agar-solidified AFM at 30 °C were harvested and suspended in ice-cold PBS (137 mM NaCl, 2.7 mM KCl, 4.3 mM Na_2HPO_4, 1.47 mM KH_2PO_4, pH 7.4) at a concentration of 0.04 $g_{fresh\ biomass}$/mL. The mixtures were then vortexed. Subsequently, the cell suspensions were loaded with a solution of 5 mM 2',7'-dichlorofluorescein diacetate (H_2DCFDA) to obtain a final probe concentration of 50 μM. These cell suspensions were incubated at 30 °C and 200 rpm during 1 h in the dark. In co-incubation experiments, a control was used for each condition, which consisted in the cell suspensions without the addition of H_2DCFDA. Finally, the cell suspensions were diluted five times and transferred to 96-well black microplates in order to measure the fluorescence intensity of the samples using a Synergy Mx / Cytation 3 microplate reader (Biotek) with the filters set to an excitation/emission of 494/522 nm. The controls (cell suspensions without H_2DCFDA) of each sample were used as blanks and their fluorescence intensities were subtracted from those of the samples (cell suspensions with H_2DCFDA) in order to remove any response background caused by cells or reagents. Simultaneously, aliquots of the same cell suspensions were also placed on microscopic slides and analysed independently by fluorescence microscopy (Leica Microsystems DM fluorescence microscope).

2.2.5 Statistical analyses

For the comet assay experiments, two independent assays were performed for each condition. The cells for the assays were collected from three independent cell cultures that were resuspended together in solution A. The mean of the tail length was obtained from at least forty comets (minimum of twenty comets analysed from each duplicate, as recommended by the protocol of Oliveira and Johansson, 2012). GraphPad Prism for IOS version 6.0 was used to carry out the statistical analyses. Differences were tested by one-way ANOVA followed by post-hoc Dunnett's and Tukey's multiple comparison tests (comet tail length, colony radial growth and fluorescence intensity) and by t-Test (specific riboflavin production). Statistical significance was established at $p < 0.05$ for the comparisons.

2.3 Results and discussion

2.3.1 The *Ashbya* Comet Assay is able to measure oxidative and non-oxidative DNA damage

The Comet Assay (Single Cell Gel Electrophoresis) is a technique that is based in the increased electrophoretic mobility of damaged DNA, allowing the establishment of a direct correlation between this parameter and the level of damage present in the sample (Collins, 2004; Oliveira and Johansson, 2012). Contrasting with its extensive use in higher eukaryotes for genotoxicity studies (Langie et al., 2015), it has been poorly explored and applied to microorganisms, notwithstanding the valuable outcomes obtained in the few studies published (Carmello et al., 2015; Cruz et al., 2016). In this work, a Comet Assay based on the protocol developed for *Saccharomyces cerevisiae* (Azevedo et al., 2011; Oliveira and Johansson, 2012) was adapted and optimized for use in *A. gossypii*. In order to validate this protocol, standard stress agents routinely used in this technique were used to induce oxidative (H_2O_2 and menadione) and non-oxidative (camptothecin; CPT) DNA damage in *A. gossypii*. Since *A. gossypii* grows exclusively in filamentous form, the two main alterations made to the protocol were related to life cycle differences between the two microorganisms. Therefore, for the successful application of this assay in *A. gossypii* some of the technical adaptations performed proved to be of major importance.

(i) Growth of *A. gossypii* cultures on solid media with the stress agent present from the inoculation start, contrasting with stress induction in *S. cerevisiae* that is carried out after an initial growth period in liquid medium and for a shorter period of time. This adaptation facilitated the monitoring of morphological and physiological alterations caused by the stress agents in the filamentous fungus.

(ii) During growth, spore formation starts to occur in older parts of the *A. gossypii* mycelia, which hampers the obtaining of a pure protoplasts suspension (required for the comet assay). Therefore, after protoplast formation, paraffin was added to the suspension in order to create two phases, the upper one with the hydrophobic spores and the lower with the protoplasts (Nieland and Stahmann, 2013). The omission of this step from the protocol completely compromised the assay, as the presence of spores in the sample obstructed the visualization of the comets (Appendix: Figure A2.1).

(iii) The variability observed in the control samples (*e.g.*, existence of comet tails) still captures much attention and is a central topic of discussion among the users of the comet assay (Møller et al., 2014). This variability is often associated with the presence of replication forks in the

sample or with older cells, as the culture advances towards the stationary phase (Azevedo et al., 2011). In the specific case of *A. gossypii*, not much can be done regarding the former, since this fungus owns multinucleated mycelia that divide asynchronously (Anderson et al., 2013). However, regarding the latter, collection of the older zones of the colonies (the central area corresponding to the inoculum halo) was avoided.

With the newly developed *Ashbya* Comet Assay we were able to measure the DNA damage in cells of the *A. gossypii* strain ATCC 10895 growing on media containing different concentrations of H_2O_2 (Figure 2.1). Cells exposed to this stress agent presented significantly longer comet tail lengths than the control (cells growing in the absence of H_2O_2), indicating increased DNA damage. Besides the comet tail length, the percentage of DNA in the comet tail (another independent DNA damage parameter) was measured as well, indicating also increased DNA damage in cells growing on media containing H_2O_2 (Appendix: Figure A2.2).

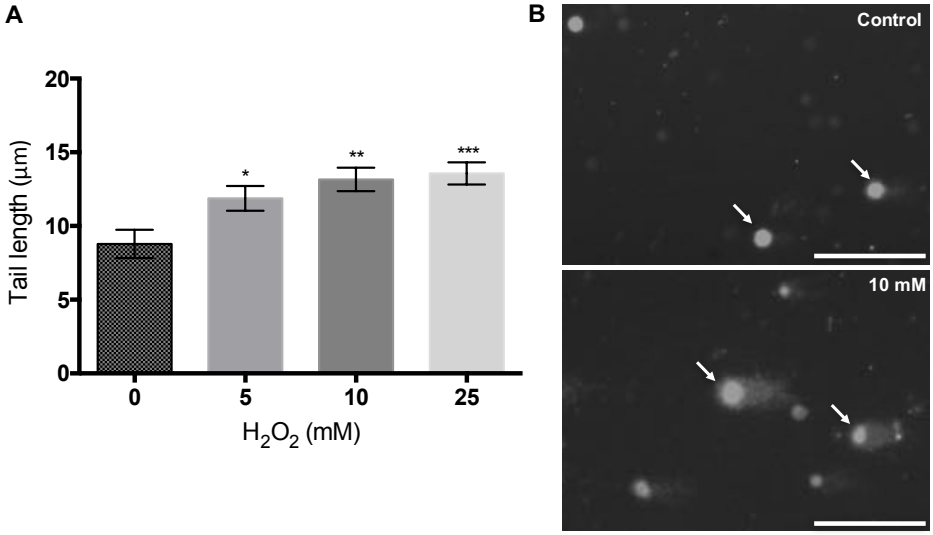


Figure 2.1. Measurement of H_2O_2-mediated oxidative DNA damage in *A. gossypii* ATCC 10895 with the *Ashbya* Comet Assay. **(A)** Data are presented as mean ± standard error of the mean of the tail length of at least forty comets obtained from two independent experiments for each concentration (as described in Materials and methods). Before harvesting, cells were grown for three days at 30 °C on agar-solidified AFM containing different concentrations of H_2O_2 (5, 10 or 25 mM). Asterisks represent significant differences compared to the control (0 mM H_2O_2). * ($p < 0.05$), ** ($p < 0.01$) and *** ($p < 0.001$). **(B)** Representative images of the comets obtained with the Comet Assay protocol adapted in this work for control cells (0 mm H_2O_2) and cells exposed to 10 mM H_2O_2. DNA was stained with GelRed™. White bar = 50 µm.

Exposure of *A. gossypii* to increasing concentrations of H_2O_2 proportionally affected its growth, as the radial growth in the presence of this compound was 92 % (5 mM), 79 % (10 mM) and 51 % (25 mM) of that of the control condition (Table 2.1).

Table 2.1. Colony radial growth of *A. gossypii* ATCC 10895 after three days of growth at 30 °C on agar-solidified AFM containing different concentrations of H_2O_2. Data are presented as mean ± standard deviation of three biological replicates. Superscript letters represent significant differences compared to the control (0 mM H_2O_2).

Condition (mM H_2O_2)	**Radial growth (mm)**
0	31 ± 1^{a}
5	28 ± 0^{d}
10	24 ± 0^{d}
25	16 ± 1^{e}

a,d – $p < 0.001$; a,e – $p < 0.0001$

DNA damage caused by two additional stress agents, menadione (oxidative) and CPT (non-oxidative), could also be measured with the *Ashbya* Comet Assay. Similar to H_2O_2, menadione causes DNA damage through a ROS mechanism, whereas CPT causes strand breaks through the inhibition of DNA topoisomerase I (Liu et al., 2000). Longer comet tails were detected in cells exposed to these two types of stress agents, with all the concentrations tested presenting significant differences compared to the control (Figure 2.2). Once again, the percentage of DNA in the comet tail corroborated the results obtained with the comet tail length, with the single exception for the concentration of 1 µM of menadione (Appendix: Figure A2.3). In this condition, although a higher percentage of DNA in the comet tail (21.0 ± 11.6 %) was observed, the difference to the control (14.1 ± 10.6 %) was not statistically significant. Contrary to H_2O_2, these stress agents did not affect the radial growth of *A. gossypii* at the concentrations tested (Appendix: Table A2.1). Altogether, these results support the reproducibility of this new protocol, validating it for measuring oxidative and non-oxidative DNA damage.

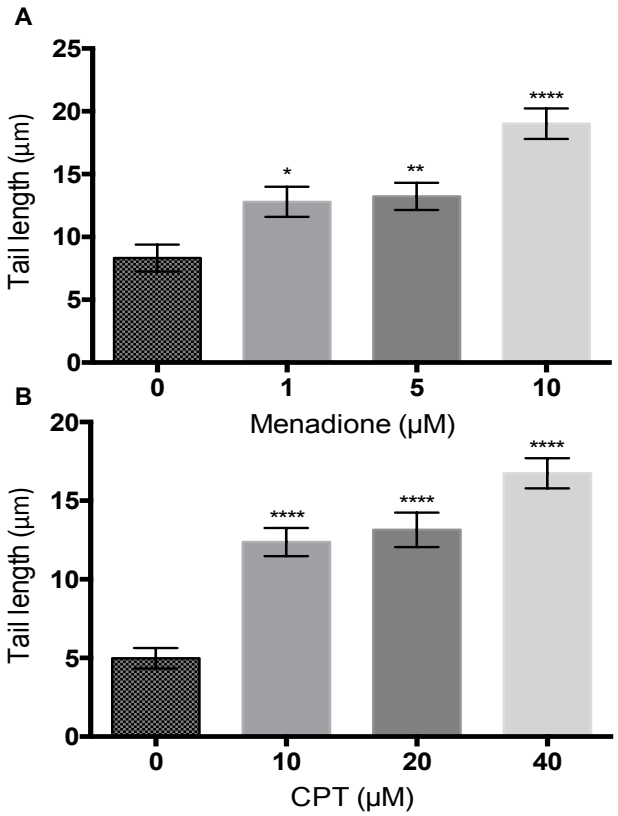


Figure 2.2. Exposure to **(A)** menadione (oxidative agent) or **(B)** camptothecin (CPT; non-oxidative agent) induces DNA damage in *A. gossypii* ATCC 10895. Data are presented as mean ± standard error of the mean of the tail length of at least forty comets obtained from two independent experiments for each concentration (as described in Materials and methods). Before harvesting, cells were grown for three days at 30 °C on agar-solidified AFM containing different concentrations of menadione (1, 5 or 10 µM) and CPT (10, 20 or 40 µM). Asterisks represent significant differences compared to the control (0 µM menadione/CPT). * ($p < 0.05$), ** ($p < 0.01$) and **** ($p < 0.0001$).

The Comet Assay protocol optimized here is the first developed for use in *A. gossypii*, offering a reliable and flexible way to study chemicals' genotoxicity. To the extent of our knowledge, only two other protocols were developed for filamentous fungi over the last 15 years, *Neurospora crassa* (Bhanoori and Venkateswerlu, 1998) and *Sordaria macrospora* (Hahn and Hock, 1999). Since *A. gossypii* is one of the most sensitive fungal species to oxidative stress (Nikolaou et al., 2009), a trait that is closely related with riboflavin overproduction (Kavitha and Chandra, 2014; Walther and Wendland, 2012), this protocol becomes a very useful tool to study the unexplored link between genome integrity and riboflavin overproduction in this filamentous fungus.

2.3.2 Light exposure during growth affects riboflavin production and increases DNA damage and intracellular oxidation in *A. gossypii*

Aiming its biotechnological exploitation, the key reactions and pathways for riboflavin overproduction in *A. gossypii* have been studied at extremely comprehensive levels (Aguiar et al., 2015). On the other hand, the regulatory and ecological mechanisms behind this trait remain largely unknown. The overproduction of riboflavin by *A. gossypii* has been assumed as a stress response of the fungus due to its connection with oxidative stress (Kavitha and Chandra, 2014; Walther and Wendland, 2012) and has also been suggested to benefit the fungus by protecting its spores against UV-irradiation (Stahmann et al., 2001). However, the interaction of endogenous riboflavin with UV light is known to cause cellular damages, particularly at the DNA level (Alam et al., 2015; Besaratinia et al., 2007; Lloyd et al., 1990). Thus, to assess the effects of riboflavin overproduction on the *A. gossypii* genome integrity, after validation of the *Ashbya* Comet Assay, it was used to measure the DNA damage in two different strains: the sequenced strain ATCC 10895 and the riboflavin-overproducing strain A8, which also produce high amounts of alcohols as VOCs compared with other *A. gossypii* strains (as observed in Chapter V). For this work, it is worth of noting that strain A8 is able to produce up to 10-fold more riboflavin than strain ATCC 10895 (Table 2.2).

Table 2.2. Colony radial growth and specific riboflavin production for the *A. gossypii* strains ATCC 10895 and A8, measured after three days of growth on agar-solidified AFM at 30 °C, in the dark or exposed to light. Data are presented as mean ± standard deviation of at least five biological replicates. Superscript letters represent significant differences between specific riboflavin productions by the same strain under different conditions.

Strain (condition)	Radial growth (mm)	Riboflavin ($mg/g_{dry\ weight}$)
ATCC 10895	28 ± 1	2 ± 1
ATCC 10895 (light)	26 ± 2	2 ± 1
A8	16 ± 2	15 ± 3[a]
A8 (light)	17 ± 1	22 ± 3[c]

a,c – $p < 0.01$

To investigate the influence of light on DNA damage, these strains were incubated in the dark or under exposure to a fluorescent lamp emitting light with a spectral wavelength distribution close to that of the sunlight (Tarrant, 1968). While no differences were detected between the comet tail length of the two strains when they were grown in the dark, significantly longer comet tails were observed in strain A8 when exposed to light in comparison with strain ATCC 10895 under the same condition (Figure 2.3).

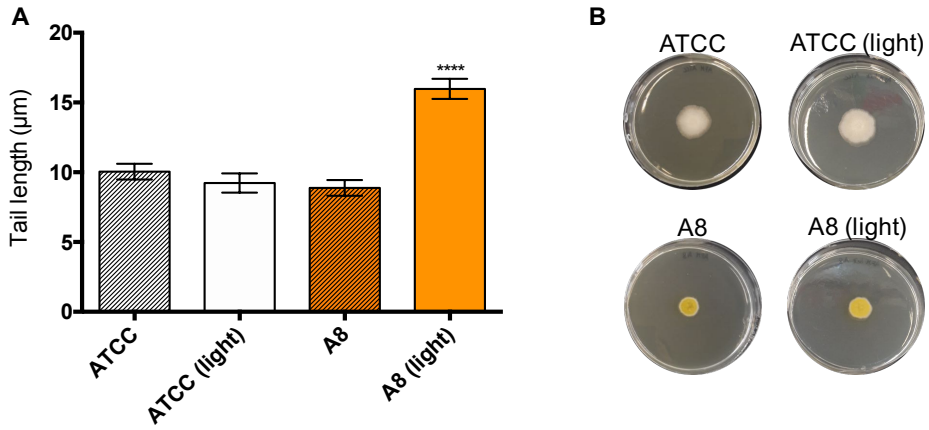


Figure 2.3. Exposure to light during growth induces DNA damage in the *A. gossypii* riboflavin-overproducing strain A8, but not in strain ATCC 10895. **(A)** Data are presented as mean ± standard error of the mean of the tail length of at least forty comets obtained from two independent experiments for each condition (as described in "Materials and methods"). Before harvesting, cells were grown for three days on agar-solidified AFM at 30 °C, in the dark or exposed to light. Asterisks represent significant differences between strains and conditions. **** ($p < 0.0001$). **(B)** Representative images of the colonies from where cells were harvested for DNA damage measurement with the *Ashbya* Comet Assay.

The filamentous fungus *A. gossypii* occurs in nature mainly in the warmer parts of the planet and therefore its exposure to light (sunlight) should be high (Stahmann et al., 2001; Dietrich et al., 2013). The results obtained here with light, at intensity near to that used to maintain microalgae cultures (Fernandes et al., 2013), strongly indicate that the overproduction of riboflavin increases the accumulation of DNA damage. The role of riboflavin as a photosensitizer with effects at the physiological and molecular levels was already reported in microorganisms (Lloyd et al., 1990) and in higher eukaryotes (Alam et al., 2015; Besaratinia et al., 2007). In their work with *E. coli*, Lloyd and colleagues (Lloyd et al., 1990) demonstrated that a riboflavin auxotrophic strain exposed to a broad spectrum of near-UV light (320–400 nm) presented decreased survival rates when subjected to non-limiting riboflavin supplementation, as compared to limiting riboflavin

supplementation. In turn, the survival rates of the parental strain (prototrophic for riboflavin) were practically unaffected by this type of light exposure when subjected to the same supplementation conditions. Therefore, the susceptibility of this auxotrophic strain to the photosensitizer effects of riboflavin should derive from its necessity to uptake riboflavin from the medium (Lloyd et al., 1990). When exposed to a similar light spectrum, embryonic fibroblasts of mice treated with riboflavin displayed increased DNA damage compared to non-treated ones (Besaratinia et al., 2007). Moreover, diabetic mice treated with riboflavin and exposed to a fluorescent lamp also accumulated more DNA damage than those without treatment (Alam et al., 2015). Thus, one can assume that the accumulation of riboflavin by vegetative cells of *A. gossypii* may act as a stressor when light exposure is not avoided.

Following the reported indications that riboflavin acts as a photosensitizer through the generation of ROS from the excitation of its isoalloxazine ring (Alam et al., 2015), evidences of its photo-induced oxidative effects in *A. gossypii* were found using the fluorescent redox-sensitive probe H_2DCFDA. This lipophilic probe has the ability to permeate the cells. Therein, it is deacetylated to H_2DCF by esterases, becoming hydrophilic and consequently held inside the cells. When oxidants are present it oxidizes to DCF, whose fluorescence can be detected at an excitation/emission range of 492–495/517–527 nm (Cruz et al., 2016). As shown in Figure 2.4A, exposure to light induced a significant increase in the fluorescence intensity of riboflavin-overproducing cells (from strain A8) loaded with H_2DCFDA, revealing an increased intracellular oxidation (higher ROS accumulation) under this condition. Conversely, the non-overproducing strain ATCC 10895 presented residual intracellular oxidation in both conditions. Additionally, the representative images obtained by microscopy clearly depicted the high oxidation level of the riboflavin-overproducing strain A8 when exposed to light (Figure 2.4B). A strain-related bias of these results can be excluded, since these effects were exclusively found with light exposure, having the riboflavin-overproducing strain presented statistically similar values to the non-overproducing strain when it was cultivated in the dark. Taking this into account, these results indicate that riboflavin, accumulated intracellularly by *A. gossypii*, acts as a photosensitizer agent that causes DNA damage through a mechanism triggered by oxidative stress.

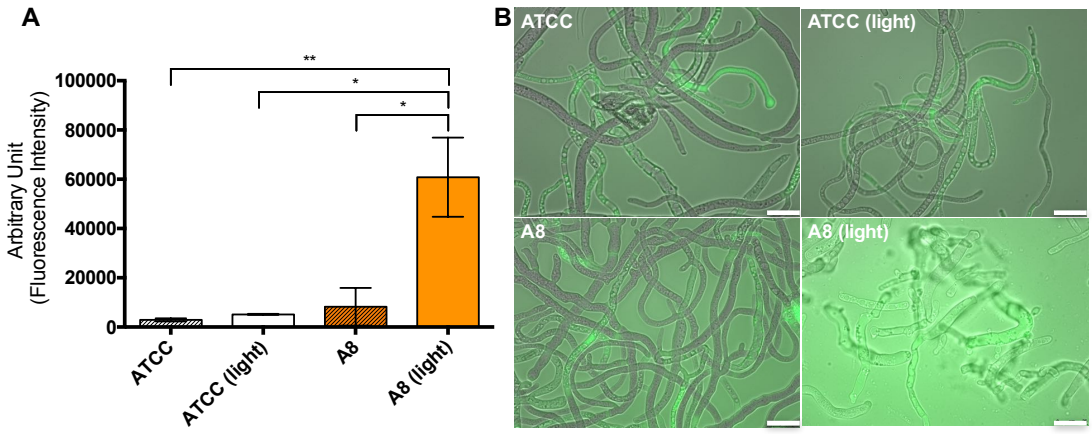


Figure 2.4. Exposure to light during growth induces intracellular ROS accumulation in the *A. gossypii* riboflavin-overproducing strain A8, but not in strain ATCC 10895. **(A)** Fluorescence intensity of cell suspensions loaded with H_2DCFDA determined by fluorimetry (as described in Material and methods) presented as mean ± standard deviation of two biological replicates. Asterisks represent significant differences between strains and conditions. * ($p < 0.05$) and ** ($p < 0.01$). **(B)** Representative overlaid images (obtained from bright-field and fluorescence microscopy) of *A. gossypii* cell suspensions loaded with H_2DCFDA. White bar = 25 µm. Before harvesting, cells were grown for three days on agar-solidified AFM at 30 °C, in the dark or exposed to light.

Over the years, riboflavin overproduction has been interconnected with sporulation and environmental stress. The link of this trait with sporulation has been established either through the addition of external second messengers (cAMP) to the medium (Stahmann et al., 2001) or through the deletion of positive regulators of sporulation, such as the gene *AgSOK2* (Wasserstrom et al., 2017). In both cases, a concomitant negative effect towards sporulation and riboflavin production was observed. In turn, environmental conditions, in the form of nutritional (Schlösser et al., 2007) or oxidative (Kavitha and Chandra, 2014; Walther and Wendland, 2012) stresses have also been connected with riboflavin overproduction. In the latter case, addition to the medium of exogenous oxidative agents (H_2O_2 and menadione) increased riboflavin production through the oxidative stress-responsive transcription factor AgYap1p (Walther and Wendland, 2012). In light of these observations, the overproduction of riboflavin by *A. gossypii* was proposed to serve as an ecological defence mechanism for this insect-dependent plant pathogen against the harsh environmental conditions (rich in ROS and alkaloids) it may face in its natural habitats (Dietrich et al., 2013; Walther and Wendland, 2012). Our results show that riboflavin-overproducing strains are highly susceptible to photo-induced oxidative DNA damage (Table 2.3 and Figure 2.4), an event accompanied by increased riboflavin production (Table 2.2). The fact that this increase in riboflavin

production was only observed in cells presenting high intracellular ROS accumulation (Figure 2.4) reinforces the link between oxidative stress and riboflavin overproduction by *A. gossypii*. Since the production of ROS, via consumption of oxygen in a so-called oxidative burst, is one of the earliest plant's defence strategies against pathogenic infections, the overproduction of riboflavin may act as a scavenging mechanism that protects both *A. gossypii* and its insect vectors against this plant's attack (Walther and Wendland, 2012; Dietrich et al., 2013). While oxidative stress has been shown to trigger riboflavin production (Kavitha and Chandra, 2014; Walther and Wendland, 2012), our results suggest that the interaction of riboflavin with light leads to ROS-mediated oxidative stress and DNA damage in overproducing cells. Previously, riboflavin overproduction was suggested to play a photoprotectant role for the spores of *A. gossypii*, as the addition of external riboflavin to spore suspensions produced a photo-protective effect against UV light (Stahmann et al., 2001). However, here we show that riboflavin acts as a photosensitizer in *A. gossypii* cells. While the ability of *A. gossypii* spores to uptake riboflavin is unknown, their hydrophobic nature may prevent such mechanism (Stahmann et al., 2001). Therefore, one can assume that riboflavin exerts negative photosensitizing effects mainly when it is accumulated intracellularly. Supporting evidences for this can also be found in *E. coli* (Loyd et al., 1990). Since riboflavin produced by *A. gossypii* is predominantly stored in the vacuole or excreted to the extracellular medium (Förster et al., 1990), one may presume that *A. gossypii* evolved this adaptation to prevent the photosensitizing effects of riboflavin here described, as already hypothesized by Stahmann et al. (2001).

Finally, it is worth to note that exposure to light led to a 1.5-fold increase in riboflavin production by the overproducing strain A8 in comparison with the same strain cultivated in the dark (Table 2.2). Exploration of the oxidative trigger to design strategies to improve the biotechnological production of riboflavin by *A. gossypii* was already reported (Kavitha and Chandra, 2014; Walther and Wendland, 2012). These strategies focused in promoting oxidative stress with external agents (H_2O_2 and menadione) at doses that are not limiting for growth but sufficient to induce a response in riboflavin production. Here, using a similar rationale, we show that light can also be used to positively impact riboflavin production in riboflavin-overproducing *A. gossypii* strains, with the advantage that no extra chemical compound needs to be added to the medium. Altogether, the results reported here draw attention for the importance of controlling the exposure to light of biotechnological riboflavin production processes with *A. gossypii*. From now on, one must bear in mind that testing riboflavin-overproducing strains in dark steel fermenters or in glass bioreactors under random-light conditions may retrieve quite different results.

2.4 References

Alam MM, Iqbal S, Naseem I. Ameliorative effect of riboflavin on hyperglycemia, oxidative stress and DNA damage in type-2 diabetic mice: Mechanistic and therapeutic strategies. Arch Biochem Biophys 2015;584:10–9.

Aguiar TQ, Silva R, Domingues L. *Ashbya gossypii* beyond industrial riboflavin production: A historical perspective and emerging biotechnological applications. Biotechnol Adv 2015;33:1774–86.

Azevedo F, Marques F, Fokt H, Oliveira R, Johansson B. Measuring oxidative DNA damage and DNA repair using the yeast comet assay. Yeast 2011;28:55–61.

Besaratinia A, Kim S, Bates SE, Pfeifer GP. Riboflavin activated by ultraviolet A1 irradiation induces oxidative DNA damage-mediated mutations inhibited by vitamin C. Proc Natl Acad Sci USA 2007;104:5953–8.

Bhanoori M, Venkateswerlu G. The alkaline single cell gel electrophoresis: a new test for assessing DNA single strand breaks in *Neurospora crassa*. Mutat Res 1998;405:29–34.

Brancato FP, Golding NS. The diameter of the mold colony as a reliable measure of growth. Mycologia 1953;45:848–64.

Carmello JC, Pavarina AC, Oliveira R, Johansson B. Genotoxic effect of photodynamic therapy mediated by curcumin on *Candida albicans*. FEMS Yeast Res 2015;15:fov018.

Collins AR. The comet assay for DNA damage and repair: principles, applications, and limitations. Mol Biotechnol 2004;26:249–61.

Cruz M, Antunes P, Paulo L, Ferreira AM, Cunha A, C. Almeida-Aguiar C, et al. Antioxidant and dual dose-dependent antigenotoxic and genotoxic properties of an ethanol extract of propolis. RSC Adv 2016;6:49806.

Dietrich FS, Voegelli S, Kuo S, Philippsen P. Genomes of *Ashbya* fungi isolated from insects reveal four mating-type loci, numerous translocations, lack of transposons, and distinct gene duplications. G3 (Bethesda) 2013;3:1225–39.

Fernandes B, Teixeira J, Dragone G, Vicente AA, Kawano S, Bišová K, et al. Relationship between starch and lipid accumulation induced by nutrient depletion and replenishment in the microalga *Parachlorella kessleri*. Bioresour Technol 2013;144:268–74.

Förster C, Santos MA, Ruffert S, Krämer R, Revuelta JL. Physiological consequence of disruption of the *VMA1* gene in the riboflavin overproducer *Ashbya gossypii*. J Biol Chem 1999; 274:9442–8.

Hahn A, Hock B. Assessment of DNA damage in filamentous fungi by single cell gel electrophoresis, comet assay. Environ Toxicol Chem 1999;18:1411–24.

Kavitha S, Chandra TS. Effect of vitamin E and menadione supplementation on riboflavin production and stress parameters in *Ashbya gossypii*. Process Biochem 2009;44:934–8.

Kavitha S, Chandra TS. Oxidative stress protection and glutathione metabolism in response to hydrogen peroxide and menadione in riboflavinogenic fungus *Ashbya gossypii*. Appl Biochem Biotechnol 2014;174:2307–25.

Langie S, Azqueta A, Collins AR. The comet assay: past, present, and future. Front Genet 2015;6:266.

Ledesma-Amaro R, Buey RM, Revuelta JL. Increased production of inosine and guanosine by means of metabolic engineering of the purine pathway in *Ashbya gossypii*. Microb Cell Factories 2015;14:58.

Liu LF, Desai SD, Li TK, Mao Y, Sun M, Sim SP. Mechanism of action of camptothecin. Ann N Y Acad Sci 2000;922:1–10.

Lloyd RE, Rinkenberger JL, Hug BA, Tuveson RW. Growing *Escherichia coli* mutants deficient in riboflavin biosynthesis with non-limiting riboflavin results in sensitization to inactivation by broad-spectrum near-ultraviolet light (320-400 nm). Photochem Photobiol 1990;52:897–901.

Magalhães F, Aguiar TQ, Oliveira C, Domingues L. High-level expression of *Aspergillus niger* β-galactosidase in *Ashbya gossypii*. Biotechnol Prog 2014;30:261–8.

Møller P, Loft S, Ersson C, Koppen G, Dusinska M, Collins A. On the search for an intelligible comet assay descriptor. Front Genet 2014 17;5:217.

Nieland S, Stahmann KP. A developmental stage of hyphal cells shows riboflavin overproduction instead of sporulation in *Ashbya gossypii*. Appl Microbiol Biotechnol 2013;97:10143–53.

Nikolaou E, Agrafioti I, Stumpf M, Quinn J, Stansfield I, Brown AJ. Phylogenetic diversity of stress signalling pathways in fungi. BMC Evol Biol 2009;9:44.

Oliveira R, Johansson B. Quantitative DNA Damage and Repair Measurement with the Yeast Comet Assay. In: Lotte Bjergbæk, editor. DNA Repair Protocols, Methods in Molecular Biology 2012. New York: Springer Science + Business Media, 101–9.

Ostling O, Johanson KJ. Microelectrophoretic study of radiation-induced DNA damages in individual mammalian cells. Biochem Biophys Res Commun 1984;123:291–8.

Schlösser T, Wiesenburg A, Gätgens C, Funke A, Viets U, Vijayalakshmi S, et al. Growth stress triggers riboflavin overproduction in *Ashbya gossypii*. Appl Microbiol Biotechnol 2007;76:569–78.

Silva R, Aguiar TQ, Domingues L. Blockage of the pyrimidine biosynthetic pathway affects riboflavin production in *Ashbya gossypii*. J Biotechnol 2015;193:37–40.

Stahmann KP, Arst Jr HN, Althöfer H, Revuelta JL, Monschau N, Schlüpen C, et al. Riboflavin, overproduced during sporulation of *Ashbya gossypii*, protects its hyaline spores against ultraviolet light. Environ Microbiol 2001;3:545–50.

Tarrant AWS. The spectral power distribution of daylight. Lighting Res Technol 1968;33:75–82.

Walther A, Wendland, J. *Yap1*-dependent oxidative stress response provides a link to riboflavin production in *Ashbya gossypii*. Fungal Genet Biol 2012;49:697–707.

Wasserstrom L, Dünkler A, Walther A, Wendland J. The APSES protein Sok2 is a positive regulator of sporulation in *Ashbya gossypii*. Mol Microbiol 2017;106:949–60.

CHAPTER III

Physiological characterization of a pyrimidine auxotroph exposes link between uracil phosphoribosyltransferase regulation and riboflavin production in *Ashbya gossypii*

The work reported on this chapter was published in:

Silva R*, Aguiar TQ*, Oliveira C, Domingues L. Physiological characterization of a pyrimidine auxotroph exposes link between uracil phosphoribosyltransferase regulation and riboflavin production in *Ashbya gossypii*. New Biotechnol 2019;50:1–8. *Equal contributions.

Abstract

The blockage of the *de novo* pyrimidine biosynthetic pathway at the orotidine-5'-phosphate decarboxylase level was previously demonstrated to affect riboflavin production in the industrial producer fungus *Ashbya gossypii*. However, the molecular basis for the unusual sensitivity to uracil displayed by the pyrimidine auxotroph *A. gossypii Agura3* was unknown. Here, uridine was shown to be the only intermediate of the pyrimidine salvage pathway able to fully restore this mutant's growth. Conversely, uracil, which is routinely used to rescue pyrimidine auxotrophs, had a dose-dependent growth-inhibitory effect. Uracil phosphoribosyltransferase (UPRTp) is the pyrimidine salvage pathway enzyme responsible for converting uracil to uridine monophosphate in the presence of phosphoribosyl pyrophosphate (PRPP). Characterization of the *A. gossypii* UPRT, as produced and purified from *Escherichia coli*, revealed that uracil concentrations above 1 mM negatively affected its activity, thus explaining the hypersensitivity of the *Agura3* mutant to uracil. Accordingly, overexpression of the AgUPRTp encoding-gene in *A. gossypii Agura3* led to similar growth on rich medium containing 5 mM uracil or uridine. Decreased UPRTp activity ultimately favours the preservation of PRPP, which otherwise may be directed to other pathways. In *A. gossypii*, increased PRPP availability promotes overproduction of riboflavin. Thus, this UPRT modulation mechanism reveals a putative means of saving precursors essential for riboflavin overproduction by this fungus. A similar uracil-mediated regulation mechanism of the UPRT activity is reported only in two protozoan parasites, whose survival depends on the availability of PRPP. Physiological evidence here discussed indicate that it may be extended to other distantly related flavinogenic fungi.

3.1 Introduction

The use of auxotrophies as tools for genetic modification of microbial strains is widely employed in molecular microbiology. However, there are some recognized problems associated with their use, such as a lack of clarity regarding how much nutrient supplementation is required for each auxotrophy and microorganism (Çakar et al., 1999; Pronk, 2002). Auxotrophy for pyrimidines, resulting from blockage of the *de novo* pyrimidine biosynthetic pathway at the orotidine 5'-phosphate decarboxylase level (encoded by *URA3* or corresponding ortholog in non-yeast species) or at the orotate phosphoribosyltransferase level (encoded by *URA5* or homologs), is one of the most used among microbes (Çakar et al., 1999; Kelly et al., 1988; Pronk, 2002). As standard procedure, these mutants require the supply of exogenous uracil to rescue their growth, thus being termed uracil auxotrophs.

Uracil enters the pyrimidine salvage pathway and is converted to uridine monophosphate (UMP) in a one-step reaction catalysed by uracil phosphoribosyltransferase (UPRT), thus re-establishing the biosynthesis of pyrimidines (Figure 3.1). While efficient in restoring growth of the majority of the pyrimidine auxotrophs, the supply of exogenous uracil is unable to fully overcome the effects of this auxotrophy in some fungi, which require the supply of exogenous uridine. Among them are *Candida albicans* (Kelly et al., 1988), *Ashbya gossypii* (*syn*. *Eremothecium gossypii*) (Aguiar et al., 2014), *Debaryomyces hansenii* (*syn*. *Candida famata*) (Seda-Miró et al., 2007), *Candida guilliermondii (syn*. *Pichia guilliermondii*) (Millerioux et al., 2011), *Aspergillus fumigatus* (D'Enfert et al., 1996) and *Aspergillus nidulans* (Sun et al., 2013). Despite the importance of this apparently uncommon phenotype, it is poorly understood at the molecular level.

A. gossypii is a filamentous fungus of considerable industrial and biological significance, due to its capacity to overproduce riboflavin (vitamin B_2) and to its unique genetic and biological features (Aguiar et al., 2015; 2017). The genetic blockage of its pyrimidine pathway at the *AgURA3* level (orotidine 5'-P to UMP) leads to increased riboflavin production on standard Ashbya Full Medium (AFM), a phenotype that is reverted when extra uridine/uracil (≥0.5/1 mM) is added to the medium (Silva et al., 2015). Unlike *ura3* mutants from the closely related yeasts *Saccharomyces cerevisiae* and *Kluyveromyces* sp. (Gomes et al., 2014), the *A. gossypii Agura3* mutant not only requires the supply of exogenous uridine to fully overcome its auxotrophy, but its growth is also inhibited by high uracil concentrations (Aguiar et al., 2014; Silva et al., 2015). Thus, the *ura3* mutation, a common genetic alteration among microorganisms, has a profound impact not only on the growth but also on the physiology of this fungus.

In order to elucidate the molecular mechanism(s) underlying the unusual phenotypes of this *A. gossypii* pyrimidine auxotroph, here its growth was analysed on media containing different pyrimidine supplements, envisioning the detection of bottlenecks in the pyrimidine salvage pathway. This allowed the identification of limitations at the AgUPRTp level (Figure 3.1). Characterization of recombinant AgUPRTp revealed a type of metabolic enzyme regulation previously unknown in *A. gossypii*. Moreover, common features with other organisms, such as unrelated protozoan parasites (Soysa et al., 2013; Wilson et al., 2012) and other flavinogenic fungi, were identified and discussed, thus extending the impact of this study.

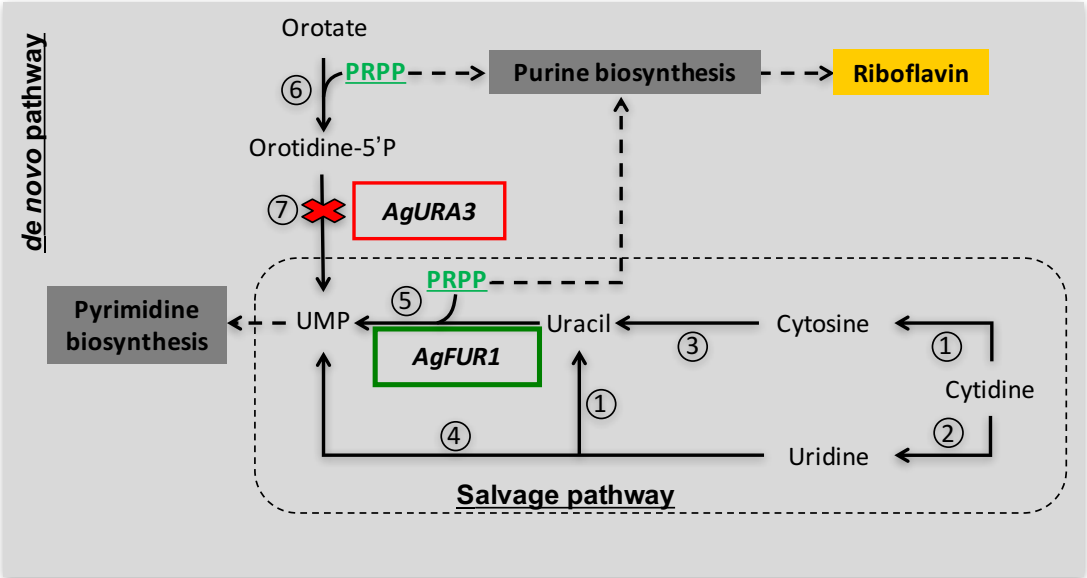


Figure 3.1. Schematic representation indicating the *de novo* and salvage pathways of pyrimidine ribonucleotides. Red × marks where the *de novo* pyrimidine biosynthetic pathway is blocked in the *A. gossypii Agura3* uracil auxotroph. Dashed arrows indicate a multi-step pathway. UMP: uridine monophosphate; PRPP: phosphoribosyl pyrophosphate. Numbers indicate the enzymes involved in each step of the pyrimidine pathways. 1: nucleosidase/uridine nucleosidase; 2: cytidine deaminase; 3: cytosine deaminase; 4: uridine kinase; 5: uracil phosphoribosyltransferase; 6: orotate phosphoribosyltransferase; 7: orotidine-5'-phospate decarboxylase.

3.2 Materials and methods

3.2.1 Strains and media

The *A. gossypii Agura3* strain (*Agura3*Δ::*lox*P) (Aguiar et al., 2014), a uridine/uracil auxotroph derived from the parental strain *A. gossypii* ATCC 10895, was used in this study. For *AgFUR1* overexpression, the AFR052C ORF (NCBI Reference Sequence: NM_210953.1) was isolated from the *A. gossypii* genome by PCR (5'cggaattcATGaaaagttttagtgcccg and 5'ccgctcgagTCAtatgcagtagtaccgg) and cloned between the *Eco*RI and *Xho*I restriction sites of the plasmid pFMT (Magalhães et al., 2014), under the regulation of the strong constitutive promoter *AgTEF*. The resulting plasmid (pFMT*AgFUR1*) was then transformed into the *Agura3* strain as previously described (Magalhães et al., 2014). Stock cultures of these strains were kept as spores suspended in spore buffer containing 200 g/L glycerol, 8 g/L NaCl and 0.25 % (v/v) Tween 20 and stored at −80 °C. Stock cultures of these strains were maintained as spores suspended in Spore Buffer (200 g/L glycerol, 8 g/L NaCl and 0.25 % (v/v) Tween 20) at −80 °C. Spores were prepared as previously described in Chapter II. Agar-solidified minimal medium (MM; 6.7 g/L yeast nitrogen base, 20 g/L glucose and 1 g/L $CaCO_3$), synthetic complete (SC) medium (Sherman et al., 1986) (without uracil) buffered with 1 g/L $CaCO_3$ and AFM (10 g/L tryptone, 10 g/L yeast extract, 20 g/L glucose, 1 g/L myo-inositol) were used for the growth of *A. gossypii* strains. Where indicated, 200 μg/mL geneticin (G418) was added to the medium for plasmid maintenance. *Escherichia coli* NZY5α and NZYBL21 (DE3) (NZYTech) were used for plasmid construction and recombinant protein production, respectively. *E. coli* strains were grown in LB medium (5 g/L yeast extract, 10 g/L tryptone, 10 g/L NaCl) supplemented with 100 μg/mL ampicillin for selection.

3.2.2 Radial growth conditions for *A. gossypii* strains

Agar-solidified MM, SC or AFM supplemented with uracil, uridine, cytosine or cytidine at 0, 1, 4 or 5 mM was inoculated with 10 μL of a suspension of spores (10^7 spores/mL) and incubated at 30 °C for 8 days. Colony radial growth (Brancato and Golding, 1953) was determined daily by measuring the diameter of colonies in 90 mm diameter Petri dishes in two perpendicular directions, through two guide lines previously drawn on the lower outer face of the plates. Three biological replicates were used for each condition. Images of the colony morphology were recorded using a Molecular Imager ChemiDoc™ XRS + Imaging System (Bio-Rad) with the Image Lab 4.0 software at day 8 of growth. The lag phase corresponded to the time (in days) that no growth was observed beyond the inoculum halo. The maximum radial growth rate was obtained through the

slope of the trend line of a linear regression applied to the radial growth curve excluding the lag phase. The percentage of relative growth was determined by normalizing the maximum radial growth of each condition by the maximum radial growth obtained with 5 mM uridine.

3.2.3 AgUPRTp sequence analysis, recombinant production and purification

Multiple protein sequence alignment was performed with Clustal Omega (Sievers et al., 2011) (https://www.ebi.ac.uk/Tools/msa/clustalo/) using default parameters and FigTree v1.4.3 (http://tree.bio.ed.ac.uk/software/figtree/) was used to visualize the phylogenetic tree produced by Clustal Omega. Amino acid sequences were retrieved from NCBI (National Center for Biotechnology Information; https://www.ncbi.nlm.nih.gov/). The full-length *AgFUR1* cDNA, with codons optimized for recombinant expression in *E. coli* and flanked by *Nco*I and *Xho*I recognition sites at the 5'- and 3'-end, respectively, was synthesized by NZYTech. The *AgFUR1* synthetic gene was excised from the carrying plasmid by digestion with *Nco*I and *Xho*I and ligated to the pETM20 vector (EMBL) in fusion with the N-terminal thioredoxin A (TrxA) and His_6 tags (linked to the cloning site by a TEV protease recognition sequence) (Costa et al., 2013), and the construct was transformed into chemically competent NZY5α *E. coli* cells (NZYTech). The AgUPRTp expression plasmid (pETM*AgFUR1*) was then transformed into the *E. coli* expression strain NZYBL21 (DE3) (NZYTech). A transformant colony was picked and grown in 100 mL of LB medium containing 100 μg/mL ampicillin to an OD_{600nm} of 0.5, and protein expression was induced with 0.2 mM isopropyl-β-D-thiogalactopyranoside (IPTG) for 16 h at 18 °C. Cells were recovered by centrifugation (at 4 °C for 15 min at 10,000 rpm) from 20 mL culture fractions and lysed with NZY Bacterial Cell Lysis Buffer (NZYTech) supplemented with 1 mM PMSF, according to the manufacturer's instructions. Soluble cell-free extracts were collected by centrifugation and incubated with 0.5 mL of HisPur™ Ni-NTA Resin (Thermo Fisher Scientific) for purification of the recombinant fusion protein. Purification was conducted according to the manufacturer's instructions as given for the batch method, using 50 mM Tris pH 8.0, 150 mM NaCl (Tris-NaCl buffer) with 20 mM imidazole as equilibration buffer, and Tris-NaCl buffer with 40 mM or 300 mM imidazole as washing and elution buffer, respectively. For TrxA-His_6 partner removal, the purified fusion protein was digested with TEV-His_6 protease overnight at 4 °C at the ratio of 1:20 (w/w) in equilibration buffer. Elution buffer was previously exchanged with equilibration buffer using a PD MidiTrap G-25 column (GE Healthcare). The cleaved AgUPRTp was then purified from the fusion tags and protease by reverse purification using the same resin and above-mentioned protocol, but in which the target protein

was collected from the resin washing steps. Purified protein was analysed by SDS-PAGE using 15 % (w/v) acrylamide gels, followed by BlueSafe staining (NZYTech). Predicted size for cleaved AgUPRTp was 26.3 kDa. Imidazole was removed from the protein using the PD MidiTrap G-25 column (GE Healthcare). The concentration of recombinant AgUPRTp was estimated from the absorbance at 280 nm using the respective molar extinction coefficient (ϵ = 13785 1/(M.cm)). Purified AgUPRTp was stored at 4 °C until use.

3.2.4 Enzyme activity assays

AgUPRTp enzyme activity was determined spectrophotometrically by measuring the conversion of uracil into UMP as previously described (Natalini et al., 1979; Soysa et al., 2013). To determine the effect of uracil concentration on AgUPRTp activity, the assay mixture consisted of TMD 50 buffer (50 mM Tris-HCl, 5 mM $MgCl_2$, and 2 mM DTT, pH 7.5) with 1 mM phosphoribosyl pyrophosphate (PRPP) and uracil concentrations ranging from 10 μM to 1.25 mM. To assess the influence of different PRPP concentrations on AgUPRTp activity, the assay mixture consisted of TMD 50 buffer with 0.5 mM uracil, and PRPP concentrations ranging from 25 μM to 2 mM. For each condition tested and prior to the assay, the background absorbance was set to zero to remove any response caused by substrates or reagents. Enzyme activity measurements were performed using a V-560 UV/Vis Spectrophotometer (Jasco) at 30 °C, and reactions were initiated by the addition of approximately 2 μg of enzyme to the assay mixture (1 mL final volume in a 1 cm quartz cuvette). The assays were based on the differential molar absorption coefficients between uracil and UMP at 280 nm ($\Delta\epsilon$ = 1407.5 1/(M.cm)). An increase in absorbance was observed due to the formation of UMP, which was monitored for up to 2 min. Initial rates were calculated from the linear part of each reaction progress curve, converted to specific enzyme activity (μmol/min.$mg_{protein}$) and then plotted against substrate concentration.

3.2.5 Statistical analyses

GraphPad Prism for IOS version 6.0 was used for all statistical analyses. Differences between *A. gossypii´*s growths were tested by two-way ANOVA followed by Tukey's multiple comparison test. The analysis of differential AgUPRTp activity was conducted by one-way ANOVA followed by Dunnett´s multiple comparison test. Statistical significance was established at $p < 0.05$ for the comparisons.

3.3 Results and discussion

The growth of *A. gossypii Agura3* can only be fully restored by the addition of uridine to the medium (Aguiar et al., 2014), being inhibited by high uracil concentrations (Silva et al., 2015). A similar phenotype has been reported for uracil auxotrophs of *A. nidulans* (Sun et al., 2013). Although not experimentally demonstrated, the growth-inhibitory effect of high uracil concentrations observed in *A. nidulans* pyrimidine auxotrophs was proposed to be linked with misincorporation of uracil into the DNA. This seems not to be the case for *A. gossypii*, since the parental strain of *Agura3* (ATCC 10895) did not display deficient growth when grown at high concentrations of uracil (Appendix: Figure A3.1) and no evidence was found for genomic DNA damage under these conditions using different DNA electrophoretic techniques (Appendix: Figure A3.2). Therefore, *per se*, the presence in the medium of a high content of the pyrimidine supplement is not deleterious for growth of this fungus, becoming detrimental only when uracil metabolism is required. Thus, this study focused on the characterization of the *A. gossypii* pyrimidine salvage pathway, which according to the available genomic information (the *Ashbya* Genome Database) (Gattiker et al., 2007) has two independent routes by which UMP can be synthesized, one via AgUPRTp and the other via uridine kinase, which converts uridine directly into UMP (Figure 3.1).

3.3.1 Growth-rescuing effect of various pyrimidine supplements on *A. gossypii Agura3*

In an attempt to identify potential rate-limiting steps in the *A. gossypii* pyrimidine salvage pathway, the colony radial growth of *A. gossypii Agura3* was characterized on agar-solidified minimal medium (MM) supplemented with different concentrations (1, 4 or 5 mM) of one of the four intermediates in the pyrimidine salvage pathway, namely uracil, uridine, cytosine or cytidine (Table 3.1).

Table 3.1. Maximum radial growth rates and lag phases of *A. gossypii Agura3* on agar-solidified MM supplemented with different concentrations of intermediates from the pyrimidine salvage pathway. Data are representative of three biological replicates. Radial growth rates are expressed as mean ± standard deviation. Superscripts represent significant differences ($p < 0.05$) between values of the same column (supplement concentration).

	Maximum radial growth rate (mm/day)			**Lag phase (days)**		
	1 mM	4 mM	5 mM	1 mM	4 mM	5 mM
Uridine	11 ± 1^{a}	11 ± 0^{a}	13 ± 0^{a}	3	2	2
Uracil	6 ± 0^{b}	3 ± 0^{d}	n.d.	3	3	7
Cytosine	–	4 ± 0^{c}	7 ± 1^{b}	–	5	4
Cytidine	7 ± 1^{b}	6 ± 1^{b}	7 ± 1^{b}	5	3	3

n.d., not determined, because for this condition, growth was only observed in the last day (8th day), which impeded the determination of the maximum radial growth rate; –, no growth beyond the inoculum halo.

This range of concentrations was chosen based on previous results showing that this strain's growth is highly hampered by uracil concentrations ≥5 mM and minimally affected by ≤1 mM uracil (Silva et al., 2015). In MM, even with the lowest concentration tested (1 mM), the radial growth of *Agura3* on uridine was superior to that obtained with 5 mM of any other pyrimidine supplement (Figure 3.2).

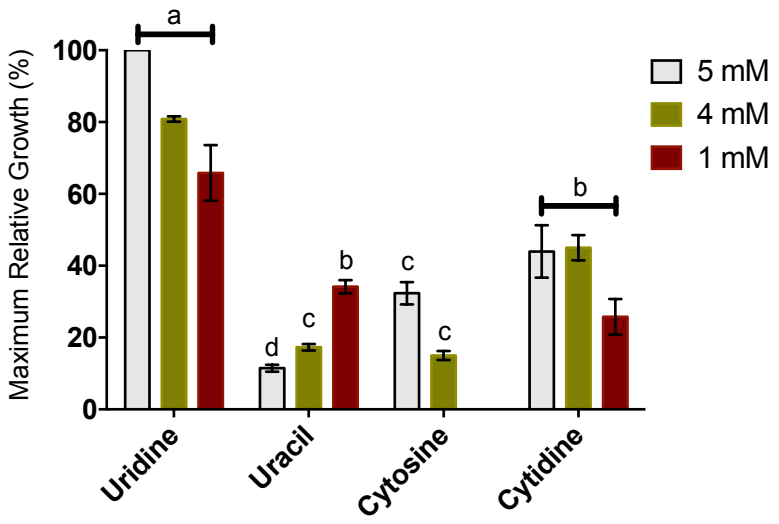


Figure 3.2. Maximum relative growth of *A. gossypii Agura3* on agar-solidified MM supplemented with different concentrations of intermediates from the pyrimidine salvage pathway. The percentage of maximum relative growth was normalized to the radial growth of the best condition tested (5 mM uridine). Data are representative of three biological replicates after 8 days of growth. Letters represent significant differences ($p < 0.05$) between bars with the same supplement concentration.

In addition to MM, two other media with distinct basal composition, one defined (SC) and one rich (AFM), were also supplemented with 5 mM uracil, uridine or cytosine and used to test the growth of *A. gossypii Agura3* (Figure 3.3A and B). Uracil is usually supplied at concentrations below 5 mM to rescue the growth of uracil auxotrophs of other fungi. Thus, to confirm that the growth-inhibitory effect of uracil is not common among fungal pyrimidine auxotrophs, we tested the growth of the frequently used *S. cerevisiae* CEN.PK113-5D (*ura3-*), *Yarrowia lipolytica* Po1f (*leu- ura- Δaep Δaxp SUC+*) and *K. marxianus* KMS2 (*ura3-*) in SC and verified that their growth was not affected by up to 10 mM uracil in the medium (Appendix: Figure A3.3).

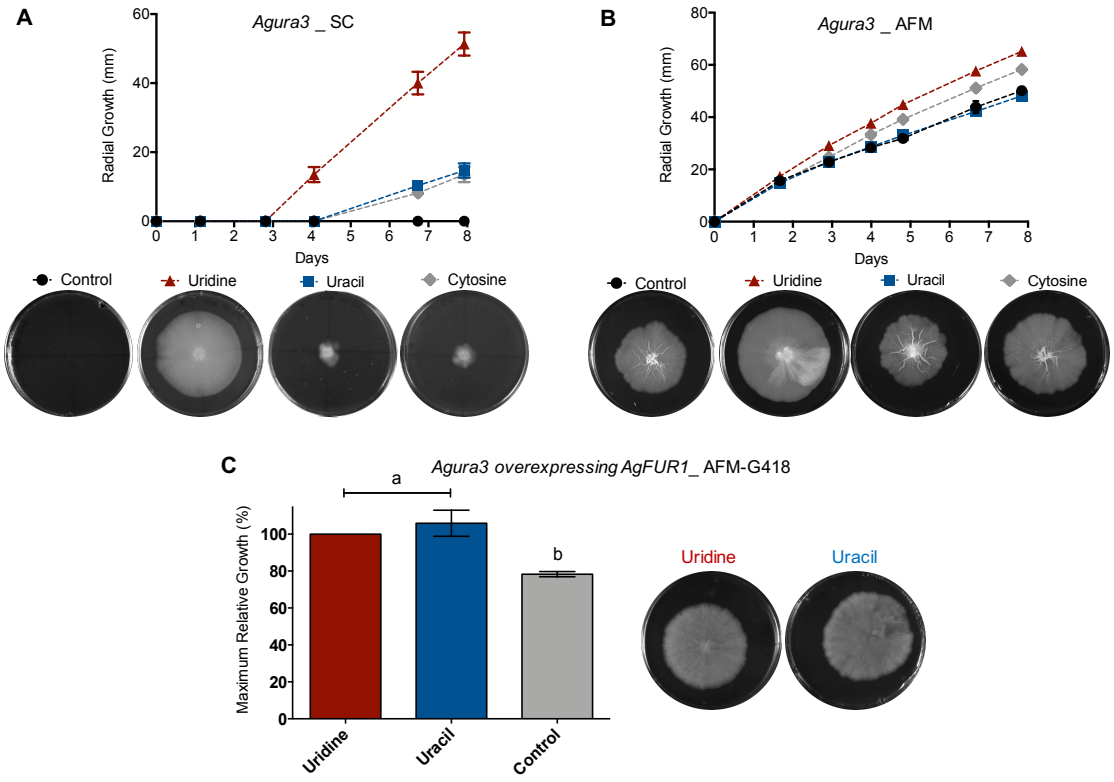


Figure 3.3. Radial growth curves and colony morphologies of *A. gossypii Agura3* on agar-solidified **(A)** SC or **(B)** AFM supplemented with 5 mM uridine, uracil or cytosine. **(C)** Maximum relative growth and colony morphology of *A. gossypii Agura3* overexpressing the gene Ag*FUR1* on agar-solidified AFM supplemented with 5 mM uridine or uracil. Letters represent significant differences ($p < 0.05$) between bars (supplementation). The control conditions represent media without added supplement. The growth observed in AFM without any added supplement is due to the presence of small quantities of various pyrimidines in the complex constituents of this rich medium. Data represent the average ± standard deviation from three (A and B) or two (C) biological replicates. Where not seen, error bars were smaller than the symbols. Images were recorded after 8 days of growth.

Regardless of the medium and supplement concentration, uridine always performed the best in rescuing the growth of the *A. gossypii Agura3* mutant (Table 3.1; Figures 3.2, 3.3A and 3.3B). Uridine supplementation also produced the shortest lag phases. In contrast, uracil failed to completely rescue the growth of the *Agura3* mutant. Moreover, increasing concentrations of this supplement were increasingly detrimental for the growth of this auxotroph (Table 3.1; Figure 3.2 and 3.3A). Cytosine, which is metabolized into uracil before conversion to UMP through the AgUPRTp route (Figure 3.1), was also unable to fully restore growth (Figure 3.2 and 3.3), but a positive correlation was observed between cytosine concentration and growth (Table 3.1; Figure 3.2). On the other hand, cytidine, which can be metabolized into UMP via UPRT or uridine kinase,

exceeded uracil and cytosine, but not uridine, in rescuing growth (Table 3.1; Figure 3.2). Morphologically, the colonies grown on media supplemented with uracil or cytosine presented an irregular shape, contrasting with the normal circular shape displayed on uridine-supplemented media (Figure 3.3A and B). In addition, wrinkled colonies were observed on rich AFM supplemented with uracil or cytosine, whereas smooth flat colonies were found in plates with uridine (Figure 3.3B).

Uridine can be directly metabolized by *A. gossypii* into UMP without going through the AgUPRTp route. Thus, altogether, these results identified the AgUPRTp-catalysed reaction as the likely rate-limiting step in the *A. gossypii* pyrimidine salvage pathway responsible for the dose-dependent detrimental effect of uracil on the growth of *Agura3*. Indeed, overexpression of the AgUPRTp encoding-gene in *Agura3* led to improved growth on AFM containing 5 mM uracil, to an extent that the maximum radial growth obtained with uracil was no longer statistically different from that obtained with the same amount of uridine (Figure 3.3C).

3.3.2 AgUPRTp sequence analysis, recombinant production and purification

AgUPRTp is a 232 amino acids-long protein encoded by the ORF AFR052C (syntenic homolog of *S. cerevisiae* gene *FUR1*) (Figure 3.4A). Highly conserved regions across UPRTs from organisms of different kingdoms and even superkingdoms (Li et al., 2007) are also conserved in AgUPRTp. The AgUPRTp amino acid sequence shares high identity (~ 80 %) with the UPRTs from closely related yeasts, such as *S. cerevisiae* and *K. marxianus*, and 53 % with the well-characterized UPRTs from the distantly related protozoan parasites *Leishmania donovani* and *Toxoplasma gondii*. Curiously, despite belonging to closely related parasites, the UPRTs from *L. donovani* and *T. gondii* share less identity between each other (49 %) than with that of *A. gossypii* (Figure 3.4B).

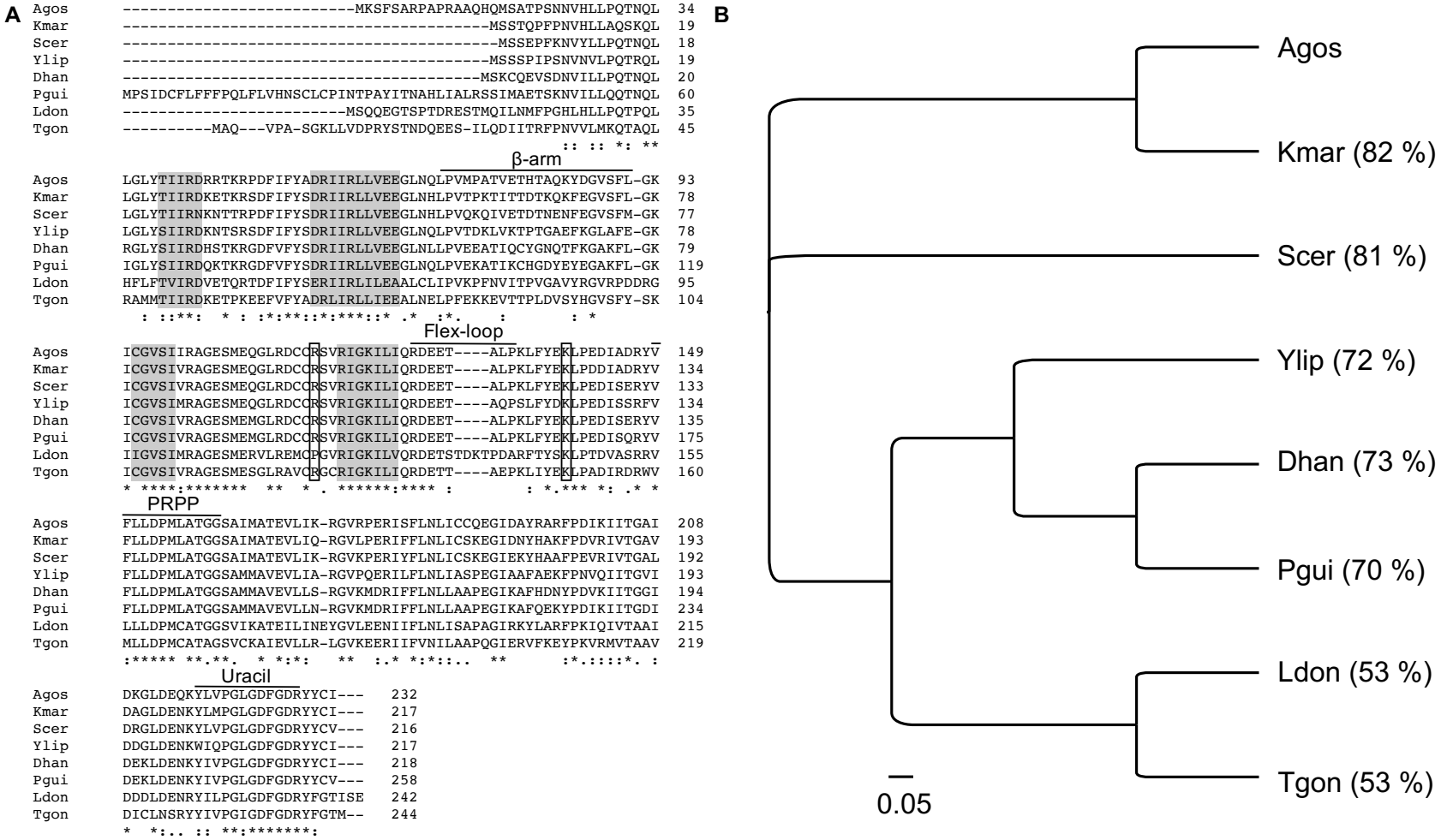

A
Agos ----------MKSFSARPAPRAAQHQMSATPSNNVHLLPQTNQL 34
Kmar ----------MSSTQPFPNVHLLAQSKQL 19
Scer ----------MSSEPFKNVYLLPQTNQL 18
Ylip ----------MSSSPIPSNVNVLPQTRQL 19
Dhan ----------MSKCQEVSDNVILLPQTNQL 20
Pgui MPSIDCFLFFFPQLFLVHNSCLCPINTPAYITNAHLIALRSSIMAETSKNVILLQQTNQL 60
Ldon ----------MSQQEGTSPTDRESTMQILNMFPGHLHLLPQTPQL 35
Tgon ----------MAQ---VPA-SGKLLVDPRYSTNDQEES-ILQDIITRFPNVVLMKQTAQL 45
β-arm
Agos LGLYTIIRDRRTKRPDFIFYADRIIRLLVEEGLNQLPVMPATVETHTAQKYDGVSFL-GK 93
Kmar LGLYTIIRDKETKRSDFIFYSDRIIRLLVEEGLNHLPVTPKTITTDTKQKFEGVSFL-GK 78
Scer LGLYTIIRNKNTTRPDFIFYSDRIIRLLVEEGLNHLPVQKQIVETDTNENFEGVSFM-GK 77
Ylip LGLYSIIRDKNTSRSDFIFYSDRIIRLLVEEGLNQLPVTDKLVKTPTGAEFKGLAFE-GK 78
Dhan RGLYSIIRDHSTKRGDFVFYSDRIIRLLVEEGLNLLPVEEATIQCYGNQTFKGAKFL-GK 79
Pgui IGLYSIIRDQKTKRGDFVFYSDRIIRLLVEEGLNQLPVEKATIKCHGDYEYEGAKFL-GK 119
Ldon HFLFTVIRDVETQRTDFIFYSERIIRLILEAALCLIPVKPFNVITPVGAVYRGVRPDDRG 95
Tgon RAMMTIIRDKETPKEEFVFYADRLIRLLIEEALNELPFEKKEVTTPLDVSYHGVSFY-SK 104
Flex-loop
Agos ICGVSIIRAGESMEQGLRDCCRSVRIGKILIQRDEET----ALPKLFYEKLPEDIADRYV 149
Kmar ICGVSIVRAGESMEQGLRDCCRSVRIGKILIQRDEET----ALPKLFYEKLPDDIADRYV 134
Scer ICGVSIVRAGESMEQGLRDCCRSVRIGKILIQRDEET----ALPKLFYEKLPEDISERYV 133
Ylip ICGVSIMRAGESMEQGLRDCCRSVRIGKILIQRDEET----AQPSLFYDKLPEDISSRFV 134
Dhan ICGVSIVRAGESMEMGLRDCCRSVRIGKILIQRDEET----ALPKLFYEKLPEDISERYV 135
Pgui ICGVSIVRAGESMEMGLRDCCRSVRIGKILIQRDEET----ALPKLFYEKLPEDISQRYV 175
Ldon IIGVSIMRAGESMERVLREMCPGVRIGKILVQRDETSTDKTPDARFTYSKLPTDVASRRV 155
Tgon ICGVSIVRAGESMESGLRAVCRGCRIGKILIQRDETT----AEPKLIYEKLPADIRDRWV 160
PRPP
Agos FLLDPMLATGGSAIMATEVLIK-RGVRPERISFLNLICCQEGIDAYRARFPDIKIITGAI 208
Kmar FLLDPMLATGGSAIMATEVLIQ-RGVLPERIFFLNLICSKEGIDNYHAKFPDVRIVTGAV 193
Scer FLLDPMLATGGSAIMATEVLIK-RGVKPERIYFLNLICSKEGIEKYHAAFPEVRIVTGAL 192
Ylip FLLDPMLATGGSAMMAVEVLIA-RGVPQERILFLNLIASPEGIAAFAEKFPNVQIITGVI 193
Dhan FLLDPMLATGGSAMMAVEVLLS-RGVKMDRIFFLNLLAAPEGIKAFHDNYPDVKIITGGI 194
Pgui FLLDPMLATGGSAMMAVEVLLN-RGVKMDRIFFLNLLAAPEGIKAFQEKYPDIKIITGDI 234
Ldon LLLDPMCATGGSVIKATEILINEYGVLEENIIFLNLISAPAGIRKYLARFPKIQIVTAAI 215
Tgon MLLDPMCATAGSVCKAIEVLLR-LGVKEERIIFVNILAAPQGIERVFKEYPKVRMVTAAV 219
Uracil
Agos DKGLDEQKYLVPGLGDFGDRYYCI--- 232
Kmar DAGLDENKYLMPGLGDFGDRYYCI--- 217
Scer DRGLDENKYLVPGLGDFGDRYYCV--- 216
Ylip DDGLDENKWIQPGLGDFGDRYYCI--- 217
Dhan DEKLDENKYIVPGLGDFGDRYYCI--- 218
Pgui DEKLDENKYIVPGLGDFGDRYYCV--- 258
Ldon DDDLDENRYILPGLGDFGDRYFGTISE 242
Tgon DICLNSRYYIVPGIGDFGDRYFGTM-- 244
B
Agos
Kmar (82 %)
Scer (81 %)
Ylip (72 %)
Dhan (73 %)
Pgui (70 %)
Ldon (53 %)
Tgon (53 %)
0.05

Figure 3.4.

Figure 3.4. *Continued*. Alignment of AgUPRTp with other UPRTs and corresponding phylogenetic tree. **(A)** UPRTp amino acid sequences from *A. gossypii* (Agos, NP_985599), *K. marxianus* (Kmar, XP_022674246), *S. cerevisiae* (Scer, NP_011996), *Y. lipolytica* (Ylip, XP_506088), *D. hansenii* (Dhan, XP_002770455), *P. guilliermondii* (Pgui, XP_001482408), *L. donovani* (Ldon, XP_003864273) and *T. gondii* (Tgon, XP_002364470). Four conserved regions from human to prokaryotes are shaded in grey (Li et al., 2007). The residues that constitute a β-arm, a flex-loop and the PRPP and uracil binding sites identified previously (Schumacher et al., 1998) are marked with black lines. Boxed residues represent positions where mutations were reported to increase resistance to 5-Flucytosine or 5-Fluorouracil. Asterisks (*) represent fully conserved residues, colons (:) represent residues with strongly similar properties and periods (.) represent residues with weakly similar properties. **(B)** Phylogenetic tree resultant from the alignment performed by ClustalO, which was drawn with FigTree v1.4.3. Indicated values represent the percentage of sequence identity to AgUPRTp.

Important secondary structures described for the *T. gondii* UPRTp, as well as the binding regions for its substrates, PRPP and uracil (Li et al., 2007), are indicated in Figure 3.4A. While the PRPP and uracil binding regions are highly conserved across species, the β-arm and the flex-loop zones only share a degree of conservation across closely related species. In *C. albicans*, resistance to 5-flucytosine (5-FC) was associated with decreased UPRT activity due to the substitution of the arginine residue corresponding to R_{126} in AgUPRTp by cysteine (C) (Dodgson et al., 2004). None of the 8 UPRTs aligned here have a cysteine in that position, the arginine residue being conserved among 7 of them. 5-FC is an antifungal prodrug that is metabolized by cytosine deaminase into 5-fluorouracil (5-FU), which relies on its catalysis by UPRT to exert toxicity (Dodgson et al., 2004; Ritt et al., 2013). In *Leishmania infantum*, substitution of the lysine corresponding to K_{139} in AgUPRTp by a threonine (T) was found to contribute to increased resistance to 5-FU (Ritt et al., 2013). This lysine is also conserved among the UPRTs aligned in Figure 3.4A.

Since the *in silico* analysis of the AgUPRTp did not highlight any particular feature that could account for limitations in its enzymatic activity, experimental characterization of this enzyme was carried out. The *AgFUR1* gene with codons optimized for expression in *E. coli* was cloned into an expression plasmid and subsequently expressed in *E. coli* BL21. AgUPRTp was initially produced as an insoluble protein at induction temperatures of 37 and 18 °C (Appendix: Figure A3.4), but by N-terminal fusion to TrxA it was subsequently expressed mostly in soluble form (Figure 3.5). Over 2 mg of purified TrxA-AgUPRTp fusion protein was obtained per 20 mL of bacterial culture induced at 18 °C with IPTG. AgUPRTp was then cleaved efficiently from TrxA with TEV protease and further

purified (Figure 3.5), with an overall yield of 0.3 mg of pure AgUPRTp per mg of fusion protein. The cleaved and purified AgUPRTp could be observed in SDS-PAGE gel as a single band of ~26 kDa, consistent with its calculated molecular weight, and was stable when stored at 4 °C in Tris-NaCl buffer for at least 1 week.

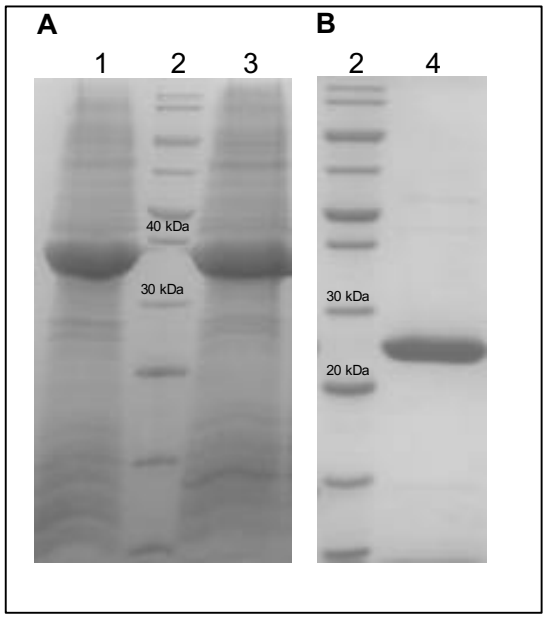


Figure 3.5. SDS-PAGE analyses of the **(A)** production and **(B)** purification of AgUPRTp from *E. coli*. Lane 1, crude extract of cells producing AgUPRTp fusion with TrxA (TrxA-AgUPRTp); Lanes 2, molecular weight marker; Lane 3, supernatant containing the soluble protein fraction after lysis of the TrxA-AgUPRTp producing cells; Lane 4, AgUPRTp cleaved and purified from TrxA-AgUPRTp.

3.3.3 AgUPRTp activity is negatively affected by high uracil concentrations

The purified recombinant AgUPRTp was enzymatically active, catalysing the phosphoribosylation of uracil to UMP in the presence of PRPP (Figure 3.6). Maximum activity was obtained with 0.4-0.5 mM uracil in the presence of 1 mM PRPP, decreasing thereafter with increasing uracil concentrations. On the other hand, activity in the presence of 0.5 mM uracil and at varying concentrations of PRPP was maximal at 0.75-1 mM PRPP, remaining constant thereafter.

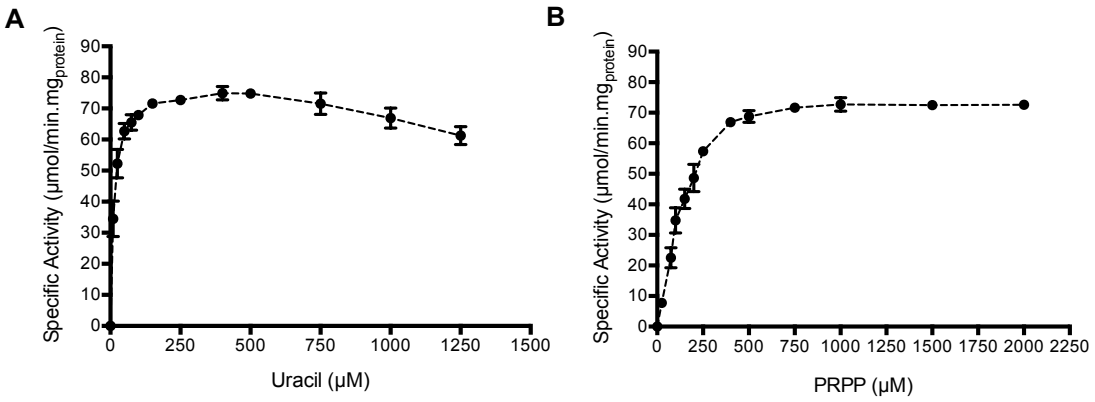


Figure 3.6. AgUPRTp activity at varying concentrations of uracil and PRPP. Specific AgUPRTp activity was determined spectrophotometrically as a function of uracil concentration in the presence of **(A)** 1 mM PRPP, and as a function of PRPP concentration in the presence of **(B)** 0.5 mM uracil concentration. Data represent average ± standard deviation from three experimental replicates.

Lastly, as shown in Figure 3.7, uracil concentrations ≥1 mM negatively affected AgUPRTp activity in a statistically significant way, such that with 1.25 mM uracil, catalytic activity was approximately 80 % of maximum. This dose-dependent effect of uracil on AgUPRTp activity could not be circumvented by the addition of more PRPP. These observations are in line with what was observed in terms of growth of the *A. gossypii Agura3* mutant, for which uracil concentrations above 1 mM were increasingly deleterious (Table 3.1; Figure 3.2).

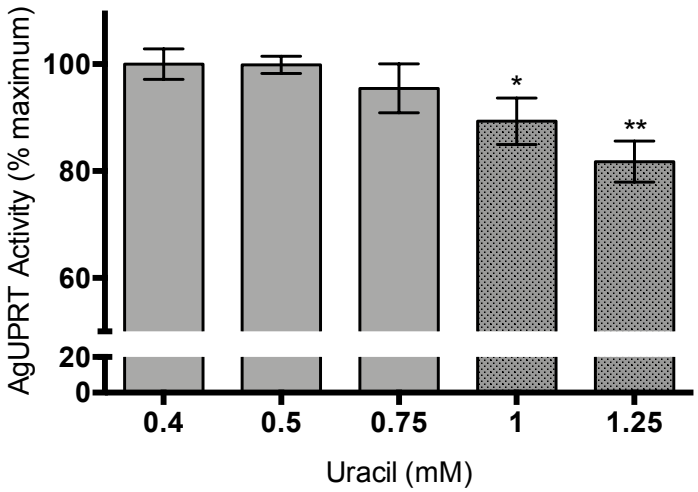


Figure 3.7. Effect of increasing uracil concentrations on AgUPRTp activity. AgUPRTp activity was determined spectrophotometrically at a set-saturating PRPP concentration (1 mM) and represented as percentage of the maximum activity. Data represent average ± standard deviation from three experimental replicates. Asterisks represent significant differences (* $p < 0.05$; ** $p < 0.01$) compared to the maximum activity.

UPRT is an enzyme that is highly conserved across species (Ghosh et al., 2015) and has been characterized in several organisms, from prokaryotes (Andersen et al., 1992) to humans (Li et al., 2007). Among them, the UPRTs from the protozoan parasites *L. donovani* and *T. gondii* have also been described to be negatively affected by high uracil concentration (Soysa et al., 2013). Moreover, the growth of an *L. donovani* pyrimidine auxotroph was shown to be (i) inhibited by increasing concentrations of uracil, (ii) not completely rescued by cytosine, and (iii) only fully restored when uridine was used as supplementation (Wilson et al., 2012), thus revealing a surprising, but also striking similarity to what was observed here with *A. gossypii Agura3*.

The conversion of uracil to UMP catalysed by UPRT is dependent on the presence of PRPP, an essential precursor shared by the purine and pyrimidine pathways, both *de novo* and salvage pathways (Hove-Jensen, 1988; Switzer, 1969). In turn, the purine biosynthetic pathway is essential for the production of guanosine-5-triphosphate (GTP), one of the precursors for riboflavin production. Indeed, a direct correlation between increased availability of PRPP and riboflavin overproduction by *A. gossypii* was previously demonstrated (Jiménez et al., 2008), which may explain the riboflavin-overproducing phenotype displayed by the *Agura3* mutant (Silva et al., 2015). Overproduction of riboflavin is a key differentiating trait of *A. gossypii*, not only at the biotechnological level but also ecologically, as it has been suggested that *A. gossypii* overproduces riboflavin as a detoxifying (Dietrich et al., 2013; Walther and Wendland, 2012) and protective mechanism (Stahmann et al., 2001). Although the regulatory mechanisms involved in riboflavin overproduction remain largely unknown, the biological relevance of the negative regulation of AgUPRTp activity by high uracil concentration is most likely related with this trait, for which it may well contribute as a mechanism to preserve PRPP for purine (and ultimately riboflavin) biosynthesis. Apart from ATP, which is present at mM levels, the average physiological concentrations of purines and pyrimidines for the routine functioning of the cell are in the μM range (Traut, 1994). Therefore, after these requirements are satisfied, PRPP can be channelled for the generation of precursors (GTP) for the production of riboflavin, which in *A. gossypii* is highly active in the late stages of growth and can easily reach very high concentrations (up to 20 g/L) (Revuelta et al., 2017; Schwechheimer et al., 2016).

Evidence supporting this hypothesis can be found in the almost perfect parallel with the events in *L. donovani* and *T. gondii*. Since protozoan parasites lack the *de novo* purine biosynthetic pathway, they must scavenge nutritionally essential purines from their hosts (Wilson et al., 2012), which they do through the purine salvage pathway, activity of which relies on two other PRPP-

dependent enzymes. Therefore, the biological relevance for the presence in these parasites of a uracil-mediated regulation mechanism of UPRT has been linked with the increased need of PRPP for purine biosynthesis (Soysa et al., 2013). Although the PRPP needs of each organism are for different purposes, the fact that *A. gossypii*, *L. donovani* and *T. gondii* have UPRTs which, after reaching a maximum activity, are negatively affected by increasing uracil concentrations strongly indicates that this mechanism may exist to favour purine synthesis when the pyrimidine requirements are satisfied.

A further independent and remarkable support to this hypothesis is the fact that uracil auxotrophs from other highly flavinogenic fungi, such as the yeasts *P. guilliermondii* and *D. hansenii*, are also unable to grow well in medium supplemented with uracil alone (Millerioux et al., 2011; Seda-Miró et al., 2007). These reports indicate that the hypersensitivity to uracil observed in *A. gossypii Agura3* extends to pyrimidine auxotrophs of other flavinogenic fungi and suggest that the UPRT modulation mechanism also exists in these fungi, just as the phenotypes and corresponding molecular mechanisms observed in *L. donovani* extend to other protozoan parasites (*e.g., T. gondii*) (Soysa et al., 2013).

3.4 Conclusions

Here, it is shown that high uracil concentrations negatively affect AgUPRTp activity, which can explain the growth impairment observed in the *A. gossypii Agura3* auxotroph when increasing concentrations of this pyrimidine intermediate are present in the medium. Until now, this phenomenon had been only reported to exist in protozoan parasites. The present findings demonstrate that this type of mechanism exists beyond the requirement for survival and can be extended to microorganisms that are phylogenetically distant from parasites. Moreover, since uracil auxotrophs are regularly used as backgrounds in genetic and metabolic engineering strategies, awareness is raised to these unusual phenotypes that may interfere with the correct assessment of strain modification outcomes.

From a biotechnological point of view, understanding the mechanisms behind the biosynthesis of high-value products by natural microbial producers is essential to develop stable and long-lasting biotechnological processes. After years of improving riboflavin production yields and titers in *A. gossypii*, the unravelling of new regulatory mechanisms involved in its biosynthesis will ensure the maintenance of this paradigm process in the successful industrial track. Contributing to that, the modulation mechanism of the AgUPRTp activity reported here reveals a new way of economizing essential metabolic precursors for riboflavin overproduction by *A. gossypii*.

3.5 References

Aguiar TQ, Dinis C, Domingues L. Cre-*lox*P-based system for removal and reuse of selection markers in *Ashbya gossypii* targeted engineering. Fungal Genet Biol 2014;68:1–8.

Aguiar TQ, Silva R, Domingues L. *Ashbya gossypii* beyond industrial riboflavin production: A historical perspective and emerging biotechnological applications. Biotechnol Adv 2015;33:1774–86.

Aguiar TQ, Silva R, Domingues L. New biotechnological applications for *Ashbya gossypii*: Challenges and perspectives. Bioengineered 2017;4:309–15.

Andersen PS, Smith JM, Mygind B. Characterization of the *upp* gene encoding uracil phosphoribosyltransferase of *Escherichia coli* K12. Eur J Biochem 1992;204:51–6.

Brancato FP, Golding NS. The diameter of the mold colony as a reliable measure of growth. Mycologia 1953;45:848–64.

Çakar ZP, Sauer U, Bailey JE. Metabolic engineering of yeast: the perils of auxotrophic hosts. Biotechnol Lett 1999;21:611–6.

Costa SJ, Almeida A, Castro A, Domingues L, Besir H. The novel Fh8 and H fusion partners for soluble protein expression in *Escherichia coli*: a comparison with the traditional gene fusion technology. Appl Microbiol Biotechnol 2013;97:6779–91.

D'Enfert C, Diaquin M, Delit A, Wuscher N, Debeaupuis JP, Huerre M, Latge JP. Attenuated virulence of uridine-uracil auxotrophs of *Aspergillus fumigatus*. Infect Immun 1996;64:4401–5.

Dietrich FS, Voegelli S, Kuo S, Philippsen P. Genomes of *Ashbya* fungi isolated from insects reveal four mating-type loci, numerous translocations, lack of transposons, and distinct gene duplications. G3 (Bethesda) 2013;3:1225–39.

Dodgson AR, Dodgson KJ, Pujol C, Pfaller MA, Soll DR. Clade-specific flucytosine resistance is due to a single nucleotide change in the *FUR1* gene of *Candida albicans*. Antimicrob Agents Chemother 2004;48: 2223-7.

Gattiker A, Rischatsch R, Demougin P, Voegeli S, Dietrich FS, Philippsen P, Primig M. Ashbya Genome Database 3.0: a cross-species genome and transcriptome browser for yeast biologists. BMC Genom 2007;8:9.

Ghosh AC, Shimell M, Leof ER, Haley MJ, O'Connor MB. UPRT, a suicide-gene therapy candidate in higher eukaryotes, is required for *Drosophila* larval growth and normal adult lifespan. Sci Rep 2015;5:13176.

Gomes D, Aguiar TQ, Dias O, Ferreira EC, Domingues L, Rocha I. Genome wide metabolic re-annotation of *Ashbya gossypii*: new insights into its metabolism through a comparative analysis with *Saccharomyces cerevisiae* and *Kluyveromyces lactis*. BMC Genom 2014;15:810.

Hove-Jensen, B. Mutation in the phosphoribosylpyrophosphate synthetase gene (*prs*) that results in simultaneous requirements for purine and pyrimidine nucleosides, nicotinamide nucleotide, histidine, and tryptophan in *Escherichia coli*. J Bacteriol 1988;170:1148–52.

Jiménez A, Santos MA, Revuelta JL. Phosphoribosyl pyrophosphate synthetase activity affects growth and riboflavin production in *Ashbya gossypii*. BMC Biotechnol 2008;8:67–78.

Kelly R, Miller SM, Kurtz MB. One-step gene disruption by cotransformation to isolate double auxotrophs in *Candida albicans*. Mol Gen Genet 1988;214:24–31.

Li J, Huang S, Chen J, Yang Z, Fei X, Zheng M, et al. Identification and characterization of human uracil phosphoribosyltransferase (UPRTase). J Hum Genet 2007;52:415–22.

Magalhães F, Aguiar TQ, Oliveira C, Domingues L. High-level expression of *Aspergillus niger* β-galactosidase in *Ashbya gossypii*. Biotechnol Prog 2014;30:261–8.

Millerioux Y, Clastre M, Simkin AJ, Marais E, Sibirny AA, Noël T, et al. Development of a *URA5* integrative cassette for gene disruption in the *Candida guilliermondii* ATCC 6260 strain. J Microbiol Methods 2011;84:355–8.

Natalini P, Ruggieri S, Santarelli I, Vita A, Magni G. Baker's yeast UMP: pyrophosphate phosphoribosyltransferase. Purification, enzymatic and kinetic properties. J Biol Chem 1979;254:1558–63.

Pronk JT. Auxotrophic yeast strains in fundamental and applied research. Appl Environ Microbiol 2002;68:2095–100.

Revuelta JL, Ledesma-Amaro R, Lozano-Martinez P, Díaz-Fernández D, Buey RM, Jiménez A. Bioproduction of riboflavin: a bright yellow history. J Ind Microbiol Biotechnol 2017;44:659–665.

Ritt JF, Raymond F, Leprohon P, Légaré D, Corbeil J, Ouellette M. Gene amplification and point mutations in pyrimidine metabolic genes in 5-fluorouracil resistant *Leishmania infantum*. PLoS Negl Trop Dis. 2013;7:e2564.

Schumacher MA, Carter D, Scott DM, Roos DS, Ullman B, Brennan RG. Crystal structures of *Toxoplasma gondii* uracil phosphoribosyltransferase reveal the atomic basis of pyrimidine discrimination and prodrug binding. EMBO J 1998;17:3219–32.

Schwechheimer SK, Park EY, Revuelta JL, Becker J, Wittmann C. Biotechnology of riboflavin. Appl Microbiol Biotechnol 2016;100:2107–19.

Seda-Miró JM, Arroyo-González N, Pérez-Matos A, Govind NS. Impairment of cobalt-induced riboflavin biosynthesis in a *Debaryomyces hansenii* mutant. Can J Microbiol 2007;53:1272–7.

Sherman F, Fink GR, Hicks JB. Methods in Yeast Genetics: A Laboratory Course Manual. New York: Cold Spring Harbor Laboratory Press; 1986.

Sievers F, Wilm A, Dineen D, Gibson TJ, Karplus K, Li W, et al. Fast, scalable generation of high-quality protein multiple sequence alignments using Clustal Omega. Mol Syst Biol 2011;7:539.

Silva R, Aguiar TQ, Domingues L. Blockage of the pyrimidine biosynthetic pathway affects riboflavin production in *Ashbya gossypii*. J Biotechnol 2015;193:37–40.

Soysa R, Wilson ZN, Elferich J, Forquer I, Shinde U, Riscoe MK, et al. Substrate inhibition of uracil phosphoribosyltransferase by uracil can account for the uracil growth sensitivity of *Leishmania donovani* pyrimidine auxotrophs. J Biol Chem 2013;288:29954–64.

Stahmann KP, Arst Jr HN, Althöfer H, Revuelta JL, Monschau N, Schlüpen C, et al. Riboflavin, overproduced during sporulation of *Ashbya gossypii*, protects its hyaline spores against ultraviolet light. Environ Microbiol 2001;3:545–50.

Sun XY, Zhu JF, Bao L, Hu CC, Jin C, Harris SD, et al. *pyrG* is required for maintaining stable cellular uracil level and normal sporulation pattern under excess uracil stress in *Aspergillus nidulans*. Sci China Life Sci 2013;56:467–75.

Switzer RL. Regulation and mechanism of phosphoribosylpyrophosphate synthetase. I. Purification and properties of the enzyme from *Salmonella typhimurium*. J Biol Chem 1969;244:2854–63.

Traut TW. Physiological concentrations of purines and pyrimidines. Mol Cell Biochem 1994;140:1–22.

Walther A, Wendland J. *Yap1*-dependent oxidative stress response provides a link to riboflavin production in *Ashbya gossypii*. Fungal Genet Biol 2012;49:697–707.

Wilson ZN, Gilroy CA, Boitz JM, Ullman B, Yates PA. Genetic dissection of pyrimidine biosynthesis and salvage in *Leishmania donovani*. J Biol Chem 2012;28**:**12759–70.

CHAPTER IV

Exploration of the *Ashbya gossypii* pyrimidine auxotroph *Agura3* for orotic acid production

Abstract

Orotic acid (orotate) is an intermediate of the *de novo* pyrimidine biosynthetic pathway present in microorganisms and also in humans. Its application as a mineral carrier in formulations of nutraceutical supplements and its use as precursor of nucleotides and pyrimidine-derived compounds are widely explored. Biotechnological production of this compound by microorganisms requires the use of a pyrimidine auxotrophic strain, since it is the blockage of the *de novo* pyrimidine biosynthesis downstream the formation of orotic acid that leads to its accumulation and excretion. However, this phenotype is not always observed in eukaryotic microorganisms, suggesting that additional metabolic features must be present in orotic acid-producing species. Through characterization of the pyrimidine auxotroph *Agura3* we demonstrate here that *Ashbya gossypii* is among the eukaryotic species able to accumulate and excrete orotic acid to the culture medium. In light of previous evidences, a putative mitochondrial dihydroorotate dehydrogenase encoded by *AgURA9* is highlighted as a metabolic determinant for this phenotype. Envisioning the future development of a cost-effective orotic acid production process employing *A. gossypii*, the *Agura3* strain was further engineered with the overexpression of a gene involved in glycerol metabolism (*AgGUP1*) and characterized in different media containing cheap complex nutrients and/or industrial wastes. This strain demonstrated a superior consumption profile of glycerol, an abundant carbon source in the main by-product of the industrial biodiesel production, as well as improved glycerol-dependent tolerance to hyperosmotic stress conditions, which are frequently encountered in industrial fermentations. Altogether, *A. gossypii Agura3*, which was previously reported to display a riboflavin-overproducing phenotype, was identified here as a suitable host for the production of a novel high-value compound, orotic acid. Furthermore, a flexible and robust chassis strain for the production of high-value chemicals from industrial by-products was constructed based on this genetic background, *Agura3*_GUP1, which is harnessed for orotic acid and riboflavin production.

4.1 Introduction

Orotic acid is an intermediate of the *de novo* biosynthetic pathway of pyrimidines. It was firstly isolated from cow's milk in the beginning of the last century (1905) (Takayama and Furuya, 1989) and known as vitamin B_{13}. However, as it synthesis occurs in microorganisms and also in humans, this classification was abandoned (Takayama and Furuya, 1989; Wishart et al., 2018b). It is a minor constituent of the diet, mainly found in dairy products and some vegetables (such as carrots and beets). The commercial interest on this chemical relies on the use of its salt, orotate. Orotate is the conjugated base of orotic acid and, for a matter of simplicity, independently of its state it will be mentioned as orotic acid (Carvalho et al., 2016). Orotic acid is used in combination with minerals such as magnesium and calcium ("magnesium and calcium orotate"), since it acts as a carrier that improves their transportation into cells (Wishart et al., 2018a). These formulations are widely appreciated as supplements for athletes and people in general. In addition, as a key intermediate of the *de novo* pyrimidine biosynthesis, it is used as a precursor of nucleotides and pyrimidine-derived compounds (Carvalho et al., 2016).

Despite several bacteria have been reported to accumulate orotic acid, its biotechnological production by fermentation has been explored in pyrimidine auxotrophs of the bacterium *Corynebacterium glutamicum* (Takayama and Furuya, 1989; Takayama and Matsunaga, 1991). In these prokaryotes, blockage of the pyrimidine biosynthesis, generally at the orotidine 5'-phosphate decarboxylase level, seems to be the only requiring metabolic condition for their orotic acid-producing phenotype. However, when eukaryotes are inspected, other enzymatic factors appear to be also involved in this phenotype. For instance, the uracil-auxotroph *Scura3Δ* of the model yeast *Saccharomyces cerevisiae* does not display orotic acid production (Nezu and Shimokawa, 2004), but a similar mutant of the pre-whole genome duplication (pre-WGD) yeast *Kluyveromyces lactis* (*Klura3Δ*) produces large amounts of orotic acid in standard yeast extract-peptone-glucose (YPD) media (Carvalho et al., 2016). On the other hand, other yeast reported to produce orotic acid, *Candida albicans Caura3Δ*, only does so when YPD is supplemented with acetate (Nezu and Shimokawa, 2004). In Carvalho et al. (2016), the presence in *K. lactis* of a mitochondrial dihydroorotate dehydrogenase (DHOD; EC 1.3.5.2) encoded by *KlURA9*, which for instance is lacking in *S. cerevisiae*, was found to be of major importance for orotic acid production. While important metabolic features were disclosed in their work, the process developed by Carvalho et al. (2016) for orotic production with *K. lactis Klura3Δ* was performed using YPD. This commercial medium composition is not valued in industrial biotechnological processes since the

production of high-value chemicals should be ideally exploited from low-cost and environmental-friendly substrates (please see Chapter I). Therefore, the approach adopted for the process with *C. glutamicum*, in which a culture medium based in industrial by-products was optimized for orotic acid production (Takayama and Matsunaga, 1991), should be preferably followed.

Ashbya gossypii is a pre-WGD member of the Saccharomycetaceae family. In this filamentous fungus, unlike the purine biosynthetic pathway, which is strongly connected with the riboflavin overproduction phenotype of this fungus (Aguiar et al., 2015), investigation on pyrimidine biosynthesis is limited. However, *A. gossypii* presents some interesting singularities regarding the metabolic regulation of purine and pyrimidine biosynthesis that deserve attention (see Chapter III). For instance, the *de novo* pyrimidine biosynthesis pathway of this fungus, in contrast with *S. cerevisiae* and similarly to *K. lactis*, owns a putative mitochondrial DHOD (encoded by *AgURA9*). This fact suggests that an orotic acid-producing phenotype could be displayed by *A. gossypii* (Figure 4.1) and therefore the exploration of the *Agura3* pyrimidine auxotroph of this filamentous fungus (Aguiar et al., 2014) for orotic acid production should be considered.

In order to develop sustainable biotechnological processes, the identification of high-value chemicals should be conjugated with the exploitation of low-cost substrates. Glycerol is a by-product accumulated in several industrial processes, namely in biodiesel and bioethanol production processes (Klein et al., 2016). For instance, the amounts accumulated during biodiesel production are extremely relevant. Since this crude glycerol contains some contaminants it is considered a waste stream (Islam et al., 2017). Moreover, in comparison with sugars like glucose, utilization of glycerol in biotechnological processes may present some metabolic advantages, such as: (i) it does not exert the Crabtree effect and therefore higher biomass yields could be achieved; (ii) since it presents a superior degree of reduction, higher production yields can be obtained for some chemicals (Islam et al., 2017; Klein et al., 2016). Despite this, glycerol waste streams have been rather overlooked in comparison with other renewable raw materials (*e.g.*, lignocellulosic biomass). This is partly due to the fact that the leading eukaryotic industrial model, *S. cerevisiae*, has a reduced innate capacity to utilize glycerol as carbon source (Swinnen et al., 2013). *A. gossypii* presents a good ability to grow in glycerol (Ribeiro et al., 2012). Still, this carbon source has been poorly explored, being only tested for recombinant protein production (Magalhães et al., 2014).

With this in mind, the production of orotic acid by the pyrimidine auxotroph *A. gossypii Agura3*, harnessed for improved riboflavin production (Silva et al., 2105), was in here first disclosed. In addition, since glycerol was chosen as a suitable substrate for this end, the *Agura3*

mutant was further engineered to cope with the culture conditions envisaged. Finally, different low-cost medium formulations were tested to identify cheap substrates appropriate for the production of orotic acid, envisioning the economical feasibility of this novel biotechnological process employing *A. gossypii*.

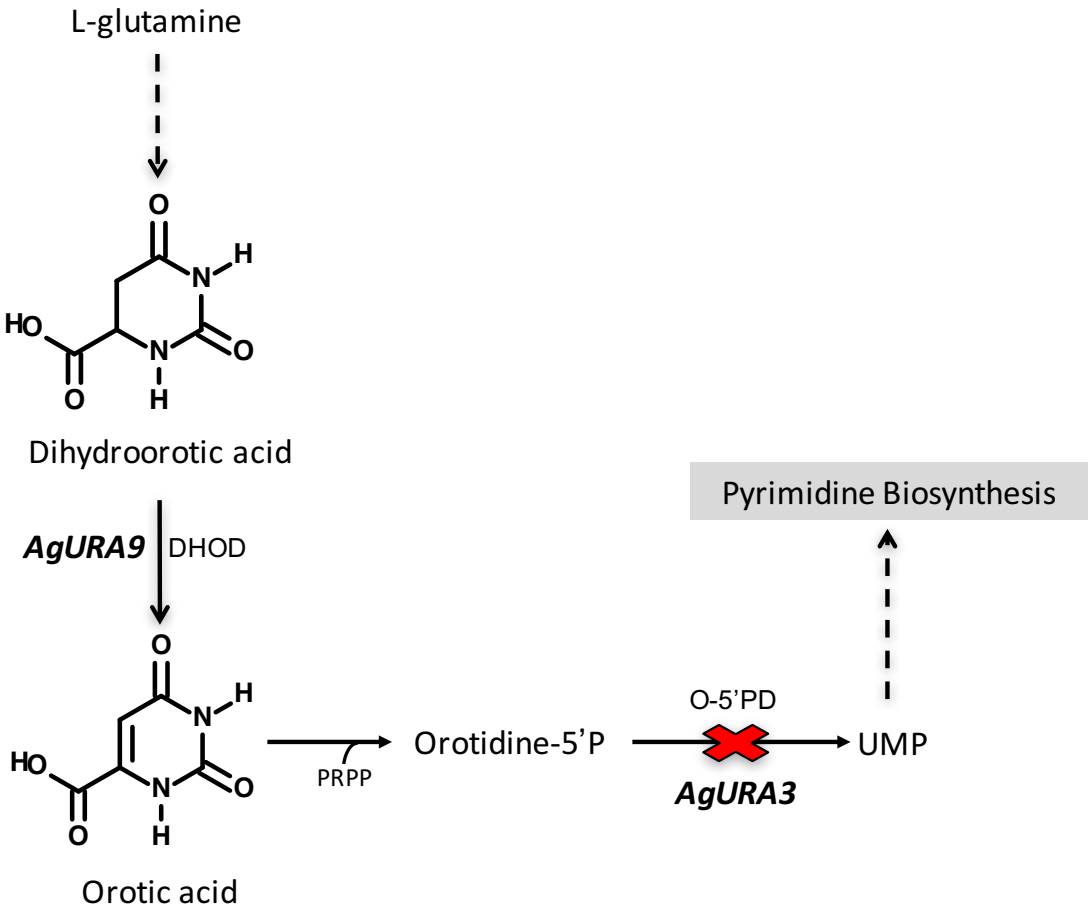


Figure 4.1. Schematic representation of the *de novo* biosynthetic pathway of pyrimidines in *A. gossypii*. Red × marks where the *de novo* pyrimidine biosynthetic pathway is blocked in the *A. gossypii Agura3* auxotroph. Dashed arrows indicate a multi-step pathway. Relevant gene names are represented in italic and bold. Acronyms near the gene names represent the corresponding enzyme: DHOD, dihydroorotate dehydrogenase; O-5'PD, orotidine-5'-phosphate decarboxylase. UMP: uridine monophosphate.

4.2 Material and methods

4.2.1 Strains

The *A. gossypii* strains used and generated during this study are listed in Table 4.1. The pyrimidine auxotroph studied in Chapter III, *A. gossypii Agura3* strain (Aguiar et al., 2014), was the core genetic background used. Stock cultures of these strains were kept as spores suspended in spore buffer containing 200 g/L glycerol, 8 g/L NaCl and 0.25 % (v/v) Tween 20 and stored at −80 °C. Spores were prepared as previously described in Chapter II.

Table 4.1. *A. gossypii* strains and primers used in this work. Lower case sequences correspond to homologous recombination sites.

***A. gossypii* strains**	**Relevant genotype**	**Parental strain**	**Reference**
ATCC 10895	Sequenced strain; Non-engineered	–	Prof. P. Philippsen, (University of Basel)
Agura3	*Agura3Δ*	ATCC 10895	Aguiar et al. (2014)
ATCC_GUP1	*loxP-KanMX4-loxP-*P_{AgGPD}*-AgGUP1*	ATCC 10895	This work
*Agura3*_GUP1	*Agura3Δ*, *loxP-KanMX4-loxP-*P_{AgGPD}*-AgGUP1*	*Agura3*	
Primers	**Sequence (5' – 3')**		**Purpose**
loxPK-GPDp-GUP1-fw	tacgtttgttatcacgtgctgaagtataacaggtttcaaattacagcgtgtt gcaacaacgactacttcacttgcaagagGTCGACAACCCTTAA TTTACCG		Overex[1]
loxPK-GPDp-GUP1-rv	gctaatcgggcgtctagcgcttccaaggagaacaaccggctcacgca cgtgagcgttgcatcccagagcgaatggagcatCTGTGCGGTGT GTATGTG		Overex[1]
AgGUP1p-fw	TGAAGGGACTATACTACCTACGT		Overex[1]/homok[2] confirmation
kanB-rv	CTGCAGCGAGGAGCCGTAAT		Overex[1]/homok[2] confirmation
AgGUP1-rv	GGGGTACCCACAATGAGGTAGTATGTGGCG		Overex[1]/homok[2] confirmation

[1]Overex. refers to the construction of the *AgGUP1* overexpression module. [2]Homokaryotic genotype.

4.2.2 Media and fermentations

AFM (10 g/L yeast extract, 10 g/L tryptone, 1 g/L myo-inositol and 20 g/L glucose) was the primary medium used for investigating orotic acid production. In alternative to glucose, glycerol was also used at different concentrations (AFM-glycerol). Additionally, some low-cost medium formulations were also tested, which contained complex nutrients and/or industrial wastes such as crude glycerol (GLY_{CR}), raw yeast extract (RYE; Kelbert et al., 2015), corn steep liquor (CSL; Pereira et al., 2010) and sugarcane molasses (SM). GLY_{CR} was kindly provided by CVR-Centre for Waste Valorisation (Guimarães, Portugal) and before use it was pre-treated to eliminate soap and methanol, essentially as described in Ruhal et al. (2011). GLY_{CR} was first diluted in distilled water (1:4 v/v) to reduce the viscosity of the fluid. The pH of the mixture was then adjusted to 3 with HCl (6 M) to convert soap into free fatty acids. The precipitate formed was separated from the mixture by centrifugation at 7000 rpm for 10 min. Next, the pH was adjusted to 12 with KOH (5 M) and the suspension filtrated through qualitative filter paper (Advantec) in order to remove suspended debris. Then, the pH of the filtrate was adjusted to 6.8 – 7. Finally, the methanol contained in the solution was removed by autoclaving and the concentration of glycerol quantified by high-performance liquid chromatography (HPLC). GLY_{CR} was then added to medium formulations at a final concentration equivalent to approximately 25 g/L glycerol. The origin and preparation mode of the RYE and CSL are reported in Kelbert et al. (2015) and (Pereira et al., 2010), respectively. SM was kindly provided by RAR: Refinarias de Açúcar Reunidas, S.A. (Porto, Portugal) and used at a final concentration equivalent to approximately 25 g/L sucrose. Whenever indicated, $CaCO_3$ (2 g/L) was used to buffer the medium. All the constituents of each media were sterilized together by autoclaving. As standard procedure, fermentations were performed in 250 mL shake-flasks with a working volume of 50 mL and carried out at 28 °C in an orbital shaker at 200 rpm. The inoculum was set to approximately 10^8 spores/L. However, since different growth conditions and medium formulations were tested, they are described in the "4.3 Results and discussion" section and figure legends. Fermentations were carried out in biological duplicates.

The experiment in controlled bioreactor was conducted in a 3.7 L Bioengineering's RALF with a working volume of 1.5 L at 30 ± 0.5 °C, 300 rpm agitation and 2 vvm aeration rate. The bioreactor was equipped with a condenser cooled with water to prevent evaporation. The bioreactor was inoculated with approximately 5 g of fresh biomass from an overnight pre-inoculum in AFM (10 g/L glucose). Samples were withdrawn at desired times and filtrated. Biomass was collected for cell dry weight determination and the filtrate stored at -20 °C for further analysis of orotic acid.

Cell dry weight (CDW) was determined by filtration, collection of the mycelium into a pre-weighed dried tube and drying at 105 °C until constant weight (~24 h).

4.2.3 Construction of the integration cassette and transformation of *A. gossypii* strains

DNA manipulations were made using standard molecular biology procedures (Domingues, 2017). For the overexpression of the *AgGUP1* gene (AFL067W; NCBI Reference Sequence: NM_210835.2) the transformation cassette used to substitute the native promoter of the gene was constructed as follows: the promoter sequence of the *AgGPD* gene and the *loxP-KanMX-loxP* selectable marker, conferring resistance to geneticin (G418), was amplified by PCR using specific primers (Table 4.1) from a vector described in Chapter V. These primers were used to introduce recombinogenic flanks for the *AgGUP1* locus corresponding to regions starting upstream 50 bp from the start codon and downstream the ATG initiation codon (Figure 4.2). This overexpression module was used to transform spores of *A. gossypii* using the Cre-*lox*P system (Aguiar et al., 2014). The primary heterokaryotic transformants were selected on agar-solidified AFM containing 250-300 g/L geneticin (G418). Selection of *A. gossypii* homokaryotic clones was performed through the germination of uninucleated haploid spores obtained from the primary heterokaryotic transformants on agar-solidified AFM-G418. The correct genomic integration of the cassette as well as the homokaryotic genotype of each clone were confirmed by analytical PCR (Appendix: Figure A4.1). For this purpose, a pin-head of mycelium from single colonies was suspended in 30 µL of extraction buffer (0.05 M carbonate buffer pH 6.9, 2 % (w/v) PVP 40, 0.2 % (w/v) BSA and 0.05 % (v/v) Tween 20) and incubated for 10 min at 100 °C. Afterwards, the tubes were centrifuged at maximum speed. The supernatant was used as template in the PCR reactions using the specific primers listed in Table 4.1.

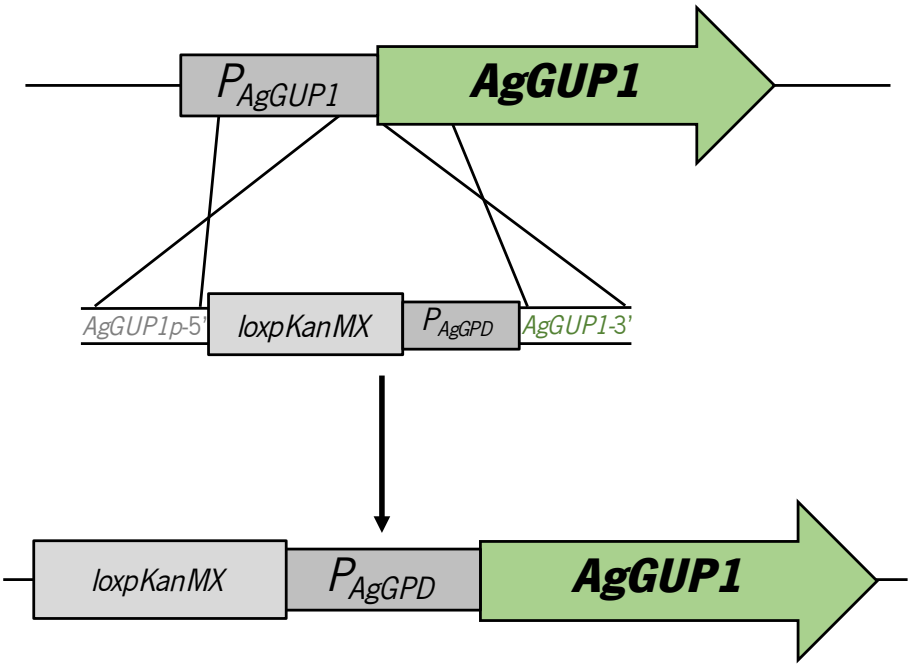


Figure 4.2. Engineering strategy and integration cassette used for the overexpression of *AgGUP1*.

4.2.4 Radial growth of *A. gossypii* strains in hyperosmotic stress conditions

Agar-solidified AFM containing 1 M KCl and 30 mM glycerol were inoculated with 10 µL of a suspension of spores (10^7 spores/mL) and incubated at 30 °C for 7 days. The control condition consisted in agar-solidified AFM. Colony radial growth (Brancato and Golding, 1953) was determined daily by measuring the diameter of colonies in 90 mm diameter Petri dishes in two perpendicular directions, through two guide lines previously drawn on the lower outer face of the plates. Radial growths were performed in biological duplicates.

4.2.5 Analytical methods

The concentration of glucose, glycerol and sucrose in the supernatant of fermentation samples was determined by HPLC using a BioRad Aminex HPX-87H (300 × 7.8 mm) column at 60 °C and 0.005 M sulfuric acid as eluent in a flow rate of 0.6 mL/min. The corresponding peaks were detected using a Knauer-IR intelligent refractive index detector. The orotic acid present in the supernatant of fermentation samples was quantified by ultra high-performance liquid chromatography (UHPLC) using a SHIMADZU Nexera X2 UHPLC chromatograph. The column used for separation was a BRISA LC2 C18 (250 mm × 4.6 mm, 5 µm particle size; from Teknokroma, Spain) maintained at room temperature. Column effluent was monitored at 280 nm using a SHIMADZU SPD-M20A diode array detector. The eluent used was 25 mM K_2HPO_4/KH_2PO_4 (pH

7.0) at a flow rate of 0.5 mL/min during a total run of 40 min (Carvalho et al., 2016). Orotic acid standard was obtained from Acros Organics (Belgium). Samples for orotic acid quantification were diluted with 500 mM NaOH when appropriate.

Riboflavin was measured as described in Ledesma-Amaro et al. (2015) with slight modifications. Briefly, 350 μL of supernatant from fermentation samples was mixed with 350 μL HCl (0.1 M) for extracellular riboflavin determination. A calibration curve was performed using pure riboflavin dissolved in 1 mM NaOH, which was processed in an identical way to the samples. Riboflavin concentration was determined spectrophotometrically at a wavelength of 445 nm. Measurements were performed in 96-well plates (200 μL/well) using a Synergy Mx / Cytation 3 microplate reader (Biotek). Three technical replicates were performed for each sample.

4.3 Results and discussion

4.3.1 *A. gossypii Agura3* produces and excretes orotic acid to the medium

Initial assessment of orotic acid production by *A. gossypii Agura3* in shake-flask cultivations revealed that this strain is able to produce orotic acid in the range of g/L from both glucose and glycerol (Figure 4.3) and that the orotic acid produced is mostly (if not exclusively) excreted to the extracellular medium, since no relevant differences were found between its concentration in the supernatant and total culture broth (lysed cells plus supernatant). Similarly to what was previously observed in *K. lactis* (Carvalho et al., 2016), time-course analysis of orotic acid production by *A. gossypii Agura3* showed a production kinetics associated with growth, which seems to stabilize at the stationary phase (Figure 4.3).

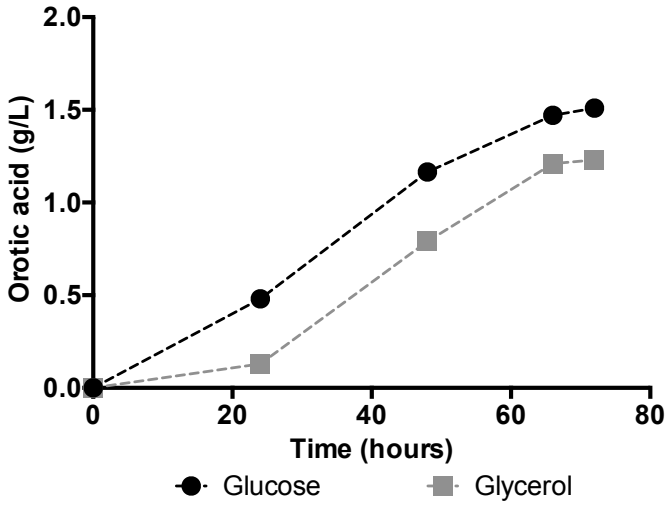


Figure 4.3. Time-course quantification of the orotic acid produced and excreted by *A. gossypii Agura3* during growth at 28 °C and 200 rpm in AFM (20 g/L glucose) or AFM-glycerol (20 g/L glycerol). Cultivations were stopped when the concentration of orotic acid stabilized. Data represent average values and standard deviations of biological duplicates. Where not seen, error bars were smaller than the symbols.

In glucose, the amounts of orotic acid produced by *A. gossypii Agura3* (1.51 ± 0.04 g/L) were slightly higher than those observed in glycerol (1.23 ± 0.04 g/L). However, when the concentration of orotic acid apparently stabilized, after 72 h of growth, glucose was already depleted from AFM cultivations, whereas 5.83 ± 0.58 g/L glycerol remained present in AFM-glycerol cultivations. At this time point, biomass production was similar in glucose (5.52 ± 0.33 g_{CDW}/L) and glycerol (5.73 ± 0.07 g_{CDW}/L).

As expected, orotic acid was not detected in *A. gossypii* ATCC 10895 cultivations. On the other hand, addition of 5 mM uridine to AFM abolished the production of orotic acid by *A. gossypii Agura3*. Thus, these results indicate that: (i) blockage of the *de novo* pyrimidine biosynthesis downstream the formation of orotic acid (*e.g.*, *Agura3Δ*) lead to the accumulation and subsequently excretion of this compound, as reported for *K. lactis* (Carvalho et al., 2016); (ii) when high amounts of intermediates of the pyrimidine salvage pathway (such as uridine) are present in the medium, this pathway is recruited and the metabolic flux through the *de novo* biosynthesis is reduced or null (as discussed in Chapter III). Notwithstanding these metabolic particularities, the major genetic determinant for orotic acid production appears to be the *AgURA9* gene. As previously reported, *K. lactis* owns two putative DHODs, KlUra1p (cytosolic; EC 1.3.98.1) and KlUra9p (mitochondrial; EC 1.3.5.2), whereas *S. cerevisiae*, *A. gossypii* and *C. albicans* only have one: ScUra1p (EC 1.3.98.1), AgUra9p (EC 1.3.5.2) (Gomes et al., 2014) and CaUra9p (EC 1.3.5.2) (Gojković et al., 2004), respectively. Given these genetic idiosyncrasies and the fact that, among these microorganisms, uracil auxotrophs of *S. cerevisiae* are the only unable to accumulate orotic acid (Nezu and Shimokawa, 2004), the existence of a putative mitochondrial DHOD is here highlighted as a determinant metabolic factor for orotic acid accumulation by eukaryotic microorganisms.

Interestingly, detection of orotic acid production from glycerol at production levels comparable to those obtained with glucose, even though glycerol is consumed at slower consumption rates, indicates that this polyol is a suitable carbon source for the production of high-value chemicals by *A. gossypii*. Therefore, in order to evaluate the flexibility of this production process, the characterization and optimization of glycerol consumption by *A. gossypii* was further explored.

4.3.2 Effects of *AgGUP1* overexpression on the glycerol consumption profile and hyperosmotic stress tolerance of *A. gossypii Agura3*

Major factors driving the development of a microorganism as a cell factory are the expansion of its substrate range utilization, together with the increasing of its consumption or co-consumption efficiency (Nielsen et al., 2016; Yadav et al., 2012). In addition, improvement of the robustness of the host towards industrial conditions is also constantly sought (Czajka et al., 2017). In *S. cerevisiae*, *GUP1* was firstly identified as a glycerol transporter by Holst et al. (2000), who reported its involvement in the growth of this yeast from glycerol (as energy and carbon source), as well as in cell recovery from hyperosmotic stress when glycerol was present in the medium.

Although other functions have been associated with *ScGUP1* far beyond glycerol metabolism, overexpression of the *ScGUP1* revealed to be an effective strategy to increase the glycerol consumption of *S. cerevisiae* strains (Jung et al., 2011; Yu et al., 2010a). The function of the *A. gossypii* synthetic homolog of this gene (*AgGUP1*) was never characterized at the molecular and cellular level. However, we have previously overexpressed the gene *AgGUP1* and its homolog from *S. cerevisiae* (*ScGUP1*) in *A. gossypii* ATCC 10895 through the use of a multi-copy plasmid (Silva, 2014 – MSc Thesis; unpublished results). The resulting strains (especially the strain overexpressing the native *AgGUP1*) presented enhanced glycerol consumption and improved hyperosmotic tolerance when glycerol was present in the medium. Given these previous outcomes, here we aimed at transferring these phenotypes to the *Agura3* strain in order to improve its performance on glycerol and to increase its robustness towards hyperosmotic stress conditions. We previously used a multi-copy vector to overexpress the *GUP1* genes, but the use of episomal vectors raises stability issues that are critical for industrial biotechnological applications. Therefore, here we overexpressed the native *AgGUP1* gene by replacing its native promoter by the strong and constitutive *AgGPD* promoter (Figure 4.2).

As shown in Figure 4.4, the glycerol consumption profile of the strain overexpressing the *AgGUP1* through a stable integrative overexpression cassette (*Agura3*_GUP1) was compared with that of the parental strain (*Agura3*) and, as expected, *Agura3*_GUP1 demonstrated a slight but consistent improvement in glycerol utilization, being able to consume almost completely all the glycerol present in AFM-glycerol after 8 days (192 h). At this time point, approximately 5 g/L of glycerol was still present in the *Agura3* cultures. Regarding orotic acid, the overexpression of *AgGUP1* did not affect negatively its production. In these culture conditions, the concentration of orotic acid stabilized after 72 – 96 h, when almost half of the carbon source initially supplied was consumed.

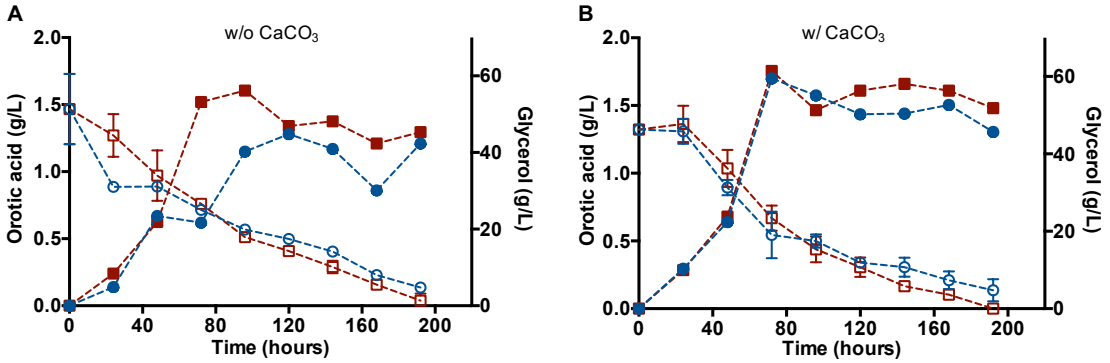


Figure 4.4. Orotic acid production and glycerol consumption by *A. gossypii Agura3* and *A. gossypii Agura3*_GUP1 in AFM-glycerol **(A)** without $CaCO_3$ and **(B)** with $CaCO_3$ (2 g/L). *A. gossypii Agura3* is represented by circles (●) and *A. gossypii Agura3*_GUP1 by squares (■). Filled symbols represent orotic acid and empty symbols glycerol. Strains were grown for 8 days at 28 °C and 200 rpm. Data represent average values and standard deviations of biological duplicates. Where not seen, error bars were smaller than the symbols.

In addition to the standard AFM-glycerol formulation (Figure 4.4A), we also tested the buffering of the medium with $CaCO_3$ (Figure 4.4B) for the following reason: *A. gossypii Agura3* has a genetic background harnessed for improved riboflavin production (Silva et al., 2015) and riboflavin production is favoured in the pH range of 6.0 – 7.0, which is near the buffering capacity of $CaCO_3$. In this condition (Figure 4.4B), riboflavin production for *A. gossypii Agura3* was 73.5 ± 14.5 mg/L, while for *Agura3*_GUP1 it was 58.1 ± 1.8 mg/L (vs 46.6 ± 4.9 mg/L without $CaCO_3$). Altogether, these results demonstrated that the beneficial effects of *AgGUP1* overexpression for glycerol consumption are achieved in strain *Agura3*_GUP1 without negatively affecting riboflavin and/or orotic acid production (Figure 4.4).

Given that glycerol was described to act as a major osmoprotectant for *A. gossypii* cells (Förster et al.,1998) and that in *S. cerevisiae* ScGup1p has an important and complementary role in counteracting hyperosmotic stress conditions (Holst et al., 2000; Yu et al., 2010b), the overexpression of *AgGUP1* could bring an additional benefit to *A. gossypii Agura3* by improving its hyperosmotic stress tolerance. Increasing concentrations of ionic (KCl) and non-ionic (sorbitol) osmotic stress agents gradually affected the radial growth of *A. gossypii* (Silva, 2014 – MSc Thesis; unpublished results). KCl had a more pronounced effect, being able to abolish the growth of the ATCC 10895 strain at concentrations of 1 M. This stress could be counteracted by the strain overexpressing *AgGUP1*. However, this was only observed when small concentrations of glycerol were present in the medium, suggesting that the improvement in hyperosmotic stress tolerance

was dependent on external glycerol. Thus, to assess the hyperosmotic stress tolerance of *A. gossypii Agura3*_GUP1, this strain was grown on agar-solidified AFM containing an osmotic stress agent (1 M KCl) and 30 mM glycerol, and its growth was compared with that of the parental strain (*Agura3*) (Figure 4.5).

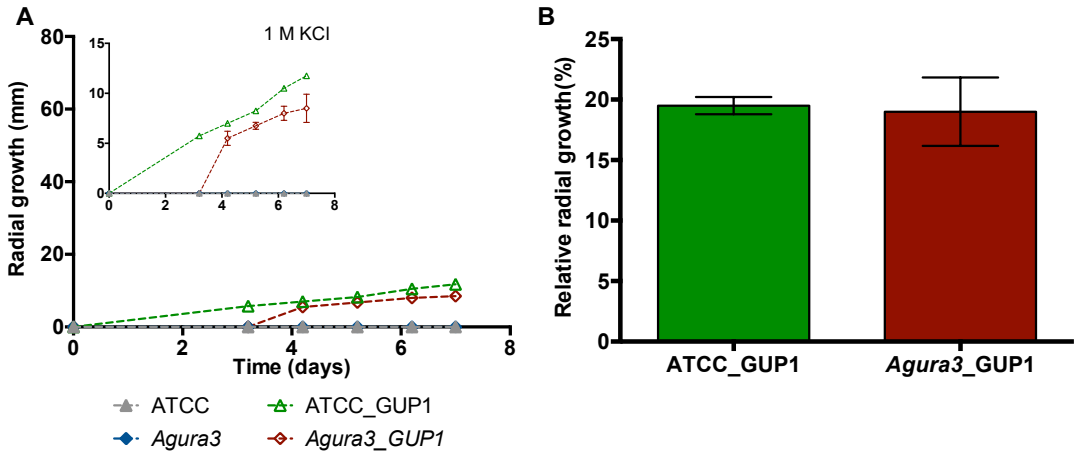


Figure 4.5. **(A)** Radial growth of *A. gossypii* strains on agar-solidified AFM with 1 M KCl. Strains were grown for 7 days at 30 °C. The small graphic represents the same data but with smaller scale of the vertical axis to allow a better comparison. **(B)** Relative radial growth (%) of strains overexpressing *AgGUP1* (ATCC_GUP1 and *Agura3*_GUP1). Relative growth was obtained by calculating the ratio between the final radial growth of each strain in 1 M KCl and in the AFM without KCl. Data represent average values and standard deviations. Where not seen, error bars were smaller than the symbols.

By analysing Figure 4.5A we confirmed that the overexpression of *AgGUP1* improved the radial growth of all strains at hyperosmotic stress conditions that completely abolish the growth of the parental strains (*Agura3* and ATCC 10895). Interestingly, the improvement was similar for both overexpressing strains (Figure 4.5B), which under hyperosmotic stress conditions present 20 % of the radial growth observed in control conditions. Glycerol is the major osmoprotectant used by *A. gossypii* under hyperosmotic stress conditions (Förster et al., 1998). Under these conditions, the preferential mechanism adopted by *A. gossypii* cells to accumulate glycerol is through its biosynthesis. This is also observed in *S. cerevisiae* (Blomberg and Adler, 1989; Förster et al., 1998; Holst et al., 2000). Given the connection of the improved hyperosmotic stress phenotype here observed with the presence of exogenous glycerol in the medium, we propose that the overexpression of *AgGUP1* complement the main response mechanism of *A. gossypii* to strong hyperosmotic stress conditions (glycerol biosynthesis) by being involved in the uptake of exogenous

glycerol when this is available. This is particularly relevant since *A. gossypii* is among the most sensitive fungi to osmotic stress (Nikolaou et al., 2009).

In sum, the overexpression of *AgGUP1* revealed to be a flexible metabolic/physiological engineering strategy that allowed enhancing the consumption of glycerol, a carbon source abundantly present in industrial wastes, while simultaneously improved the *A. gossypii* robustness towards osmotic stress, one of the stresses encountered in industrial fermentations by microbial cell factories. Furthermore, these improvements were added up to a genetic background (*Agura3*) that was already harnessed for riboflavin and orotic acid production.

4.3.3 Exploring culture conditions for orotic acid production by *A. gossypii*

Once a novel bioproduct coming from the exploration of the *A. gossypii* natural metabolism was identified (orotic acid) and a promising chassis constructed (*Agura3*_GUP1), we further looked at exploring the most suitable culture conditions for orotic acid production. In many biotechnological processes, the attainment of proper production titers requires the use of well-controlled bioreactors. Thus, *A. gossypii Agura3*_GUP1 was grown in controlled bioreactor, where agitation, aeration and pH of the culture were monitored throughout the fermentation. However, no marked improvement was detected in comparison with the previous shake-flask fermentations using similar medium composition (AFM; 20 g/L glucose) (Figure 4.6). An additional fermentation in similar conditions of agitation and aeration rate was performed in controlled bioreactor using AFM-glycerol (20 g/L glycerol) with again no noticeable improvement in orotic acid production when compared to shake-flask culture (data not shown).

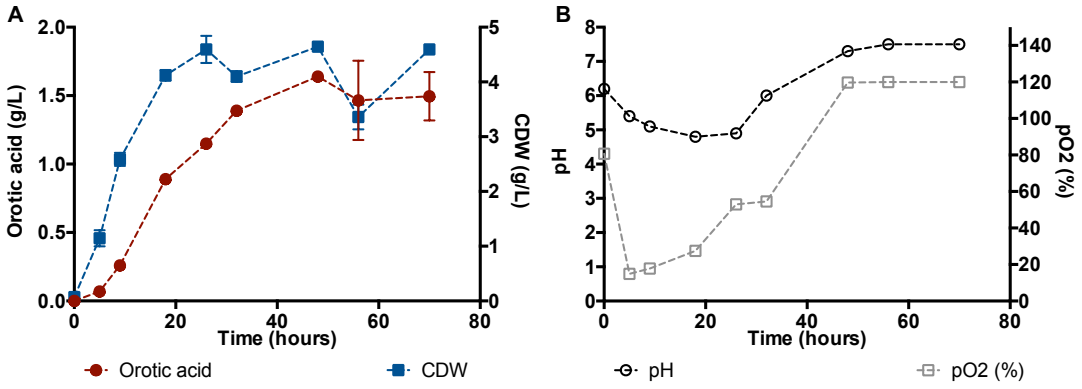


Figure 4.6. Performance of *A. gossypii Agura3*_GUP1 during a controlled bioreactor fermentation using AFM (20 g/L glucose). **(A)** Orotic acid and biomass production (CDW) and **(B)** pH and dissolved oxygen concentration (pO2) profiles during 3 days (72 h) of culture at 30 °C using 300 rpm of agitation and 2 vvm of aeration.

Curiously, Carvalho et al. (2016) have also reported no improvement in orotic acid production by *K. lactis Klura3* upon shifting from shake-flasks to bioreactor fermentations. Taken this into account we proceeded with the exploration and understanding of the most suitable culture conditions for orotic acid production by *A. gossypii* in shake-flasks, since this is the most convenient system for screening multiple conditions.

Since the *de novo* pyrimidine pathway is linked to the respiratory chain in *A. gossypii* and *K. lactis* through a mitochondrial DHOD, a good oxygenation of the culture should be determinant for orotic acid production by *A. gossypii*, similarly to what was previously observed for *K. lactis* (Carvalho et al., 2016). To assess the effect of culture oxygenation in shake-flask, *Agura3*_GUP1 was grown under different aeration conditions in AFM-glycerol using 40 g/L of this carbon source (Figure 4.7). To provide a higher level of aeration, the ratio between working volume/shake-flask capacity was increased from 1:5 to 1:10. For that, the headspace in shake-flasks was increased by reducing the working volume of the medium (25 mL in shake-flasks of 250 mL; 25/250 mL) or by using a shake-flask with higher capacity (50 mL in shake-flasks of 500 mL; 50/ 500 mL).

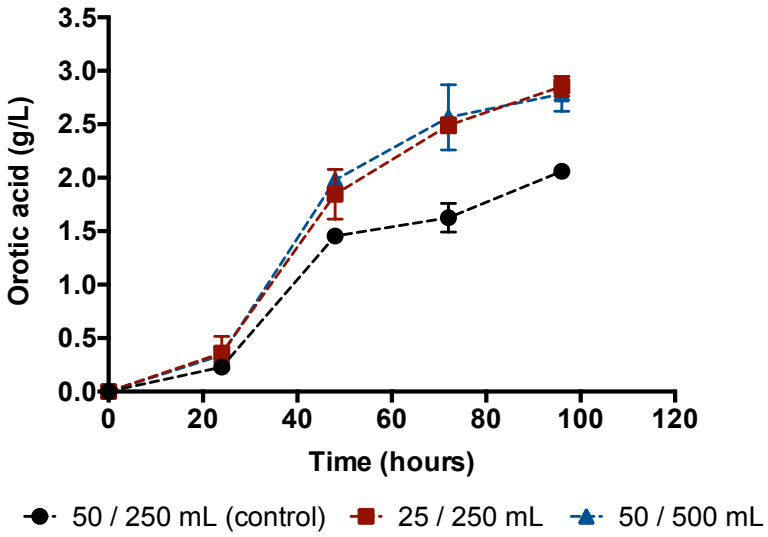


Figure 4.7. Effect of aeration on orotic acid production by *A. gossypii Agura3*_GUP1 during shake-flask fermentation in AFM-glycerol (40 g/L glycerol). Superior levels of aeration were achieved by increasing the headspace in shake-flasks (to a ratio of 1:10) through reduction of the working volume of the medium (25 mL in shake-flasks of 250 mL) or by using a shake-flask with higher capacity (50 mL in shake-flasks of 500 mL). The control condition consisted in 50 mL of working volume in shake-flaks of 250 mL (ratio of 1:5). Strains were grown at 28 °C and 200 rpm. Data represent average values and standard deviations of biological duplicates. Where not seen, error bars were smaller than the symbols.

As seen in Figure 4.7, the production of orotic acid in shake-flask was positively affected by increased aeration, with similar improvements achieved in both conditions tested (25/250 mL and 50/500 mL). In these conditions, after 96 h a maximum concentration of 2.85 ± 0.09 g/L of orotic acid was reached. This represents an increase of 39 % in orotic acid production in comparison with the control condition (50/250 mL). We also evaluated orotic acid production using 50 mL cultures in baffled flasks of 500 mL and the improvements to the control condition remained similar. Thus, these results in shake-flask system suggest that a good culture oxygenation is indeed important for orotic acid production by *A. gossypii*. Together with the general preference of *A. gossypii* for aerobic culture conditions, these data highlight the suitability of this filamentous fungus as a host for the production of orotic acid.

Furthermore, envisioning the future formulation of a low-cost production medium, low-cost industrial by-products were assessed as culture medium components for the production of orotic acid and other high-value products by *A. gossypii*. Hence, crude glycerol (GLY_{CR}) and sugarcane molasses (SM) were tested as carbon sources and raw yeast extract (RYE) and corn steep liquor (CSL) as complex supplements. GLY_{CR} is the main by-product of the biodiesel industry, being accumulated in large amounts during this industrial process (10 % of the total biodiesel produced; Islam et al., 2017). SM is a by-product from the sugar manufacturing industry and it is mainly rich in sucrose (Lozano-Martínez et al., 2016). In turn, CSL is a by-product of corn starch processing and a rich source of amino acids, minerals and vitamins (Pereira et al., 2010), while RYE coming from the brewery industry is a very complex supplement containing at large extent proteins but also many micronutrients (Kelbert et al., 2015; Schwechheimer et al., 2018). Thus, the production of orotic acid by *A. gossypii Agura3*_GUP1 from different combinations of these substrates was tested in shake-flasks fermentation. As can be seen in Figure 4.8, *A. gossypii* was able to produce orotic acid from all the medium formulations shown, which are exclusively made of low-cost substrates.

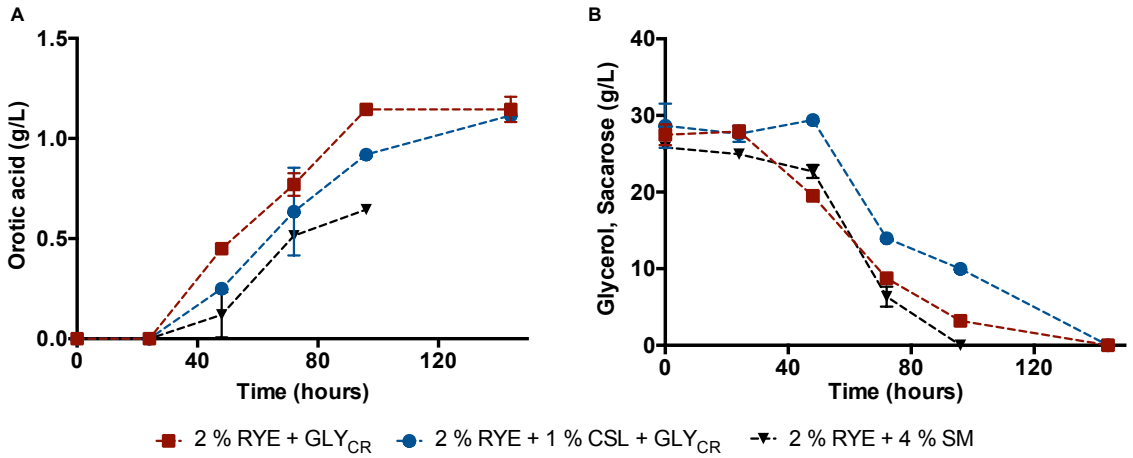


Figure 4.8. **(A)** Orotic acid production and **(B)** carbon source consumption by *Agura3*_GUP1 in shake-flask fermentations using crude glycerol (GLY$_{CR}$; ~2.5 % v/v) or sugarcane molasses (SM; ~2.5 % w/v) as main carbon source. Fermentations were carried out at 28 °C and 200 rpm in 250 mL shake-flasks containing 25 mL medium. The percentages (%) indicated for RYE, CSL are expressed in w/v. All medium formulations were buffered with 2 g/L $CaCO_3$. Data represent average values and standard deviations of biological duplicates. Where not seen, error bars were smaller than the symbols.

Noteworthy, from a medium formulation constituted by 2 % RYE + GLY$_{CR}$, *A. gossypii* *Agura3*_GUP1 was able to produce 1.15 ± 0.02 g/L of orotic acid after 96 h. Moreover, riboflavin production could also be visually detected (data not show) in this condition. Additional concentrations of RYE (4 %) and CSL (2 and 3 %) were tested, but no orotic acid production was detected in these conditions. Thus, these results clearly demonstrate that *A. gossypii* not only withstands these industrial by-products but also produces multiple high-value chemicals from a medium completely based on industrial by-products.

Overall, insights into the culture requirements for orotic acid production were acquired. The baseline production levels obtained here are comparable to those reported for other eukaryotic microorganisms (Carvalho et al., 2016; Nezu and Shimokawa, 2004). Thus, all the conditions are now gathered for the optimization of a bioprocess for the production of orotic acid simultaneously with other high-value products (riboflavin) employing *A. gossypii*, which demonstrated to be able of producing them from industrial by-products. Nevertheless, in order to guarantee elevated metabolic flux through the *de novo* pyrimidine biosynthetic pathway, further genetic engineering might be needed, in particular the overexpression or the introduction of additional copies of key gene(s) of this pathway (*e.g.*, *AgURA9*).

4.4 Conclusions

In this work, *A. gossypii* is presented as a novel host for the production of orotic acid due to its innate metabolic features. Inspection of the pyrimidine biosynthetic pathway of orotic acid-producing eukaryotic microorganisms exposed the putative mitochondrial DHOD encoded by *AgURA9* as a key metabolic determinant for the accumulation of orotic acid by the *Agura3* pyrimidine auxotroph. In addition, engineering of this pyrimidine auxotroph with the overexpression of a gene involved in glycerol metabolism (*AgGUP1*) improved its consumption profile of a main industrial by-product from biodiesel production (glycerol) while simultaneously increased its robustness towards hyperosmotic stress. This new *A. gossypii* strain can now serve as a chassis for further genetic optimization of the *de novo* pyrimidine biosynthetic pathway flux towards orotic acid production. Moreover, since this strain displayed simultaneous production of orotic acid and riboflavin from a medium completely based on industrial by-products, groundwork is set for developing low-cost medium formulations optimized for the production of multiple high-value chemicals.

4.5 References

Aguiar TQ, Dinis C, Domingues L. Cre-loxP-based system for removal and reuse of selection markers in *Ashbya gossypii* targeted engineering. Fungal Genet Biol 2014;68:1–8.

Aguiar TQ, Silva R, Domingues L. *Ashbya gossypii* beyond industrial riboflavin production: A historical perspective and emerging biotechnological applications. Biotechnol Adv 2015;33:1774–86.

Blomberg, A., Adler, L. Roles of glycerol and glycerol-3-Phosphate dehydrogenase (NAD+) in acquired osmotolerance of *Saccharomyces cerevisiae*. J Bacteriol 1989;171:1087–92.

Brancato FP, Golding NS. The diameter of the mold colony as a reliable measure of growth. Mycologia 1953;45:848–64.

Carvalho N, Coelho E, Gales L, Costa V, Teixeira JA, Moradas-Ferreira P. Production of orotic acid by a *Klura3Δ* mutant of *Kluyveromyces lactis*. J Biosci Bioeng 2016;121:625–30.

Czajka J, Wang Q, Wang Y, Tang Y. Synthetic biology for manufacturing chemicals: constraints drive the use of non-conventional microbial platforms. Appl Microbiol Biotechnol 2017;101:7427–34.

Domingues L. PCR: Methods and Protocols. 1st ed., New York: Springer; 2017.

Förster C, Marienfeld S, Wendisch VF, Krämer R. Adaptation of the filamentous fungus *Ashbya gossypii* to hyperosmotic stress: different osmoresponse to NaCl and mannitol stress. Appl Microbiol Biotechnol 1998;50:219–26.

Gomes D, Aguiar TQ, Dias O, Ferreira EC, Domingues L, Rocha I. Genome wide metabolic re-annotation of *Ashbya gossypii*: new insights into its metabolism through a comparative analysis with *Saccharomyces cerevisiae* and *Kluyveromyces lactis*. BMC Genomics 2014;15:810.

Gojković Z, Knecht W, Zameitat E, Warneboldt J, Coutelis JB, Pynyaha Y, et al. Horizontal gene transfer promoted evolution of the ability to propagate under anaerobic conditions in yeasts. Mol Genet Genomics 2004;271:387–93.

Holst B, Lunde C, Lages F, Oliveira R, Lucas C, Kielland-Brandt MC. *GUP1* and its close homologue *GUP2*, encoding multimembrane-spanning proteins involved in active glycerol uptake in *Saccharomyces cerevisiae*. Mol Microbiol 2000;37:108–24.

Islam ZU, Klein M, Aßkamp MR, Ødum ASR, Nevoigt E. A modular metabolic engineering approach for the production of 1,2-propanediol from glycerol by *Saccharomyces cerevisiae*. Metab Eng. 2017;44:223–35.

Jung JY, Hyun SY, Jinwon L, Min-Kyu O. Production of 1,2-Propanediol from glycerol in *Saccharomyces cerevisiae*. J Microbiol Biotechnol 2011;21:846–53.

Kelbert M, Romaní A, Coelho E, Pereira FB, Teixeira JA, Domingues L. Lignocellulosic bioethanol production with revalorization of low-cost agroindustrial by-products as nutritional supplements. Ind Crops Prod 2015;64:16–24.

Klein M, Islam ZU, Knudsen PB, Carrillo M, Swinnen S, Workman M, et al. The expression of glycerol facilitators from various yeast species improves growth on glycerol of *Saccharomyces cerevisiae*. Metab Eng Commun 2016;3:252–7.

Ledesma-Amaro R, Serrano-Amatriain C, Jiménez A, Revuelta JL. Metabolic engineering of riboflavin production in *Ashbya gossypii* through pathway optimization. Microb Cell Fact 2015b;14:163.

Lozano-Martínez P, Buey RM, Ledesma-Amaro R, Jiménez A, Revuelta JL. Engineering *Ashbya gossypii* strains for *de novo* lipid production using industrial by-products. Microb Biotechnol 2017;10:425–33.

Magalhães F, Aguiar TQ, Oliveira C, Domingues L. High-level expression of *Aspergillus niger* β-galactosidase in *Ashbya gossypii*. Biotechnol Prog 2014;30:261–8.

Nezu T, Shimokawa O. Acetate-mediated production of orotic acid by *ura3* mutants of *Candida albicans*. Microbiol Immunol 2004;48:783–5.

Nielsen J, Keasling JD. Engineering Cellular Metabolism. Cell 2016;164:1185–97.

Nikolaou E, Agrafioti I, Stumpf M, Quinn J, Stansfield I, Brown AJP. Phylogenetic diversity of stress signalling pathways in fungi. BMC Evol Biol 2009;9:44.

Pereira FB, Guimarães PM, Teixeira JA, Domingues L. Optimization of low-cost medium for very high gravity ethanol fermentations by *Saccharomyces cerevisiae* using statistical experimental designs. Bioresour Technol 2010;101:7856–63.

Ribeiro O, Domingues L, Penttilä M, Wiebe MG. Nutritional requirements and strain heterogeneity in *Ashbya gossypii*. J Basic Microbiol 2012;52:582–9.

Ruhal R, Aggarwal S, Choudhury B. Suitability of crude glycerol obtained from biodiesel waste for the production of trehalose and propionic acid. Green Chem 2011;13:3492–98.

Schwechheimer SK, Becker J, Peyriga L,, Portais JC, Wittmann C. Metabolic flux analysis in *Ashbya gossypii* using 13C-labeled yeast extract: industrial riboflavin production under complex nutrient conditions. Microb Cell Fact 2018;17:162.

Silva R. Exploitation of *Ashbya gossypii* for the production of high-value products from glycerol feedstocks. MSc thesis 2014, University of Minho, Portugal.

Silva R, Aguiar TQ, Domingues L. Blockage of the pyrimidine biosynthetic pathway affects riboflavin production in *Ashbya gossypii*. J Biotechnol 2015;193:37–40.

Takayama K, Furuya A. Microbial Production of Orotic Acid (Vitamin B13). In: Vandamme EJ, editor. Biotechnology of Vitamins, Pigments and Growth Factors. Elsevier, Applied Biotechnology Series; 1989. p. 285–97.

Takayama and Matsunaga. Process for producing orotic acid by fermentation. US Patent No. 1991/5,013,656.

Wishart DS, Feunang YD, Guo AC, Lo EJ, Marcu A, Grant JR, et al. DrugBank 5.0: a major update to the DrugBank database for 2018. Nucleic Acids Res 2018a;46: D1074–82.

Wishart DS, Feunang YD, Marcu A, Guo AC, Liang K, Vázquez-Fresno R, et al. HMDB 4.0: the human metabolome database for 2018. Nucleic Acids Res 2018b;46:D608–D17.

Yadav VG, De Mey M, Lim CG, Ajikumar PK, Stephanopoulos G. The future of metabolic engineering and synthetic biology: towards a systematic practice. Metab Eng 2012;14:233–41.

Yu KO, Kim SW, Han SO. Engineering of glycerol utilization pathway for ethanol production by *Saccharomyces cerevisiae*. Bioresour Technol 2010a;101: 4157–61.

Yu KO, Kim SW, Han SO. Reduction of glycerol production to improve ethanol yield in an engineered *Saccharomyces cerevisiae* using glycerol as a substrate. J Biotechnol 2010b;150:209–14.

CHAPTER V

Metabolic engineering of *Ashbya gossypii* for deciphering the *de novo* biosynthesis of γ-lactones

The work reported on this chapter was published in:

Silva R, Aguiar TQ, Coelho E, Jiménez A, Revuelta JL, Domingues L. Metabolic engineering of *Ashbya gossypii* for deciphering the *de novo* biosynthesis of γ-lactones. Microb Cell Fact 2019; https://doi.org/10.1186/s12934-019-1113-1.

Abstract

Lactones are highly valuable cyclic esters of hydroxy fatty acids that find application as pure fragrances or as building blocks of speciality chemicals. While chemical synthesis often leads to undesired racemic mixtures, microbial production allows obtaining optically pure lactones. The production of a specific lactone by biotransformation depends on the supply of the corresponding hydroxy fatty acid, which has economic and industrial value similar to γ-lactones. Hence, the identification and exploration of microorganisms with the rare natural ability for *de novo* biosynthesis of lactones will contribute to the long-term sustainability of microbial production. In this study, the innate ability of *Ashbya gossypii* for *de novo* production of γ-lactones from glucose was evaluated and improved. Characterization of the volatile organic compounds produced by nine strains of this industrial filamentous fungus in glucose-based medium revealed the noteworthy presence/production of seven chemically different γ-lactones. To decipher and understand the *de novo* biosynthesis of γ-lactones from glucose, we developed metabolic engineering strategies focused on the fatty acid biosynthesis and the β-oxidation pathways. Overexpression of *AgDES589*, encoding a desaturase for the conversion of oleic acid (C18:1) into linoleic acid (C18:2), and deletion of *AgELO624,* which encodes an elongase that catalyses the formation of C20:0 and C22:0 fatty acids, greatly increased the production of γ-lactones (up to 6.4-fold; $(7.6 \pm 0.8) \times 10^3$ $\mu g/g_{Cell\ Dry\ Weight}$). Further substitution of *AgPOX1*, encoding the exclusive acyl-CoA oxidase in *A. gossypii*, by a codon-optimized *POX2* gene from *Yarrowia lipolytica*, which encodes a specific long chain acyl-CoA oxidase, fine-tuned the biosynthesis of γ-decalactone to a relative production of more than 99 %. This study demonstrates the potential of *A. gossypii* as a model and future platform for *de novo* biosynthesis of γ-lactones. By means of metabolic engineering, key enzymatic steps involved in their production were elucidated. Moreover, the combinatorial metabolic engineering strategies developed resulted in improved *de novo* biosynthesis of γ-decalactone. In sum, these proof-of-concept data revealed yet unknown metabolic and genetic determinants important for the future exploration of the *de novo* production of γ-lactones as an alternative to biotransformation processes.

5.1 Introduction

Lactones are volatile organic compounds (VOCs) derived from the lipid metabolism. They are chemically classified as cyclic esters of hydroxy fatty acids and find application mainly as pure fragrances and flavours or as building blocks of specialty chemicals (Kourist and Hilterhaus, 2015). These compounds are naturally present in ripe fruits, such as peach and strawberry, and contribute extensively to their complex aroma and flavour (Sánchez et al., 2013; Sánchez-Sevilla, 2014). Concentrations of few mg/L of lactones provide the consumer a wide variety of sensorial perceptions ranging from fruity to creamy notes. Consequently, lactones can be found in products of the food and cosmetics industries, reaching a world market volume of hundreds of tons per year (Braga et al., 2018). The most relevant lactone commercialized is γ-decalactone, characterized by a strong peach-like odour.

Lactones are still mainly obtained by chemical synthesis (Braga et al., 2018). However, this type of process often leads to undesired racemic mixtures, has the problem of not being well accepted by the consumers and withstands serious environmental problems linked to fossil fuels (Hanko et al., 2018; Kourist and Hilterhaus, 2015). Therefore, microbial production has appeared as a sustainable biotechnological alternative that offers the possibility to obtain pure lactones.

Microbial production of lactones has been accomplished through biotransformation processes, where an immediate precursor of lactones (an hydroxy fatty acid) is added to the production media to be converted into the desired lactone. The majority of the biotransfomation processes explored at the industrial scale use the yeast *Yarrowia lipolytica* to convert ricinoleic acid (*e.g.*, from castor oil) to γ-decalactone. Following the same enzymatic pathway, the change of the precursor leads to the production of a different lactone (Kourist and Hilterhaus, 2015). For instance, the use of 10-hydroxystearic acid results in the production of γ-dodecalactone (An et al., 2013). Thus, in these processes, the production of a particular lactone entirely relies on the availability of the corresponding precursor. This is a major drawback, since these precursors often have economic value and industrial applicability equivalent to that of lactones (Patel et al., 2016). Moreover, castor oil, the raw substrate most commonly used, is connected to health and safety issues concerning its extraction from the plant *Ricinus communis* (Audi et al., 2005).

Given all of the above, the identification and engineering of microbial systems with the unusual natural ability for *de novo* biosynthesis of lactones from sustainable and highly accessible carbon sources, such as carbohydrates, constitutes a major challenge to this field. These microbial candidates should be able to efficiently transform carbohydrates into biolipids and consequently

convert them into lactones. To the extent of our knowledge, only three microbial species were previously studied for the *de novo* biosynthesis of lactones: two filamentous fungi, *Fusarium poae* (Latrasse et al., 1993) and *Trichoderma viride* (Collins et al., 1972; Fadel et al, 2015); and one yeast, *Sporidiobolus salmonicolor* (Dufossé et al., 1997; Haffner and Tressl, 1996). However, a comprehensive overview of this biosynthetic process is lacking and there is very little information regarding the genetic and enzymatic machinery involved.

Ashbya gossypii is a filamentous fungus of the Saccharomycetaceae family that has been used in the industrial production of riboflavin (vitamin B_2) for almost 30 years (Revuelta et al., 2016; Schwechheimer et al., 2016) and which presents important industrial advantages (Aguiar et al., 2015). Moreover, the molecular and *in silico* tools available for its engineering are steadily growing and omics data are becoming increasingly available (Aguiar et al., 2017). Together with these technical advantages, *A. gossypii* owns a very rich and heterogeneous metabolism mainly modulated by riboflavin overproduction (as exemplified in Chapter III), but being able to produce many other metabolites such as aromatic VOCs (Ravasio et al., 2014). In addition, since riboflavin is produced from the lipids that this fungus is able to biosynthesize (Schwechheimer et al., 2018) and to accumulate (Ledesma-Amaro et al., 2014a; Stahmann et al., 1994), *A. gossypii* shows up as a suitable microbial model for studying and modulating the production of the fatty acid-derived VOCs: lactones. Therefore, in this study, the innate potential of several *A. gossypii* strains to biosynthesize lactones was evaluated and metabolic engineering strategies towards the fatty acid biosynthesis and the β-oxidation pathways were performed (Figure 5.1A) with the objective of deciphering and understanding the intricate *de novo* biosynthesis of lactones in *A. gossypii*.

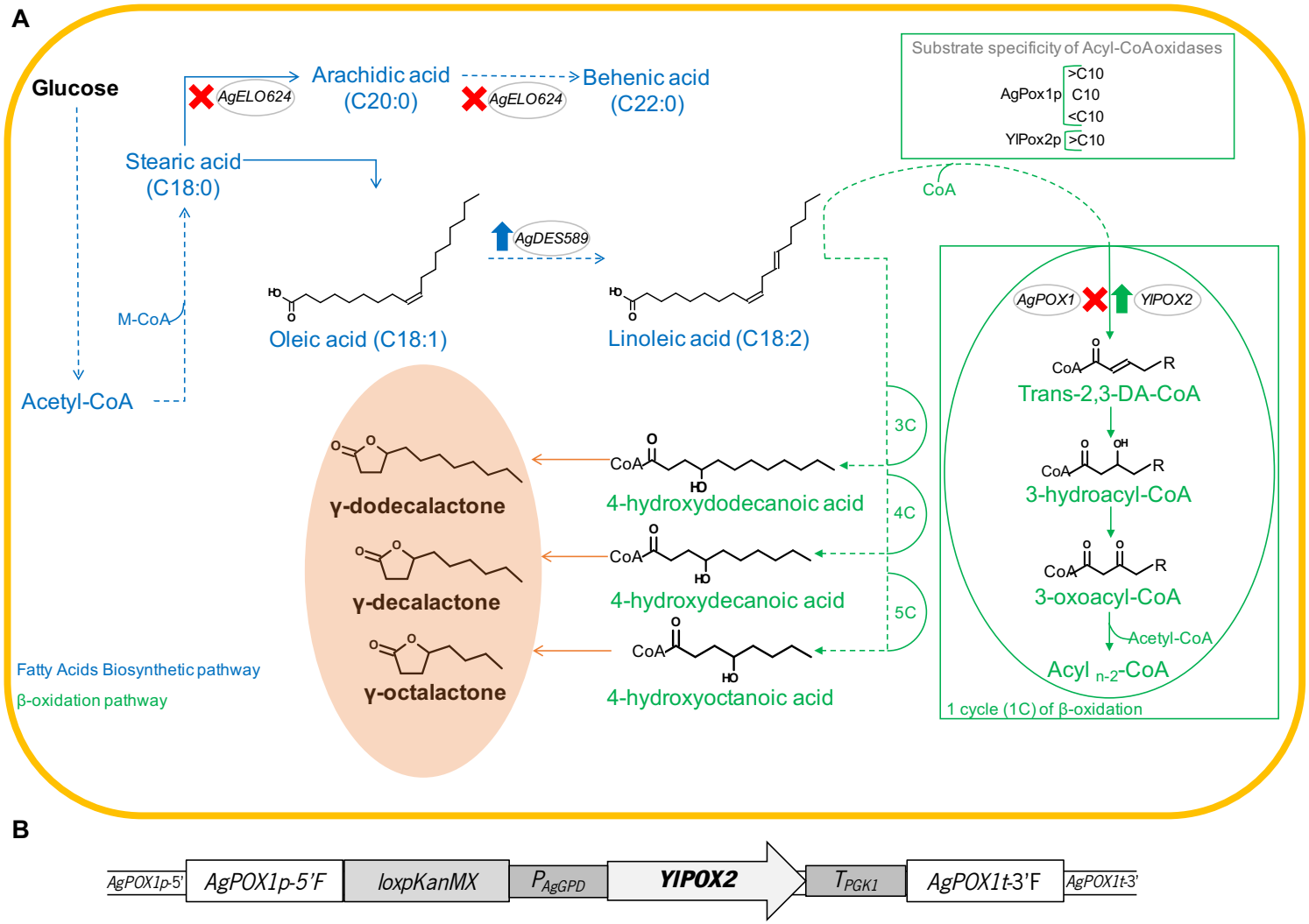


Figure 5.1. *Continued.*

Figure 5.1. *Continued.* Metabolic engineering of the *de novo* biosynthesis of lactones in *A. gossypii*. **(A)** Schematic diagram of the interconnection between the metabolic pathways involved in the *de novo* biosynthesis of lactones. An $acyl_{n-2}$-CoA represents a fatty acid from which two carbons of the initial chain length were removed after 1 cycle of β-oxidation. **(B)** Heterologous overexpression cassette constructed using the Golden-Gate rapid assembly. Grey-circled names represent the genes targeted for engineering. Dashed lines represent multi-reactions. Abbreviations used: M-CoA, malonyl-CoA; trans-2,3-DA-Coa, trans-2,3-dehydroacyl-CoA.

5.2 Materials and methods

5.2.1 Chemicals

The following chemicals with the corresponding purity were used as standards for the gas chromatography-mass spectrometry (GC–MS) analysis: 3-methyl-1-butanol (≥ 99.8 %), 2-phenylethanol (≥ 99 %) and γ-octalactone (> 98 %) from Fluka; γ-valerolactone (> 98 %) from TCI; γ-caprolactone (> 98 %), γ-nonalactone (> 98 %), γ-decalactone (≥ 98 %), γ-dodecalactone (≥ 97%) and γ-undecalactone (≥ 98 %) from Sigma-Aldrich.

5.2.2 Strains and media

The *A. gossypii* strains used and generated during this study are listed in Table 5.1. These strains were maintained on agar-solidified AFM (10 g/L yeast extract, 10 g/L tryptone, 1 g/L myo-inositol and 20 g/L glucose) or agar-solidified MA2 medium (20 g/L peptone, 2 g/L yeast extract, 0.6 g/L myo-inositol and 20 g/L glucose, pH 6.8). For longer periods, stock cultures of these strains were kept as spores suspended in spore buffer containing 200 g/L glycerol, 8 g/L NaCl and 0.25 % (v/v) Tween 20 and stored at −80 °C. Spores were prepared as previously described in Chapter II. The *S. cerevisiae* CEN.PK113-7D (MAT α, MAL2-8c, SUC2; INSA, France) and *Y. lipolytica* W29 (ATCC 20460:CLIB89) used for comparative purposes during the screening of the volatile compounds were maintained on agar-solidified YPD medium (10 g/L yeast extract, 20 g/L peptone and 20 g/L glucose). *Escherichia coli* DH5α strain served as host for the cloning experiments and was grown on agar-solidified LB medium (10 g/L tryptone, 5 g/L yeast extract and 10 g/L NaCl, pH 7.0) containing, when appropriate, 100 µg/mL ampicillin, 50 µg/mL kanamycin or 100 µg/mL spectinomycin for the selection and maintenance of plasmids.

Table 5.1. *A. gossypii* strains used and generated in this work.

***A. gossypii* strains**	**Relevant genotype**	**Parental strain**	**Reference**
ATCC 10895	Sequenced strain; Non-engineered	–	Prof. P. Philippsen, (University of Basel)
MUCL 29450	Non-engineered	–	Ribeiro et al. (2012)
IMI 31268	Non-engineered	–	
CBS 109.26	Non-engineered	–	
A5	Non-engineered	–	Ledesma-Amaro et al. (2015)
A7	Non-engineered	–	
A8	Non-engineered	–	
A9	Non-engineered	–	
A10	Non-engineered	–	
DES589	P_{AgGPD}-*AgDES589*	ATCC 10895	Ledesma-Amaro et al. (2014b)
elo624Δ	*Agelo624Δ*	ATCC 10895	
DES589/ elo624Δ	P_{AgGPD}-*AgDES589, Agelo624Δ*	DES589	This work
YlPOX2	*Agpox1Δ::loxP-KanMX4-loxP-* P_{AgGPD}-*synYlPOX2*	ATCC 10895	
DES589/ elo624Δ/ YlPOX2	P_{AgGPD}-*AgDES589, Agelo624Δ, Agpox1Δ::loxP-KanMX4-loxP-* P_{AgGPD}-*synYlPOX2*	DES589/ elo624Δ	

5.2.3 Culture conditions for the analysis of the VOCs produced by *A. gossypii* non-engineered strains

As not all the *A. gossypii* strains are able to sporulate under laboratory conditions (Ribeiro et al., 2012), the inocula for the screening of VOCs were made as follows. Grown mycelium of each strain was scrapped off an agar-solidified AFM plate and digested with 4 mg/mL lysing enzymes from *T. harzianum* (Sigma-Aldrich) in order to obtain more homogeneously dispersed mycelium. Subsequently, this was used to prepare a pre-inoculum in MA2 medium that was grown for 48 h in order to obtain a reproducible and normalized amount of mycelium for all strains. Finally, 1 mL of this pre-inoculum was used to inoculate 250 mL shake-flasks with 50 mL of MA2 medium. *A. gossypii* cultures were carried out at 28 °C and 200 rpm. After 48 h, the total culture broth was separated by vacuum filtration using Advantec Qualitative Filter Paper (grade 2). The filtrates were

immediately filtered again through 0.2 μm membrane filters and stored at −20 °C until GC-MS analysis. The mycelium retained in the filter paper was washed with distilled water and used for cell dry weight (CDW) determination. CDW was then measured by collecting the mycelium into a pre-weighed dried tube and drying at 105 °C until constant weight (~24 h).

5.2.4 Construction of integration cassettes and transformation of *A. gossypii*

DNA manipulations were made using standard molecular biology procedures (Domingues, 2017). Different transformation cassettes were constructed either for the deletion of native genes or for the overexpression of heterologous genes. For the deletion of the *AgELO624* gene (AFR624W; NCBI Reference Sequence: NM_212307.1), the entire open reading frame (ORF) was replaced by a cassette comprising a *loxP-KanMX-loxP* marker that was obtained by PCR amplification using specific primers (Appendix: Table A5.1). These primers were used to introduce recombinogenic flanks for the *AgELO624* ORF in both sides, corresponding to regions upstream the start codon and downstream the stop codon of the gene. For the overexpression of the heterologous *POX2* gene from *Y. lipolytica* (NCBI Reference Sequence: XM_505264.1), the ORF was codon-optimized for the *A. gossypii* codon usage. This gene was obtained from Integrated DNA Technologies (IDT®). This synthetic gene was then amplified using specific primers (Appendix: Table A5.1) and subsequently cloned in a pBluescript SK (-) vector. Besides the codon-optimized *YlPOX2* gene, the heterologous overexpression cassette contained two recombinogenic flanks, a selection marker *loxP-KanMX-loxP*, and the regulatory *AgGPD* promoter and *AgPGK1* terminator sequences (Figure 5.1B). The recombinogenic flanks of this cassette were targeted to *AgPOX1* locus. Thus, the entire ORF of the *AgPOX1* gene (AER358C; NCBI Reference Sequence: NM_210568.2) was completely replaced by the *YlPOX2* overexpression cassette. The *AgPOX1* recombinogenic flanks were also PCR-amplified using specific primers (Appendix: Table A5.1) and cloned in a pBluescript SK (-) vector. The modules comprising the selection marker and the regulatory sequences were amplified and cloned previously (Ledesma-Amaro et al., 2014a). Finally, all the modules of the overexpression cassette were verified by DNA sequencing and assembled together with the acceptor vector using the *Bsa*I restriction enzyme, accordingly with the Golden-Gate method previously described (Engler et al., 2009; Ledesma-Amaro et al., 2018). Before transformation in *A. gossypii*, the heterologous overexpression cassette (Figure 5.1B) was linearized by enzymatic restriction with *Sap*I.

Spores of *A. gossypii* ATCC 10895 were transformed with the corresponding cassettes

using the Cre-*lox*P system (Aguiar et al., 2014), which enabled the elimination and reuse of the selection marker through the expression of a Cre recombinase in *A. gossypii* as described previously (Serrano-Amatriain et al., 2016). The primary heterokaryotic transformants were selected on agar-solidified MA2/AFM containing 250-300 g/L geneticin (G418). Selection of *A. gossypii* homokaryotic clones was performed through the germination of uninucleated haploid spores obtained from the primary heterokaryotic transformants on agar-solidified MA2/AFM-G418. The correct genomic integration of each cassette as well as the homokaryotic genotype of each clone were confirmed by analytical PCR (Appendix: Figure A5.1) and DNA sequencing. For this purpose, a pin-head of mycelium from single colonies was suspended in 30 µL of extraction buffer (0.05 M carbonate buffer pH 6.9, 2 % (w/v) PVP 40, 0.2 % (w/v) BSA and 0.05 % (v/v) Tween 20) and incubated for 10 min at 100 °C. Afterwards, the tubes were centrifuged at maximum speed. The supernatant was used as template in the PCR reactions using the specific primers listed in Appendix: Table A5.1.

5.2.5 Culture conditions for the analysis of the *de novo* biosynthesis of γ-lactones by *A. gossypii* engineered strains

The cultures of the engineered strains were initiated with the inoculation of 10^7 spores in 50 mL of AFM and carried out in 250 mL shake-flasks at 28 °C and 200 rpm. After 72 h, the mycelium and filtrate were collected and treated as described above.

5.2.6 Volatiles extraction and analysis by GC–MS

Volatiles were analysed by GC–MS (Gas chromatography–mass spectrometry) after extraction from 8 mL samples with 400 µL of dichloromethane, with 4-nonanol as internal standard. A gas chromatograph Varian 3800 with a 1079 injector and an ion-trap mass spectrometer Varian Saturn 2000 was used. 1 µL injections were made in splitless mode (30 s) in a Sapiens-Wax MS column (30 m; 0.15 mm; 0.15 µm film thickness, Teknokroma). Carrier gas was helium 49 (Praxair) at a constant 1.3 mL/min flow. Detector was set to electronic impact mode with an ionization energy of 70 eV, a mass acquisition range from 35 to 260 m/z and 610 ms acquisition interval. Oven temperature was initially set to 60 °C for 2 min and then raised from 60 to 234 °C at a rate of 3 °C/min, raised from 234 to 260 °C at 5 °C/min and finally maintained at 260 °C for 10 min. Injector temperature was 250 °C with 30 mL/min split flow. Compounds were identified using MS Workstation version 6.9 (Varian) software, by comparing mass spectra

and retention indices with those of pure standards mentioned above. Volatiles were quantified as 4-nonanol equivalents.

5.2.7 Statistical analyses

GraphPad Prism for IOS version 6.0 was used to carry out the statistical analyses. Differences to a control strain were analysed by one-way ANOVA followed by Dunnett's multiple comparison test. When no control strain is indicated, the analyses were made by one-way ANOVA followed by Tukey´s multiple comparison test. Unless indicated otherwise, statistical significance was established at $p < 0.05$ for the comparisons.

5.3 Results and discussion

5.3.1 *A. gossypii* predominantly produced γ-lactones and higher alcohols as VOCs

A complete metabolic profiling of the VOCs produced by *A. gossypii* was performed to understand its innate potential to biosynthesize lactones. Nine *A. gossypii* strains obtained from different collections (Table 5.1) were screened in glucose-based media (MA2). From this screening, it was possible to identify 31 to 50 different VOCs in each strain. Total production of VOCs was quantified (Figure 5.2A) after 48 h of culture, when glucose was already depleted from the medium. By grouping these compounds according to their chemical structure into families of commercially valuable aromas, it was possible to notice that *A. gossypii* strains produced predominantly higher alcohols and γ-lactones (Figure 5.2B). Higher alcohols represented 43 % – 87 % of the VOCs produced by *A. gossypii*, while γ-lactones had a relative representation of 6 % – 57 %. On the other hand, the yeasts *Saccharomyces cerevisiae* and *Y. lipolytica* demonstrated an almost exclusive production of higher alcohols and absence of γ-lactones production (Figure 5.2B). These results confirm the distinctive trait of *A. gossypii* for *de novo* biosynthesis of γ-lactones.

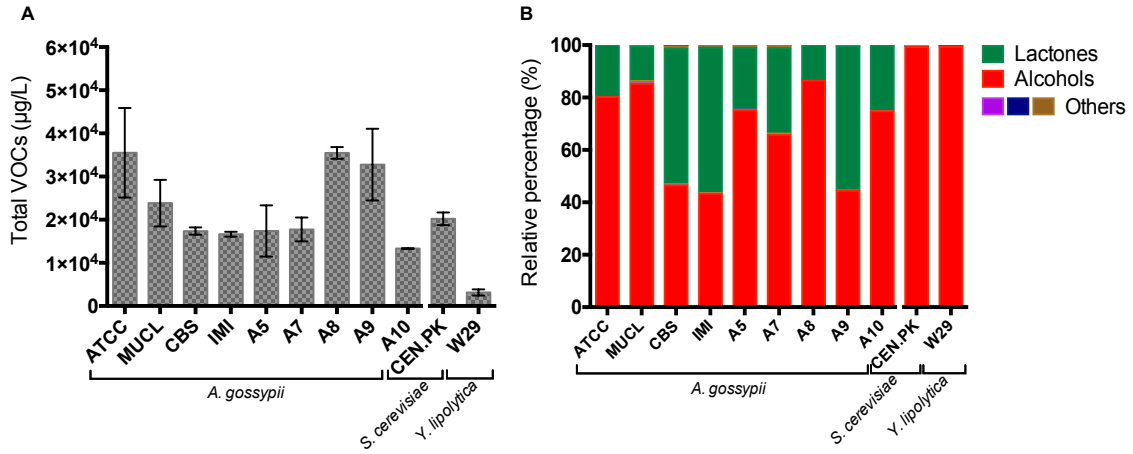


Figure 5.2. Quantitative and qualitative VOCs profiling by GC-MS of *A. gossypii* strains. **(A)** Total VOCs production. **(B)** Distribution of the VOCs produced by families of aromas according to their chemical structure and their relative presence in each strain. The *S. cerevisiae* CEN.PK113-7D (CEN.PK) and *Y. lipolytica* W29 were used as controls to help evaluate which VOCs were distinctively produced by *A. gossypii*. Cultures were carried out in MA2 medium for 48 h. Data are presented as mean ± standard deviation of at least two biological replicates.

Seven chemically different γ-lactones were identified during the growth phase of this fungus (from 24 h onward), namely γ-valerolactone (PubChem CID: 7921), γ-caprolactone

(PubChem CID: 12756), γ-octalactone (PubChem CID: 7704), γ-nonalactone (PubChem CID: 7710), γ-decalactone (PubChem CID: 12813), γ-undecalactone (PubChem CID: 7714) and γ-dodecalactone (PubChem CID: 16821). All the γ-lactones here detected were identified using pure standards. Their identification was also confirmed by the presence of the molecular ion peak of *m/z* 85 in the MS spectrum, which is characteristic of γ-lactones as listed in the National Institute of Standards and Technology (NIST). In addition, it can be assumed that *A. gossypii* did not produce δ-lactones since the molecular ion peak of *m/z* 99, representative of δ-lactones, was not identified in any of the MS spectra (Table 5.2). When compared with other microorganisms, the chemical diversity of the γ-lactones biosynthesized by *A. gossypii* and the relative short time needed for their production (2 days) is noteworthy. Only three (*T. viride*; 12 days) (Fadel et al., 2015), four (*S. salmonicolor*; 12 days) (Dufossé et al., 1997) and five (*F. poae*; 8 days) (Latrasse et al., 1993) γ-lactones were detected in the other reported lactone-producing fungi. Regarding the other predominant family of VOCs, the two major higher alcohols detected were 2-phenylethanol and isoamyl alcohol (Appendix: Figure A5.2), which is in accordance with data previously reported for the ATCC 10895 strain (Ravasio et al., 2014).

Table 5.2. MS fragmentation pattern for each γ-lactone. Numbers between brackets represent percentages of m/z ions.

Compound	Characteristic ions
γ-valerolactone	56(100) + 85(69) + 41(64) + 39(56) + 43(38)
γ-caprolactone	85(100) + 57(25) + 39(17) + 55(16) + 56(13)
γ-octalactone	85(100) + 57(22) + 39(14) + 41(11) + 55(9)
γ-nonalactone	85(100) + 57(20) + 39(16) + 41(13) + 55(11)
γ-decalactone	85(100) + 57(20) + 39(16) + 41(15) + 55(15)
γ-undecalactone	85(100) + 57(27) + 41(19) + 55(16) + 128(12)
γ-dodecalactone	85(100) + 39(24) + 57(24) + 55(24) + 41(23)

5.3.2 The major lactone produced by *A. gossypii* was γ-decalactone

The distinctive nature of *A. gossypii* for *de novo* biosynthesis of γ-lactones from glucose was extensive to all strains tested. However, among the seven γ-lactones biosynthesized, one was clearly produced with major prevalence, γ-decalactone. Compared to the other six γ-lactones (Figure 5.3A), γ-decalactone was produced in concentrations two orders of magnitude higher,

reaching (2.8 ± 0.6) × 10^3 $\mu g/g_{CDW}$ (Figure 5.3B). Regarding the six minor γ-lactones detected, their concentration in the medium was not uniformly distributed, being γ-dodecalactone the most representative among them (Figure 5.3A). On the other hand, the specific production of γ-lactones was heterogeneous among the different strains (Figure 5.3). For instance, the best γ-decalactone-producing strain (concerning average specific production) was strain A9, while strain A10 was superior for γ-dodecalactone biosynthesis. Strain heterogeneity in *A. gossypii* was previously reported regarding growth rates in different carbon sources (Ribeiro et al., 2012) and also regarding nucleosides production (Ledesma-Amaro et al., 2015). Therefore, when investigating *A. gossypii* for the purpose of its development as a cell factory, the exploration of this specie's biodiversity gives a more comprehensive understanding of its potential.

Noteworthy, four of the seven γ-lactones produced by *A. gossypii* were detected in volumetric concentrations above their odour perception threshold (Appendix: Table A5.2) (Coelho et al., 2015; Jackson, 2009). Therefore, these active fragrances possibly contribute to the characteristic aroma released from the cultures of this fungus. Specifically, γ-decalactone seems to be the major contributor among the fragrances produced from the *A. gossypii* strains tested.

Since these results revealed a yet unknown potential of *A. gossypii* for *de novo* biosynthesis of γ-lactones from sugar-based media, the native pathways involved in γ-lactone formation merited further elucidation.

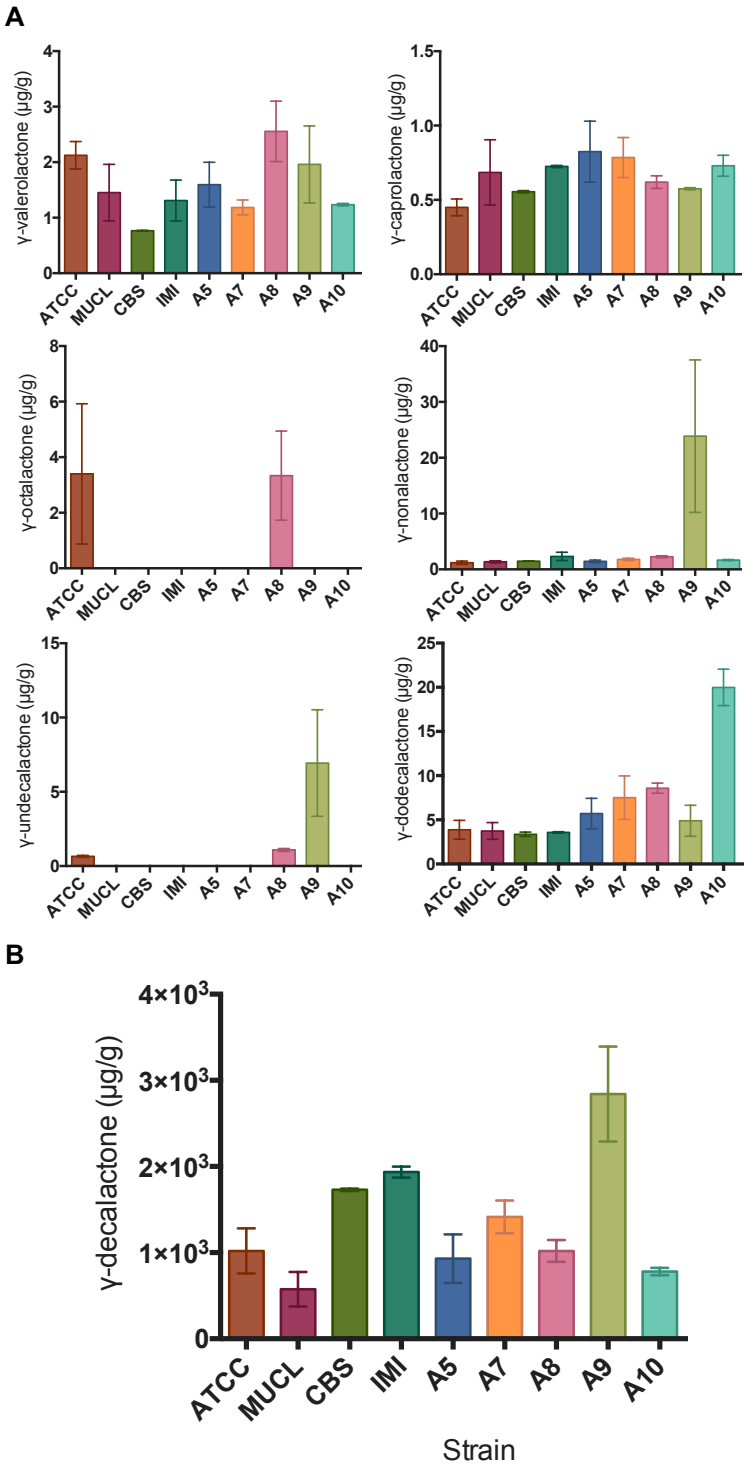


Figure 5.3. Specific productions ($\mu g/g_{CDW}$) of the seven chemically different γ-lactones identified in cultures of *A. gossypii*. **(A)** Production levels of the minor γ-lactones identified. **(B)** Production levels of the major γ-lactone identified, γ-decalactone. Data are presented as mean ± standard deviation of at least two biological replicates.

5.3.3 Redirection of the metabolic fluxes of the fatty acid biosynthesis modulated the *de novo* biosynthesis of γ-lactones in *A. gossypii*

Lactones are VOCs derived from the fatty acid metabolism. In natural producers, such as peach (*Prunus persica* L. Batsch) or strawberry (*Fragaria* × *ananassa*) fruits, the direct precursors for lactones biosynthesis are unsaturated fatty acids (Sánchez et al., 2013; Sánchez-Sevilla et al., 2014). In *A. gossypii*, more than 80 % of the total fatty acids accumulated during growth in sugar-based media are unsaturated (Ledesma-Amaro et al., 2014a). Of these, oleic acid (C18:1) represents more than 50 % of the total fatty acid composition (Ledesma-Amaro et al., 2014b). A first experimental indication that oleic acid could positively contribute for the biosynthesis of lactones in *A. gossypii* was obtained from fermentations where glucose was substituted by oleic acid as the carbon source. While the production of γ-decalactone remained similar, oleic acid stimulated the biosynthesis of some minor lactones, such as γ-dodecalactone, which in this condition was produced in amounts 100-fold higher than in glucose-based medium (data not shown). These data indicated oleic acid as an important precursor for the *de novo* biosynthesis of γ-lactones and is in good agreement with the fact that oleic acid is the starting point for the production of γ-dodecalactone in biotransformation processes (An et al., 2013). Furthermore, oleic acid was identified as a central intermediate in the biosynthesis of lactones in the yeast *S. salmonicolor* (Haffner and Tressl, 1996).

Thus, to confirm this hypothesis and to assess whether the biosynthesis of γ-lactones from glucose could be improved through the redirection of the oleic acid metabolic flux in the *A. gossypii's* fatty acid biosynthetic pathway, two genetic modifications were designed: i) the overexpression of the gene *AgDES589*, encoding a desaturase for the conversion of oleic acid into linoleic acid (EC 1.14.19.6); and ii) the deletion of the gene *AgELO624*, encoding an elongase that catalyses the formation of fatty acids of C20:0 and C22:0 (EC 2.3.1.199) (Figure 5.1A). It is worth of noting that the fatty acid profile of *A. gossypii* is characterized by the presence of 4 % – 8 % of fatty acids longer than C18 (Ledesma-Amaro et al., 2014a; 2014b). The background chosen for the genetic modifications was the best characterized and sequenced strain ATCC 10895 (ATCC).

The engineered strains were tested in AFM sugar-based medium. The transition from MA2 to AFM is justified by superior biomass production obtained with this medium that led to a higher volumetric production of γ-lactones (~10-fold; Figure 5.4A).

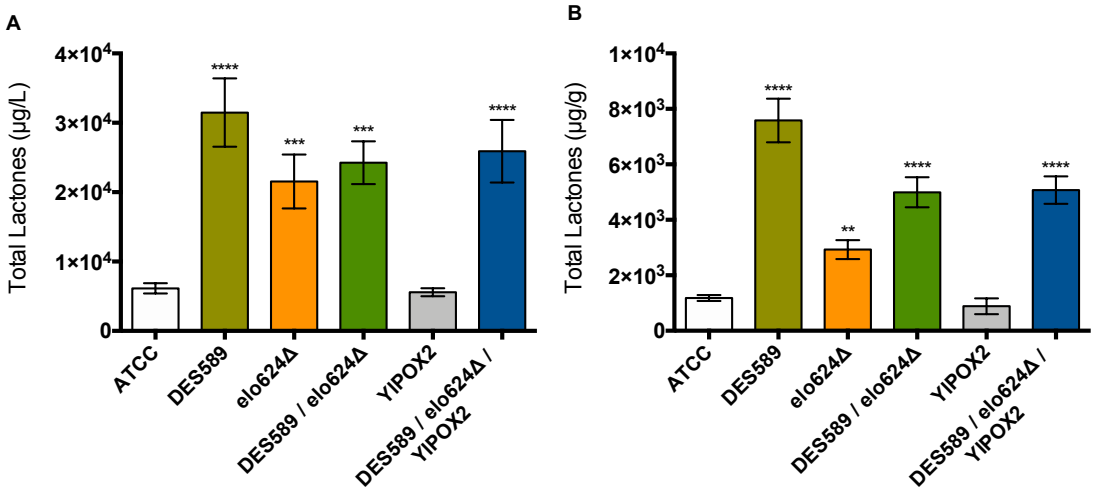


Figure 5.4. Improved biosynthesis of γ-lactones by engineered *A. gossypii* strains. **(A)** Volumetric (µg/L) and **(B)** specific (µg/g_{CDW}) production of total γ-lactones. Data are presented as mean ± standard deviation of three biological replicates. Cultures were carried out in AFM for 72 h. Asterisks represent significant differences to the control (ATCC). **($p < 0.01$), ***($p < 0.001$) and ****($p < 0.0001$).

The time point chosen for the comparisons was 72 h, when all the glucose was already depleted from the medium, because a small but increasing trend in the production of γ-lactones by the ATCC strain was observed between 24 h – 72 h. In comparison with the parental strain, the overexpression of *AgDES589* led to the most pronounced improvement, with a 6.4-fold increase in the specific production of γ-lactones (µg/g_{CDW}; Figure 5.4B). However, this overexpression did not increase evenly the production of all the γ-lactones, being this strain (DES589) significantly enriched mainly in γ-octalactone and γ-decalactone, and slightly enriched in γ-dodecalactone (Table 5.3).

Table 5.3. Specific production ($\mu g/g_{CDW}$) of different γ-lactones by engineered *A. gossypii* strains. Underlined values represent the percentage (%) of γ-decalactone regarding the total γ-lactones produced by different high-producing engineered strains. Data are presented as mean ± standard deviation of three biological replicates. Superscript letters represent significant differences to the control (ATCC) between values of the same column. Superscript letters of underlined values represent significant differences between relative productions. a,b ($p < 0.05$), a,c ($p < 0.01$), a,d ($p < 0.001$) and a,e ($p < 0.0001$).

γ-lactones	ATCC	DES589	elo624Δ	DES589/ elo624Δ	YlPOX2	DES589/elo624Δ /YlPOX2
γ-octalactone	–	$(1.3 \pm 0.2)^{a} \times 10^{2}$	–	$(1.1 \pm 0.1)^{a} \times 10^{2}$	–	$(3.2 \pm 1.0)^{d} \times 10^{1}$
γ-nonalactone	–	6 ± 2	–	3 ± 0	–	–
γ-decalactone	$(1.2 \pm 0.1)^{a} \times 10^{3}$	$(7.4 \pm 0.8)^{e} \times 10^{3}$	$(2.9 \pm 0.3)^{c} \times 10^{3}$	$(4.9 \pm 0.5)^{e} \times 10^{3}$	$(8.8 \pm 2.9)^{a} \times 10^{2}$	$(5.0 \pm 0.5)^{e} \times 10^{3}$
		$\underline{98.0 \pm 0.2^{a}}$		$\underline{97.7 \pm 0.2^{a}}$		$\underline{99.3 \pm 0.1^{e}}$
γ-undecalactone	–	3 ± 1	–	2 ± 0	–	2 ± 1
γ-dodecalactone	3 ± 1^{a}	$(1.4 \pm 0.3)^{b} \times 10^{1}$	2 ± 0^{a}	3 ± 0^{a}	3 ± 1^{a}	2 ± 1^{a}

(–), not detected and considered 0 for the statistical tests

AgDES589 was previously shown to be transcriptionally inhibited by the product (linoleic acid) (Ledesma-Amaro et al., 2014b). In addition, enzyme feedback regulation by products was reported for other desaturases (Ledesma-Amaro et al., 2014b). Therefore, gene and/or protein engineering of AgDes589p to eliminate potential regulatory mechanisms could further potentiate the positive effect of this enzyme on the biosynthesis of lactones in *A. gossypii*.

In turn, strain elo624Δ produced 2.5-fold more lactones, specifically γ-decalactone. This result suggests that very long fatty acids (C20 to C26) are not ideally used as precursors for lactones biosynthesis. This may be related with their saturated nature. Even if shortened in the β-oxidation pathway, these fatty acids would not become an appropriate substrate for AgDes589p. Moreover, as the other elongase encoded in the *A. gossypii* genome (AgElo586p) is able to elongate fatty acids of C18:0 and C20:0 with poor efficiency (Ledesma-Amaro et al., 2014b), its deletion would be expected to further improve lactones' biosynthesis.

Finally, combination of the two genetic modifications in strain DES589/elo624Δ resulted in a 4.2-fold increase in lactone production, reflected exclusively in the two main γ-lactones produced by strain DES589, γ-octalactone and γ-decalactone (Figure 5.4B; Table 5.3).

Together, these results clearly show that the deregulation of the fatty acid biosynthetic pathway at the C18 level significantly modulated the biosynthesis of γ-lactones in *A. gossypii*. Oleic acid, the main fatty acid accumulated by *A. gossypii*, is a central metabolite. As shown in Table 5.3, the biosynthesis of γ-lactones increased upon blockage of its conversion into longer fatty acids (strain elo624Δ). Moreover, before entering the β-oxidation pathway, oleic acid is very likely to undergo additional chemical modifications. In accordance, the overexpression of the gene *AgDES589*, which promotes the desaturation of oleic acid (C18:1) into linoleic acid (C18:2) (Figure 5.1), was shown to strongly enhance the biosynthesis of γ-lactones. In strawberry fruit, the expression of the gene *FaFAD1*, encoding a Δ12 fatty acid desaturase, was positively correlated with the γ-decalactone content in fruits (Sánchez-Sevilla et al., 2014). A homologue of *FaFAD1* in peach fruit was also connected with lactone biosynthesis (Sánchez et al., 2013). A BLAST® (https://blast.ncbi.nlm.nih.gov/Blast.cgi) retrieved *FaFAD1* as an ortholog of *AgDES589*. AgDes589p shares 39 % amino acid identity with *Fa*Fad1p (Appendix: Figure A5.3). In contrast, no orthologs of the *AgDES589* gene were found in the closely related yeast *S. cerevisiae* or in other post-WGD species of the Saccharomycetaceae. Therefore, *AgDES589* is one of the underlying genetic differences conferring *A. gossypii* the ability for *de novo* biosynthesis of γ-lactones.

Interestingly, and just as FaFad1p, two amino acid residues important for the catalytic

activity (Sánchez et al., 2013) are conserved between AgDes589p and hydroxylases (*e.g.*, *R. comunis* RcFah12p) or bifunctional hydroxylase/desaturases (*Lesquerella fendleri* bifunctional LfAh12p), rather than with exclusive desaturases (*e.g.*, *Arabidopsis thaliana* AtFad2p). This suggests that AgDes589p could be an enzyme with both desaturase and hydroxylase activity. *Y. lipolytica*, the workhorse used for the production of γ-decalactone by biotransformation, also owns a protein similar to AgDes589p (Appendix: Figure A5.3). However, this enzyme is only conserved in one of the amino acids critical for the hydroxylase activity. Not owning enzyme(s) able to catalyse the formation of hydroxy fatty acids from oleic acid could be the reason why the production of γ-decalactone by this yeast is only reported from hydroxy fatty acids (*e.g.*, ricinoleic acid) (Kourist and Hilterhaus, 2015), despite the major accumulation of oleic acid inside the cells (Blazeck et al., 2014). Thus, studying the activities of these enzymes is of pivotal importance to further understand their role in the *de novo* biosynthesis of lactones.

In fruits (Sánchez et al., 2013; Sánchez-Sevilla et al., 2014), the biosynthesis of γ-lactones has been proposed to start from the hydration or hydroxylation of unsaturated fatty acids. Considering our data, we propose that the cellular pools of oleic acid (18:1), naturally synthesized and accumulated by *A. gossypii* (Ledesma-Amaro et al., 2014a), are directed to linoleic acid formation (18:2) by the introduction of an additional unsaturation (Figure 5.1). In turn, linoleic acid should be hydrated to form hydroxy fatty acids by a yet unidentified enzyme, similarly to what was proposed for fruits (Sánchez et al., 2013; Sánchez-Sevilla et al., 2014). As mentioned above, we cannot exclude that AgDes589p may also possess hydroxylase activity and therefore be able to catalyse the conversion of oleic acid into hydroxy fatty acids. These lactones' precursors are then shortened at the β-oxidation pathway, generating 4-hydroxy acids of different lengths. Finally, it is widely accepted that γ-lactones are formed by spontaneous lactonisation (Kourist and Hilterhaus, 2015; Sánchez et al., 2013; Sánchez-Sevilla et al., 2014) (Figure 5.1).

5.3.4 Combinatorial engineering fine-tuned the biosynthesis of γ-decalactone in *A. gossypii*

Pure lactones obtained by microbial production are preferred instead of racemic mixtures, because the former facilitates downstream processing (Kourist and Hilterhaus, 2015). The operations used for that end have been liquid-liquid two-phase extraction and distillation, which are designed to purify one lactone (Blaser and Federsel, 2010; Thomas, 2013). Since the application as pure fragrances is the most relevant route for their commercialization, fine-tuning the

biosynthesis of γ-lactones towards a particular one and therefore create tailored engineered strains is envisaged. Hence, the *AgPOX1* gene was replaced by a heterologous overexpression cassette containing a *POX2* gene from *Y. lipolytica* (Figure 5.1A). *AgPOX1* codifies for the exclusive acyl-CoA oxidase (EC 1.3.3.6) encoded in the *A. gossypii* genome that catalyses the first reaction of the β-oxidation pathway (Ledesma-Amaro et al., 2014a), while *YlPOX2* codifies for a specific long chain acyl-CoA oxidase (EC 1.3.3.6) with activity for C11–C18 fatty acids (Wang et al., 1999). With this modification, the degradation of fatty acids in the β-oxidation pathway should stop at the C10 level and consequently the biosynthesis of lactones shorter than γ-decalactone would be prevented. Furthermore, this strategy would confirm the role of the β-oxidation pathway in the *de novo* biosynthesis of lactones by *A. gossypii*.

The overexpression of *YlPOX2* did not produce any significant effect on the total production (Figure 5.4) nor on the profile of γ-lactones biosynthesized (Table 5.3) as compared with the parental strain. However, fine-tuning was accomplished by combining the three genetic modifications in strain DES589/elo624Δ/YlPOX2. This strain presents a similar production of γ-decalactone and lower production of γ-octalactone when compared to strains DES589 and DES589/elo624Δ (Table 5.3). Noteworthy, the percentage of γ-decalactone produced by this strain was significantly higher than that obtained with the other two overproducer strains, DES589 and DES589/elo624Δ (Table 5.3). This fine-tuning occurred at an extent that γ-decalactone represented 99.3 % of the total γ-lactones produced, confirming that the specificity of the acyl-CoA oxidase in the β-oxidation contributes to the qualitative profile of the final product.

5.4 Conclusions

An efficient microorganism for the *de novo* biosynthesis of lactones should: i.) present a superior ability to transform carbohydrates into fatty acids; ii.) possess the genetic machinery for the conversion of the latter into lactones. Here, we show that *A. gossypii* fulfils these two requisites. Taken together, these results indicate that the fatty acid biosynthesis and the β-oxidation are the central pathways involved in the *de novo* biosynthesis of γ-lactones in *A. gossypii*. Regarding the first, *A. gossypii* has been successfully engineered to synthesize biolipids not only from hexoses (Lozano-Martínez et al., 2016), but also from pentoses (Díaz-Fernández et al., 2017), expanding its potential as a model for studying the biosynthesis of lactones from different sugars.

Moreover, by means of metabolic engineering, this work elucidates key enzymatic steps for *de novo* biosynthesis of γ-lactones in *A. gossypii* and shows how this can be further improved and fine-tuned. To the extent of our knowledge, this is the first example of improved *de novo* biosynthesis of γ-lactones achieved by an engineered microorganism. The realization of microbial *de novo* biosynthesis of γ-lactones is of upmost importance, paving the way for the sustainable production of these valuable compounds with a broad range of biological or odorant properties.

5.5 References

Aguiar TQ, Dinis C, Domingues L. Cre-*lox*P-based system for removal and reuse of selection markers in *Ashbya gossypii* targeted engineering. Fungal Genet Biol 2014;68:1–8.

Aguiar TQ, Silva R, Domingues L. *Ashbya gossypii* beyond industrial riboflavin production: A historical perspective and emerging biotechnological applications. Biotechnol Adv 2015;33:1774–86.

Aguiar TQ, Silva R, Domingues L. New biotechnological applications for *Ashbya gossypii*: Challenges and perspectives. Bioengineered 2017;8:309-15.

An J, Joo Y, Oh D. New biotransformation process for production of the fragrant compound γ-dodecalactone from 10-hydroxystearate by permeabilized *Waltomyces lipofer* cells. Appl Environ Microbiol 2013;79:2636–41.

Audi J, Belson M, Patel M, Schier J, Osterloh J. Ricin poisoning: a comprehensive review. JAMA 2005;294:2342–51.

Blaser HU, Federsel H. Asymmetric catalysis on industrial scale: challenges, approaches and solutions, 2nd ed. 2010 Weinheim: Wiley-VCH.

Blazeck J, Hill A, Liu L, Knight R, Miller J, Pan A, et al. Harnessing *Yarrowia lipolytica* lipogenesis to create a platform for lipid and biofuel production. Nat Commun 2014;5:3131.

Braga A, Guerreiro C, Belo I. Generation of flavors and fragrances through biotransformation and *de novo* synthesis. Food Bioprocess Tech 2018;11:2217–28.

Coelho E, Vilanova M, Genisheva Z, Oliveira JM, Teixeira JA, Domingues L. Systematic approach for the development of fruit wines from industrially processed fruit concentrates, including optimization of fermentation parameters, chemical characterization and sensory evaluation. LWT - Food Sci Technol 2015;62:1043–52.

Collins RP, Halim AF. Characterization of the major aroma constituent of the fungus *Trichoderma viride*. J Agr Food Chem 1972;20:437–8.

Díaz-Fernández D, Lozano-Martínez P, Buey RM, Revuelta JL, Jiménez A. Utilization of xylose by engineered strains of *Ashbya gossypii* for the production of microbial oils. Biotechnol Biofuels 2017;10:3.

Domingues L. PCR: Methods and Protocols. 1st ed., New York: Springer; 2017.

Dufossé L, Féron G, Latrasse A, Guichard E, Spinnler HE. Chirality of the gamma-lactones produced by *Sporidiobolus salmonicolor* grown in two different media. Chirality 1997:9;667-71.

Engler C, Gruetzner R, Kandzia R, Marillonnet S. Golden gate shuffling: a one pot DNA shuffling method based on type IIs restriction enzymes. PLoS One 2009;4:e5553.

Fadel HHM, Mahmoud MG, Asker MMS, Lotfy SN. Characterization and evaluation of coconut aroma produced by *Trichoderma viride* EMCC-107 in solid state fermentation on sugarcane bagasse. Electron J Biotechnol 2015;18: 5–9.

Haffner T, Tressl R. Biosynthesis of (R)-γ-decanolactone in the yeast *Sporobolomyces odorus*. J Agric Food Chem 1996;44:1218-23.

Hanko EKR, Denby CM, Sànchez I, Nogué V, Lin W, Ramirez KJ, et al. Engineering β-oxidation in *Yarrowia lipolytica* for methyl ketone production. Metab Eng 2018;48:52–62.

Jackson RS. Olfactory Sensations. In:_ Wine Tasting: A Professional Handbook 2009. Academic Press: Burlington, San Diego, London.

Kourist R, Hilterhaus, L. Microbial Lactone Synthesis Based on Renewable Resources. In: Kamm B (eds) Microorganisms in Biorefineries. Microbiology Monographs 2015. Springer: Berlin, Heidelberg.

Latrasse A, Guichard E, Piffaut C, Fournier N, Dufossé L. Chirality of the γ-lactones formed by *Fusarium poae* INRA 45. Chirality 1993;5:79–84.

Ledesma-Amaro R, Buey RM, Revuelta JL. Increased production of inosine and guanosine by means of metabolic engineering of the purine pathway in *Ashbya gossypii*. Microb Cell Fact 2015;14:58.

Ledesma-Amaro R, Jiménez A, Revuelta JL. Pathway grafting for polyunsaturated fatty acids production in *Ashbya gossypii* through Golden-Gate rapid assembly. ACS Synth Biol 2018;7:2340–7.

Ledesma-Amaro R, Santos MA, Jiménez A, Revuelta JL. Strain design of *Ashbya gossypii* for single-cell oil production. Appl Environ Microbiol 2014a;80: 1237–44.

Ledesma-Amaro R, Santos MA, Jiménez A, Revuelta JL. Tuning single-cell oil production in *Ashbya gossypii* by engineering the elongation and desaturation systems. Biotechnol Bioeng 2014b;111:1782–91.

Lozano-Martínez P, Buey RM, Ledesma-Amaro, R, Jiménez A, Revuelta JL. Engineering *Ashbya gossypii* strains for *de novo* lipid production using industrial by-products. Microb Biotechnol 2016;10:425–33.

Magalhães F, Aguiar TQ, Oliveira C, Domingues L. High-level expression of *Aspergillus niger* β-galactosidase in *Ashbya gossypii*. Biotechnol Prog 2014;30:261–8.

Patel VR, Dumancas GG, Viswanath LKK, Maples R, Subong BJJ. Castor oil: properties, uses, and optimization of processing parameters in commercial production. Lipid Insights 2016;9:1–12.

Ravasio D, Wendland J, Walther A. Major contribution of the Ehrlich pathway for 2-phenylethanol/rose flavor production in *Ashbya gossypii*. FEMS Yeast Res 2014;14:833–44.

Revuelta JL, Ledesma-Amaro R, Lozano-Martinez P, Díaz-Fernández D, Buey RM, Jiménez A. Bioproduction of riboflavin: a bright yellow history. J Ind Microbiol Biotechnol 2016;44:659–65.

Ribeiro O, Domingues L, Penttilä M, Wiebe MG. Nutritional requirements and strain heterogeneity in *Ashbya gossypii*. J Basic Microbiol 2012;52:582–9.

Sánchez G, Venegas-Calerón M, Salas JJ, Monforte A, Badenes ML, Granell A. An integrative "omics" approach identifies new candidate genes to impact aroma volatiles in peach fruit. BMC Genomics 2013;23:343.

Sánchez-Sevilla JF, Cruz-Rus E, Valpuesta V, Botella MA Amaya I. Deciphering gamma-decalactone biosynthesis in strawberry fruit using a combination of genetic mapping, RNA-Seq and eQTL analyses. BMC Genomics 2014;15:218.

Schwechheimer SK, Becker J, Peyriga L, Portais JC, Sauer D, Müller R, et al. Improved riboflavin production with *Ashbya gossypii* from vegetable oil based on 13C metabolic network analysis with combined labeling analysis by GC/MS, LC/MS, 1D, and 2D NMR. Metab Eng 2018a;47:357–73.

Schwechheimer SK, Park EY, Revuelta JL, Becker J, Wittmann C. Biotechnology of riboflavin. Appl Microbiol Biotechnol 2016;100:2107–19.

Serrano-Amatriain C, Ledesma-Amaro R, López-Nicolás R, Ros G, Jiménez A, Revuelta JL. Folic acid production by engineered *Ashbya gossypii*. Metab Eng 2016;38:473–82.

Stahmann KP, Kupp C, Feldmann SD, Sahm H. Formation and degradation of lipid bodies found in the riboflavin-producing fungus *Ashbya gossypii*. Appl Microbiol Biotechnol 1994;42:121–7.

Thomas WD. Purification of butyrolactone. United States Patent No. 4,851,085. 2013.

Wang HJ, Le Dall MT, Wach Y, Laroche C, Belin JM, Gaillardin C, et al. Evaluation of acyl coenzyme A oxidase (Aox) isozyme function in the n-alkane-assimilating yeast *Yarrowia lipolytica*. J Bacteriol 1999;181:5140–8.

CHAPTER VI

General conclusions and future perspectives

This thesis had the major goal of expanding the biotechnological applications of *A. gossypii*, moving from a well-settled industrial riboflavin production process into alternative production processes having this fungus as cell factory. Thus, this thesis was dedicated to the continuous exploration of the *A. gossypii*'s natural metabolism through the physiological and molecular characterization of existing strains (non-engineered and engineered), envisioning the identification of novel high-value chemicals and the development of strategies to further improve their biosynthesis. Overall, the main goals were achieved and the main conclusions obtained throughout the developed work are summarized as follows.

Riboflavin overproduction will always be the major distinctive trait of *A. gossypii*, as exemplified in Chapters II and III. The key pathways leading to riboflavin overproduction are well understood, but the regulatory and ecological mechanisms behind this trait remain largely unknown. The *Ashbya* Comet Assay was developed in Chapter II to help assess whether riboflavin overproduction was connected with photo-induced genotoxic effects. This protocol allowed detecting superior accumulation of DNA damage in a riboflavin-overproducing *A. gossypii* strain, as well as increased intracellular oxidation and riboflavin production, when it was exposed to sun-mimicking light during growth. In addition to be a new and independent report suggesting that the overproduction of riboflavin by *A. gossypii* acts as an ecological defence mechanism, this study offers new opportunities for optimizing current riboflavin production processes. Despite this additional association, the specific ecological role of riboflavin overproduction still remains unknown.

In Chapter III, the physiological and molecular characterization of a pyrimidine auxotroph harnessed for riboflavin production allowed identifying a conserved enzyme of the pyrimidine salvage pathway whose activity is dependent on the presence of uracil and phosphoribosyl pyrophosphate (PRPP), AgUPRTp, as the cause for the unusual hypersensitivity of this *Agura3* mutant to uracil. The modulation of this enzyme appears to be a mechanism that favours the preservation of PRPP for the synthesis of riboflavin precursors. These results, besides providing a link between the main trait of *A. gossypii* and non-related metabolic pathways (pyrimidine biosynthesis), demonstrated the extension of the impact that riboflavin overproduction has over its metabolism.

It was through further characterization of this engineered strain (*Agura3*) that the production of a novel high-value chemical was identified in Chapter IV. The *Agura3* pyrimidine auxotroph is able to accumulate and excrete orotic acid to the culture medium. This phenotype is

most likely conferred by the presence of a putative mitochondrial AgUra9p in the *de novo* pyrimidine biosynthetic pathway. As discussed in Chapter I, the exploitation of novel targets should not only be based on its commercial value, but also take into account the innate potential of the microbial host, as well as the combination of its production with cost-effective feedstocks. Therefore, the overexpression of *AgGUP1* in the *Agura3* background allowed the construction of a strain with improved glycerol utilization, a carbon source widely present in industrial waste streams. This genetic modification also increased the hyperosmotic stress tolerance of this strain, depending on the presence of glycerol in the medium. This strain (*Agura3*_GUP1) is thus a promising chassis, not only for the production of orotic acid but also for other high-value chemicals such as riboflavin, since it has an improved substrate utilization capacity and robustness towards stresses encountered in industrial environments. The enhancement of orotic acid production in *A. gossypii* should now pass by increasing the metabolic flux towards the *de novo* biosynthesis of pyrimidine ribonucleotides through the overexpression of genes at the beginning of the pathway (*e.g.*, *AgURA2*) and by integrating metabolic engineering strategies with the optimization of culture and process conditions.

To finalize, we add another class of compounds that may be explored as target products in *A. gossypii* based on the rationale that making the most out of the natural metabolism of this filamentous fungus is the more appropriate path for designing novel biotechnological applications. Thus, it was demonstrated in Chapter V that *A. gossypii* has innate potential as a model for *de novo* biosynthesis of γ-lactones from sugars. These valuable fragrances had only been biotechnologically exploited through biotransformation process, which limited their production from more sustainable feedstocks. Thus, by means of metabolic engineering of its fatty acid biosynthesis and β-oxidation pathways, key steps of *de novo* biosynthesis of γ-lactones in *A. gossypii* were deciphered and engineered, which allowed increasing and fine-tuning the biosynthesis of these compounds. This approach resulted not only on the first report of an engineered microorganism with improved *de novo* biosynthesis of γ-lactones as also served as proof of principle for their exploitation from carbon sources widely present in renewable raw materials and industrial by-products. Due to the intricate nature of the *de novo* biosynthesis of γ-lactones, which involves several pathways, resolving the corresponding carbon fluxes by isotopic labelling analysis would allow a comprehensive and complete view of the underlying metabolism involved. As already done for riboflavin, this would lead to the elaboration of strategies to further improve their production in *A. gossypii*.

In sum, in this thesis, an attempt to establish a framework around which biotechnological applications for *A. gossypii* could be systematically identified and studied was performed. The specific contributions provided herein (Figure 6.1), translated into the exploration of two novel high-value chemicals (orotic acid and γ-lactones), were only possible to achieve due to an in-depth characterization and understanding of the *A. gossypii* metabolism and cellular biology, accumulated over more than 30 years of fundamental and applied research.

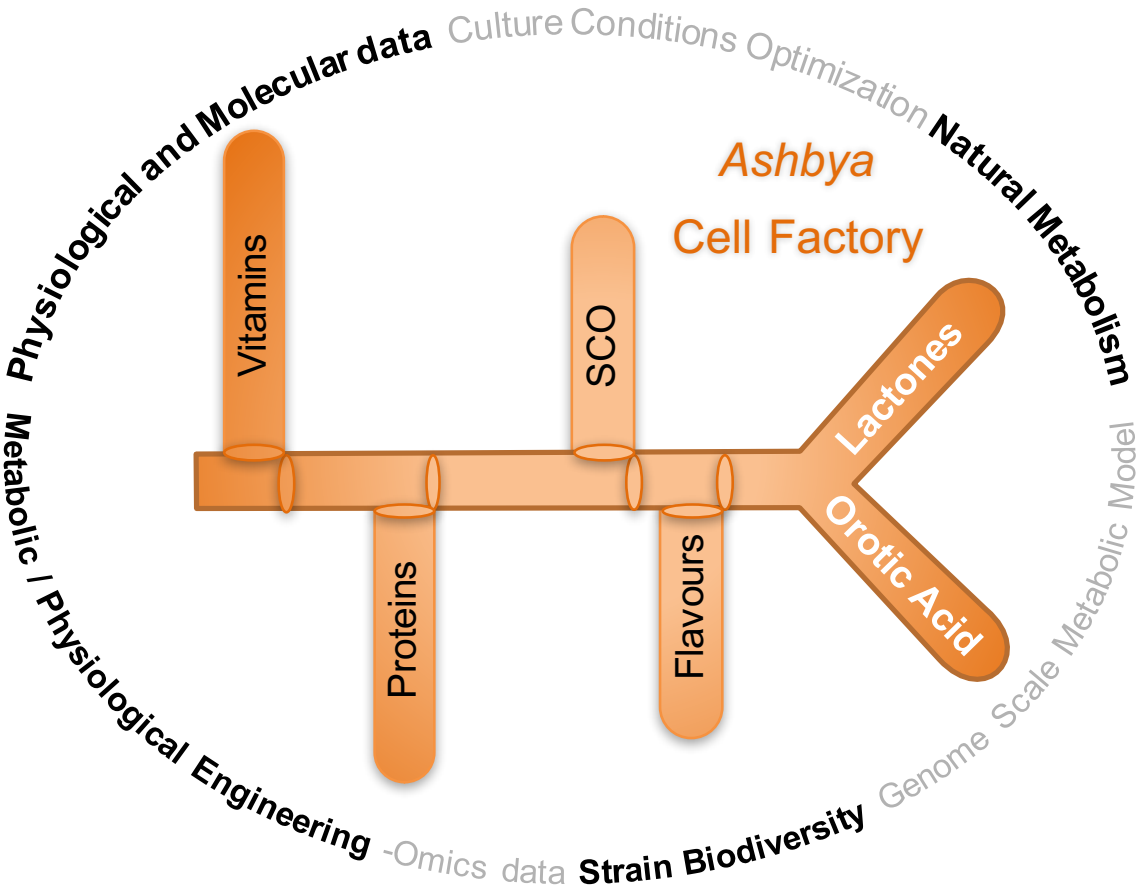


Figure 6.1. Graphical schematic representation of the contributions of this thesis for the development of *A. gossypii* as a cell factory. The biotechnological applications identified and explored here are shown in white. The scientific and technical approaches most applied during this thesis are written in bold in the closing circle.

The exploitation of this fungus natural metabolism and strain biodiversity will help not only to identify novel biotechnological applications but also strains with superior potential. However, it is of upmost importance that in the future, genetic engineering starts to be applied in strains other than the ATCC 10985. In this regard, strains isolated from industrial environments would be an interesting source of promising chassis. Moreover, engineering these strains for already explored

compounds (*e.g.*, strain A9 for production of γ-lactones) could bring valuable insights to boost the development of these bioprocesses. For this end, genome sequencing of these strains would also be valuable. Regarding the construction of strains, the implementation of an adapted and effective CRISPR-Cas system for *A. gossypii* should be done. Although the molecular tools currently available (*e.g.*, Cre-*lox*P system) allow to satisfactorily engineer this filamentous fungus, they are still time-consuming due to the need to introduce more than one genetic modification in a sequential manner. Moreover, the accumulation of *lox*P scars resulting from the sum of the genetic modifications performed could generate genomic instability, and consequently loss of fitness by the strains. On the other hand, the rapid and precise testing of engineered strains depends on cost-effective high-throughput screening methodologies that guarantee the characterization of phenotypes under different process conditions, as it is done in industrial yeasts like *Saccharomyces cerevisiae*. However, the filamentous nature of this fungus makes it difficult to obtain disperse and reproducible growth under mini-scale culture conditions and therefore optimization of high-throughput screening methodologies for *A. gossypii* will be required.

Fermentation is the operation unit that has most impact on the cost of biotechnological processes, mainly due to the cost of feedstocks. Thus, besides developing high-producing and robust engineered strains, it is also crucial to combine their improved traits with the selection of cheap raw materials. Preferably, the use of industrial by-products as substrates will significantly reduce the cost of the process, while also contributing to a circular economy. While for industrial models, such as *S. cerevisiae*, this subject has been thoroughly addressed, for *A. gossypii*, the range of substrates studied is limited. Therefore, after achieving the milestone of constructing proof-of-principle strains, such as the ones presented in Chapters IV and V, further engineering should be combined and integrated with the optimization of production conditions. In this future development phase, the medium composition and the culture conditions should be optimized with the aid of statistical experimental designs. For this end, the industrial by-products and complex nutrients pre-identified in Chapter IV serve as good starting variables for this end, not only for the production of orotic acid, but also for riboflavin, lactones and others.

As a final remark, the outcomes obtained in this thesis reinforce that the biotechnological potential of *A. gossypii* goes far beyond riboflavin production. Thus, the physiological and metabolic potential evidenced herein by *A. gossypii* should not be overlooked, since the existence of well-established protocols for industrial riboflavin production is expected to facilitate the implementation of novel biotechnological applications.

APPENDIX

CHAPTER II

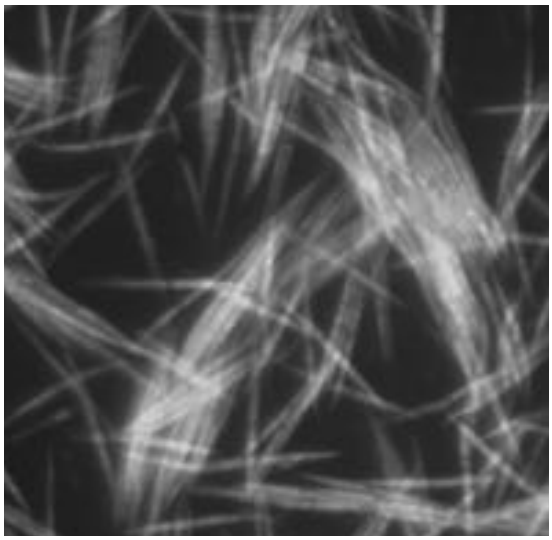


Figure A2.1 Representative image of the microscopic field obstructed with *A. gossypii* spores, which if not removed by using paraffin, impeded the visualization of the comets and consequently the comet assay protocol adapted in this work.

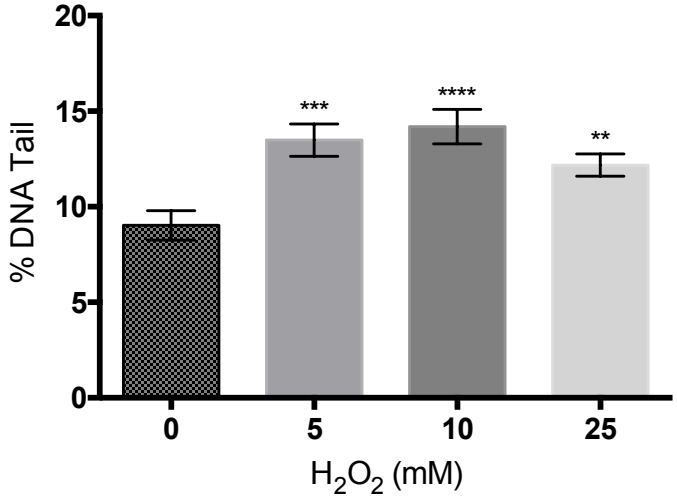


Figure A2.2. Measurement of H_2O_2-induced DNA damage in *A. gossypii* ATCC 10895. Data are presented as mean ± standard error of the mean of the % DNA tail of at least forty comets obtained from two independent experiments for each concentration of H_2O_2 (5, 10 or 25 mM). Experimental procedure is described in the Materials and methods section of Chapter II. Statistical differences were tested by one-way ANOVA followed by post-hoc Dunnett's multiple comparison tests. Asterisks represent significant differences compared to the control (0 mM H_2O_2). ** ($p < 0.01$), *** ($p < 0.001$) and **** ($p < 0.0001$).

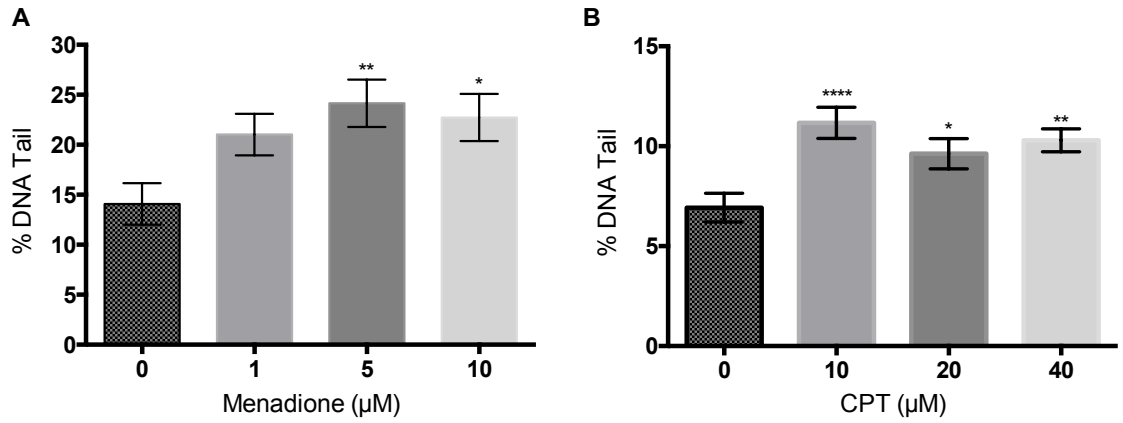


Figure A2.3. Exposure to **(A)** menadione or **(B)** camptothecin (CPT; non-oxidative agent) induces DNA damage in *A. gossypii* ATCC 10895. Data are presented as mean ± standard error of the mean of the % DNA tail of at least forty comets obtained from two independent experiments for each concentration of menadione (1, 5 or 10 μM) and CPT (10, 20 or 40 μM). Experimental procedure is described in the Materials and methods section of Chapter II. Statistical differences were tested by one-way ANOVA followed by post-hoc Dunnett's multiple comparison tests. Asterisks represent significant differences compared to the control (0 μM menadione/CPT). * ($p < 0.05$), ** ($p < 0.01$) and **** ($p < 0.0001$).

Table A2.1. Colony radial growth of *A. gossypii* ATCC 10895 after three days of growth at 30 °C on agar-solidified AFM containing different concentrations of menadione or CPT. Data are presented as mean ± standard deviation of three biological replicates.

Condition	**Radial growth (mm)**
Menadione (μM)	
0	32 ± 0
1	33 ± 0
5	32 ± 1
10	32 ± 1
CPT (μM)	
0	28 ± 0
10	27 ± 1
20	28 ± 0
40	28 ± 1

CHAPTER III

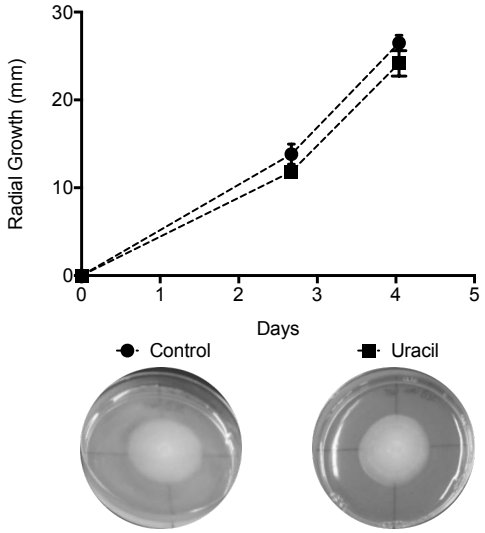


Figure A3.1. Radial growth curve and colony morphology of *A. gossypii* ATCC 10895 at 30 °C on agar-solidified SC supplemented with 5 mM of uracil. The control condition represents medium without any added supplement. Data represent the average ± standard deviation from three biological replicates. Where not seen, error bars were smaller than the symbol. Images were recorded after 4 days of growth. Previously, we observed that the addition of uracil to SC medium negatively affected the growth of *A. gossypii* ATCC 10895, the parental strain of the *Agura3* mutant (Silva et al., 2015; see section "3.5 References"). However, during this study we realized that happened due to inadequate buffering of the medium pH, which after addition of a basic uracil stock solution increased to values that impair the growth of *A. gossypii* ATCC 10895. With this medium pH issue overcome, here we show that the growth and morphology of *A. gossypii* ATCC 10895 on SC medium is not affected by the presence of 5 mM uracil or cytosine. In fact, concentrations of uracil up to 10 mM did not affect the phenotype of this strain (data not shown).

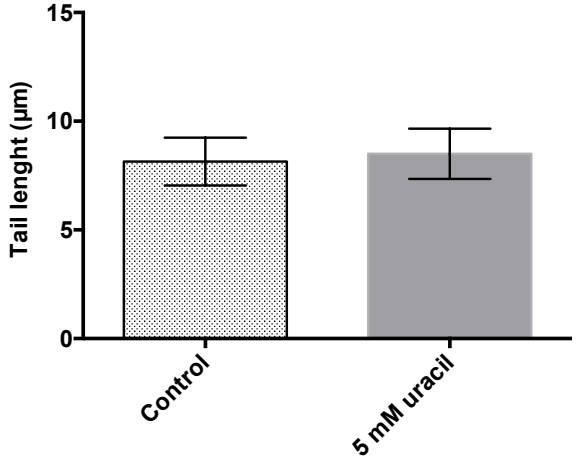


Figure A3.2. DNA damage was assessed by the *Ashbya* Comet Assay (single cell gel electrophoresis) in cells exposed to 5 mM uracil during 7 days of growth on solid SC medium. Control condition represents medium without uracil. Data are presented as mean ± standard error of the mean of the tail length of 50 comets analyzed by condition. Experimental procedure applied for the Comet Assay is described in the "2.2 Materials and methods" section of Chapter II.

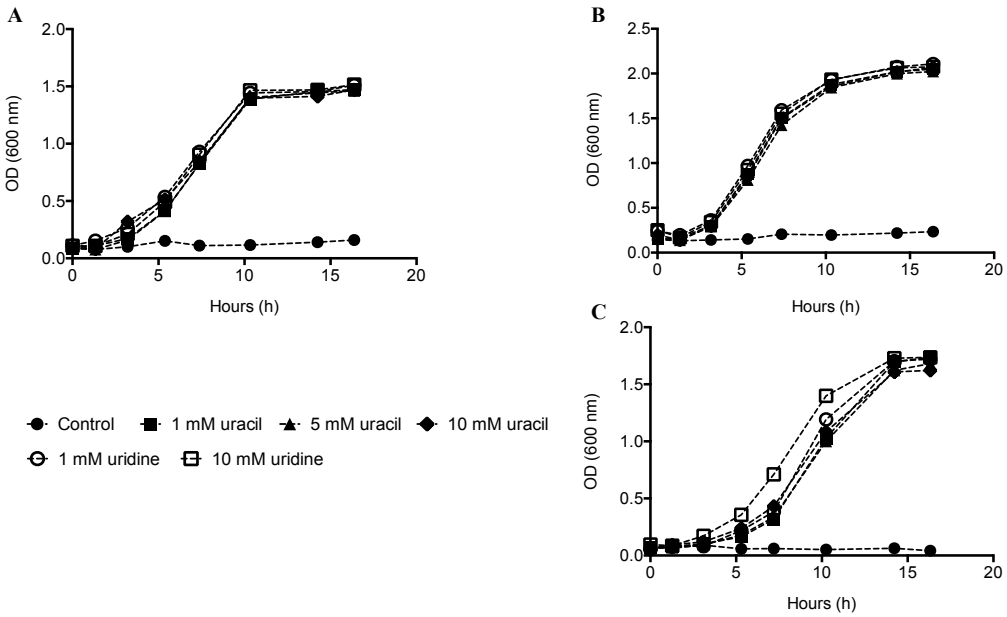


Figure A3.3. Growth curve (OD_{600nm}) of pyrimidine auxotrophic **(A)** *S. cerevisiae* CEN.PK113-5D, **(B)** *K. marxianus* KMS2 and **(C)** *Y. lipolytica* Po1f in liquid SC medium supplemented with different concentrations of uracil or uridine. Control condition represents medium without any added supplement. Data represent average ± standard deviation from three biological replicates. Where not seen, error bars were smaller than the symbol. Growths were performed in 24-well microplates containing 1 mL of medium at 30 °C and 200 rpm. The inoculum was defined to an initial OD_{600nm} of 0.1 from an overnight pre-inoculum in YPD (10 g/L yeast extract, 20 g/L peptone, 20 g/L glucose). The optical density at 600 nm was measured using a Synergy Mx / Cytation 3 microplate reader (Biotek) at the indicate time points.

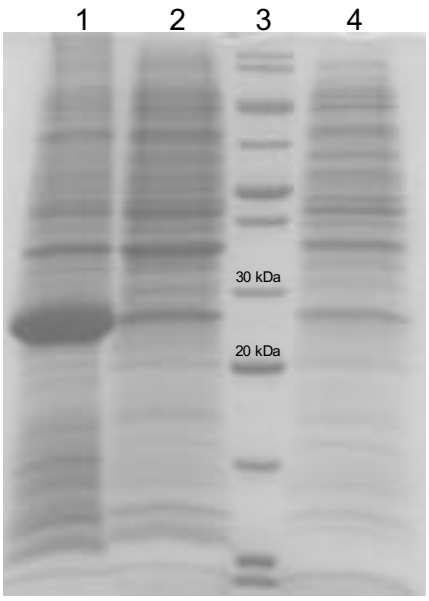


Figure A3.4. SDS-PAGE analyses of the production AgUPRTp from *E. coli* without any fusion partner. Lane 1, insoluble fraction; Lane 2, soluble fraction; Lane 3, molecular weight marker; Lane 4, whole protein content of non-induced cells. Both insoluble and soluble fractions were obtained after lysis of cells producing AgUPRTp.

CHAPTER IV

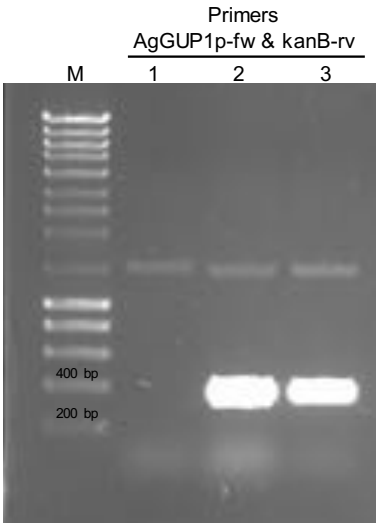


Figure A4.1. Confirmation of correct genomic integration of *AgGUP1* overexpression cassette upstream the initiator codon of *AgGUP1*. Expected size of amplification using primers annealing outside the overexpression cassette integration (AgGUP1p-fw) and within the *KanMX* selection marker (kanB-rv) of the cassette: 378 bp. Lane M, molecular weight marker; Lane 1, ATCC 10895 (WT); Lane 2, ATCC_GUP1; Lane 3, *Agura3*_GUP1.

CHAPTER V

Table A5.1. Primers used in this work. Lower case sequences correspond to homologous recombination sites. Recognition sequences for restriction enzymes are underlined.

Primers	Sequence (5'– 3')	Purpose
ELO624W-del5	gttagttcaacataagtaagcgttacaccactgcggaagccgttattc ataactccatataactgtctgagtttggtgcttcaatatttacctcaatat gcGGATCCCCGGGTTAATTAA	*AgELO624* deletion
ELO624W-del3	gagtatgtaacagcgccaaacaagatctagaagattaaactaccatt agaggaagagtttatcgatctatccaacatatataataacgtaatcag agttaGAATTCGAGCTCGTTTAAAC	*AgELO624* deletion
elo624-fw	ACTCTGCCAAGTATGCACTCCGT	*AgELO624Δ*/homok[2] confirmation
kanB-rv	CTGCAGCGAGGAGCCGTAAT	*AgELO624Δ*/ *YlPOX2* overex[1] confirmation
elo624-rv	CGCTCTTCTGCAGCAATGCTC	*AgELO624Δ*/homok[2] confirmation
(GATG)-YlPOX2-fw	TTTGGTCTCAGATGAACCCCAACAACACTGG	*YlPOX2* overex[1]
(TAGT)-YlPOX2-rv	AAAGGTCTCAACTATTCCTCATCAAGCTCGCA	*YlPOX2* overex[1]
(ACAC)-AgPOX1L-fw	TTTGGTCTCAACACAGTAGCGAAACACCCGAGAA	*YlPOX2* overex[1]
(ATCA)-AgPOX1L-rv	TTTGGTCTCATGATCTTGTCGATCCTTGGCTGCT	*YlPOX2* overex[1]
(ACGC)-AgPOX1R-fw	TTTGGTCTCAACGCTTGAGTCTATCTCTGCTCGCTG	*YlPOX2* overex[1]
(CTTG)-AgPOX1R-rv	TTTGGTCTCACAAGTAGCGAGAATATGCTAGAGGTA CG	*YlPOX2* overex[1]
YlPOX2-b-fw	TGGGCCATGGCTCCAACCTG	*YlPOX2* sequencing
YlPOX2-c-rv	GGACCTTGGCGGCCTGGAAT	*YlPOX2* sequencing
POX1-a3-fw	GCCCGGGTAACCAAACCTTA	*YlPOX2* overex[1]/ homok[2] confirmation
POX1-a3_rv	CTTGCGTGCCAGCTTAATGTC	*YlPOX2* homok[2] confirmation

[1] *YlPOX2* overex. refers to the construction of the *YlPOX2* overexpression module. [2]Homokaryotic genotype.

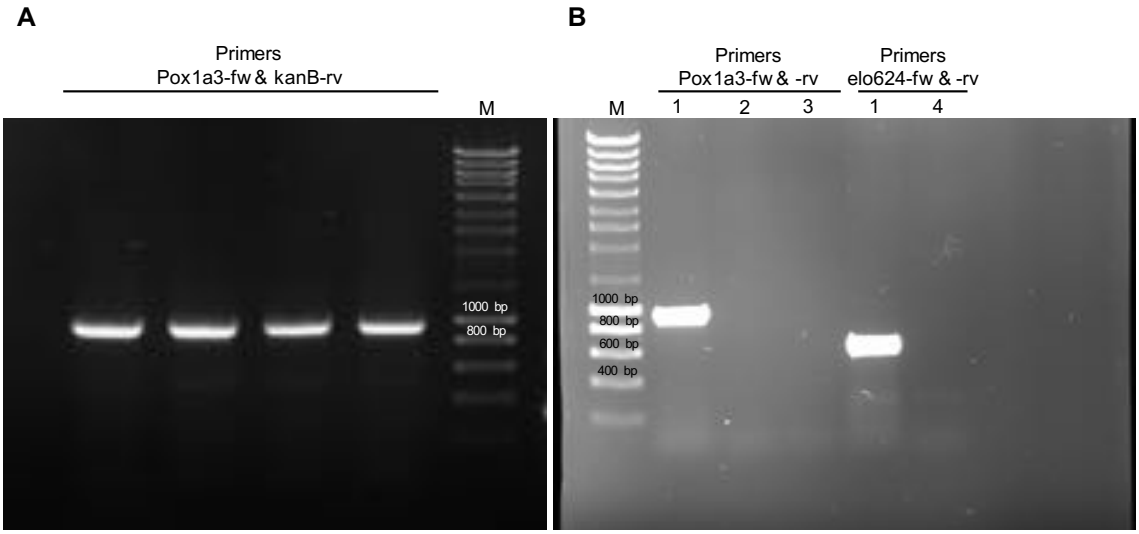


Figure A5.1. Confirmation of genotypes by analytical PCR. **(A)** Confirmation of correct genomic integration of *YlPOX2* overexpression cassette in the *AgPOX1* locus of 4 independent clones (strain DES589/elo624Δ/YlPOX2). Expected size of amplification using primers annealing outside the overexpression cassette (Pox1a3-fw) and within the *KanMX4* selection marker (kanB-rv) of the cassette: 908 bp. Lane M, molecular weight marker. The correct integration of deletion cassette of *AgELO624* gene cannot be shown since no digital image was possible to get from the equipment used. **(B)** Confirmation of homokaryotic genotype of each strain. Lane M, molecular weight marker; Lane 1, ATCC 10895 (WT); Lane 2, YlPOX2; Lane 3, DES589/elo624Δ/YlPOX2; Lane 4, DES589/ Lane elo624Δ. Expected size (Pox1a3-fw & -rv) for ATCC 10895 genotype: 894 bp. Expected size (elo624-fw & -rv) for ATCC 10895 genotype: 601 pb. Absence of WT genotypes confirms homokaryotic genotype of engineered strains.

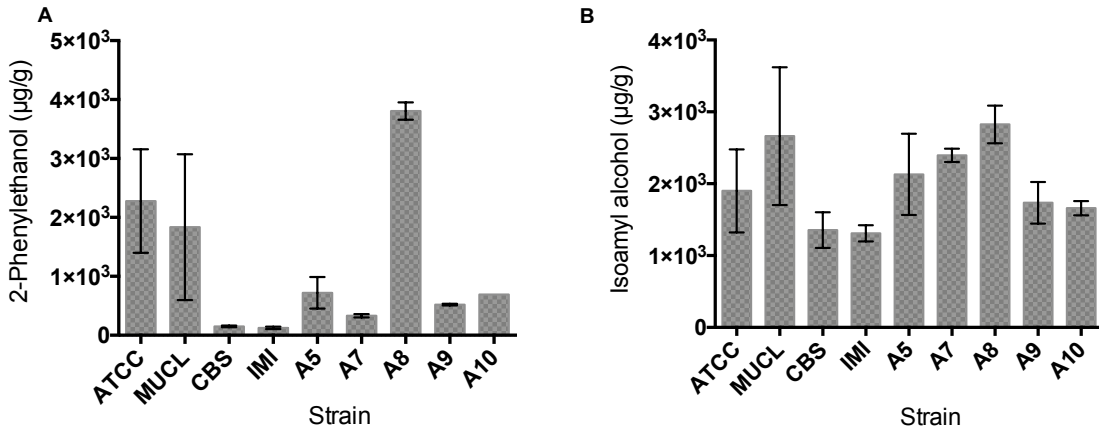


Figure A5.2. Specific productions (µg/gCDW) of the two major higher alcohols identified in cultures of non-engineered *A. gossypii* strains. Production levels of **(A)** 2-phenylethanol and **(B)** isoamyl alcohol. Data are presented as mean ± standard deviation of at least two biological replicates.

Table A5.2. Lactones produced by *A. gossypii* non-engineered strains above their odour perception threshold. Values of the thresholds either in complex (*e.g.*, wine) or simple (*e.g.*, aqueous solutions) samples were retrieved from the literature (Coelho et al., 2015; Jackson et al., 2009). Data are presented as mean of at least two biological replicates. (–), not detected or detected at concentrations below the odour perception threshold of the compound.

Strain	**γ-octalactone (1–67 μg/L)**	**γ-nonalactone (25 μg/L)**	**γ-decalactone (0.088–1 mg/L)**	**γ-dodecalactone (7 μg/L)**
ATCC	(24.34)	–	(6.89)	(26.12)
MUCL	–	–	(2.83)	(17.59)
CBS	–	–	(8.95)	(17.45)
IMI	–	–	(9.19)	(16.96)
A5	–	–	(4.05)	(24.9)
A7	–	–	(5.71)	(29.30)
A8	(15.09)	–	(4.61)	(38.75)
A9	–	(151.39)	(17.74)	(30.78)
A10	–	–	(3.21)	(82.07)

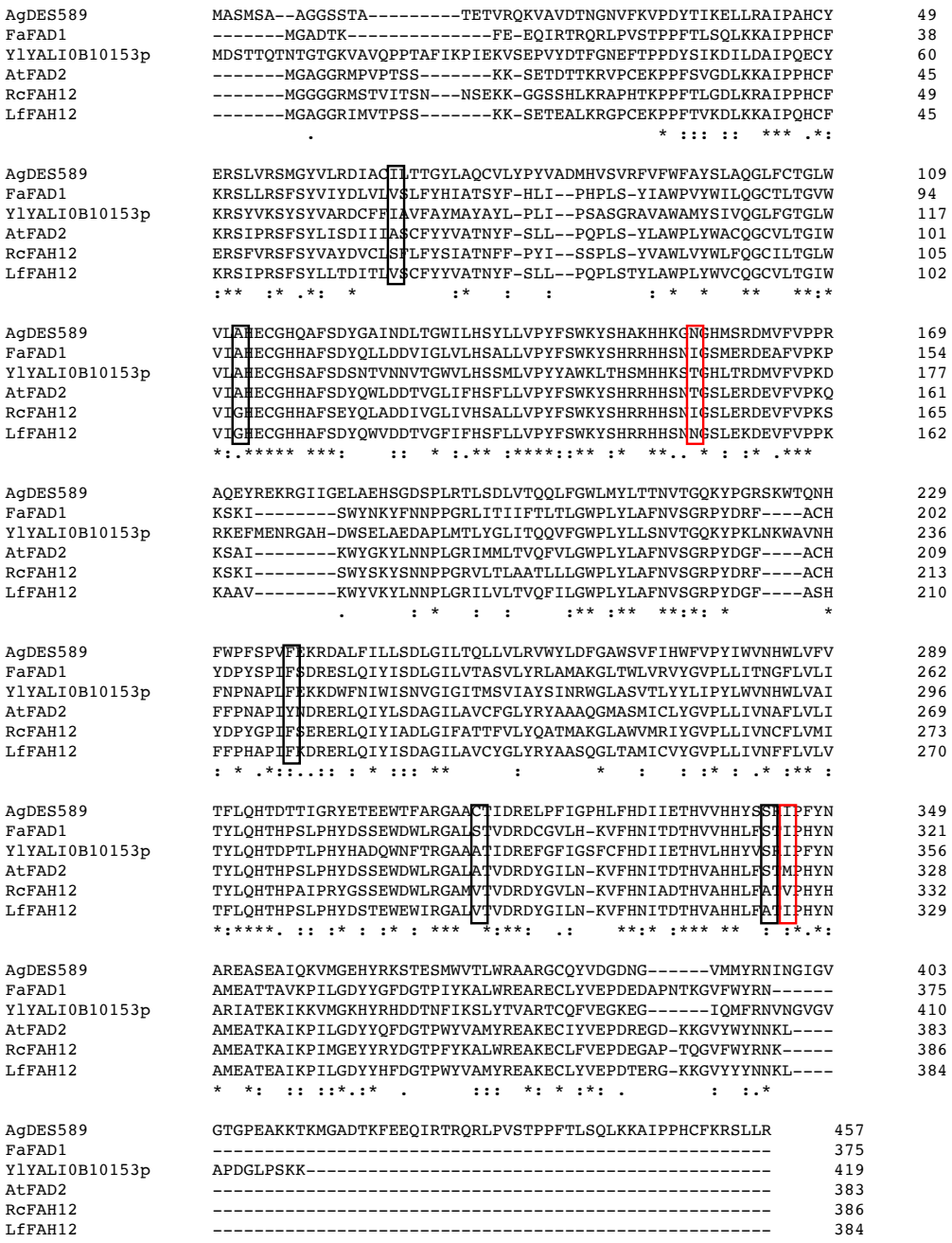


Figure A5.3. Comparison of the amino acid sequence of *A. gossypii* AgDes589p with other fatty acid desaturases, hydroxylases and bifunctional desaturase/hydroxylases. Asterisks (*) represent conserved residues, colons (:) represent residues with strong similar properties and periods (.) represent residues with weak similar properties. The amino acid residues that differ between oleate desaturases and hydroxylases are indicated in boxes. Red boxes represent the two important amino acids residues for the catalytic activity that are conserved between AgDes589p and hydroxylases or bifunctional enzymes. Accession numbers for the sequences are: *F.* x *ananassa* desaturase FaFAD1p (KF887973), *Y. lipolytica* YlYALI0B10153p (XP_500707.1), *A. thaliana* AtFAD2p (AAA32782), *R. comunis* hydroxlase RcFAH12 (AAC49010), (MDP0000288297) and *L. fendleri* bifunctional desaturase/hydroxylase LfAH12 (AAC32755).